The Pennsylvania State University

The Graduate School

Department of Food Science

EFFECT OF DISPERSED PHASE CRYSTALLIZATION ON AROMA RELEASE FROM OIL-IN-WATER EMULSIONS

A Thesis in

Food Science

by

Supratim Ghosh

Submitted in Partial Fulfillment
of the Requirements
for the Degree of

Doctor of Philosophy

May 2007

The thesis of Supratim Ghosh was reviewed and approved* by the following:

John N. Coupland
Associate Professor of Food Science
Thesis Co-Advisor
Co-Chair of Committee

Devin G. Peterson
Assistant Professor of Food Science
Thesis Co-Advisor
Co-Chair of Committee

Roberts F. Roberts
Associate Professor of Food Science

Gregory R. Ziegler
Professor of Food Science

Darrell Velegol
Associate Professor of Chemical Engineering

John D. Floros
Professor of Food Science
Head of the Department of Food Science

*Signatures are on file in the Graduate School

ABSTRACT

The release of volatile aroma compounds before or during food consumption is one of the key factors in perception of food quality. Volatile aroma release from food emulsions is governed by both thermodynamics of binding of aroma molecules to different food constituents and the kinetics of its transport within different regions of food. Lipids, being a large reservoir of aroma compounds, significantly influence aroma release from food emulsions and these effects have been well documented. However, most of these studies involve liquid lipid and effects of fat crystallization on the aroma release properties have been largely ignored.

The major difficulty faced in the comparison of the interactions of aroma compounds with solid and with liquid fats is that there is always a temperature or composition change required to initiate crystallization which might itself affect the binding properties of the system. However, by varying the temperature history of an emulsified lipid it was possible to compare aroma interactions of supercooled liquid droplets with those of crystalline droplets at the same temperature and with the same composition.

The first objective of this study was to understand the thermodynamics of aroma-solid fat interaction in oil-in-water emulsions. The partitioning of a mixture of aroma compounds (ethyl butanoate, ethyl pentanoate, ethyl heptanoate and ethyl octanoate) to model n-eicosane-in-water emulsions stabilized with sodium caseinate was studied by static headspace gas chromatography. The binding of aroma compounds by the liquid droplets was modeled in terms of the bulk oil-gas and water-gas partition coefficients and the volume fraction of the phases. However, aroma binding by solid droplets depended on the specific surface area of the droplets suggesting a surface-binding mechanism and an effective surface binding coefficient was defined for each aroma compounds as the ratio of aqueous to interfacial concentration. This value was constant up to a critical point after which it increased dramatically as the droplets bound much more volatiles.

The increase coincided with an apparent dissolution of the solid droplets in the adsorbed volatile (as measured by a decrease in the measured melting enthalpy). Using the surface binding coefficient and bulk partition coefficients it was possible to model the aroma binding by solid droplets in emulsion.

The results from eicosane emulsion were also compared with triglyceride emulsions prepared with hydrogenated palm stearin (HPS) and Salatrim® (Short And Long chain Acyl TRIglyceride Molecules). For all aroma compounds, equilibrium aroma release from solid droplet emulsions was significantly higher than that for liquid droplet emulsions. It was found that while the partitioning of volatile aroma compounds from emulsion does not depend on the type of liquid oil used, the interactions between solid fat droplets and aroma compounds are significantly influenced by the nature of the crystalline fat. Notably, partitioning into the headspace was much lower for emulsions with solid triglyceride droplets than that for solid alkane droplets.

The second objective of this work was to investigate the kinetics of aroma release from solid fat and liquid oil in emulsion droplets. Emulsions (eicosane or HPS) were mixed with a mixture of aroma compounds and transferred to a model mouth. The glass vessel was sealed and the emulsion was allowed 15 s for the aroma compounds to release into the headspace before a nitrogen flow was used to sweep the headspace out of the container and into a mass spectrometer detector. The change in aroma concentration in the headspace was plotted with time and it was found that with the start of gas flow the aroma concentration increases sharply to a maximum value and thereafter decreases as the rate that aroma compounds are swept out of the glass vessel is exceeded by the rate at which it is released into the gas phase by the emulsion. The rate of release from solid fat droplets was higher than that from liquid oil droplets emulsions. For emulsions with solid fat droplets rate of release decreased with droplet size, particularly for higher molecular weight aroma compounds and release from solid HPS was slower than solid eicosane. By manipulating the aroma content, the initial aroma release profile of the solid droplet

emulsion can be matched to that of a liquid droplet emulsion with higher aroma content with resulting considerable savings of these food ingredients.

TABLE OF CONTENTS

LIST OF FIGURES

LIST OF TABLES

ACKNOWLEDGEMENTS

Completion of Ph.D is truly an enormous task and it would not have been possible for me without tremendous help and support of my advisers Dr. Coupland and Dr. Peterson. I must express my sincere gratitude towards my advisers. Their knowledge, hard work, positive thinking, patience and encouragement enriched me and helped me to rich my goal successfully.

I would also like to express my gratitude and thank to my committee members Dr. Ziegler, Dr. Roberts, and Dr. Velegol for their useful advice and for serving on my committee.

Special thanks to the head of the Department of Food Science Dr. Floros for giving me the opportunity to do my Ph.D at Penn State. I would like to thank all Faculty and Staffs of the Department of Food Science for their help and support throughout my journey in Penn State. I'm especially thankful to all the lab mates and the Food Science Club officers and the fellow graduate Students. They were always there when I needed and made my life at Penn State a memorable one.

I'm grateful to my family for their moral support, encouragement and care without which I would never have achieved what I have. Finally I would like to extend all my thanks to my wife, Atrayee Basu, without whose love and active support in my life finishing this thesis would not have been possible. She took care of everything so that I could solely concentrate in my research and cheered me up on the days my experiments failed. I cannot imagine completing graduate school without her help.

I dedicate this thesis to my parents Mr. Asoke Ghosh and Mrs. Purnima Ghosh for all the sacrifices they made for me. I am greatly indebted to them for their constant support to pursue my goals in life and to teach me to keep faith in God during both difficult and happy times in life.

Chapter 1

Statement of the Problem

Chemical perception of aroma occurs in the nasal cavity so volatile aroma compounds must be released from the food into the headspace gas to be perceived. Aroma release depends both on the thermodynamics of binding of the relevant molecules to different food constituents and on the kinetics of mass transport. However, as foods are complex in nature, it is difficult to separate the effect of different interactions on overall aroma release and simple model systems are used. Emulsions are widely used model systems because they can be prepared and characterized precisely and have some of the complexity of real food. In addition, many foods are themselves emulsions and importantly emulsions are often used as flavor delivery systems.

In an emulsion at equilibrium, the aroma compounds distribute among the different phases (liquid oil, aqueous and headspace gas, see Figure **1.1** a) according to the volumes of the phases and the relevant partition coefficients. Liquid oils are reservoirs for hydrophobic aroma compounds, and their presence can significantly reduce headspace aroma concentration above an oil-in-water emulsion. However, very few studies have considered the effect of solid lipid droplets in emulsions, and most of these have concluded that aroma compounds are inert to solid fat. Thus in a solid droplet emulsion, aroma compounds would be excluded from the droplets (Figure **1.1** b). It has also been proposed that if the aroma compounds are added to liquid droplets, they would be entrapped as the fat crystallizes (Figure **1.1** c)

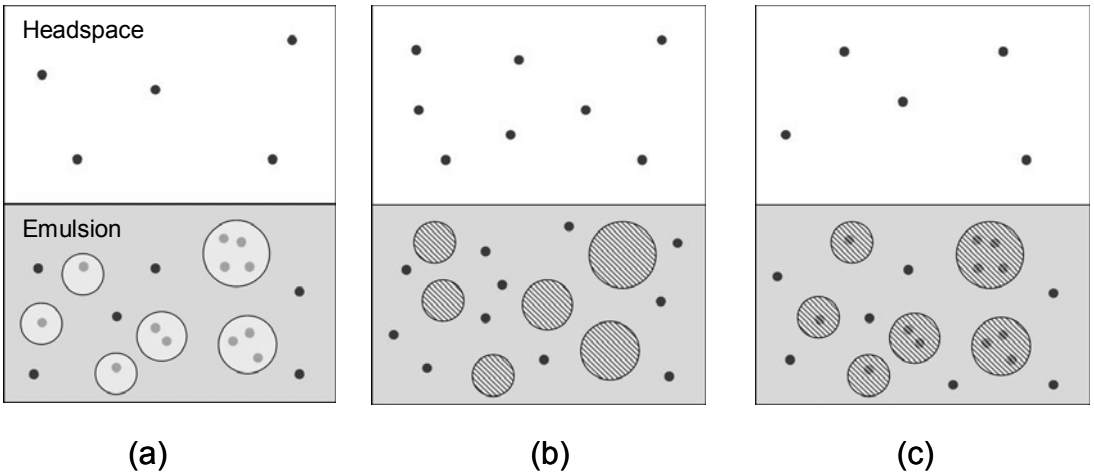

Figure **1.1**: Schematic diagram of oil-in-water emulsions showing the distribution of aroma compounds among the headspace, aqueous phase and oil droplets (a) aroma compounds are partitioned into the liquid oil, (b) aroma compounds cannot interact with inert solid droplets, and (c) aroma compounds added before fat crystallization and are entrapped inside the solid droplets.

One of the major problems faced in the study of aroma release from emulsions containing solid droplets is that either the composition of the lipid or the temperature of the emulsion must be changed in order to initiate fat crystallization, both of which might independently alter the aroma interactions. My solution to this problem exploits the fact that emulsified lipids crystallize at a lower temperature than the corresponding bulk oil while the melting points of bulk and emulsified forms are similar. Figure **1.2** shows a thermogram for an eicosane-in-water emulsion. The exothermic peak on cooling corresponds to fat crystallization while the endothermic peak on heating corresponds to melting. Therefore, the same lipid in an emulsion is stable at 30°C as either a supercooled liquid droplets or crystalline solid droplets. In the present work, this approach has been used to compare the aroma release from solid and liquid droplet emulsion containing the same lipid at the same temperature.

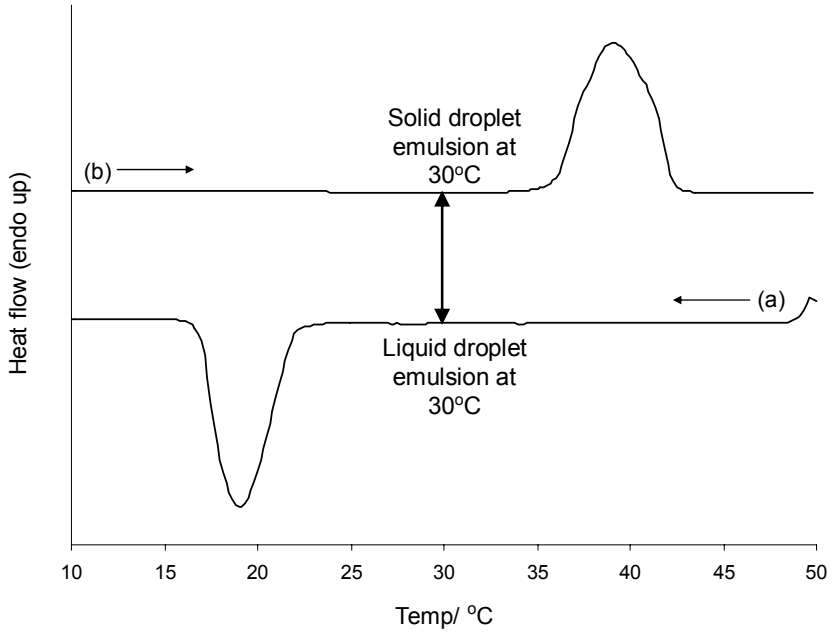

Figure **1.2**: Differential Scanning Calorimeter thermogram of 40 wt% n-eicosane emulsion stabilized with 2 wt% sodium caseinate solution during (a) cooling and (b) heating cycle. The emulsion was temperature cycled at $5^{o}C\ min^{-1}$.

Throughout this thesis, a homologous series of four ethyl esters, namely, ethyl butanoate (EB) ethyl pentanoate (EP), ethyl heptanoate (EH) and ethyl octanoate (EO), is used as model aroma compounds. Ethyl esters are known to be chemically unreactive with the different emulsion ingredients. By using a homologous series we were able to compare aroma compounds with a range of different polarities and molecular weights.

Goal, Objective and Thesis Layout.

The overall goal of my work was to investigate the effect of fat crystallization on the aroma release properties of oil-in-water emulsions. In order to accomplish this goal the specific objectives of my research were to understand the:

1. thermodynamics of aroma- solid fat interactions in oil-in-water emulsions

2. kinetics of aroma release from solid and liquid droplets in oil-in-water emulsions

Chapter 3, 4 and 5 are concerned with the equilibrium or static aroma release properties of solid and liquid droplet emulsions (i.e., Objective 1). I started with a simple alkane (n-eicosane) as a model lipid (Chapter 3) so that the underlying principles of aroma-solid fat interactions can be distinguished without the complex behavior of crystallization in triglycerides. The thermodynamic model developed in Chapter 3 was further modified in next chapter (Chapter 4) in order to include melting of solid droplets in presence of excess amount of aroma. In Chapter 5 I compared the aroma release properties of eicosane with food triglycerides; hydrogenated palm stearin (HPS) was selected because previously published work showed that solid HPS was inert to aroma compounds and Salatrim® was selected based on a hypothesis that the diversity of its fatty acid chain length might accommodate foreign aroma compounds in its crystal structure.

The kinetics of aroma release from solid and liquid droplet emulsion was studied in Chapter 6 (i.e., Objective 2). Emulsions were placed in "model mouth", a sealed, stirred, thermostatted glass vessel, and the aroma compounds released into the headspace were swept away with gas flow to a mass spectrometer detector. In this chapter aroma release from eicosane emulsions was compared with the release kinetics from HPS emulsions. I also use this chapter to show some of the ways that a solid lipid emulsion could be used as a novel aroma delivery vehicle. The last chapter of the thesis (Chapter 7) is written as conclusions to summarize the work and to recommend some thoughts for future work.

As well as aroma, the stability of food emulsions also influences their quality. Often, food emulsions are frozen to improve their shelf life (e.g., sauces) or as a necessary part of the food itself (e.g., ice cream) but very often the thawed emulsion is significantly destabilized and sometimes completely broken down into an oily and an aqueous phase. Therefore, in order to improve food quality it would be necessary to

understand the basic mechanism of freeze-thaw stability of food emulsions. A series of studies on the the effect of continuous phase crystallization on the stability of emulsions are also included in an appendix. While this is a related problem (i.e, phase transitions in emulsions), it does not fit with the overall goal of the thesis and are treated as a separate section. In appendix A I review the current published knowledge on freeze-thaw stability of emulsions. In the next chapter (appendix B) I studied the basic mechanism of freeze-thaw destabilization by using a homologous series of alkane-in-water emulsions prepared with different emulsifiers. The last section is a study showing how the freeze-thaw stability can be improved by changing the emulsion aqueous phase composition (Appendix B). Appendix A and B have also been co-authored with other researchers and these have been included in the thesis because of my significant contribution to those works. Consents from other co-workers were also obtained before including the Chapters in my thesis.

Chapters 3-7 of this thesis are presented in the form of manuscripts co-authored with my advisors each with a separate introduction, materials and method, results and discussion, conclusion and references. Parts of Chapter 2 are a book chapter with one of my advisors in which I describe the current state of knowledge on aroma release from emulsions. Some of the experimental data in the later chapters that had been published at time of completion of the chapter are included in that section.

The structure of the thesis is presented in Table **1.1**.

Table **1.1**: Schematic outline of the thesis

Chapter	Paper	Objective covered
1	Statement of problems	
2	Literature review Ghosh, S.; Coupland, J. N., Influence of food microstructure on flavor interactions. In Understanding and controlling the microstructure of complex foods, McClements, D. J., Ed. Woodhead Publishing: Cambridge, UK, 2007; Chapter 19 (in press)	
3	Ghosh, S.; Peterson, D. G.; Coupland, J. N., Effects of droplet crystallization and melting on the aroma release properties of a model oil-in-water emulsion. *Journal of Agricultural and Food Chemistry* 2006**,** 54, (5), 1829-1837.	1
4	Ghosh, S.; Peterson, D. G.; Coupland, J. N. In *Flavor binding by solid and liquid emulsion droplets*, Food Colloids 2006, Montreux, 2006; Dickinson, E., Ed. Royal Society of Chemistry, UK.	1
5	Ghosh, S.; Peterson, D. G.; Coupland, J. N., Aroma release from solid and liquid droplet emulsions: effect of lipid type	1
6	Ghosh, S.; Peterson, D. G.; Coupland, J. N., Temporal aroma release profile of solid and liquid droplet emulsions	2
7	Conclusions	
Appendix A	Ghosh, S.; Coupland, J. N. in Factors affecting the freeze-thaw stability of emulsions, International Hydrocolloid Conference, Trondheim, Norway, 2006 (in press)	
Appendix B	Cramp, G. L.; Docking, A. M.; Ghosh, S.; Coupland, J. N., On the stability of oil-in-water emulsions to freezing. *Food Hydrocolloids* 2004, 18, (6), 899-905.	
Appendix C	Ghosh, S.; Cramp, G. L.; Coupland, J. N., Effect of aqueous composition on the freeze-thaw stability of emulsions. *Colloids and Surfaces a-Physicochemical and Engineering Aspects* 2006, 272, (1-2), 82-88.	

Chapter 2

Literature Review

2.1 Introduction

Emulsions are a key structural component of numerous natural and processed foods and impact the product quality (McClements, 2004). An improved understanding of the basic physiochemical and sensory properties of food emulsions would therefore provide the key information to tailor the quality of these food products. For example, the flavor properties of food emulsions can be significantly affected by various emulsion properties (i.e. fat content, solid fat index). Considering that flavor is one of the most important factors in determining food choice (Taylor, 1996), defining the mechanisms that governs the flavor delivery properties of food emulsions would be useful.

The aim of this review is to discuss some of the underlying principles of emulsion properties and flavor delivery. We begin with a discussion of basic theory of emulsion formation, characterization, stability and phase transition. We then review some of the thermodynamic and kinetics models of aroma release from emulsions and their experimental validation methods.

2.2 Basic Emulsion Science

2.2.1 Definition

Emulsions are dispersions of one phase into another continuous phase. The basic terminology of dispersions owes its origin to Ostwald, who pointed out that eight types of

dispersions of mutually insoluble substances could exists between solid, liquid and gas considering one as dispersed and other as continuous phase (Ostwald, 1919). He further distinguished between dispersions as molecular (particle size < 0.001μm), colloidal (particle size 0.001μm to 0.1μm) and coarse (particle size > 0.1μm). These limits are quite arbitrary and are defined in terms of the physical and thermodynamic properties of the dispersions thus obtained. A more recent distinction comes from the term micro and macroemulsions. A microemulsion is a thermodynamic stable dispersion of two immiscible phases, i.e. they form spontaneously and are stable indefinitely, are optically clear and their characteristic particle size lies between 0.01 to 0.001 μm. They are characterized by ultralow interfacial tensions (less than 10^{-2} mN/m) (Becher, 2001; Binks, 1998). Macroemulsions are commonly called emulsions and can be defined as heterogeneous systems, consisting of at least one immiscible phase intimately dispersed in another in the form of droplets, whose diameter in general exceeds 0.1mm. Such systems are stabilized by additives such as surface-active agents, thickening agents, finely divided solids etc.

Commonly used food emulsions are liquid/liquid emulsions. Although other types of emulsions like gas/liquid (whipped toppings) are also in use. In food emulsions the two immiscible liquids are usually oil and water, with one of the liquids dispersed as small spherical droplets in the other. Emulsions can be classified according to distribution of oil and water phases. Oil-in-water emulsion consists of oil droplets dispersed in aqueous phase (e.g. milk, coffee creamers, mayonnaise, soups, sauces), and water-in-oil emulsions are dispersions of water droplets in oil phase (e.g. margarine, butter and spreads). In the present work we are concerned with the properties of oil-in-water emulsions.

2.2.2 Emulsion Ingredients and Their Functions

A considerable number of foods exist either partly or wholly as emulsions, or have been in an emulsified state at times during their processing (McClements, 2004). Food emulsions are compositionally complex materials which contain a wide variety of different chemical constituents. In addition to oil and water, a typical food emulsion contains emulsifiers, thickening agents, buffering systems, preservatives, antioxidants, chelating agents, sweeteners, salt, preservatives, colorants and flavors (Dickinson, 1992; McClements, 2004). The overall physiochemical and organoleptic properties of a food emulsion depends on the type and amount of these ingredients and their physical distribution, i.e., in the dispersed phase, the continuous phase or at the interface.

2.2.2.1 Lipid

In oil-in-water emulsions, the dispersed phase consists of food oils which are almost always triglycerides. (Although, because of the chemical complexity of real food lipids, many researchers have used simple alkanes as model lipids to systematically study the consequences of droplet crystallization in emulsions (Awad, 2002; Dickinson, Kruizenga, Povey and van der Molen, 1993).) Fats and oils influence the nutritional, organoleptic and physiochemical properties of food emulsions in a variety of ways. The characteristic turbid, cloudy or opaque appearance of emulsion is largely due to scattering of light by the dispersed oil droplets (McClements, 2002). Perceived creaminess of the food emulsion as well as its viscosity increases with the lipid content and droplet concentration of emulsions. Lipid also influences emulsion texture by crystallization and forming fat crystal network and hence modifying its mechanical strength against external force (Narine and Marangoni, 2002). The perceived flavor of food emulsions is also significantly influenced by the amount and nature of lipid used (Buttery, 1973; Relkin, Fabre and Guichard, 2004; van Ruth, King and Giannouli, 2002).

2.2.2.2 Water

The aqueous phase of an oil-in-water emulsion contains a variety of water soluble functional ingredients and their solubility, partitioning and chemical reactivity depends on the interaction with water (McClements, 2004). Crystallization of water has a significant effect on the emulsion's stability and physiochemical properties. Freezing of water adversely affects freeze-thaw stability of emulsions (Cramp, Docking, Ghosh and Coupland, 2004; Thanasukarn, Pongsawatmanit and McClements, 2004b). Many food emulsions are designed to be freeze-thaw stable (e.g. frozen sauces) and special additives and modified formulations are needed for them (Ghosh, Cramp and Coupland, 2006a; Thanasukarn, Pongsawatmanit and McClements, 2004a).

2.2.2.3 Emulsifiers

Emulsifiers are one of the most important ingredients in emulsion stabilization. Oil and water are almost completely mutually insoluble yet commonly coexist in the form of emulsions. There is thermodynamic pressure for a complete phase separation but this is kinetically retarded largely by amphiphilic materials absorbed at the interface and hence lowering the interfacial tension. Different types of stabilizing structural entities may occur at the oil-water interface, e.g. low molecular weight surfactants, amphiphilic biopolymers and solid particles. Small molecule surfactants consist of a hydrophilic head group attached to a hydrophobic tail group. Their principal role is to lower the surface tension at the oil-water interface and hence stabilize the emulsion. However, they may affect other emulsion properties by forming micelles in the continuous phase (Lindman, 2001), interacting with other biopolymers (Courthaudon, Dickinson and Dalgleish, 1991) and by influencing fat crystallization in the oil droplets (McClements, 1993). Depending on their structure, small molecule surfactants can be classified into ionic (fatty acid salts and sodium stearoyl lactate), zwitterionic (lecithin and other phospholipids) and nonionic (monoglycerides, Tweens or polyoxyethelyne sorbitan fatty acid mono esters, sucrose fatty acid esters etc.) groups. Biopolymers that have significant amount of both polar and

nonpolar residues tend to be surface active and polysaccharides (e.g. gum Arabic, modified starches) and more importantly proteins (e.g. Caseins, whey protein concentrate, gelatins, egg protein) are the two most important types of biopolymers used in food emulsions. Biopolymers form thick layers at the interface and sterically stabilize the droplets from coalescence. Stabilization of food emulsion with adsorbed solid particles is known as Pickering stabilization (Binks, Clint, Mackenzie, Simcock and Whitby, 2005; Garti, 2002; Rousseau, 2000a) and important examples include egg yolk particles in mayonnaise (Dalgleish, 2004) and fat particles in whipped cream (Rousseau, 2000a; 2002). To impart stabilization of emulsions the solid particle (fat crystals in many cases) must be adsorbed at the droplet interface. The formation of these stabilizing crystals can also be due to the solidification of surfactants previously adsorbed at the interface (monoglycerides) or by migration of crystals toward the droplet interface from the interior of the oil droplets (Rousseau, 2000a).

2.2.3 Emulsion Formation

Emulsions are usually created with a mechanical device, a homogenizer, which supplies energy in order to disrupt and disperse a lipid phase into an aqueous phase in the presence of a surfactant system and potentially other ingredients. Typically, homogenization is (at least) a two-step process. Oil and water are coarsely mixed to form large droplets which are subsequently disrupted into smaller one further stages of homogenization (secondary homogenization). During homogenization, the size of the droplets formed depends on two opposing process: droplet disruption and droplet re-coalescence (McClements, 2004).

2.2.3.1 Droplet Disruption

Whether a large droplets will disrupt into smaller ones depends on the balance between the forces that hold the droplets together (interfacial force) and that tries to pull

them apart (disruptive force generated by the homogenizer) (Walstra, 1993). The interfacial force is given by the Laplace pressure which for a sphere is given as $p_L=2\gamma/r$, where γ is the interfacial tension and r is the radius of the sphere. This pressure is responsible for holding the spherical shape of a droplet and to deform or disrupt it during homogenization considerably larger force is needed (McClements, 2004; Walstra, 1993). From the Laplace pressure expression, it can be seen that the force required to disrupt the droplets increases with a decrease in droplet radius. Thus smaller droplets are harder to break than larger ones and most homogenization processes have a minimum droplet size that can be achieved under given conditions however long they are run. Additionally the force needed to disrupt a droplet increases with surface tension so adsorbed surfactants (which lower interfacial tension) facilitate homogenization.

The disruptive force acting on the droplets depends on the nature of flow properties in a homogenizer. Commonly achieved flow regimes are laminar, turbulent and cavitational flow. Laminar flow is predominant in lower flow rates while turbulence occurs at very high flow rates (depending on the Reynolds number). The dominant flow regimes in large scale industrial homogenizers are turbulent. Turbulence occurs when the Reynolds number of the flow exceeds some critical value (>2500) (Walstra, 2003b). Turbulent flow is characterized by the formation of eddies (Walstra, 1993). Generation of eddies in turbulent flow is critical in droplet disruption. Extremely high shear and pressure gradients are associated with these eddies which cause droplet deformation and disruption (Gopal, 1968; Walstra, 1993).

The relative magnitude of disruptive forces and interfacial forces can be expressed by the Weber number (We) (Walstra, 1983) and when the Weber number is exceeds some critical value (We_{cr}), droplets tend to be disrupted. Schubert and Armbuster (1992) showed that that We_{cr} is minimum when the ratio of viscosities of the two phases is between 0.1 and 1, and increases significantly when it is below 0.05 or above 5. This is because at low viscosity ratio (<0.05) the droplets can becomes extremely elongated before any disruption occurs and at high values (>5) the time needed

for deformation of the drop will be longer than the time of rotation of the drop to a new orientation hence altering the distribution of forces acting upon it (Schubert and Armbruster, 1992).

Walstra and Smulders (1998) derived a relationship between the maximum droplet size that can persist a homogenization process. The authors proposed that droplet size will decrease with the decrease in interfacial tension and increase in shear rate and viscosity of the continuous phase. If the continuous phase is of low viscosity a much higher shear rate is need in order to decrease the droplet size (Walstra and Smulder, 1998).

2.2.3.2 Droplet Re-coalescence

The emulsifiers present in the solution during homogenization adsorbed on the freshly generated droplet surface and prevent them against coalescing to each other. Droplet coalescence due to collision between the droplets is especially very rapid during the homogenization process itself because of very high mechanical pressure created in the homogenizer. To prevent coalescence, sufficient amount of emulsifiers need to quickly adsorb to the newly generated surface of droplets. Therefore, in order to get smaller droplets the time taken by the emulsifiers to adsorb on the surface should be much lower than the time required for droplet-droplet collision.

Apart from preventing droplet coalescence, emulsifiers also have other important effects during homogenization. From the Laplace pressure expression it can be seen that the interfacial force of the droplets and hence the force required to disrupt the droplets decreases with decrease in interfacial tension. In the presence of emulsifiers, interfacial tension decreases which facilitates the droplets disruption during homogenization (McClements, 2004).

2.2.3.3 Homogenizers

Different type of homogenization devices are used to prepare emulsions. Each device has been developed based on its specific application and advantages. High speed mixers are generally used to prepare direct dispersion of bulk oil and surfactant solution. Colloid mills and high pressure valve homogenizers are commonly used industrial homogenizers to prepare fine emulsions (Fellows, 2000). Colloids mills are used for medium to high viscosity materials whereas high pressure valve homogenizers are used for low to medium viscosity products (Pandolfe, 1991). In colloid mills, the rapid rotation of rotors against a stator generates high shear stress on the coarse emulsion which breaks up the large droplets into smaller one. High pressure valve homogenizers operate by passing the coarse emulsion through a narrow valve where intense disruptive force creates droplets break up (Pandolfe, 1991). Homogenizers based on high-powered ultrasonics have also been used to prepare food emulsions (Gopal, 1968). Unlike the other two, ultrasonic homogenizers operate under cavitational flow where high intensity ultrasonic waves generates intense shear and pressure gradient in the coarse emulsion which disrupt the droplets due to cavitational effects (Gopal, 1968).

2.2.4 Emulsion Characterization – Particle Size Distribution

Many of the properties of an emulsion including stability, appearance, texture and flavor depend on its droplet size (McClements, 2004). Therefore, determination of droplet size is of prime importance in order to characterize an emulsion. However, most of the emulsions are polydisperse, meaning that they have a range of different size of droplets. So, rather than a single number for droplet size, emulsion should be characterized by a distribution of particle size by expressing the fraction of droplets in different size ranges. The fraction of droplets in different size range can be expressed in several different ways, including number, mass, volume or surface area distribution (Walstra, 2003b). It is sometimes useful to express the particle size of an emulsion by a

mean and width of a distribution. There are different ways of expressing the mean of a particle size distribution, for example (Walstra, 2003b):

Number-length mean diameter $$d_{10} = \frac{\sum_{i=1} N_i d_i}{\sum_{i=1} N_i} \quad (2.1)$$

Area-volume mean diameter $$d_{32} = \frac{\sum_{i=1} N_i d_i^3}{\sum_{i=1} N_i d_i^2} \quad (2.2)$$

Volume fraction-length mean diameter $$d_{43} = \frac{\sum_{i=1} N_i d_i^4}{\sum_{i=1} N_i d_i^3} \quad (2.3)$$

Where, N_i is the total number of particles in the ith size range and d_i is the droplet diameter in the respective size range. Here d_{10} is the number average mean diameter of the distribution. The two most commonly used method of expressing mean particle size of emulsions are area-volume mean diameter (d_{32}, a function of volume fraction and total interfacial area) and volume-length mean diameter (d_{43}, volume ratio of the droplets in each size range multiplied by the mid point diameter of that range) (McClements, 2004). It should be noted that d_{43} is more sensitive to the presence of large droplets in an emulsion than d_{32} (Walstra, 2003b).

For a fairly monodisperse emulsion the value of different mean diameter are similar, however with the increase in polydispersity they increasingly vary. Thus for an emulsion with a wide distribution of particle size the width of the distribution also need to be reported. The width of a particle size distribution can be conveniently expressed by the standard deviation of the size distribution weighted with the particles' surface area, divided by d_{32} (Walstra, 2003b). The range of width of distribution in food emulsions is generally between 0.5 to 1 (Walstra, 2003b). If the width of the distribution is large, the

shape of the distribution should also be described. (e.g., skewed, log-normal, truncated or bimodal) (McClements, 2004).

Instruments for determination of particle size distribution. Several different instruments have been developed to measure particle size distribution of food emulsions. Of these some of the most commonly used techniques are microscopy, static and dynamic light scattering, Electric sensing zone (i.e., Coulter counter), sedimentation, and ultrasonic spectrometry (McClements, 2004). The instrument used in the present work is based on static light scattering or laser diffraction light scattering technique. In this method a monochromatic light beam (generated by a He-Ne gas laser, λ=0.63 μm) is passed through a sample cell containing the diluted emulsion (oil volume fraction < 0.05%) and the light scattered by the droplets of the emulsion is collected by an array of photosensitive detectors. The intensity of the scattered light is measured as a function of scattering angle and data is analyzed by a computer. Generally the smaller the particle size of droplets, the more the scattered light would be (McClements, 2004). Finally using Mie theory of approximation the particle size distribution is calculated that gives the best fit with the experimental scattering data (Kerker, 1969). The use of Mie theory requires the refractive index of the dispersed phase and the continuous phase as a supplied data. In modern light scattering instrument a number of additional technique has been used, for example, more than one laser source and measuring intensity of backscattered light so that the instrument can be used for a wide range of emulsion droplet size (typical range of 0.02 to 2000μm) (Rawle, 2004).

2.2.5 Emulsion Stability

Emulsions are thermodynamically unstable systems because of their large excess surface energy due to the small droplet size. However, they can be kinetically stabilized for considerable periods of time. The stability of an emulsion is characterized by the capacity to resist changes in its physicochemical properties over time (McClements,

2004). The requirements for kinetic stability depends on the type of food product, e.g., mayonnaise, salad dressings and cream liquor must remain stable for a long time (i.e., months to years) whereas controlled destabilization of emulsion is required in some food products (e.g., butter, ice cream, whipped cream).

Physically, emulsions can be destabilized by several processes including creaming, flocculation, coalescence, partial coalescence and Ostwald ripening (Dickinson, 1992; Dickinson and Stainsbay, 1982), whereas, lipid oxidation is a major cause of chemical destabilization of emulsions (McClements and Decker, 2000). The properties of food emulsion can also be adversely affected by microbial growth. In the following section, some of the mechanisms of emulsion destabilization are discussed.

2.2.5.1 Creaming

Creaming is the separation of oil droplets as a layer at the top of an oil-in-water emulsion due to a density contrast between the continuous and dispersed phases (McClements, 2004). Creaming is reversible, i.e., the droplets can be re-dispersed uniformly by gentle mixing (Dickinson and Stainsby, 1988). The rate of creaming in a highly dilute emulsion can be determined using Stokes' law considering that oil droplets with a layer emulsifier on its surface behave like rigid particles. According to Stokes' law, when a particle moves at a constant velocity through a surrounding liquid the force acting on it due to gravity should be equal to the hydrodynamic frictional force acting against it. According to Stokes's law the equation for the creaming rate of an isolated spherical particle is:

$$v_{stokes} = \frac{2g\Delta\rho r^2}{9\eta} \tag{2.4}$$

Where, v_{stokes} is the velocity of the droplet and $\Delta\rho$ is density difference of the dispersed and continuous phase, r is the radius of the droplet, η is the viscosity of the surrounding continuous phase and *g* the acceleration due to gravity. From Equation 2.4 it can be seen that creaming rate in an emulsion can be effectively reduced by increasing aqueous phase viscosity, decreasing droplet size and matching the density of the two phases. A low value of v_{stokes} (e.g., <1 mm/day) would mean the emulsion would be stable to creaming (Dickinson 1992). Stokes' law however, ignores the effects of Brownian motion of emulsions droplets which favors random distribution of droplets throughout the emulsion (Hiemenz and Rajagopalan, 1997). A mathematical expression for droplet distribution involving both creaming and Brownian motion has been developed (Walstra, 1996a). It was shown that Brownian motion may retard creaming for emulsions with droplet size lower than 0.1 μm and creaming would be completely inhibited when the droplet radii would be less than 10 nm (McClements, 2004), which is essentially the case for microemulsions.

Typical food emulsions differ significantly from the dilute conditions assumed in the derivation of Stokes' law. The creaming velocity in a concentrated emulsion is less than the value predicted by Stokes' law (Dickinson and Stainsby, 1988; Hunter, 1989). At sufficient high droplet volume fraction (i.e., close packing of droplets), creaming can eventually be stopped

Experimental determination of creaming. Creaming can be simply measured as the relative heights of different layers formed in an emulsion after a certain time. For this method to work, it must be possible to visually distinguish between the droplet depleted lower serum layer, any intermediate emulsion layer and the top cream layer. In a more advanced methods a monochromatic beam of near infrared light is directed thorough an emulsion as in clear glass tube (Chanamai and McClements, 2000). The variation of droplet concentration in the emulsion as function of height in the tube can be calculated from the transmitted and/or scattered light using a suitable calibration curve.

2.2.5.2 Flocculation

If two particles stay together for much longer time then they would do in the absence of any colloidal forces, they are said to be aggregated (Walstra, 2003b). If the process of aggregation is reversible, that is if the droplets are associate with each other without losing their individual identities and can be separated easily, they are flocculated (McClements, 2004) while on the other hand strong and irreversible aggregation is known as coagulation. Flocculation increases the rate of creaming in dilute oil-in-water emulsion which reduces emulsion shelf-life. However, in concentrated emulsions flocculation significantly increases emulsion viscosity, increasing its shelf life by minimizing the rate of creaming.

The rate of flocculation in an emulsion depends on two factors: the frequency of collision between the droplets and the proportion of collisions that lead to the formation of a semi-permanent link (McClements, 2004). Collision between the droplets in an emulsion can result from Brownian motion, gravitational flow or by applied mechanical forces (McClements 2004). In all cases, the frequency of collisions can be reduced by reducing the droplet concentration. Collision frequency due to Brownian motion and gravitational flow decreases with increases in viscosity of the continuous phase. Reducing the applied shear rate can also reduce collision due to mechanical forces (McClements 2004).

Not every collision between the droplets leads to flocculation. and the fraction that does is expressed as the collision efficiency which depends on the colloidal and hydrodynamic interactions among the droplets (Friberg and Larsson, 1997). The most effective way of preventing flocculation in emulsions is by modifying the colloidal interactions between the droplets. This can be done by adding ionic emulsifiers so that electrostatic repulsion between the droplets will prevent them from coming together. Many emulsions are also sterically stabilized against flocculation by biopolymers or nonionic emulsifiers. However biopolymers can cause bridging flocculation when there is

insufficient present in order to cover the individual droplet surfaces and hence multiple droplets share the same biopolymer chain and are connected by it (Dickinson, 2003).

Non-adsorbing colloidal particles (e.g., surfactant micelles) (McClements, 1994), hydrocolloids and modified starch (Chanamai and McClements, 2001; Dickinson, Goller and Wedlock, 1995) or casein submicelles (Dickinson and Golding, 1997) sometimes create an attractive interaction between the droplets that can be enough to induce flocculation (Walstra, 2003b). The colloidal particles are excluded from the narrow region from the surface of droplets to a distance equal to the radius of the colloidal particle. There is a concentration gradient between this region and the bulk aqueous phase and an associated osmotic pressure which drives the droplets to flocculate (Walstra, 1996b). Depletion flocculation is observed when the nonadsorbed colloidal particle concentration exceeds a critical value but above the added particles may also increase the emulsion viscosity and prevent subsequent creaming (Chanamai and McClements, 2001).

Experimental determination of flocculation. Flocculation can be monitored using variety of techniques based on particle size measurement or inferred from an increase in the viscosity of the emulsion (McClements, 2004). Care must be taken to ensure that measured changes in droplet size are due to flocculation and not any other mechanism (e.g., coalescence or Ostwald ripening). Flocculation can be reversed by gentle agitation or by adding small molecule surfactants which can break the floc into its constituent droplets. Thus droplet size would be decreased only if flocs are present.

2.2.5.3 Coalescence

Coalescence is defined as the process by which two or more liquid oil droplets merge to form a larger droplet (McClements, 2004). Coalescence leads to the formation of larger droplets thereby increasing creaming rate and finally forming a separate oil layer at the top of the emulsion. During the manufacture of certain products (e.g. butter

and whipped cream) coalescence is desirable and a limited amount of coalescence in the mouth, contributes to the oily lubricity and perhaps the perceived creaminess of food. However, in most cases coalescence is usually undesirable and causes a reduction in shelf life.

In most cases coalescence in an emulsion is initiated by the following process: droplet encounter, droplet deformation, film formation between the droplets, film thinning and film rupture (van Aken, 2004). Depending on the physical processes involved, it can be divided into two major classes: homogeneous and heterogeneous coalescence (van Aken, 2004). Homogeneous coalescence occurs entirely due to interaction between the droplets while heterogeneous coalescence involves presence of a third phase during coalescence, for example, fat crystals and shearing in a confined space. In the following paragraphs, the processes leading to coalescence are discussed.

For coalescence to occur, two droplets must first approach each other in close proximity (van Aken, 2004). The rate of encounter depends on the mechanisms of droplet movement in emulsions in a similar manner as discussed in Section 2.2.5.2 for interactions leading to flocculation (McClements, 2004). When the droplets are sufficiently close together they start to interact with each other and the droplets deformed so that part of its surface flattened to form a thin film between them (Figure **2.1)** . The droplet flattening occurs when the external forces acting on the droplets exceed the internal Laplace pressure (Walstra, 2003b). The tendency of droplets to be deformed can be described by the dimensionless Weber number (We, defined as the ratio of the local external force to the internal Laplace pressure). If We<1, the droplets remain undeformed, while for We>1, a flat thin film will be formed between the droplets (Figure **2.1)** (McClements, 2004). In turbulent flow the outflow of continuous phase from the thin spacing between the approaching droplets increases which may drag along the adsorbed interfacial layer with it (Figure **2.1)**. This generates a spot on the surface with low surfactant concentration and hence high interfacial tension which may initiate film rupture and coalescence.

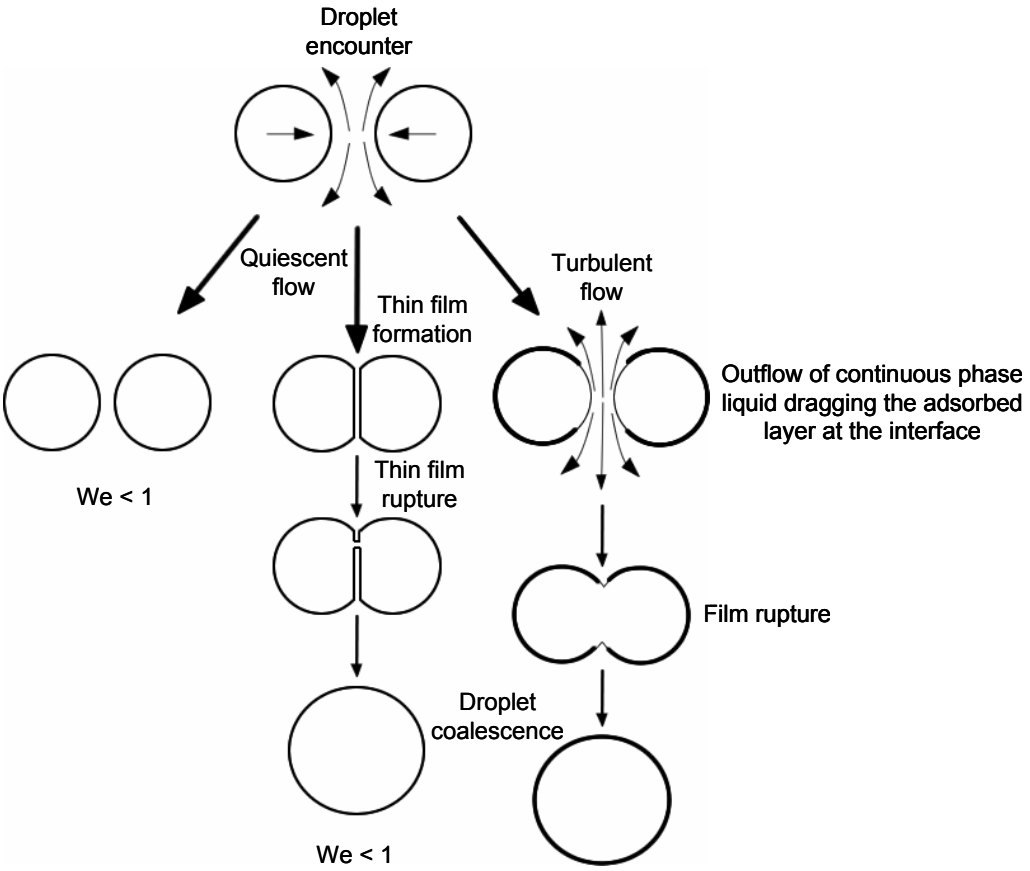

Figure **2.1**: Coalescence induced by quiescent and turbulent flow.

Film rupture is the final step in the coalescence process (van Aken, 2004). It occurs when a hole formed in the thin film become larger than the critical size such that it will grow spontaneously leading to coalescence. Different mechanisms of film rupture have been proposed by several authors. The relative importance of these mechanisms depends on the nature of the interfacial membrane, characteristics of the continuous phase and emulsion environmental conditions.

Rupture by spontaneous hole formation. The thin film can be ruptured by spontaneous formation of hole through which dispersed phase liquid forms a continuous bridge between two adjacent droplet surfaces (van Aken, 2004). This mechanism of film rupture can be applied for coalescence of small molecule surfactant stabilized emulsion

and it is strongly dependent on the nature of the emulsifiers at the oil-water interface. A theoretical description of this mechanism known as “oriented wedge theory” was developed by Kabalnov and Wennerstrom (1996). According to this theory, the monolayer bending energy at the oil-water interface affects the free energy of “coalescence transition state”. In this model surfactant molecules are depicted as wedges. If the surfactants are such that tail group cross-sectional area greater than head group, the spontaneous curvature of the monolayer fits that of the hole edge and film rupture occurs (Figure **2.2)** (Kabalnov and Wennerstrom, 1996). These types of surfactants typically have low HLB (hydrophilic-lipophilic balance) numbers and tend to form micelles in the oil phase (van Aken, 2004). On the other hand, if the surfactant head group cross-sectional area is greater than the cross-sectional area of the tail group, the monolayer of surfactant at the edge of the hole surface would be “frustrated”, and hole formation will not occur spontaneously (Figure **2.3**) (Kabalnov and Wennerstrom, 1996). These surfactants are of high HLB type and they tend to form micelles in the aqueous phase (van Aken, 2004).

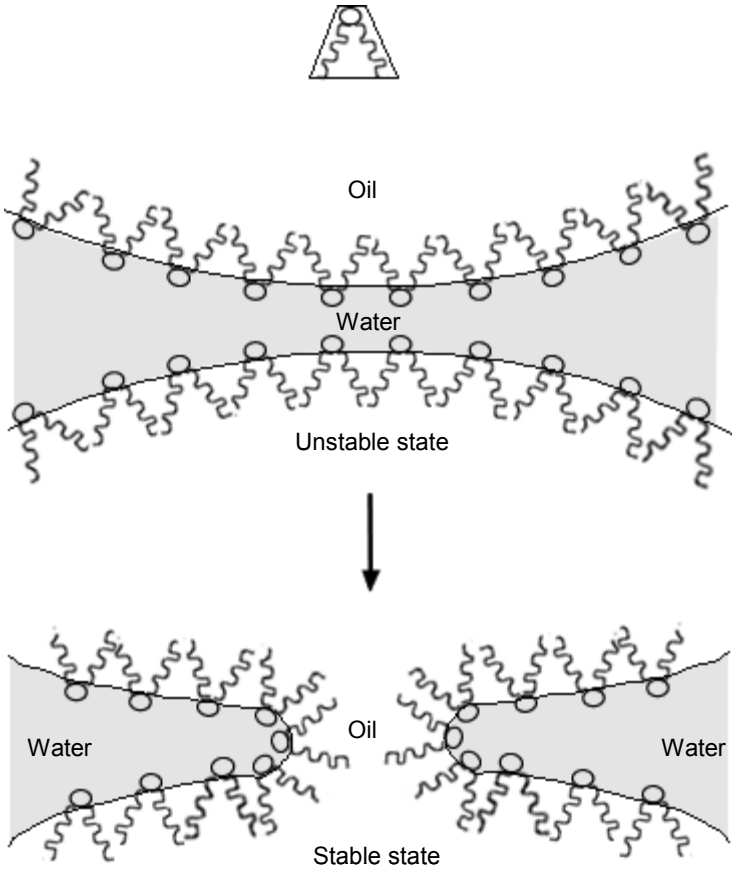

Figure **2.2**: Oriented wedge model for droplet coalescence. Coalescence is more favorable for surfactants with tail group cross-sectional area greater than head group

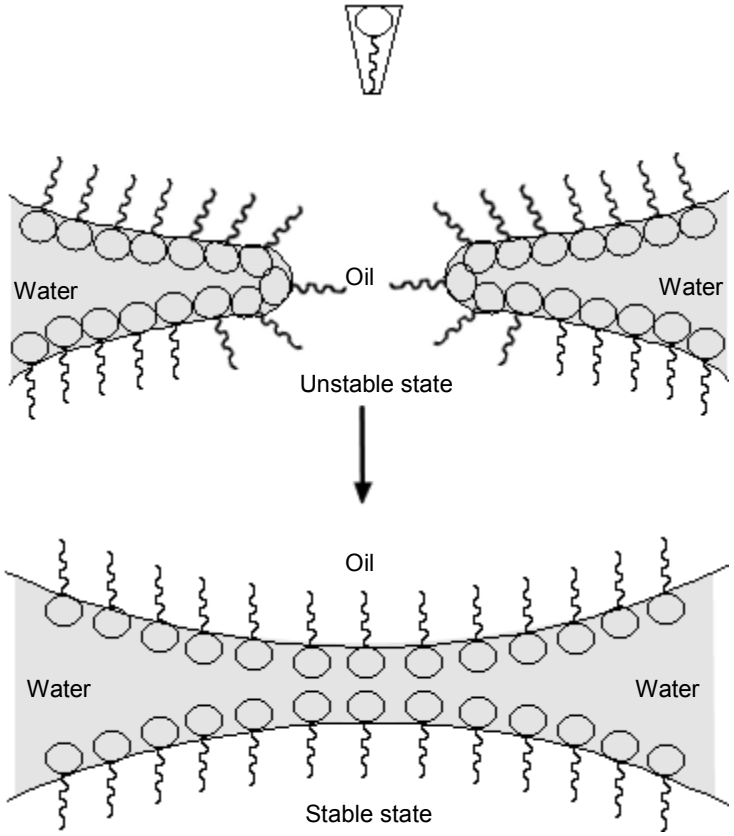

Figure **2.3**: Oriented wedge model for droplet coalescence. Coalescence is less favorable for surfactants with head group cross-sectional area greater than tail group

Rupture by the presence of vacancies on the interface. If the adsorption of surfactant at the interface is insufficient to completely cover the surface then collision between two bare surfaces can lead to immediate coalescence without the need for a hole to develop (Figure **2.4)** (Kashchiev and Exerowa, 1980). This type of coalescence can be seen for both small molecule surfactant and protein stabilized emulsions. Van Aken and coworkers showed that the stability of emulsion sharply changes when protein concentration in emulsion reach saturation adsorption (van Aken and Zoet, 2000).

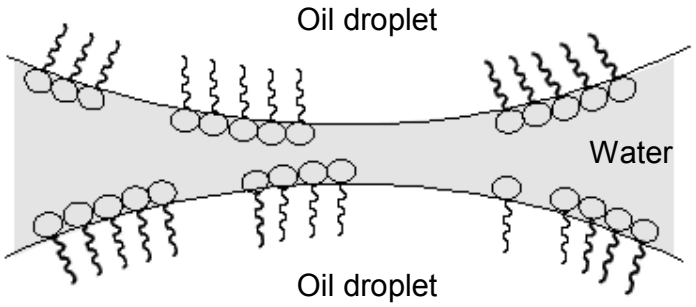

Figure **2.4**: Film rupture by the presence of vacancies on the interface due to unsaturation of the interface

Rupture by film stretching. When emulsions are placed under very high stress acting parallel to the droplet interface, some of the emulsifier molecules may be dragged along the interface leading to bare patches on the droplet surface (emulsifier depleted regions). If the emulsifier depleted regions of two droplets come into close proximity to each other during encounter, they coalesce due to film rupture by the presence of vacancies (McClements, 2004; van Aken, 2004). This mechanism will only be applicable for systems where rate of emulsifier adsorption form the continuous phase is lower than the rate of shear and droplet encounter. Van Aken and coworkers showed coalescence by film stretching due to externally applied force in highly concentrated protein stabilized emulsion (van Aken, 2002). As the highly concentrated droplets are in a deformed state, externally applied stress cannot relax by slip between the droplet surfaces (Figure **2.5)** .

This type of highly concentrated close packed structure can also be created by increasing the osmotic pressure (Bibette, 1992) and freezing the continuous phase of emulsion (Cramp, et al., 2004; Ghosh, et al., 2006a)

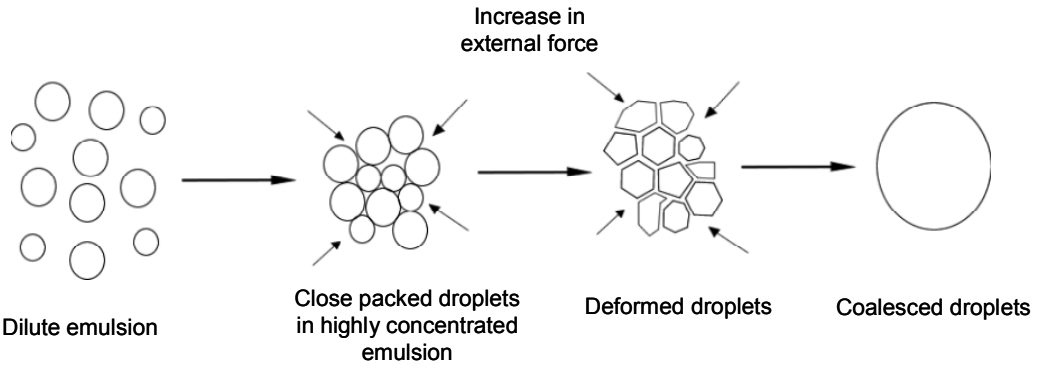

Figure **2.5**: Formation of highly concentrated emulsion – leads to film rupture by application of external force

Experimental determination of coalescence. Coalescence can be determined by measuring or observing the change in droplet size of an emulsion. Optical, confocal or electron microscopes are used to record coalescence in emulsion (McClements, 2004). Coalescence can also be measured indirectly by determining the amount of free oil separated from an oil-in-water emulsion. The amount of free oil can be measured by solvent extraction of emulsion (Ghosh, et al., 2006a) or by adding an oil soluble dye to the emulsion which will be diluted only if free oil is present in the emulsion (Palanuwech, Potineni, Roberts and Coupland, 2003).

2.3 Phase Transitions

A phase transition is the spontaneous conversion of one phase into another (Atkins and Paula, 2006) and in the present work the solid liquid-phase, transition will be reviewed. Formation of a solid phase from liquid is known as crystallization. For

crystallization to be spontaneous, the Gibbs free energy of the solid state must be lower than that of the liquid state. However, a spontaneous transition predicted from thermodynamics can be too slow to achieve in reality and the kinetics of crystallization needs to be taken into account

2.3.1 Phase Diagrams

The phase diagram of a substance shows the regions of pressure, temperature and composition at which various phases are thermodynamically stable (Atkins and Paula, 2006). A phase diagram can be understood in terms of Gibbs phase rule which states that an equilibrium relation between a number of components (*C*) and phases (*P*) depends on the degrees of freedoms available (*F*):

$$F=C-P+2 \tag{2.5}$$

For a one component system, such as oil, $F=3-P$ so if only one phase is present (P=1), F=2 and both pressure and temperature can be varied independently without affecting the number of phases. If $P=2$ two phases are in equilibrium (e.g., solid fat and liquid oil), and according to phase rule, $F=1$, Thus only one variable, pressure or temperature can be specified independently and the other is fixed by the thermodynamic rules. However, if three phases are in equilibrium ($P=3$, e.g., ice, water and steam), F=0, and the system will be invariant and this special condition is defined by a characteristic temperature and pressure for any substance and is represented by a point in the phase diagram (triple point).

For a two component system ($C=2$), $F=4-P$. Thus at constant pressure, the degree of freedom will be $3-P$, which has a maximum value of 2 (for a single phase system). These two remaining degree of freedoms are temperature and composition. As food are often stored and used at normal atmospheric pressure, the most common phase diagram for food systems is temperature – composition map at a constant pressure.

In this thesis, the phase behavior of binary mixtures of water and sugar has been used to study the composition of system under investigation (Appendix C). Phase behavior of mixture of triacylglycerols or complex fats is also important in order to understand properties of different foods containing fats (e.g. chocolates) and has been discussed by several authors (Hartel, 2001; Sato, 1998).

2.3.2 Kinetics of Crystallization

The process of crystallization can be thought of as a four step process: supersaturation, nucleation – the formation of a crystalline phase from supersaturated solution, subsequent growth of nuclei until equilibrium is attained and recrystallization– reorganization of the crystalline structure to a more stable lower energy state. In the following sections the nucleation and growth of crystallization process has been discussed.

2.3.2.1 Nucleation

The various mechanisms of nucleation are shown in Figure **2.6**. Primary nucleation occurs in the absence of crystalline surfaces, whereas secondary nucleation involves active participation of secondary surfaces.

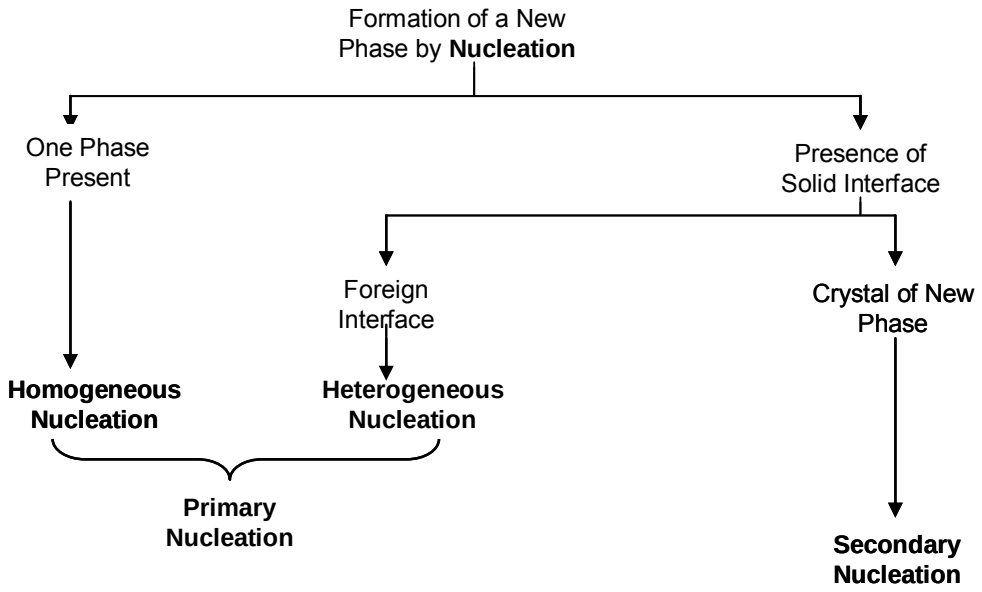

Figure **2.6**: Mechanisms of nucleation

Homogeneous nucleation occurs spontaneously in a pure liquid in the absence of any solid surface. Considerable supercooling is needed for this. When the supercooling is increased, at a specific point nucleation occurs spontaneously (Myerson and Ginde, 2001). The formation of one phase within a second generates an interfacial tension proportional to the area of contact which opposes nucleation while, formation of solid phase liberates an enthalpy of fusion proportional to the volume of the newly formed phase. Thus there is a critical radius for the nucleus (r_c) below which the surface-dependant energy cost dominates and favors nucleus melting and above which the volume-dependent energy released dominates and favors nucleus growth (Hartel, 2001):

$$r_c = \frac{2\sigma_s \nu T_f}{\Delta H_f (T_f - T)} \tag{2.7}$$

where, σ_s is the interfacial tension, ν is the molecular volume, ΔH_f is the latent heat of fusion and T_f is the crystallization temperature of the material and T is the

temperature. Up to this critical radius growth of nucleus does not induce a decrease in free energy, hence the newly formed would be unstable. Only when the radius exceeds the value of critical radius the nucleus would be stable (Rousset, 2002).

The rate of homogeneous nucleation (J, the number of nuclei formed per unit time per unit volume) can be predicted by Fisher-Turnbull equation:

$$J = \frac{NkT}{h}\exp\left(\frac{-\Delta G^*}{kT}\right)\exp\left(\frac{-\Delta G_{visc}}{kT}\right) \qquad (2.8)$$

where the free energy needed to form a nucleus (ΔG^*) and the free energy for molecular diffusion (ΔG_{visc}, the viscous energy term), N is Avogadro's number, k and h are Boltzmann's constant and Planck's constant respectively. At higher supercooling of a melt or supersaturation of a solution, the first term becomes smaller whereas the viscous energy term, ΔG_{visc}, becomes larger and the nucleation rate can decrease.

Classical homogeneous nucleation rarely occurs in real food systems and the presence of foreign nucleating sites, like dissolved impurities, or rough and pitted surface of crystallizer walls, stirrers, and baffles, induces nucleation at much lower supercooling. Nucleation in the presence of a foreign surface or catalytic impurities is called heterogeneous nucleation.

Secondary nucleation occurs near the surface of an already existing crystal of the solute. It is most commonly observed in industrial crystallizers, involving considerable agitation but it can however also occur under quiescent conditions (Walstra, 1998). The phenomenon of secondary nucleation is of considerable practical importance in determining the final size of the crystals obtained. It appears to occur at high supersaturation in systems where crystal growth is slow and has been argued to be especially important in multicomponent triglyceride mixtures (Walstra, Kloek and van Vliet, 2001).

2.3.2.2 Crystal Growth

Once stable nuclei have formed in a supercooled melt, they will continue to grow until the thermodynamic equilibrium between the melt and crystalline state has been attained (Hartel, 2001). The growth of crystals by incorporation of molecules into the lattice structure is a combined process of several steps. First, a molecule must diffuse from the bulk solution to the crystal interface, once it reaches the surface it must orient itself and find an appropriate site for incorporation into the lattice structure. For a slow growth process, incorporation occurs at most energetically favorable site, whereas, rapid growth results in a disorganized less perfect crystal structure. Finally, as a molecule from liquid becomes a part of the crystal lattice, the latent heat of fusion released must be removed from the surrounding area of crystal surface (Hartel, 2001). Any of the above process can be rate limiting in crystal growth. The rate of crystal growth is also influenced by processing parameters like temperature, rate of cooling and agitation.

2.3.3 Fat Crystallization

Natural fats and oils are complex mixtures of triglycerides and because they are a multicomponent system they melt over a range of temperatures rather than at a defined temperature The melting point of a given triglyceride molecule depends on the chain length, degree of unsaturation, the position of fatty acids on the glycerol backbone and the melting range depends on triglyceride composition, for example, cocoa butter, having a very high proportion of few triglycerides, melts quite sharply at mouth temperature.

As triglycerides are large and highly anisometric molecules, they can crystallize in many different conformations which give rise to polymorphism of fat crystals (Sato, 1988; Walstra, 2003b). The most common polymorphic forms of fat crystals are α, β' and β (Larsson, 1966; Sato, 2001). Different polymorphic forms can be characterized by their unique packing arrangement in crystalline solid, for example, the single crystal structure of α, β' and β forms of monoacid triglycerides have been identified as hexagonal,

orthorhombic and triclinic (Nawar, 1996). It was also proposed that while molecular structure of the α form can be described by disordered aliphatic chain conformation, β' and β are distinguished by intermediate packing and most dense packing, respectively. Stability of the polymorphic forms increases in the order: $\alpha < \beta' < \beta$. However, the less stable polymorphs form faster than the more stable polymorphs. The less stable forms transform into more stable forms either by solid-liquid-solid transition or by a solid to solid transition (Hartel, 2001). This complex phase transition in solid fat contributes to the slowness of fat crystallization process and sometimes it takes several months in order to reach a thermodynamically stable state (Hartel, 2001; Walstra, 2003b).

2.3.4 Fat Crystallization in Emulsions

Fat crystallization in emulsified droplets can be very different from crystallization in the bulk phase (Dickinson and McClements, 1995). Both mechanism of crystallization and structure of fat crystals is significantly influenced by emulsification.

In an oil-in-water emulsion, the dispersed phase is divided into a number of droplets of varying size. The impurities that catalyze heterogeneous nucleation in bulk oil have are isolated in a few droplets so that considerable supercooling is required in order to form solid nuclei in the vast majority of the droplets (Samis and Sato, 2002) and hence crystallization occurs through an apparently homogeneous mechanism (Coupland, 2002; Skoda and van den Tempel, 1963; Walstra and van Beresteyn, 1975). Homogeneous nucleation should only be possible if the number of impurities is much less than the number of droplets and so the importance of a homogeneous vs. a heterogeneous mechanism would depend on both the purity and source of the oil as well as the size of the droplets (Coupland, 2002).

For a nucleation to be genuinely homogeneous, the degree of supercooling should be independent of type of emulsifier used but this is not always the case suggesting the

interface itself may play a catalytic role (McClements, Dungan, German, Simoneau and Kinsella, 1993). If the hydrophobic portion of the emulsifier has a similar molecular structure as that of the triglyceride fatty acid hydrocarbon chain it can induce crystallization in oil droplet and hence increase the rate of nucleation. This type of nucleation assisted by interfacial surfactant is known as surface heterogeneous nucleation (McClements, et al., 1993; Skoda and van den Tempel, 1963; Walstra and van Beresteyn, 1975).

If an emulsion contains both solid and liquid droplets, solid droplets can induce crystallization in liquid droplets upon collision leading to interdroplet heterogeneous nucleation (Dickinson, Kruizenga and Povey, 1993; Dickinson and Povey, 1996; Hindle, Povey and Smith, 2000; McClements, Han and Dungan, 1994).

The structure of fat crystals formed in emulsified droplets is affected by the physical constraints of the droplet surface (Hindle, et al., 2000) which tend to deform the less stable and loosely packed crystal polymorphs more readily than the more stable polymorphic forms (Coupland, 2002). The polymorphic form of crystallized emulsified lipid can be controlled by adding several types of hydrophobic surfactant (Sonoda, Takata, Ueno and Sato, 2006; Ueno, Hamada and Sato, 2003). Bunjes and Koch (Bunjes and Koch, 2005) showed that by using saturated phospholipid emulsifier, the stability of metastable α form of tristearin in an emulsion could be increased.

2.3.4.1 Partial Coalescence

Most real food oils, notably milk fat, are semicrystalline over a wide temperature range. Collision between semisolid droplets in an emulsion can also promote destabilization via partial coalescence, in which a fat crystal from one droplet penetrates the lamella separating two colliding droplets (Rousseau, 2000b; Walstra, 1996b) (Figure **2.7**). As the crystal is wetted better by the oil than by water, the residual liquid oil flows out to reinforce the linkage point between them. With time, the droplets fuse more

closely to reduce the total surface area of the oil exposed to aqueous phase, but the irregular shape of the partially coalesced droplets is maintained by the mechanical strength of the fat crystal network. Upon heating of this emulsion the fat crystal network melts, allowing full coalescence. Partial coalescence is important in the processing of ice cream and butter where it is responsible for supporting the air cell structure and phase inversion, respectively.

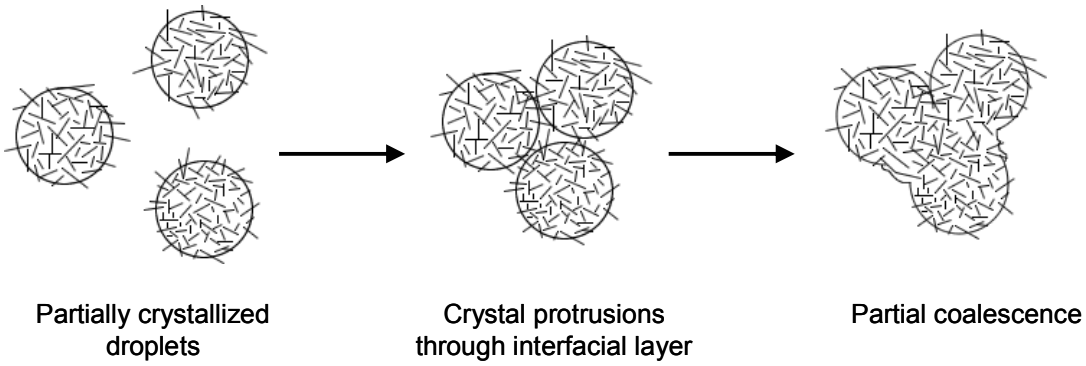

Figure **2.7**: Schematic diagram of partial coalescence

2.4 Flavor Release from Emulsions

The chemical cascade that leads to the cognitive response of flavor begins with the release of stimulating molecules from the food. Before and during consumption, the released flavor and aroma molecules interact with receptors in the mouth and nose (Figure **2.8**) (Keast, Dalton and Breslin, 2004). Different types of stimuli give rise to different classes of chemical stimulation: taste, aroma, and somestheis. Taste is generally regarded as limited to sweet, sour, bitter, salty and umami, while the list of stimuli for aroma perception is virtually unlimited. Chemical, mechanical, and thermal stimuli gives rise to somatosensory sensation that are detected in the mouth and nose and transmitted to the brain along the trigeminal, glosso, and thmoid nerves. The integration of these stimuli in the brain gives rise to the sensation of flavor (Laing and Jinks, 1996). In some cases, our appreciation of flavor is also affected by the sounds released as it is eaten (i.e., mechanical properties) as well as its visual appearance.

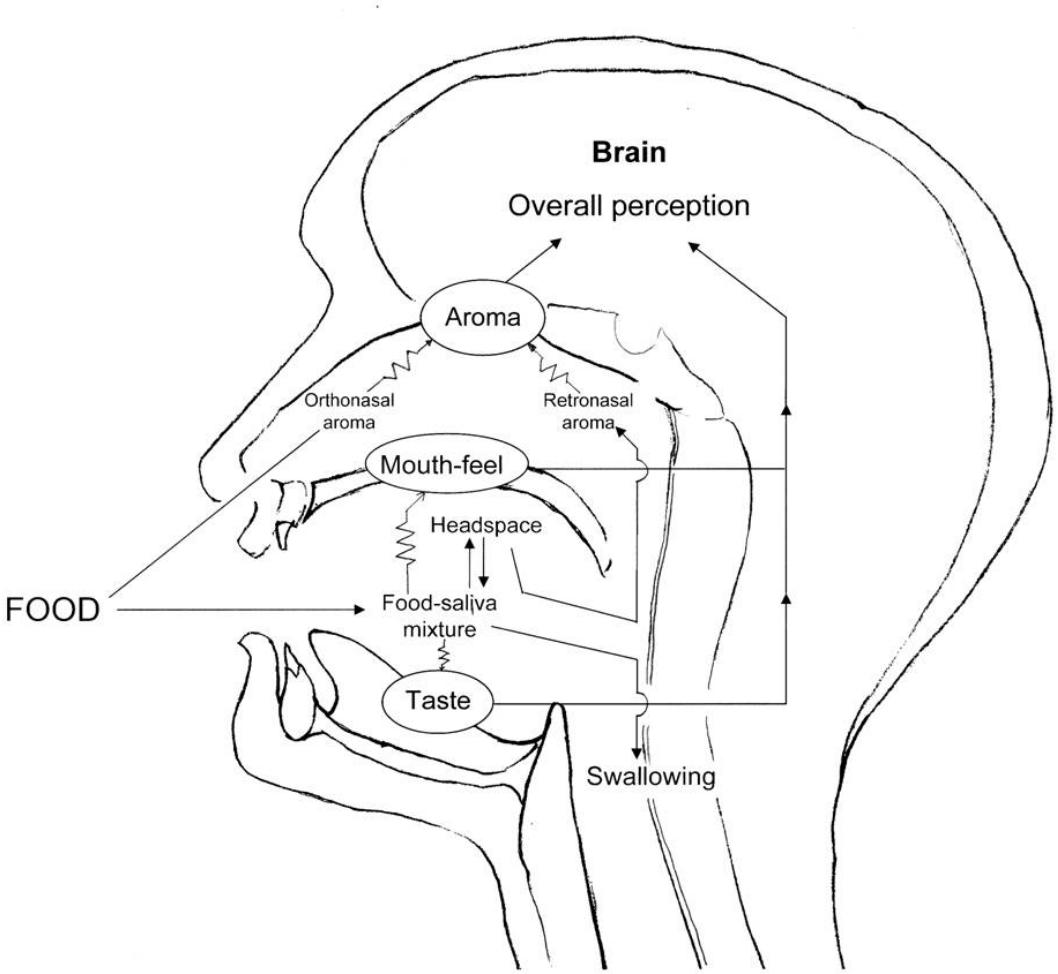

Figure **2.8**: Air flow in mouth and sites of flavor stimulation and perception (adapted with modifications from Taylor, 1996)

In summary, perception of food occurs at brain. The physiology, anatomy and neurochemistry of the signal transduction to the relevant portions of the brain are complex, and in many ways not a "food science" problem. Furthermore the identification, formation, and structure of the various molecules in foods that can stimulate a flavor response are not the foci of this work. Instead, we will address the question of how food structure controls the release of these molecules and hence their availability to the receptor cells located in the olfactory epithelium. If the flavor molecules are bound tightly to the food so they are unavailable to the nerves in the mouth and nose, then their presence will not be perceived. The gustatory and olfactory receptors are located in the mouth and nasal cavity, respectively (Figure **2.8**; note that gasses can pass from the mouth to the nose either outside the body or through the nasopharynyx), so we will be concerned with understanding the release of molecules from the food into saliva and the headspace of the orthonasal cavity.

We will begin with a thermodynamic treatment of binding before moving on to models of the kinetics of release and methods for experimental validation. The bulk of this work will address aroma release from emulsions. Emulsions are attractive candidates to model microstructural effects, because they are found in many foods and can be manufactured precisely and characterized thoroughly enough to allow reliable modeling.

2.4.1 Thermodynamics of Flavor Interactions

Flavor molecules will distribute themselves within a system so that their chemical potential is the same in all phases in which they occur. Chemical potential is a function of the affinity of a molecule for that phase so the equilibrium concentration in different phases will frequently be different. The partitioning of aroma compounds between two phases can be described as the ratio of activities of the compound in two different phases or, as the concentration of aroma molecules is typically very low, the ratio of concentrations. This is particularly important for the sense of smell as aroma perception occurs in the nose, and only those molecules in the headspace phase can be smelled while

those trapped in the food will not. The partition coefficient between a food and headspace gas, K_{gp}, is given by

$$K_{gp} = \frac{c_g}{c_p} \tag{2.12}$$

where, c_g and c_p are the concentrations in the headspace and food product phases respectively. Equation 2.12 represents the thermodynamics of flavor binding and a food with a high affinity for the flavor will have a lower K_{gp}, and consequently fewer aroma molecules available to be smelled.

The partitioning of organic compounds between air and water was measured as early as in 1935 when Butler, Ramachandani and Thomson (1935) studied the release of homologous series of organic alcohols (methanol to octanol) from aqueous solutions. Pierotti, Deal and Derr (1959) predicted the increase in volatility with molecular weight for dilute aqueous solutions of homologous series of several compounds including n-acids, alcohols, ketones, ethers and paraffins. Similarly, Buttery and coworkers (Buttery, Bomben, Guadagni and Ling, 1971; Buttery, Ling and Guadagni, 1969) measured the partition coefficients of homologous series of aldehydes, ketones, esters and alcohols in water solutions. The effect of temperature on K_{gp}, is described by the Clausius-Claperyon relationship (i.e., a logarithmic relationship between air-medium partition coefficient and temperature) (Meynier, Garillon, Lethuaut and Genot, 2003).

Partition coefficients can be measured by determining the concentration of volatiles in a closed headspace above a solution. For example, Ghosh, Peterson and Coupland (2006b) measured the headspace concentration of a series of ethyl esters in equilibrium with water. The partition coefficients were determined from the rate of increase in headspace concentration with increased concentration in the solution (Figure **2.9**). In the absence of experimental data it is possible to use chemometrics to calculate the partition coefficient from the chemical structure of the aroma molecule. Carey, Asquith, Linforth and Taylor (2002) used quantitative structure property

relationships (QSPR) to relate the partition coefficient to the physical and chemical properties of the aroma compounds. The model was developed based on experimentally determined partition coefficient and computer software calculated numerous different physiochemical terms of 39 aroma compounds. From this only the significant descriptors of partitioning behavior were utilized to build the model using a multilinear regression method. This model was tested with another 28 different aroma compounds and a good prediction of experimental results were obtained (R^2=0.83) (Carey, et al., 2002).

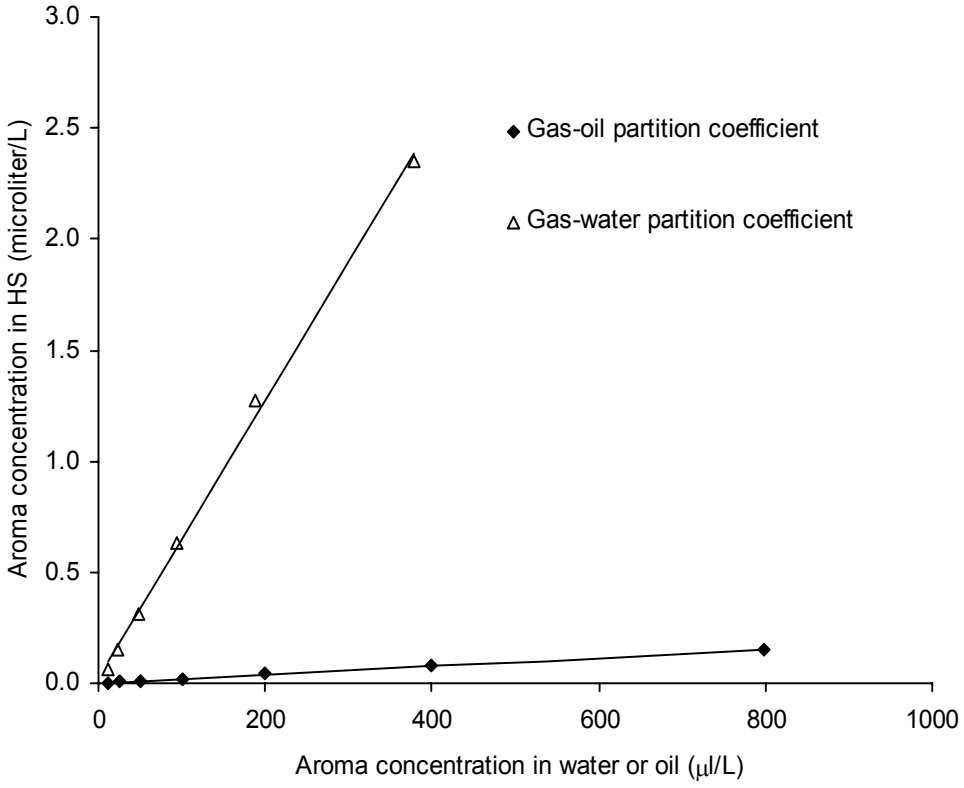

Figure **2.9**: Determination of gas-oil and gas-water partition coefficient for ethyl butanoate

A solvent with a greater affinity for the aroma molecule will tend to depress its volatility. As many aroma molecules are non-polar, their headspace concentrations will be lower over fatty foods. For example in Figure **2.9**, the headspace concentration of ethyl butanoate above oil and water is compared as a function of solution concentration. Although the headspace concentration increases linearly in both cases, there is always less present above the oil as ethyl butanoate is relatively non-polar. Some gas-oil partition coefficients are shown in Table **2.1** for comparison with the gas-water data for the same molecules. Most foods contain a mixture of oil and water and in these cases the aroma molecules will partition between both of these phases as well as with the vapor phase. Buttery, Guadagni and Ling (1973) took a simple approach to this problem and modeled the partitioning of a series of aroma molecules with a mass balance Equation:

Table **2.1**: Comparison of air-water (K_{gw}) and air-oil (K_{go}) partition coefficients ($\times 10^{-3}$) of aroma compounds

Compound		K_{gw}	K_{go}	**Temperature**
Butanal	Buttery et al. 1969, 1973	4.7	2.3	25ºC
Pentanal		6.0	1.0	
Hexanal		8.7	0.35	
Heptanal		11	0.1	
Octanal		21	0.04	
Butan-2-one	Buttery et al. 1969, 1973	1.9	1.9	25ºC
Heptan-2-one		5.9	0.1	
Isoamyl acetate	Meynier et al. 2003	4.5	0.057	30ºC
Amyl acetate		3.0	0.014	
Ethyl butanoate	Ghosh et al. 2006	7.35	0.2	30ºC
Ethyl pentanoate		9.02	0.07	
Ethyl heptanoate		18.2	0.006	
Ethyl octanoate		26.7	0.002	

$$\frac{1}{K_{ge}} = \frac{\phi_o}{K_{go}} + \frac{\phi_w}{K_{gw}} \qquad \text{or} \qquad K_{ge} = \frac{K_{gw}}{1 + (K_{ow} - 1)\phi} \tag{2.13}$$

where K_{ge} is the overall gas-emulsion partition coefficient and ϕ_o, ϕ_w are the volume fraction of lipid phase and aqueous phase in the mixture and K_{go}, K_{gw}, K_{ow} are the gas-oil, gas-water and oil-water partition coefficients respectively. Ghosh, Peterson and Coupland (2006b) successfully used Equation 2.13 to predict gas-emulsion partition coefficients values of a series of fatty acids ethyl esters (ethyl butyrate, ethyl pentanoate, ethyl heptanoate and ethyl octanoate) from oil-in-water emulsions (Figure **2.10**). Similarly, Roberts, Pollein and Watzke (2003) used a modified form of Equation 2.13 (i.e., expressing the aroma release from emulsion relative to the release of the compound at the same concentration in water) to model the effect of lipid content on the release of 10 volatile compounds from milk based emulsions. Importantly, Equation 2.13 is a function in system composition (ϕ) but not microstructure, so we would expect to see any effects of system microstructure as deviation from the model. For example, the Buttery model gave a good prediction of the headspace concentrations of one volatile molecule added to milk (ethyl pentanoate) but not for others (amyl acetate, isoamyl acetate, hexanal and t-2-hexenal) (Meynier, et al., 2003). Similarly Harrison, Hills, Bakker and Clothier (1997) showed that while Equation 2.13 gave a good description of the headspace diacetyl concentration in equilibrium with an oil-water mixture, it was not reliable when the oil and water were emulsified (with a sugar ester surfactant).

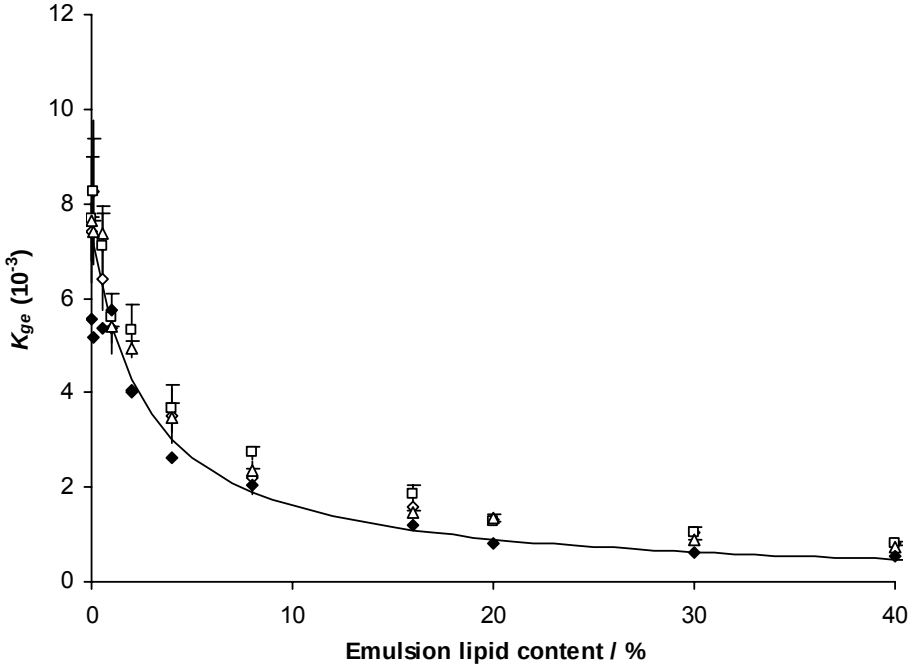

Figure **2.10**: Gas-emulsion partition coefficient of ethyl butanoate as function of emulsion lipid content. Results for emulsions with different particle sizes (d_{32}) 0.97 μm (□), 0.44 □m (♦) and 0.28 □m (Δ) are shown along with bulk lipid and water mixture (■). Predicted line (from Equation 2.13) is shown alongside the experimental data points.

One consequence of changing structure not considered in the Buttery model is the increase in interfacial area with a decrease in particle size. The chemical environment at the interface is distinct from both the oil and the water phases having a higher concentration of surfactant molecules as well as being particularly attractive for amphiphilic aroma molecules. The relative importance of surface binding can vary widely depending on the interactions between the volatile molecules and the surfactant. For example Landy and co-workers (Landy, Courthaudon, Dubois and Voilley, 1996) reported no change in volatility of ethyl hexanoate upon emulsification and regardless of the surfactant used (sodium caseinate or sucrose stearate) but a large change in air-sample partition coefficient of 2-nonanone after emulsification with sodium caseinate (Voilley, Espinosa Diaz and Landy, 2000). Guyot, Bonnafont, Lesschaeve, Issanchou, Voilley and Spinnler (1996) showed a decrease in air-emulsion partition coefficient for butyric acid due to interfacial binding by the emulsifier (sucrose stearate-palmitate ester) but no such change in volatility for δ-decalactone and diacetyl. In some cases the surface binding may result from a chemical reaction between the volatile and interfacial protein. For example, Meynier, Rampon, Dalgalarrondo and Genot (2004) showed that aldehydes such as hexanal and t-2-hexenal react with certain amino acids of whey protein and sodium caseinate forming covalent bond between the aroma compound and the protein. This might be the explanation of the observation by Meynier, Garillon, Lethuaut and Genot (2003) and Voilley, Espinosa Diaz and Landy (2000) that some volatile molecules are specifically bound by proteins at the interface.

The interface can be introduced as a third phase within Buttery's model:

$$\frac{1}{K_{ge}} = \frac{\phi_o}{K_{go}} + \frac{\phi_w}{K_{gw}} + \frac{\phi_i}{K_{gi}} \qquad (2.14)$$

where K_{gi} is the gas-interface partition coefficient defined as the ratio of concentration of aroma compound in the headspace to that at the interface (McClements, 2004). However, because it is difficult to measure the value of K_{gi} and interfacial

properties are better expressed in terms of area, the last term in Equation 2.14 can be rewritten as follows:

$$\frac{1}{K_{ge}} = \frac{\phi_o}{K_{go}} + \frac{\phi_w}{K_{gw}} + \frac{A_s K_{iw}^*}{K_{gw}} \tag{2.15}$$

where A_s is the interfacial area per unit volume of an emulsion and K_{iw}^* is the apparent surface binding coefficient (= Γ_i / c_w, Γ_i is the surface load of aroma compound i.e. the volume of aroma compound adsorbed per unit interfacial area and c_w is the aroma concentration in the aqueous phase). The effect of emulsion particle size on the gas-emulsion partition coefficient has been compared in Figure **2.11** using both the Buttery model (Equation 2.13) and the reversible surface binding model (Equation 2.15). The Buttery model is particle size independent, but according to Equation 2.15 the effective partition coefficient decreases with decreasing particle size. For large droplets (A_s tends to zero) Equation 2.15 reduces to Equation 2.13. It should be noted that this approach assumes that the emulsifier in the continuous phase does not influence the partitioning behavior.

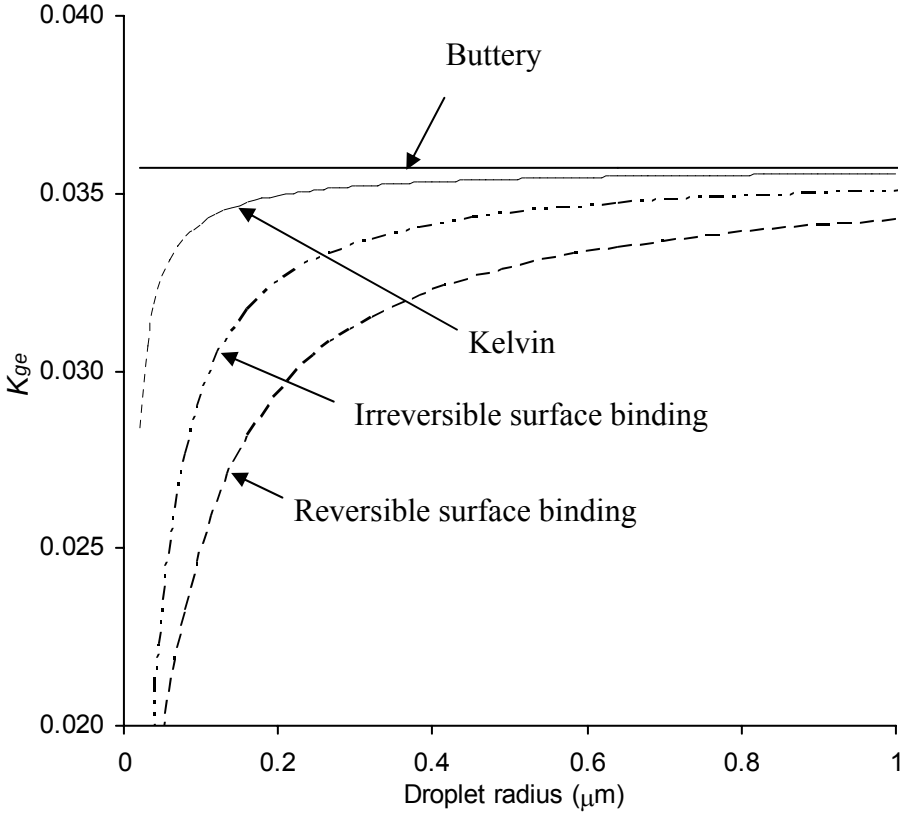

Figure **2.11**: Influence of droplet size on the gas-emulsion partition coefficient of aroma compound according to different models: volume partitioning Buttery Model (Equation 2.13); reversible surface binding model (Equation 2.17); irreversible surface binding model (Equation 2.15); and Kelvin model (Equation 2.19). The system under consideration consists of a 20 cm^3 closed vial containing 2 cm^3 of a 20% oil content emulsion. The emulsion was assumed to contain 200μl/L of a hypothetical aroma compound (K_{go} = 0.01, K_{gw} = 0.1 and K_{iw}^{*} = 10^{-7}). It was also assumed that the aroma compound can only partitioned into the dispersed lipid phase, aqueous phase, interphase and gas phase.

In Chapter 3 Equation 2.15 has been used to model equilibrium flavor distribution from solid emulsion droplets by assuming no interaction between the aroma and the crystalline droplet phase (i.e., K_{ow}=0). However, to our knowledge, this Equation has not yet been used in practice to model surface aroma binding in liquid emulsion droplets. One reason for this could be that unless the experimental conditions are carefully selected, the large affinity of many aroma molecules for the liquid oil phase can readily obfuscate the relatively minor effects of surface binding.

Equation 2.15 is applicable to reversible partitioning of aroma compounds to the interface. However, if the aroma compounds form irreversible covalent bonds with the adsorbed emulsifiers at the interface (as in the case of hexanal and t-2-hexenal with milk proteins) (Meynier, et al., 2004) volatile partitioning into the headspace would only be affected by the amount of free aroma compounds in the emulsion. McClements (McClements, 2004) used an effective gas-emulsion partition coefficient, $K^e_{ge} = c_g / c_e$, as the ratio of concentration of aroma compounds in headspace to the total amount of aroma (both free and bound) present in the emulsion (c_e). The actual gas-emulsion partition coefficient from the Buttery model (Equation 2.13) can thus be expressed as:

$$K_{ge} = \frac{c_g}{c_{e,free}} = \frac{K^{\mathrm{e}}_{\mathrm{ge}} c_e}{c_e - A_s \Gamma_i} \tag{2.16}$$

where $c_{e,free}$ is the concentration of free aroma in the emulsion which is equal to the total amount of aroma minus the aroma bound to the interface and Γ_i is the amount of aroma irreversibly bound to the interface per unit interfacial area. Replacing the value of K_{ge} from the Buttery model (Equation 2.13) Equation 2.16 can be written as:

$$\frac{1}{K^{\mathrm{e}}_{\mathrm{ge}}} = \left(\frac{c_e}{c_e - A_s \Gamma_i} \right) \left(\frac{\phi_o}{K_{go}} + \frac{\phi_w}{K_{gw}} \right) \tag{2.17}$$

If the flavor does not interact with the interface (i.e. Γ_i is negligible) then Equation 2.17 reduces to the original Buttery Equation (Equation 2.13). Predictions from Equation

2.17 are plotted in Figure **2.11** alongside the Buttery model (Equation 2.13) and reversible surface binding model (Equation 2.15). For both binding models, as the particle size increases, the interfacial area decreases and the partition coefficient tends towards that predicted by the Buttery model. Other volatile molecules with stronger affinities for the interface would show a greater deviation form the Buttery model.

A second potential consequence of reduced particle size is an increase in surface curvature which increases the internal pressure and solubility of materials in the droplets as expressed in the Kelvin equation (Walstra, 2003a):

$$s_r = s_\infty \exp(X / r) \tag{2.18}$$

where, s_r is the solubility in sphere of radius r and s_∞ is the solubility in the absence of curvature ($r = \infty$). $X = \frac{2\gamma V_D}{RT}$ where, γ is the surface tension, V_D molar volume of the dispersed phase, R is the universal gas constant and T is the temperature. If we consider the solubility as the concentration of volatile compounds in the respective phases, then the above equation can be written as:

$$K_{ow(r)} = K_{ow} \exp(X / r) \tag{2.19}$$

where, $K_{ow(r)}$ is the partition coefficient of the volatile compound in the dispersed phase droplets. Partitioning typically increases with solubility so the affinity of volatile molecules should be greater for smaller droplets and consequently the headspace concentration depressed from the bulk value predicted from Buttery's model. This can be seen in Figure **2.11** where $K_{ow(r)}$ values predicted by the Kelvin Equation were used to calculate gas –emulsion partition coefficients from Buttery model (Equation 2.13). As the particle size decreases the solubility of the aroma compounds would be greater in the droplets and hence a decrease in the K_{ge} values. However, for larger droplets the Kelvin model once more approximates to the Buttery model. Of course, the actual range of sizes

over which surface curvature effects may be important depend on the interfacial tension and molar volume of the solute.

During consumption, the volumes of the different phases in the system will change as, for example, packages are opened, air is drawn over the surface of food during sniffing, and saliva is mixed with food. The effect of changing volumes can be readily incorporated into the equilibria models, however it should be stressed that these are still describing the new equilibria formed and not the time taken to readjust. Thermodynamics is useful to tell us the direction in which molecules will move, but not the timescale it will take them to get there. It is probably reasonable to assume that in a sealed package, the aroma molecules will reach some equilibrium so, for example, the smell of a freshly opened package of coffee would be stronger if the coffee solids had lower affinity for the volatile molecules. However, once the package is opened, the equilibrium is disrupted and the distribution of volatile molecules will become a mass transfer problem.

2.4.2 Kinetics of Flavor Release

During most of the interactions with food that lead to sensation, the aroma molecules are not at equilibrium, and their distribution will change with time. For example, when a morsel of food is placed in the mouth, a saliva phase is introduced and mixed with the food as it is chewed, changing the affinity of the food for the aroma molecules and hence their partitioning behavior. Furthermore, the headspace above the emulsion is periodically being refreshed with incoming air as a result of breathing which will further dilute the volatile concentration and cause more mass transfer. Finally the food is being removed from the mouth periodically due to swallowing. Clearly, the concentration of volatile molecules reaching the aroma sensitive receptors in the nose will change over time depending on both the thermodynamics of binding and on the barriers to mass transport (de Roos, 2005). The rate of mass transfer is given by Fick's first law as the product of concentration gradient and a mass transfer coefficient. The

thermodynamic models give an indication of the driving force for mass transfer and the mass transfer coefficient describes the ability of the volatile to move through the food and is a function of microstructure.

A path taken by a volatile molecule moving from an oil droplet in a food emulsion to the headspace gas is shown schematically in Figure **2.12**. The overall rate could be limited by (i) movement in the oil phase, (ii) movement across the oil-water interface, (iii) movement in the aqueous phase (possibly affected by aqueous solutes including viscous biopolymers), or (iv) movement across the food-air interface. Which of the various microstructures are most important in the overall release kinetics depends on which is rate limiting and various theories have been developed to satisfy different assumptions (de Roos, 2000). In this section we will consider first models for release into saliva and second release into the headspace above foods. In both cases we will use a simple oil-in-water emulsion as our model for food structure.

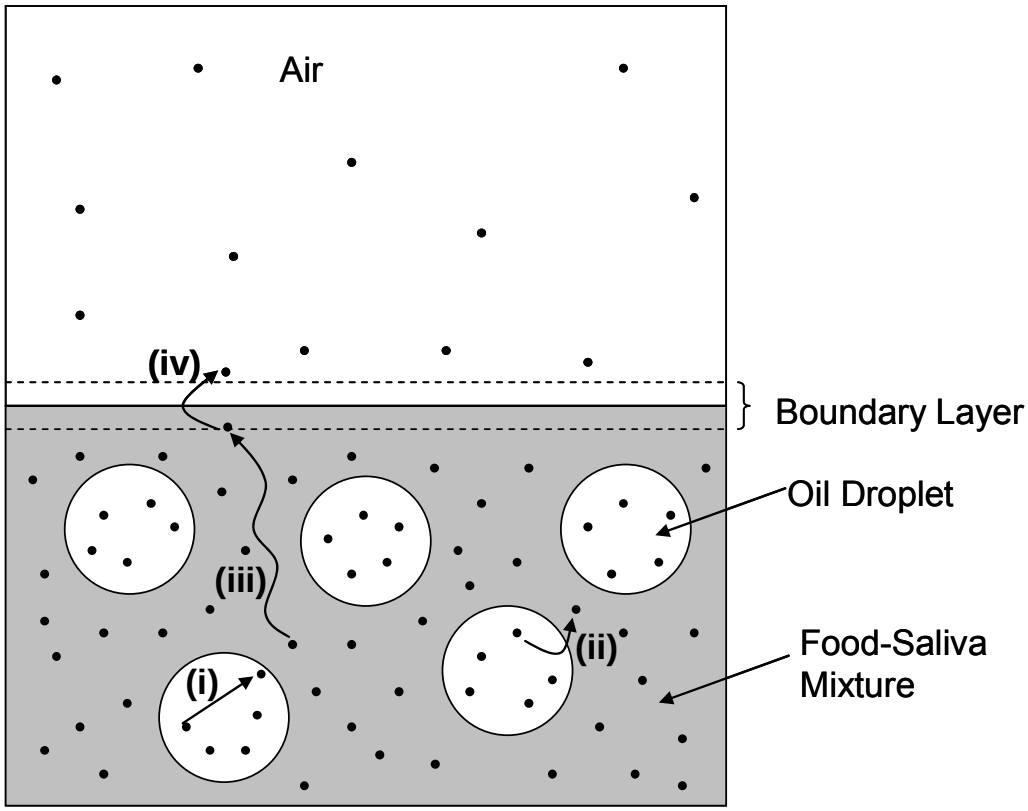

Figure **2.12**: Schematic diagram showing potential rate limiting steps that may affect the kinetics of aroma release from a food to the surrounding headspace. Black points represent aroma molecules.

2.4.2.1 Release into the Saliva

To be released from a food emulsion into the saliva, molecules must diffuse from the oil and through the aqueous phase. For our purposes, we will consider each of these in turn as the rate limiting step and model the kinetics using the Crank and Sherwood equations respectively. The Crank model assumes that the rate limiting step is the diffusion of a solute through the spherical particles surrounded by an infinite volume of a well mixed liquid (Crank, 1975). The release of non-polar molecules (K_{ow}>>1) from an oil-in-water emulsion can be described using a simplified form of the Crank model (Lian, 2000; McClements, 2004):

$$\frac{M_t}{M_0} = 1 - \exp\left[-\frac{1.2 D_o \pi^2}{K_{ow} r^2} t\right] \tag{2.20}$$

where M_o is the initial total amount of flavor compound present in the droplets and M_t is the amount diffused out of the oil droplets in time t. D_o is the diffusion coefficient of the aroma compound in the oil droplets, K_{ow} is the partition coefficient between the oil droplets and the aqueous phase, and r is the radius of the droplets. The kinetics of flavor release can be conveniently expressed as the time required for half of the total flavor to diffuse out of the droplets ($t_{1/2}$) (Lian, 2000):

$$t_{1/2} = 0.0586 \frac{K_{ow} r^2}{D_o} \tag{2.21}$$

It can be seen from Equation (2.21) that flavor release for relatively nonpolar compounds (K_{ow}>>1) from large droplets would be quite slow and hence the rate limiting process. However, for polar compounds (K_{ow}≤1) flavor release from smaller droplets would be extremely fast and hence it would not be a rate limiting process (McClements, 2004). Also the time for diffusion increases with the square of droplet radius so for micron-size oil droplets is likely to be very fast. For example, Wedzicha and Couet

(1996) used benzoic acid as a model compound and showed the kinetics of diffusion from fine (average d_{32}= 0.42 μm) droplets to the aqueous phase is extremely fast (on millisecond time scale) and unlikely to be rate limiting.

The alternative limitation to diffusion kinetics is in the bulk phase, and in this case the kinetics of flavor release rate can be expressed as (Lian, 2000):

$$\frac{M_t}{M_0} = 1 - \exp\left[-\frac{3ShD_w\pi^2}{2K_{ow}r^2}t\right] \tag{2.22}$$

where D_w is the diffusion coefficient of the aroma compound in the aqueous phase and *Sh* is the Sherwood number which is a dimensionless parameter depicting the ratio of total convective mass transport to the molecular diffusive mass transport and is a function of droplet size, density, viscosity and velocity of droplets in the medium. Note the similarities between the forms of Equations 2.20 and 2.22; they differ in that the diffusion coefficients refer to the oil and aqueous phase, respectively while the Sherwood number is introduced in the latter to model the effects of convection in the continuous phase. Mass transport within small droplets is assumed to be purely molecular diffusion unaided by convection currents and unaffected by mixing the emulsion.

The Crank (Equation 2.20, rate limited by movement in the droplets) and Sherwood (Equation 2.22, i.e., rate limited by movement in the continuous phase) have been combined in a more general model by Lian (2000) considering resistance to mass transfer in *both* locations. For flavor release from an oil-in-water emulsion the combined mass transfer equation would be:

$$\frac{M_t}{M_0} = 1 - \exp\left[-\frac{3h_oh_w}{r(h_w + K_{ow}h_o)}t\right] \tag{2.23}$$

where h_o and h_w are the individual mass transfer coefficients in the oil droplets and aqueous phase respectively and expressed as: $h_o = 3.94\frac{D_o}{rK_{ow}}$, $h_w = 0.5\frac{ShD_w}{r}$. The half time of flavor release can be shown to be:

$$t_{1/2} = 0.231 \cdot \left(\frac{0.254K_{ow}}{D_o} + \frac{2K_{ow}}{ShD_w} \right) r^2 \qquad (2.24)$$

The general model also predicts that the time required for flavor release increases with droplet diameter. If $D_o<ShD_w$ then diffusion in the oil droplet will dominate the kinetics of release and Equation 2.24 will reduce to the Crank model. Conversely if $D_o>ShD_w$ then diffusion in the continuous phase is rate limiting and Equation 2.24 reduces to the Sherwood model. According to the Stokes-Einstein relation, the diffusion coefficient is inversely proportional to solvent viscosity so we might expect for a given molecule D_o to be about an order of magnitude or so less than D_w and hence move more slowly within the droplet. This effect is counteracted by the effect of natural convection or stirring in the continuous phase which will increase Sh and hence the rate of mass transport in the continuous phase.

2.4.2.2 Release into the Headspace

The kinetics of release into saliva may be the appropriate model for the effects of food microstructure on taste perception but aroma molecules must be released into the headspace. Harrison and coworkers (Harrison and Hills, 1997a; 1997b; Harrison, et al., 1997) developed a model for mass transport from a well-mixed food into a well-mixed gas using penetration theory (Coulson and Richardson, 1993). In this model, mass transfer from the emulsion takes place when a volume element of the stirred liquid is brought to the interface with the gas for a finite period of time during which volatiles can move into the gas phase by molecular diffusion (Coulson and Richardson, 1993) (Figure **2.13**). Subsequently the volume element is again mixed with the rest of the bulk

phase and the process repeated. According to this theory the aroma concentration in a well-mixed gas phase above an emulsion is given by (Harrison, et al., 1997):

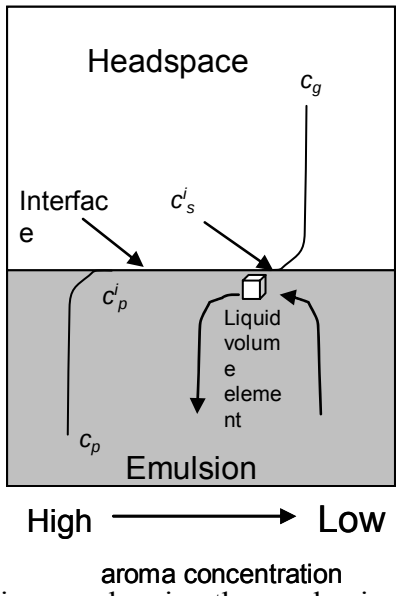

Figure **2.13**: Schematic diagram showing the mechanism for mass transfer in penetration theory (Harrison, Hills, Bakker and Clothier, 1997)

$$c_g(t) = \frac{K_{ge}c_e(0)}{\left(\frac{K_{ge}v_g}{v_e}+1\right)}\left[1-\exp\left\{-\left(\frac{v_e}{K_{ge}v_g}+1\right)\frac{Ah_d}{v_e}t\right\}\right] \qquad (2.25)$$

where h_d is the emulsion-gas interfacial mass transfer coefficient, A is the area of the emulsion-gas interface. $c_e(0)$ is the initial flavor concentration in emulsion, and v_g and v_e are the volume of gas phase and the emulsion phase respectively. The equilibrium gas phase aroma concentration is given by the first term on the right hand side of Equation 2.25 while the term in parentheses describes the kinetics of mass transport. The rate of release decreases with time before tending to zero at an equilibrium concentration affected by the oil concentration in an emulsion, Figure **2.14**). The initial rate can be calculated by expanding the exponential term in Equation 2.25 as a Taylor series and discarding the higher-order terms:

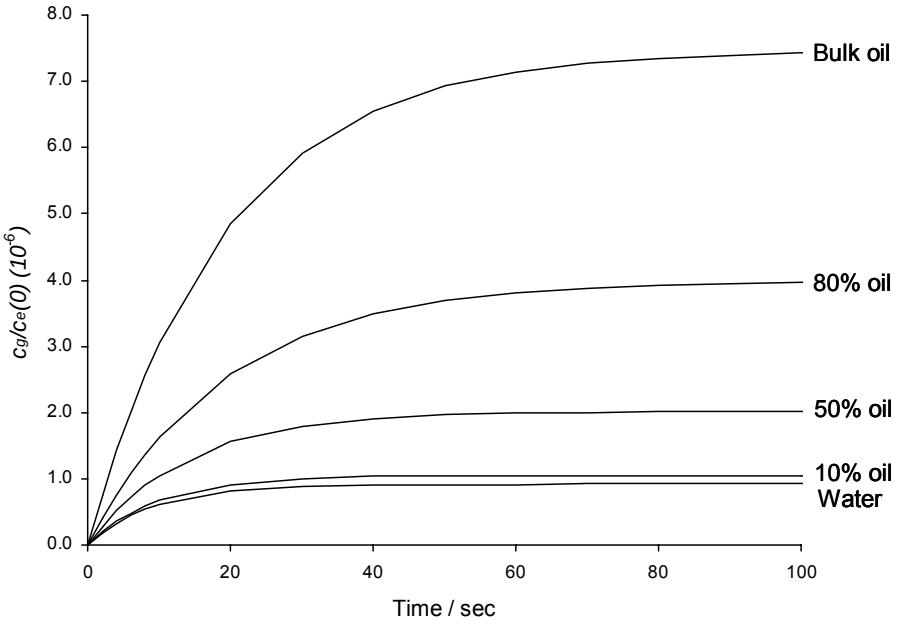

Figure **2.14**: Effect of emulsion oil content on the rate of flavor release according to Equation 2.25. Lines for water, emulsion with 10% oil, 50% oil, 80% oil, and bulk oil are shown for an aroma compound with K_{gw}=3X10^{-4} and K_{go}=9X10^{-4}. The emulsion-gas interfacial mass transfer coefficient was assumed to be 5X10^{-7}m s^{-1}. The gas-emulsion partition coefficient was calculated using the Buttery model (Equation 2.13).

$$c_g(t) = c_e(0)\frac{Ah_d}{v_g}t \tag{2.26}$$

Importantly, Equation 2.26 predicts that at short times, the headspace aroma concentration depends on the mass transfer coefficient and interfacial surface area but not the thermodynamic partition coefficient. This finding is striking, as it suggests that in short timescales, possibly similar to those during eating, the thermodynamic arguments developed in the Buttery model (Equation 2.13) may not be relevant in determining the concentration of volatiles available to the nose.

The emulsion-gas interfacial mass transfer coefficient h_d was calculated by Harrison and others by fitting experimental release kinetics from a variety of emulsions

with Equation 2.25, and then empirically modeled it as a function of droplet diameter and dispersed phase volume fraction (Harrison, et al., 1997):

$$h_d = h_w \exp\left(-3.13\times10^{-6}\,\frac{\phi}{d}\right) \tag{2.27}$$

where h_w is the mass transfer coefficient of the aroma compound in water. The mass transfer coefficient in an emulsion decreases with oil volume fraction and increases with droplet diameter (Figure **2.15**).

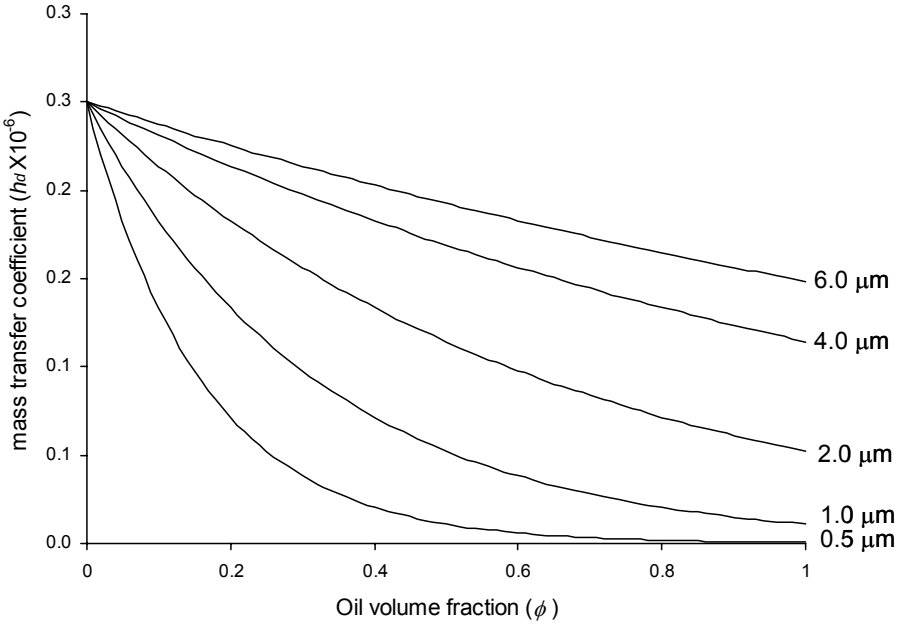

Figure **2.15**: Effect of oil concentration and droplet size on the mass transfer coefficient of a model aroma compound (mass transfer coefficient in water = 2.5X10^{-7}m s^{-1}) in an emulsion. Lines calculated using Equation 2.28 for a model aroma compound with a mass transfer coefficient in water as 2.5X10^{-7}m s^{-1}.

Harrison and coworkers (Harrison, 1998; Harrison and Hills, 1997a) subsequently expanded the model to account for some of the physiological processes of eating. For example, Harrison (1998) showed that saliva flow can affect release kinetics by diluting the lipid fraction and reducing the viscosity of the aqueous phase. The volume fraction of the emulsion was assumed to decrease exponentially with time due to saliva flow:

$$\phi(t) = \phi(0)\exp\left(-\frac{qt}{v_e}\right) \tag{2.28}$$

where $\phi(0)$ is the initial oil volume fraction of the emulsion, q is the saliva flow rate, and v_e is the volume of the emulsion in the mouth. As the oil content of the emulsion is decreasing, it will reduce the mass transfer coefficient of the aroma compounds (Figure **2.16**).

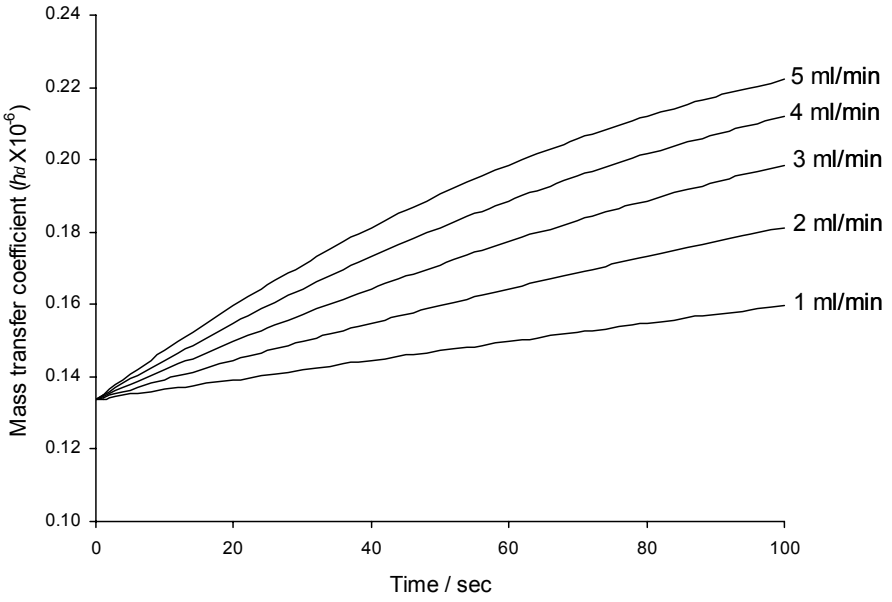

Figure **2.16**: Effect of saliva flow rate on the emulsion-gas interfacial mass transfer coefficient of a model aroma compound from an o/w emulsion (ϕ=0.2, d=1 μm) (calculated using Equations 16 and 17). The mass transfer coefficient of the same model compound in water was taken as 2.5X10-7m s^{-1}

Another model for the kinetics of release of volatile molecules into the headspace was developed recently by Lian, Malone, Homan and Norton (2004) considering two rate limiting processes for in-mouth flavor release: first the transfer of volatiles from the food particles (in this case gel particles containing emulsion droplets) to the aqueous phase and second the transfer from the well-mixed continuous aqueous phase to the headspace. The model was validated for the release of five aroma compounds and the predicted values showed a good agreement with the experimental data (Lian, et al., 2004). This work is particularly helpful in that it suggests the conditions under which different aspects of food structure can be significant. For small particles, release from the food is fast and the overall kinetics is governed by movement through the continuous phase of the food. This regime is similar to the penetration theory models of Harrison and others described above. However, if the particles of food are large, then they may offer a significant barrier to diffusion and their changing microstructure becomes important.

2.4.3 Experimental Systems to Validate Models

The models proposed above give a good quantitative description for the factors affecting the kinetics of aroma release from foods. However given the paucity of data on the composition and structure of food inside the mouth, it is hard to say which, if any, are most appropriate under a given circumstance. Various groups have developed methods to measure flavor release from foods and we will consider some of them here grouped as *in vitro*, *in vivo* and sensory techniques. The *in vitro* methods involve the construction of a model mouth and measuring the release of volatiles from foods placed in it. They have the advantage of thoroughly controlling the experimental conditions but inevitably the conditions selected may not be representative of real consumption. In the *in vivo* methods the concentration of headspace volatiles is measured directly in the gas exhaled as a human being really eats the sample. Actual chemical concentrations are measured so it is, in theory, possible to connect the measurements to mass transport models. However, the processing of the food is less well controlled and the variation in the data is consequently higher. The final group of methods bypasses any measurement of chemical

concentration and instead use user reported assessments of sensory intensity during eating. These methods have the advantage of being based on real perception, but without measurements of concentrations of chemicals it is hard to use them to assess mass transport models.

2.4.3.1 Measuring *in vitro* flavor release.

The earliest in vitro methods were dynamic headspace sampling where gas is passed either over (i.e. flushing) or through (i.e. purging) the food product to strip off the volatiles which are either trapped for subsequent analysis or passed directly to a GC detector but these devices did not have the capacity to simulate and more realistic eating conditions through mechanical mixing or the addition of saliva-like liquids. The importance of these factors was demonstrated by van Ruth, Roozen and Cozijsen (1994) who developed a model mouth by adding artificial saliva to food then using a piston pump to simulate chewing. They used this device to measure flavor release from bell pepper cuttings and compared the results with dynamic headspace measurements based on both purging and flushing with nitrogen. It was observed that flavor release from the mouth model system was significantly different from both purging and dynamic headspace sampling system. The amount of volatile components released was highest for purging system followed by mouth model and dynamic headspace analysis. Mastication produced an increase in the release of all volatile components as well as a relative increase in the release of less volatile components compared to the dynamic headspace system. Thus simple dynamic headspace analyses do not adequately predict volatile release during actual eating process and use of in-mouth model system is necessary. Whether the conditions selected in the model mouth correspond to those during real eating is not clear.

Other devices have been designed as model noses. For example, Roberts and Acree (1995) developed a retronasal aroma simulator which simulated the flow in the mouth during consumption by applying shear with a modified blender. (Their instrument

was primarily designed to analyze flavor release from liquid foods and hence effects of shearing on food microstructure were not considered.) The sample was purged with nitrogen and the volatiles were collected on a silica trap and then analyzed by gas chromatography. Similarly, Rabe Krings, Banavara and Berger (2002) developed a computer-controlled apparatus to simulate the conditions in the mouth using a large (5 l) glass reactor. A stirrer with impeller blade was used to mix the liquid food with saliva and the headspace was flushed with purified air. The whole system was controlled by a computer program which maintained different in-mouth conditions and allowed automatic sample collection over 30 seconds of simulated "drinking" (Rabe, Krings and Berger, 2004). Continuous measurements of dynamic headspace samples were made by Lee (1986) who coupled a mass spectrometer with a simple dynamic headspace model mouth system. The model mouth was a controlled temperature glass vial into which saliva was injected and mastication was simulated by adding small metal or glass balls along with the sample and shaking. The vial was flushed with helium gas and the volatiles in the carrier gas were analyzed continuously in the mass spectrometer for 2-3 minutes. This type of continuous *in-vitro* measurement of flavor release from model mouth system has been used subsequently by several research groups (Buffo, Zehentbauer and Reineccius, 2005; Springett, Rozier and Bakker, 1999; Weel, Boelrijk, Burger, Verschueren, Gruppen, Voragen and Smit, 2004).

2.4.3.2 Measuring *in vivo* flavor release.

Although model mouth systems can simulate the effects of controlled and simulated eating conditions on the release of aroma from food, it is impossible to fully duplicate the conditions inside a living mouth. *In vivo* methods have been developed to put chemical sensors inside the human body to monitor changing chemical concentrations as real food is eaten. Ideally, *in vivo* measurements should be performed without any extraction or concentration step and the analysis should be done instantaneously so that release of volatile over the short period of the eating process can be measured (Linforth, Ingham and Taylor, 1996; Taylor and Linforth, 1994; 1996). However, direct

comparison of these results with model mouth studies and mass transfer models is difficult because of the intrinsic variability of the biological experimental system and because some of the volatiles may be absorbed by biological surfaces and mucus (Linforth, Martin, Carey, Davidson and Taylor, 2002; Overbosch, Afterof and Haring, 1991).

Linforth and Taylor (1993) used direct sampling of air from mouth or nose during eating of mint flavored sweets. Reproducible measurements of the total amount of volatile released were obtained using a trapping method. These authors later used a series of traps to capture time points on the temporal release curve during eating (Linforth, et al., 1996) and were able to use this laborious method to capture volatile release profiles during the eating of sweets (Ingham, Linforth and Taylor, 1995b) and strawberries (Ingham, Linforth and Taylor, 1995a) as well as for cereal foods (Clawson, Linforth, Ingham and Taylor, 1996) and biscuits with different fat contents (Ingham, Taylor, Chevance and Farmer, 1996). The analytical protocol was vastly improved in the late 90's with the introduction of atmospheric pressure chemical ionization – mass spectrometry (APCI-MS) (Harvey and Barra, 2003; Linforth and Taylor, 1999; 2005; Taylor and Linforth, 2000; Taylor, Linforth, Harvey and Blake, 2000), proton transfer reaction – mass spectroscopy (PTR-MS) (Lindinger, Hansel and Jordan, 1998a; 1998b; Mayr, Mark, Lindinger, Brevard and Yeretzian, 2003; Yeretzian, Jordan and Lindinger, 2003) and selected ion flow tube – mass spectrometry (SIFT-MS) (Spanel and Smith, 1999). Linforth and Taylor (1999) developed an air sampling interface such that the subject could drink, eat and breathe normally while a small fraction of their breath could be sampled from the exhaled air from their nose through a deactivated fused silica capillary tube heated at 100ºC to minimize any condensation. This technique was used to study temporal release profiles of five fruit flavors from gelatin/pectin gels (Harvey, Brauss, Linforth and Taylor, 2000). Considerable variation in the time to reach maximum intensity was observed among the aroma compounds and the intensity of different aroma compounds diminished at different time during eating.

In spite of the recent advances in analytical methods, there are few studies that directly relate the structure of the food to the *in vivo* concentration of volatiles. In a recent study Lian, Malone, Homan and Norton (2004) used APCI-MS to study real time in-mouth flavor release from gelled emulsion particles and oil-in-water emulsions. The gelled emulsion particles were made by spraying oil-in-water emulsion containing Na-alginate into a solution of calcium chloride, thus inducing rapid gelation to form entrapped oil droplets in a continuous gel phase. The gelled emulsion particles were dispersed in a flavored solution of xanthan gum. As this product was eaten, the flavor was released from the food and passed through the nasal cavity (the retronasal route) and then was exhaled through the nose into an APCI probe linked to a mass spectrometer for analysis of kinetics of flavor release.

2.4.3.3 Measuring the sensation of flavor release

Flavor perception is a complex phenomena involving transfer of chemical stimulation generated at different receptors during food consumption to the specific regions of the brain. The brain then interprets the signal from the sensation so that we sense the flavor of the food. Instrumental techniques such as *in vivo* breath analysis can give measurements of the concentrations of relevant aroma molecules in the stream of gasses passing through the nose but not the sensations they elicit and sensory analysis is the necessary complementary technique (Taylor, 1996). In its simple form, sensory analysis involves rating the intensity and quality of the taste or flavor of a food compared to some predetermined standard. These types of descriptive sensory analysis are normally done with a selected group of individuals who are trained to detect qualitative or quantitative changes in the food flavor. The product profile can be generated based on overall sensory characteristics as well as any particular characteristics of a food product (Murray, Delahunty and Baxter, 2001). This type of static judgment of food flavor can be considered as the average of total sensation over the duration of food consumption. However, the perception of flavor type/intensity will change during the process of consumption. This can be tracked using time intensity (TI) sensory measurements where

the panelists are asked to record the changing intensity of food flavor during eating (Cliff and Heymann, 1993; Dijksterhuis and Piggott, 2001). Some of the mostly used parameters are maximum intensity (I_{max}), time to reach maximum intensity (t_{max}), area under the curve and slope of increasing and decreasing intensity (Cliff and Heymann, 1993).

Sensory analysis can be used to investigate the effects of food structure. For example, Moore, Dodds, Turnbull and Crawford (2000) prepared a composite gel by dispersing fat particles in aqueous protein matrix and flavored with ethyl butyrate and used a panel to measure the time-intensity (TI) sensory properties. They developed a model for flavor release following the method of Harrison and Hills (1997a) but extended to include the effect of swallowing and chewing in the mouth, evaporation of volatile flavor in respired air at the back of the mouth, and adsorption in the nose. The final differential equations were solved numerically to simulate one minute of a flavor release experiment and compared to the sensory TI data. The model gave a reasonable initial prediction for the average TI scores (across all panelists) until about 30 seconds when there was a sudden drop in sensory intensity while the model predicted a gradual reduction. The authors argued that changes in the swallowing pattern between the experiment and model simulation was responsible for this deviation (Moore, et al., 2000). Interestingly, gel texture and the fat droplet size had no significant influence on the flavor perception.

However, to fully relate the response in the eater with the properties of the eaten it is necessary to combine sensory scores with actual measurements of the concentration of the stimulant. Such a synchronized approach was used by Baek, Linforth, Blake and Taylor (1999) who compared the sensory TI curve with instrumental (APCI-MS) breath analysis of the flavor release curve from model gelatin-sucrose gels. The gels were prepared with varying gelatin content but with a fixed amount of a single aroma compound. It was found that with increasing gelatin content, the maximum perceived intensity decreases but there were no significant difference in the maximum in-nose volatile concentrations. Hence the maximum concentration of volatile present in the nose

does not correlate with the perceived sensory intensity. Surprisingly, the rate of change of nasal volatile concentration showed a better correlation with the sensory results indicating the importance of temporal aspects of flavor release in perception.

If the rate of flavor release is important for perception, then does the time to reach maximum flavor release coincide with the time to perceive maximum intensity? Linforth, Baek and Taylor (1999) used simultaneous instrumental and sensory analysis of volatile release from different gels with a single aroma compound. It was found that when weak gels were eaten, the time to reach maximum perceived intensity (sensory t_{max}) is longer than the time of maximum in-nose volatiles release (instrumental t_{max}), i.e. a temporal lag between the physical stimuli and its sensation was observed for short eating time. A similar observation was also made by Overbosch, Afterof and Haring (1991) and this lag was attributed to a temporal integration of the stimulus (Berglund and Lindvall, 1982; Overbosch, de Wijk, de Jonge and Koster, 1988). In contrast, when stronger gels were consumed (which required more time to eat) the maximum perceived intensity was reached faster than the maximum in-nose volatile concentration (Linforth, et al., 1999). This is because longer eating time can cause sensory adaptation to the aroma and hence a decrease in perceived intensity (Linforth, et al., 1999). Similar observations of sensory adaptation were also observed by Linforth and Taylor (1998) using mint flavored chewing gum as a model system.

2.4.4 Conclusions

Flavor is a cognitive response of the brain to a number of nervous signals originating from chemically sensitive nerves in the mouth and nose. The chemicals that stimulate those nerves are released from foods and beverages before and during consumption. This work was concerned with how the structure of the food can alter the nature of the release. Food structure can alter the thermodynamics and kinetics of release. Thermodynamically foods with a greater affinity for taste and aroma molecules will tend to release fewer of them into the saliva or headspace gasses. The

thermodynamics of release is mainly governed by the volumes and compositions of the various phases that constitute the food. Structure, as in the arrangement and size of the phases, is only really important as it introduces an additional "interphase" with different thermodynamic properties that alter the affinity of the food for the flavor. The kinetics of release is more affected by food structure but which structure are relevant depends on which provides the greatest resistance to the mass transport of the flavor. However, food structure inside the mouth is changing rapidly due to mastication and mixing with saliva so it is probably irrelevant to use measurements of food structure before eating to predict flavor release during consumption.

The most interesting recent work combines the human with the instrumental and introduces quantitative chemical measurements into the body as food is eaten (e.g., Baek, Linforth, Blake and Taylor (1999)). We suggest that real understanding will occur when these measurement are integrated with measurements of evolving food structures inside the human mouth. Various workers have approached this last problem using techniques including spitting out after intervals and measuring the residual structure (Buettner and Schieberle, 2000a; 2000b), or using X-rays or other imaging technologies to look through the cheeks and watch the movement of the food bolus (Buettner, Beer, Hannig, Settles and Schieberle, 2002). Many of these approaches are designed to understand the processes of chewing and disphagia but could be directed towards looking at how the food structure is changing.

Acknowledgements: I am grateful to Dr. T.C. Pritchard (Penn State College of Medicine) for helpful discussions.

2.5 References

Atkins, P.; Paula, J. D., *Atkins' Physical Chemistry*. 8th ed.; Oxford University Press: Oxford, UK, **2006**.

Awad, T. S., Sato, K., Fat crystallization in O/W emulsions controlled by hydrophobic emulsifier additives. In *Physical properties of lipids*, Marangoni, A. G., Narine, S.S., Ed. Marcel Dekker Inc.: New York, **2002**; pp 37-62.

Baek, I.; Linforth, R. S. T.; Blake, A.; Taylor, A. J., Sensory Perception is related to the rate of change of volatile concentration in-nose during eating of model gels. *Chemical Senses* **1999,** 24, 155-160.

Becher, P., *Emulsions : theory and practice*. 3rd ed.; American Chemical Society: Washington, D.C., **2001**.

Berglund, B.; Lindvall, T., Olfaction. In *The Nose, Upper Airway Physiology and the Atmospheric Environment*, Proctor, D. F.; Anderson, I. B., Eds. Elsevier: Amsterdam, **1982**.

Bibette, J., Stability of thin films in concentrated emulsions. *Langmuir* **1992,** 8, 3178-3182.

Binks, B. P., *Modern aspects of emulsion science*. Royal Society of Chemistry: Cambridge, UK, **1998**.

Binks, B. P.; Clint, J. H.; Mackenzie, G.; Simcock, C.; Whitby, C. P., Naturally occurring spore particles at planar fluid interfaces and in emulsions. *Langmuir* **2005,** 21, (18), 8161-8167.

Buettner, A.; Beer, A.; Hannig, C.; Settles, M.; Schieberle, P., Physiological and analytical studies on flavor perception dynamics as induced by the eating and swallowing process. *Food Quality and Preference* **2002,** 13, (7-8), 497-504.

Buettner, A.; Schieberle, P., Changes in concentration of key fruit odorants induced by mastication. In *Flavor Release*, Roberts, D. D.; Taylor, A. J., Eds. American Chemical Society: Washington, DC, **2000a**; pp 87-98.

Buettner, A.; Schieberle, P., Influence of mastication on the concentrations of aroma volatiles - some aspects of flavour release and flavour perception. *Food Chemistry* **2000b,** 71, (3), 347-354.

Buffo, R. A.; Zehentbauer, G.; Reineccius, G. A., Determination of linear response in the detection of aroma compounds by atmospheric pressure ionization-mass spectrometry (API-MS). *Journal of Agricultural and Food Chemistry* **2005,** 53, (3), 702-707.

Bunjes, H.; Koch, M. H. J., Saturated phospholipids promote crystallization but slow down polymorphic transitions in triglyceride nanoparticles. *Journal of Controlled release* **2005,** 107, 229-243.

Butler, J. A. V.; Ramchandani, C. N.; Thomson, D. W., The solubility of non-electrolytes Part I The free energy of hydration of some aliphatic alcohols. *Journal of the Chemical Society* **1935**, 280-285.

Buttery, R. G.; Bomben, J. L.; Guadagni, D. G.; Ling, L. C., Some Considerations of Volatilities of Organic Flavor Compounds in Foods. *Journal of Agricultural and Food Chemistry* **1971,** 19, (6), 1045-&.

Buttery, R. G., et al, Flavor compounds: volatilities in vegetable oil and oil-water mixtures. Estimation of odor thresholds. *Journal of Agricultural and Food Chemistry* **1973,** 21, (2), 198-201.

Buttery, R. G.; Guadagni, D. G.; Ling, L. C., Flavor compounds: volatilities in vegetable oil and oil-water mixtures. Estimation of odor thresholds. *Journal of Agricultural and Food Chemistry* **1973,** 21, (2), 198-201.

Buttery, R. G.; Ling, L. C.; Guadagni, D. G., Food Volatiles - Volatilities of Aldehydes Ketones and Esters in Dilute Water Solution. *Journal of Agricultural and Food Chemistry* **1969,** 17, (2), 385-&.

Carey, M. E.; Asquith, T.; Linforth, R. S. T.; Taylor, A. J., Modeling the partition of volatile aroma compounds from a cloud emulsion. *Journal of Agricultural and Food Chemistry* **2002,** 50, (7), 1985-1990.

Chanamai, R.; McClements, D. J., Creaming stability of flocculated monodisperse oil-in-water emulsions. *Journal of Colloid and Interface Science* **2000,** 225, 214-218.

Chanamai, R.; McClements, D. J., Depletion flocculation of beverage emulsions by gum arabic and modified starch. *Journal of Food Science* **2001,** 66, 457.

Clawson, A. R.; Linforth, R. S. T.; Ingham, K. E.; Taylor, A. J., Effect of hydration on release of volatiles from cereal foods. *Food Science and Technology-Lebensmittel-Wissenschaft & Technologie* **1996,** 29, (1-2), 158-162.

Cliff, M.; Heymann, H., Development and Use of Time-Intensity Methodology for Sensory Evaluation - a Review. *Food Research International* **1993,** 26, (5), 375-385.

Coulson, J. M.; Richardson, J. F., *Chemical Engineering*. Pergamon Press: Oxford, **1993**; Vol. 1.

Coupland, J. N., Crystallization in emulsions. *Current Opinion in Colloid & Interface Science* **2002,** 7, (5-6), 445-450.

Courthaudon, J. L.; Dickinson, E.; Dalgleish, D. G., Competitive Adsorption of Beta-Casein and Nonionic Surfactants in Oil-in-Water Emulsions. *Journal of Colloid and Interface Science* **1991,** 145, (2), 390-395.

Cramp, G. L.; Docking, A. M.; Ghosh, S.; Coupland, J. N., On the stability of oil-in-water emulsions to freezing. *Food Hydrocolloids* **2004,** 18, (6), 899-905.

Crank, J., *The Mathematics of Diffusion*. Oxford University Press: London, UK, 1975.

Dalgleish, D. G., Food emulsions: their structures and properties. In *Food Emulsions*, 4th ed.; Friberg, S. E.; Larsson, K.; Sjoblom, J., Eds. Marcel Dekker: New York, **2004**; p Chap 1.

de Roos, K. B., Physiochemical models of flavor release from foods,. In *Flavor Release*, Roberts, D. D.; A.J., T., Eds. American Chemical Society: Washington, D.C., **2000**; pp 126-141.

de Roos, K. B., How lipids influence flavor perception. In *Food Lipids - Chemistry, Flavor and Texture*, Shadidi, F.; Weenen, H., Eds. American Chemical Society: Washington, DC, **2005**; Vol. 920 ACS Symposium Series.

Dickinson, E., *Introduction to Food Colloids*. Oxford University Press: Oxford, UK., **1992**.

Dickinson, E., Hydrocolloids at interfaces and the influence on the properties of dispersed systems. *Food Hydrocolloids* **2003,** 17, 25.

Dickinson, E.; Golding, M., Depletion flocculation of emulsions containing unadsorbed sodium caseinate. *Food Hydrocolloids* **1997,** 11, 13.

Dickinson, E.; Goller, M. I.; Wedlock, D. J., Osmotic pressure, creaming and rheology of emulsions containing non-ionic polysaccharide. *Journal of Colloid and Interface Science* **1995,** 172, 192.

Dickinson, E.; Kruizenga, F.-J.; Povey, M. J. W.; van der Molen, M., Crystallization in oil-in-water emulsions containing liquid and solid droplets. *Colloids and Surfaces A: Physicochemical and Engineering Aspects* **1993,** 81, 273-279.

Dickinson, E.; Kruizenga, F. J.; Povey, M. J. W., Crystallization in oil-in-water emulsions containing liquid and solid droplets. *Colloids and Surfactant A Physiochemical and Engineering Aspects* **1993,** 81, 273-279.

Dickinson, E.; McClements, D. J., *Advances in Food Colloids*. Chapman & Hall: New York, **1995**.

Dickinson, E.; Povey, M. J. W., Crystallization kinetics in oil-in-water emulsions containing a mixture of solid and liquid droplets. *Journal of Chemical Society* **1996,** 92, 1213-1215.

Dickinson, E.; Stainsbay, G., *Colloids in Foods*. Applied Science Publishers: London, **1982**.

Dickinson, E.; Stainsby, G., Emulsion Stability. In *Advances in Food Emulsions and Forms*, Dickinson, E.; Stainsby, G., Eds. Elsevier Applied Science: New York, **1988**.

Dijksterhuis, G. B.; Piggott, J. R., Dynamic methods of sensory analysis. *Trends in Food Science & Technology* **2001,** 11, (8), 284-290.

Fellows, P., *Food Processing Technology: Principles and Practice*. 2nd ed.; Woodhead Publishers: Cambridge, UK, **2000**.

Friberg, S. E.; Larsson, K., *Food Emulsions*. 3rd ed.; Marcel Dekker, Inc.: New York, **1997**.

Garti, N., Food emulsifiers: structure-relativity relationships, design, and applications. In *Physical Properties of Lipids*, Marangoni, A. G.; Narine, S. S., Eds. Marcel Dekker, Inc.: New York, **2002**.

Ghosh, S.; Cramp, G. L.; Coupland, J. N., Effect of aqueous composition on the freeze-thaw stability of emulsions. *Colloids and Surfaces A: Physicochemical and Engineering Aspects* **2006a,** 272, 82-88.

Ghosh, S.; Peterson, D. G.; Coupland, J. N., Effects of droplet crystallization and melting on the aroma release properties of a model oil-in-water emulsion. *Journal of Agricultural and Food Chemistry* **2006b,** 54, (5), 1829-1837.

Gopal, E. S. R., Principles of Emulsion Formation. In *Emulsion Science*, Sherman, P., Ed. Academic Press: Londan, UK., **1968**; p Ch 1.

Guyot, C.; Bonnafont, C.; Lesschaeve, I.; Issanchou, S.; Voilley, A.; Spinnler, A. E., Effect of fat content on odor intensity of three aroma compounds in model emulsions: d-decalactone, diacetyl, and butyric acid. *J. Agric. Food Chem.* **1996,** 44, 2341-2348.

Harrison, M., Effect of breathing and saliva flow on flavor release from liquid foods. *J. Agric. Food Chem.* **1998,** 46, 27172735.

Harrison, M.; Hills, B. P., Effects of air flow-rate on flavour release from liquid emulsions in the mouth. *International Journal of Food Science and Technology* **1997a,** 32, (1), 1-9.

Harrison, M.; Hills, B. P., Mathematical model of flavor release from liquids containing aroma-binding macromolecules. *Journal of Agricultural and Food Chemistry* **1997b,** 45, (5), 1883-1890.

Harrison, M.; Hills, B. P.; Bakker, J.; Clothier, T., Mathematical models of flavor release from liquid emulsions. *Journal of Food Science* **1997,** 62, (4), 653-+.

Hartel, R. W., *Crystallization in Foods*. Aspen Publishers, Inc.: Gaithersburg, Maryland, **2001**.

Harvey, B. A.; Barra, J., Real time breath and headspace analysis of flavour volatiles. *European Journal of Pharmaceutics and Biopharmaceutics* **2003,** 55, (3), 261-269.

Harvey, B. A.; Brauss, M. S.; Linforth, R. S. T.; Taylor, A. J., Real-time flavor release from foods during eating. In *Flavor Release*, Roberts, D. D.; Taylor, A. J., Eds. American Chemical Society: Washington, DC, **2000**; pp 22-32.

Hiemenz, P. C.; Rajagopalan, R., *Principles of Colloid and Surface Chemistry*. 3rd ed.; Marcel Dekker: New York, NY, **1997**.

Hindle, S.; Povey, M. J. W.; Smith, K., Kinetics of crystallization in n-hexadecane and cocoa butter oil-in-water emulsions accounting for droplet collision mediated nucleation. *Journal of Colloid and Interfacial Science* **2000,** 232, 370-80.

Hunter, R. J., Foundations of Colloid Science. In Oxford University Press: Oxford, UK., **1989**; Vol. 2.

Ingham, K. E.; Linforth, R. S. T.; Taylor, A. J., The Effect of Eating on Aroma Release from Strawberries. *Food Chemistry* **1995a,** 54, (3), 283-288.

Ingham, K. E.; Linforth, R. S. T.; Taylor, A. J., The Effect of Eating on the Rate of Aroma Release from Mint-Flavored Sweets. *Food Science and Technology-Lebensmittel-Wissenschaft & Technologie* **1995b,** 28, (1), 105-110.

Ingham, K. E.; Taylor, A. J.; Chevance, F. F. V.; Farmer, L. J., Effect of fat content on volatile release from foods. In *Flavour Science: Recent Developments*, Taylor, A. J.; Mottram, D. S., Eds. Royal Society Chemistry: London, **1996**; pp 386-391.

Kabalnov, A.; Wennerstrom, H., Macroemulsion stability: The oriented wedge theory revisited. *Langmuir* **1996,** 12, (2), 276-292.

Kashchiev, D.; Exerowa, D., Nucleation mechanism of rupture of newtonian black films. I. Theory. *Journal of Colloid and Interface Science* **1980,** 77, (2), 501-511.

Keast, R. S. J.; Dalton, P. H.; Breslin, P. A. S., Flavor interaction at the sensory level. In *Flavor Perception*, Taylor, A. J.; Roberts, D. D., Eds. Blackwell Publishing: Oxford, UK, **2004**; pp 228-249.

Kerker, M., *The Scattering of Light and Other Electromagnetic Radiation*. Academic Press: New York, **1969**.

Laing, D. G.; Jinks, A., Flavour perception mechanisms. *Trends in Food Science & Technology* **1996,** 7, (12), 387-389.

Landy, P.; Courthaudon, J. L.; Dubois, C.; Voilley, A., Effect of interface in model food emulsions on the volatility of aroma compounds. *J. Agric. Food Chem.* **1996,** 44, (2), 526-530.

Larsson, K., Classification of glyceride crystal forms. *Acta Chemica Scandinavia* **1966,** 20, 2255–2260.

Lee III, W. E., A suggested instrumental technique for studying dynamic flavor release from food products. *Journal of Food Science* **1986,** 51, (1), 249-250.

Lian, G., modeling flavor release form oil containing gel particles. In *Flavor release*, Roberts, D. D.; Taylor, A. J., Eds. American Chemical Society: Washington, DC, **2000**; pp 201-211.

Lian, G. P.; Malone, M. E.; Homan, J. E.; Norton, I. T., A mathematical model of volatile release in mouth from the dispersion of gelled emulsion particles. *Journal of Controlled Release* **2004,** 98, (1), 139-155.

Lindinger, W.; Hansel, A.; Jordan, A., On-line monitoring of volatile organic compounds at pptv levels by means of proton-transfer-reaction mass spectrometry (PTR-MS) - Medical applications, food control and environmental research. *International Journal of Mass Spectrometry* **1998a,** 173, (3), 191-241.

Lindinger, W.; Hansel, A.; Jordan, A., Proton-transfer-reaction mass spectrometry (PTR-MS): on-line monitoring of volatile organic compounds at pptv levels. *Chemical Society Reviews* **1998b,** 27, (5), 347-354.

Lindman, B., Physico-chemical properties of surfactants. In *Handbook of Applied Surface and Colloid Chemistry*, Holmberg, K., Ed. John Wiley & Sons.: Chichester, UK, **2001**; Vol. 1, p Chap 19.

Linforth, R. S. T.; Baek, I.; Taylor, A. J., Simultaneous instrumental and sensory analysis of volatile release from gelatine and pectin/gelatine gels. *Food Chemistry* **1999,** 65, (1), 77-83.

Linforth, R. S. T.; Ingham, K. E.; Taylor, A. J., Time course profiling of volatile release from foods during the eating process. In *Flavour Science: Recent Developments*, Taylor, A. J.; Mottram, D. S., Eds. Royal Society of Chemistry: UK, **1996**; pp 361-368.

Linforth, R. S. T.; Martin, F.; Carey, M. E.; Davidson, J.; Taylor, A. J., Retronasal transport of aroma compounds. *Journal of Agricultural and Food Chemistry* **2002,** 50, 1111-1117.

Linforth, R. S. T.; Taylor, A. J., Measurement of volatile release in the mouth. *Food Chemistry* **1993,** 48, 115-120.

Linforth, R. S. T.; Taylor, A. J., Volatile release from mint flavored sweets. *Perfumer and Flavorist* **1998,** 23, 47-53.

Linforth, R. S. T.; Taylor, A. J. Apparatus and methods for the analysis of trace constituent in gases. 1999.

Linforth, R. S. T.; Taylor, A. J., release of flavor from emulsion under dynamic sampling conditions. In *Food Lipids - Chemistry, Flavor, Texture*, Shadidi, F.; Weenen, H., Eds. American Chemical Society: Washington, DC, 2005; Vol. 920 ACS Symposium Series.

Mayr, D.; Mark, T.; Lindinger, W.; Brevard, H.; Yeretzian, C., Breath-by-breath analysis of banana aroma by proton transfer reaction mass spectrometry. *International Journal of Mass Spectrometry* **2003,** 223, (1-3), 743-756.

McClements, D. J.; Dungan, S. R.; German, J. B.; Simoneau, C.; Kinsella, J. E., Droplet size and emulsifier type affect crystallization and melting of hydrocarbon-in-water emuslions. Journal of Food Science **1993**, 58, (5), 1148-1178.

McClements, D. J., Ultrasonic determination of depletion flocculation in oil-in-water emulsions containing a non-ionic surfactant. *Colloids and Surfaces A: Physicochemical and Engineering Aspects* **1994,** 90, 25.

McClements, D. J., Colloidal basis of emulsion color. *Current Opinion in Colloid and Interface Science* **2002,** 7, 451.

McClements, D. J., *Food Emulsions - Principles, practices, and Techniques*. 2nd ed.; CRC Press: New York, 2004.

McClements, D. J.; Decker, E. A., Lipid oxidation in oil-in-water emulsions: Impact of molecular environment on chemical reactions in heterogeneous food systems. *Journal of Food Science* **2000,** 65, (8), 1270-1282.

McClements, D. J.; Han, S.-W.; Dungan, S. R., Interdroplet heterogeneous nucleation of supercooled liquid droplets by solid droplets in oil-in-water emulsions. *Journal of American Oil Chemists' Society* **1994,** 71, 1385-1389.

Meynier, A.; Garillon, A.; Lethuaut, L.; Genot, C., Partitioning of five aroma compounds between air and skim milk, anhydrous milk fat or full fat cream. *Lait* **2003,** 83, 223-235.

Meynier, A.; Rampon, V.; Dalgalarrondo, M.; Genot, C., Hexanal and t-2-hexenal form covalent bonds with whey proteins and sodium caseinate in aqueous solution. *International Dairy Journal* **2004,** 14, (8), 681-690.

Moore, I. P. T.; Dodds, T. M.; Turnbull, R. P.; Crawford, R. A., Flavor release from composite dairy gels: a comparison between model predictions and time-intensity experimental studies. In *Flavor Release*, Roberts, D. D.; Taylor, A. J., Eds. American Chemical Society: Washington, DC, 2000; pp 381-394.

Murray, J. M.; Delahunty, C. M.; Baxter, I. A., Descriptive sensory analysis: past, present and future. *Food Research International* **2001,** 34, (6), 461-471.

Narine, S. S.; Marangoni, A. G., Structure and mechanical properties of fat crystal networks. In *Physical Properties of Lipids*, Marangoni, A. G.; Narine, S. S., Eds. Marcel Dekker, Inc.: New York, **2002**; pp 63-84.

Nawar, W. W., Lipids. In *Food Chemistry*, 3rd ed.; Fennema, O. R., Ed. Marcel Dekker, Inc.: New York, **1996**.

Ostwald, C. W. W., *A handbook of colloid-chemistry: the recognition of colloids, the theory of colloids, and their general physio-chemical properties*. 2nd ed.; P. Blakiston's Son & Co.: Philadelphia, **1919**.

Overbosch, P.; Afterof, W. G. M.; Haring, P. G. M., Flavor release in the mouth. *Food Reviews International* **1991,** 7, (2), 137-184.

Overbosch, P.; de Wijk, R.; de Jonge, T. J. R.; Koster, E. P., Temporal integration and reaction times in human smell. *Physiology and behaviour* **1988,** 45, 615-626.

Palanuwech, J.; Potineni, R.; Roberts, R. F.; Coupland, J. N., A method to determine free fat in emulsion. *Food Hydrocolloids* **2003,** 17, 55-62.

Pandolfe, W. D., Homogenizers. In *Encyclopedia of Food Science and Technology*, John Wiley & Sons.: New York, 1991; p 1413.

Pierotti, G. J.; Deal, C. H.; Derr, E. L., Activity Coefficients and Molecular Structure. *Industrial and Engineering Chemistry* **1959,** 51, (1), 95-102.

Rabe, S.; Krings, U.; Banavara, D. S.; Berger, R. G., Computerized apparatus for measuring dynamic flavor release from liquid food matrices. *Journal of Agricultural and Food Chemistry* **2002,** 50, (22), 6440-6447.

Rabe, S.; Krings, U.; Berger, R. G., Dynamic flavour release from myglyol/water emulsion: modeling and validation. *Food Chemistry* **2004,** 84, 117-125.

Rawle, A. *Basic Principles of Particle Size Analysis*; Malvern Instruments Limited, Worcestershire, UK: **2004**.

Relkin, P.; Fabre, M.; Guichard, E., Effect of fat nature and aroma compound hydrophobicity on flavor release from complex food emulsions. *Journal of Agricultural and Food Chemistry* **2004,** 52, (20), 6257-6263.

Roberts, D. D.; Acree, T. E., Simulation of retronasal aroma using a modified headspace technique: investigation of effects of saliva, temperature, shearing, and oil on flavor release. *J. Agric. Food. Chem.* **1995,** 43, 2179-2186.

Roberts, D. D.; Pollien, P.; Watzke, B., Experimental and modeling studies showing the effect of lipid type and level on flavor release from milk-based liquid emulsions. *Journal of Agricultural and Food Chemistry* **2003,** 51, 189-195.

Rousseau, D., Fat crystals and emulsion stability - a review. *Food Research International* **2000a,** 33, (3), 14.

Rousseau, D., Fat crystals and emulsion stability-a review. *Food Research International* **2000b,** 33, 3-14.

Rousseau, D., Fat crystal behavior in food emulsions. In *Physical Properties of Lipids*, Marangoni, A. G.; Narine, S. S., Eds. Marcel Dekker, Inc.: New York, 2002.

Rousset, P., Modeling crystallization kinetics of triacylglycerols In *Physical Properties of Lipids*, Marangoni, A. G.; Narine, S. S., Eds. Marcel Dekker, Inc.: New York, **2002**.

Samis, T.; Sato, K., Fat crystallization in O/W emulsions controlled by hydrophobic emulsifier additives. In *Physical Properties of Lipids*, Narcel Dekker, Inc.: New York, **2002**; pp 37-62.

Sato, K., Crystallization of fats and fatty acids. In *Crystallization and polymorphism of fats and fatty acids*, Garti, N.; Sato, K., Eds. Marcel Dekker, Inc.: New York, **1988**; pp 227-266.

Sato, K., Newest understandings of molecular structures and interactions of unsaturated fats and fatty acids. *Progress In Colloid And Polymer Science* **1998,** 108, 58-66.

Sato, K., Crystallization behaviour of fats and lipids - a review. *Chemical Engineering Science* **2001,** 56, (7), 2255-2265.

Schubert, H.; Armbruster, H., Principles of formation and stability of emulsions. *International Chemical Engineering* **1992,** 32, 14.

Skoda, W.; van den Tempel, M., Crystallization of emulsified triglycerides. *Journal of Colloid Science* **1963,** 18, 568-584.

Sonoda, T.; Takata, Y.; Ueno, S.; Sato, K., Effects of emulsifiers on crystallization behavior of lipid crystals in nanometer-size oil-in-water emulsion droplets. *Crystal Growth & Design* **2006,** 6, (1), 306-312.

Spanel, P.; Smith, D., Selected ion flow tube - Mass spectrometry: Detection and real-time monitoring of flavours released by food products. *Rapid Communications in Mass Spectrometry* **1999,** 13, (7), 585-596.

Springett, M. B.; Rozier, V.; Bakker, J., Use of fiber interface direct mass spectrometry for the determination of volatile flavor release from model food systems. *Journal of Agricultural and Food Chemistry* **1999,** 47, (3), 1125-1131.

Taylor, A. J., Volatile flavor release from foods during eating. *Critical Reviews in Food Science and Technology* **1996,** 36, (8), 765-784.

Taylor, A. J.; Linforth, R. S. T., Methodology for measuring volatile profiles in the mouth and nose during eating. In *Trends in Flavour Research*, Maarse, H.; van der Heij, D. G., Eds. Elsevier: UK, **1994**; pp 3-14.

Taylor, A. J.; Linforth, R. S. T., Flavor release in mouth. *Trends in Food Science & Technology* **1996,** 7, 444-448.

Taylor, A. J.; Linforth, R. S. T., Techniques for measuring volatile release in vivo during consumption of foods. In *Flavor Release*, Roberts, D. D.; Taylor, A. J., Eds. American Chemical Society: Washington, DC, **2000**.

Taylor, A. J.; Linforth, R. S. T.; Harvey, B. A.; Blake, B., Atmospheric pressure chemical ionisation mass spectrometry for in vivo analysis of volatile flavour release. *Food Chemistry* **2000,** 71, (3), 327-338.

Thanasukarn, P.; Pongsawatmanit, R.; McClements, D. J., Impact of fat and water crystallization on the stability of hydrogenated palm oil-in-water emulsions stabilized by whey protein isolate. *Colloids and Surfaces A: Physicochemical and Engineering Aspects* **2004a,** 246, (1-3), 49-59.

Thanasukarn, P.; Pongsawatmanit, R.; McClements, D. J., Influence of emulsifier type on freeze-thaw stability of hydrogenated palm oil-in-water emulsions. *Food Hydrocolloids* **2004b,** 18, (6), 1033-1043.

Ueno, S.; Hamada, Y.; Sato, K., Controlling polymorphic crystallization of n-alkane crystals in emulsion droplets through interfacial heterogeneous nucleation. *Crystal Growth & Design* **2003,** 3, (6), 935-939.

van Aken, G. A., Flow-induced coalescence in protein-stabilized highly concentrated emulsions. *Langmuir* **2002,** 18, (7), 2549-2556.

van Aken, G. A., Coalescence Mechanisms in Protein-Stabilized Emulsions. In *Food Emulsion*, Fourth ed.; Friberg, S. E., Larsson, K., Sjoblom, J., Ed. Marcel Dekker, Inc.: New York, **2004**; pp 299-325.

van Aken, G. A.; Zoet, F. D., Coalescence in highly concentrated coarse emulsions. *Langmuir* **2000,** 16, (18), 7131-7138.

van Ruth, S. M.; King, C.; Giannouli, P., Influence of lipid fraction, emulsifier fraction, and mean particle diameter of oil-in-water emulsions on the release of 20 aroma compounds. *Journal of Agricultural and Food Chemistry* **2002,** 50, (8), 2365-2371.

van Ruth, S. M.; Roozen, J. P.; Cozijnsen, J. L., Comparison of dynamic headspace mouth model systems for flavour release form rehydrated bell pepper cuttings. In

Trends in Flavor Research, Maarse, H.; van der Heij, D. G., Eds. Elsevier: London, **1994**; pp 59-64.

Voilley, A.; Espinosa Diaz, M. A.; Landy, P., Flavor release from emulsions and complex media. In *Flavor Release*, Roberts, D. D.; Taylor, A. J., Eds. American Chemical Society: Washington, D.C., **2000**; pp 142-152.

Walstra, P., Formation of emulsions. In *Encyclopedia of Emulsion Technology*, Becher, P., Ed. Marcel Dekker, Inc.: New York, **1983**; Vol. 1 Basic Theory, p Chap 2.

Walstra, P., Principles of emulsion formation. *Chemical Engineering Science* **1993,** 48, (2), 333-349.

Walstra, P., Dispersed systems: basic considerations. In *Food Chemistry*, 3rd ed.; Fennema, O. R., Ed. Marcel Dekker, Inc.: New York, **1996a**; p Chapter 3.

Walstra, P., Emulsion Stability. In *Encyclopedia of emulsion technology*, Becher, P., Ed. Marcel Dekker: New York, **1996b**; Vol. 4, p chapter 1.

Walstra, P., *Physical Chemistry of Foods*. Marcel Dekker, Inc.: New York, **2003**.

Walstra, P.; Kloek, W.; van Vliet, T., Fat crystal Network. In *Crystallization Process in Fats and Lipid Systems*, Garti, N.; Sato, K., Eds. Marcek Dekker: New York, **2001**; pp 289-328.

Walstra, P.; Smulder, P. E. A., Emulsion formation. In *Modern Aspects of Emulsion Science*, Binks, B. P., Ed. The Royal Society Chemistry: Cambridge, UK, **1998**; Vol. Chap 2.

Walstra, P.; van Beresteyn, E. C. H., Crystallization of milk fat in the emulsified state. *Neth. Milk Dairy J.* **1975,** 29, 35-65.

Wedzicha, B. L.; Couet, C., Kinetics of transport of Benzoic acid in emulsions. *Food Chemistry* **1996,** 55, (1), 1-6.

Weel, K. G. C.; Boelrijk, A. E. M.; Burger, J. J.; Verschueren, M.; Gruppen, H.; Voragen, A. G. J.; Smit, G., New device to simulate swallowing and in vivo aroma release in the throat from liquid and semiliquid food systems. *Journal of Agricultural and Food Chemistry* **2004,** 52, (21), 6564-6571.

Yeretzian, C.; Jordan, A.; Lindinger, W., Analysing the headspace of coffee by proton-transfer-reaction mass-spectrometry. *International Journal of Mass Spectrometry* **2003,** 223, (1-3), 115-139.

Chapter 3

Effects of Droplet Crystallization and Melting on the Aroma Release Properties of a Model Oil-in-Water Emulsions

Abstract

Aroma compounds partition between the dispersed and continuous phases in emulsion and phase transitions in the lipid droplets profoundly affect the position of the equilibrium. In the present study the release of ethyl butyrate, ethyl pentanoate, ethyl heptanoate and ethyl octanoate from a series of sodium caseinate–stabilized, n-eicosane emulsions were investigated as a function of solid and liquid lipid droplet concentration. For all compounds, headspace volatile concentrations above the solid droplet emulsions were higher than those above the liquid droplet emulsions. The interaction with liquid droplets could be modeled in terms of volume-weighted bulk partition coefficients while the more non-polar volatiles bound to the surface of solid lipid droplets. The amount of volatiles bound to solid surfaces increased with aqueous concentration up to a critical point, and then rapidly increases. The critical point corresponds to the dissolution of the solid lipid in a phase of adsorbed volatile. The binding of volatiles to both solid and liquid eicosane droplets is reversible.

3.1 Introduction

Flavor is one of the most important factors in determining food choice (Roberts and Taylor, 2000). The perception of food flavor depends on stimuli from both volatile and nonvolatile components (Laing and Jinks, 1996). The perceived aroma, unquestionably a key component of food flavor, not only depends on the type and concentration of volatile compounds present in the headspace above the food, and how they interact with appropriate sensory receptors in the nose and mouth (Overbosch, Afterof and Haring, 1991; Taylor and Linforth, 1996), but also influenced by presence of certain food components (e.g. sweetener) and food texture (Friel and Taylor, 2001; Pionnier, Nicklaus, Chabanet, Mioche, Taylor, Le Quere and Salles, 2004). Defining the mechanisms that govern the headspace volatile concentration are therefore key to understanding food flavor and ultimately a function of the absolute amount of each volatile compound present in the food and by their ability to partition into the gas phase.

Partitioning can be described thermodynamically as the ratio of activities of the compound in each phase. Since the concentration of aroma molecules is typically very low, the activity coefficients are approximately unity and activity can be replaced by concentration. Thus the partition coefficient for a volatile into the headspace above a simple liquid food can be expressed as (Wedzicha, 1988):

$$K_{gl} = \frac{c_g}{c_l} \tag{3.1}$$

where c_g and c_l are the concentration of the aroma compound in the headspace and liquid phase, respectively. However, most foods themselves consist of more than one phase and the partitioning of aroma molecules within the food also needs to be considered. An oil-water partition coefficient is similarly expressed as the ratio of

concentrations of the compound of interest in the oil phase (c_o) to that in the aqueous phase (c_w):

$$K_{ow} = \frac{c_o}{c_w} \tag{3.2}$$

So for a simple food emulsion consisting of an oil and an aqueous phase in contact with the air the overall distribution of volatile molecules would be (Buttery, Guadagni and Ling, 1973):

$$\frac{1}{K_{ge}} = \frac{\phi_o}{K_{go}} + \frac{\phi_w}{K_{gw}} \tag{3.3}$$

where K_{ge} is the overall gas-emulsion partition coefficient and ϕ_o, ϕ_w are the volume fraction of lipid phase and aqueous phase in the emulsion and K_{go} and K_{gw} are the individual gas-oil and gas-water partition coefficients respectively. Clearly from Equation 3.3, increased lipid content will reduce the volatility of hydrophobic volatile molecules more than the volatility of hydrophilic volatile molecules.

This approach has been used to describe the headspace volatile concentration in equilibrium with a food sample (Harrison, Hills, Bakker and Clothier, 1997; McNulty and Karel, 1973a; McNulty and Karel, 1973b; 1973c) and in many cases emulsions are used as model systems (Bakker and Mela, 1996; Charles, Lambert, Brondeur, Courthaudon and Guichard, 2000; McClements, 2004; Voilley, Espinosa Diaz and Landy, 2000). Several workers have studied flavor release from emulsions as influenced by the properties of the flavor molecules (Philippe, Seuvre, Colas, Langendorff, Schippa and Voilley, 2003) and their binding to the interface (Landy, Courthaudon, Dubois and Voilley, 1996; Seuvre, Espinosa Diaz and Voilley, 2002) and several other components (Meynier, Garillon, Lethuaut and Genot, 2003; O'Neill, 1996; Roberts and Pollien, 2000) and physical properties of the component phases (Guichard, 2002). However, most of

these studies involve exclusively liquid oil and the effect of fat crystallization on volatile partitioning is less well understood.

McNulty and Karel (1973b) investigated the release rates of n-alcohols (C-6, C-8) from a bulk lipid phase as a function of solid fat index and concluded that flavor diffusion primarily occurred in liquid portion of the lipid. Maier (1975) showed that solid triglycerides bind much less aroma compounds than liquid triglycerides, and proposed that sorption to solid fat occurs at the crystal surface. Roberts et al. (2003) studied the effects of solid fat content of lipid droplets on the amount of flavor release from milk-based emulsions. A significant increase in the headspace concentration of nonpolar flavor compounds was observed with an increase in solid fat content, whereas polar flavor compounds showed no significant change. It was concluded that only the liquid lipids could absorb nonpolar flavor compounds and hence fat crystallization would reduce the effective lipid content. Similar observations was also obtained by Dubois, Sergent and Voilley (1998) who studied effect of fat type on the release of aroma compounds from model cheese. The authors found that volatility of hydrophobic diallyl sulfide decreased by 20% in the presence of liquid tributyrin compared to milk fat with 15% solid triglycerides while the volatility of the more hydrophilic compound diacetyl was not affected by presence of solid fat. However, other workers (Carey, Asquith, Linforth and Taylor, 2002; Rabe, Krings and Berger, 2003) showed that the partitioning of flavors was not affected by crystallization of the lipid phase of emulsions.

In the present work the partitioning behavior of an homologous series of volatile aroma compounds was measured for a series of model emulsions containing either solid or liquid droplets as a function of lipid content and particle size. Eicosane was chosen as the model lipid for these studies, as its deep supercooling in the emulsified state allowed us to measure the partitioning behavior of solid and liquid droplets at the same temperature (see below for details). It should be mentioned that significant differences exist between eicosane (n-alkane) and other food oils (mixture of tri-acylglycerols). However, based on their similar physical properties including hydrophobicity, eicosane

was used to model complex food oil behavior. The volume partitioning approach (Equation 3.3) was used as a basis for understanding the phase behavior of the volatiles but this was further modified to show the effect of binding at the surface of the solid lipid droplets. A time-series experiment of volatile partitioning in headspace was also performed to confirm the thermodynamic reversibility of volatile binding by solid lipid.

3.2 Materials and Methods

Materials. Eicosane and hexadecane was purchased from Fisher Scientific (Springfield, NJ). Sodium caseinate, all four aroma compounds (ethyl butanoate, EB; ethyl pentanoate, EP; ethyl heptanoate, EH; and ethyl octanoate, EO) and ethyl alcohol (HPLC grade) were obtained from the Sigma Chemical Company (St. Louis, MO).

Emulsion preparation. The model system selected for this study is a fine dispersion of n-eicosane droplets stabilized with sodium caseinate. Emulsions were prepared by mixing n-eicosane (40% w/w) with sodium caseinate solution (2% w/w) containing 0.02% (w/w) thimerosal as an antibacterial agent (Sigma Chemical Company, St. Louis, MO). An initial oil-in-water emulsion pre-mix was made using a high-speed blender (Brinkmann Polytron, Brinkmann Instruments Inc., Westbury, NY) for 30 seconds. The coarse emulsions were then re-circulated through a twin-stage valve homogenizer (Niro Soavi Panda, GEA Niro Soavi, Hudson, WI) for several minutes at different pressures (15-60 MPa) to achieve multiple passes through the valves. Emulsions were prepared hot (>40°C) to ensure the lipid was liquid. The particle size distribution of the emulsions were characterized by laser diffraction particle sizing (Horiba LA 920, Irvine, CA) using a relative refractive index of 1.15. The emulsions were stored at 40ºC prior to use, and were stable over several weeks (no change in particle size and appearance).

Thermal Analysis. The crystallization and melting behavior of bulk and emulsified eicosane was determined using a differential scanning calorimeter (Perkin-Elmer DSC-7, Norwalk, CT). The instrument was calibrated against indium. Aliquots of sample (~15 mg) were temperature cycled in the DSC from 50°C to 10°C to 50°C at 5°C min^{-1} and the crystallization and melting points was taken from the onset temperature of peaks on the thermogram using Pyris data analysis software (version 3.52, Perkin-Elmer Corporation, Norwalk, CT). All analyses were conducted in triplicate.

Addition of aroma compounds to emulsions. The relative concentrations of four aroma compounds were selected so that after partitioning with an emulsion each compound would give a readily quantifiable peak from 1 ml of headspace sample on a gas chromatogram. Four aroma compounds ethyl butanoate (EB), ethyl pentanoate (EP), ethyl heptanoate (EH) and ethyl octanoate (EO) were mixed in a volumetric ratio of 1:2:20:20 and diluted in an equal volume of ethyl alcohol.

The initial 40% (w/w) emulsion was diluted with deionized water to produce a series of samples with different oil contents. Aliquots (2 mL) of each emulsion were added to 20 mL headspace (HS) vials (MicroLiter Analytical Supplies, Inc., Suwanee, GA, USA) which were temperature-cycled to produce either wholly solid or wholly liquid droplets (see below for more discussion of the crystallization behavior of emulsified n-eicosane and the temperature cycling protocol). Stock aroma solution (860 μL/L of emulsion) was added to the emulsions so that the final concentrations (μL/L) of aroma compounds in the emulsion were ethyl butanoate, 10; ethyl pentanoate, 20; ethyl heptanoate, 200; and ethyl octanoate 200. The vials were sealed with poly-(tetrafluoroethylene)/ butyl rubber septa (MicroLiter Analytical Supplies, Inc., Suwanee, GA, USA) and equilibrated at 30ºC for at least 1 hour prior to analysis. Note that work reported below shows that the headspace concentration of volatiles above both solid and liquid emulsions is independent of time for periods between one hour and over a week suggesting this equilibration time is sufficient.

Headspace analysis by gas chromatograph. After equilibration, a sample of the headspace (1 mL) was withdrawn using an autosampler (Combi-Pal, CTC Analytics, Carrboro, NC, USA) and injected into a gas chromatograph (Agilent 6890, Agilent Technologies, Palo Alto, CA, USA) equipped with a DB-5 capillary column (30 m×0.32 mm i.d. with a 1 μm film thickness) and a flame ionization detector. The operating conditions were as follows: sample was injected in splitless mode (purge value on at 1 min); inlet temperature was 200ºC, detector was 250ºC, oven program was 30ºC for 1 min, then increased at 35ºC min^{-1} from 30 to 200ºC and held for 2 min; carrier constant flow rate 2.0 mL min^{-1} (H_2). Static headspace concentrations were determined from peak areas using a standard calibration curve ($R^2 = 0.99$). All measurements are expressed as the mean and standard deviation of at least two full experimental replicates.

Gas-water and gas-oil partition coefficients for each aroma compound were determined using the same HS GC protocol as above. Mixed aroma stock [12.5 – 800 μL/L (v/v)] was added to HS vials containing 2 mL of either water or the lipid. The vials were sealed and equilibrated at 30ºC for at least 1 hour before measuring the headspace volatile concentrations by GC.

3.3 Results and Discussion

The emulsions were unimodal with approximately log-normal distributions (standard deviation of distribution ~0.19±0.2 μm). The particle size could be controlled by varying the homogenization conditions Table **3.1**.

Table **3.1**: Mean droplet size (d_{32}) of emulsions under different homogenization conditions

Homogenization Pressure (MPa)	Homogenization time (minute)	Emulsion mean droplet size (d_{32}) (μm)
14±1	3	0.97 ± 0.12
25±1	8	0.44 ± 0.05
59±1	8	0.28 ± 0.02

Crystallization of eicosane. A DSC thermogram of emulsified eicosane (40% w/w) is shown in Figure **3.1**. Both the bulk eicosane (data not shown) and emulsified eicosane droplets melted at 36°C but while the bulk lipid crystallized at 35ºC (i.e., 1°C of supercooling), emulsified eicosane droplets crystallized at 22ºC (i.e., 13ºC of supercooling). Deep supercooling is characteristic of emulsified alkanes (Cramp, Docking, Ghosh and Coupland, 2004) and is thought to be due to a homogeneous nucleation mechanism (Coupland, 2002). The supercooled eicosane is very stable and it was possible to maintain liquid droplets at 30°C for several weeks without measurable crystallization. Therefore by adjusting the temperature history of the eicosane emulsion it was possible to produce either solid or liquid lipid droplets of the same chemical composition at the same temperature (30°C):

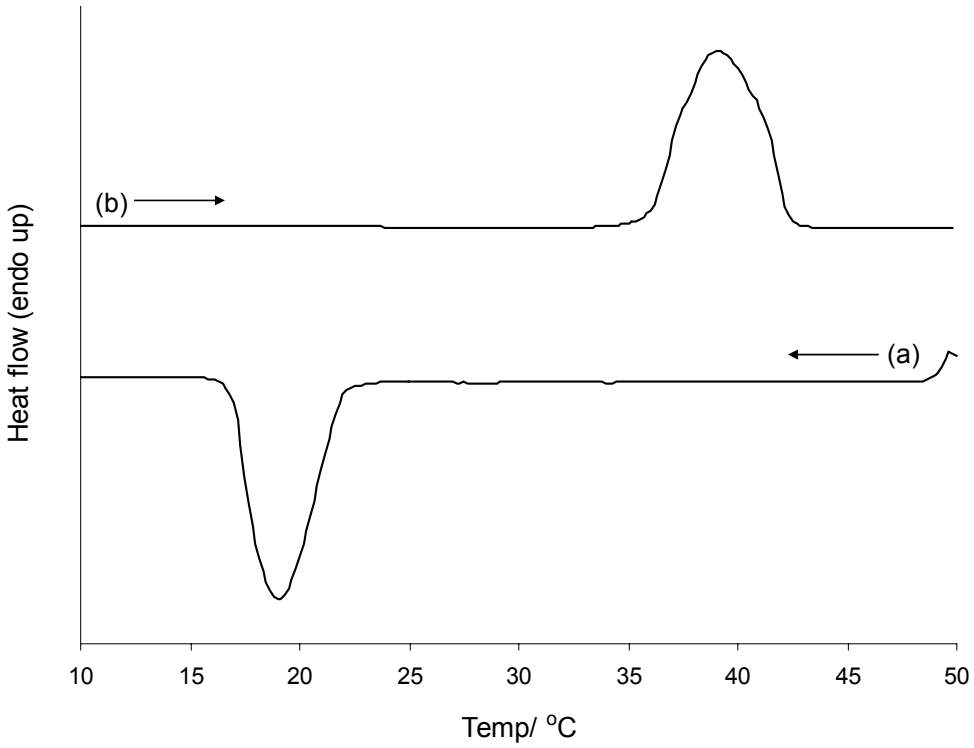

Figure **3.1**: Thermogram of n-eicosane emulsion during (a) cooling, (b) heating. The emulsion was 40 wt% lipid stabilized with 2 wt% sodium caseinate solution and was cooled and heated at 5°C min^{-1}.

- solid lipid droplets: cool from storage temperature (40°C) to 10°C to induce crystallization then reheat to the experimental temperature (30°C).
- liquid lipid droplets : cool from the storage temperature (40°C) to the experimental temperature (30°C).

Note that while an emulsion is defined as a fine dispersion of one liquid in a second, largely immiscible liquid (McClements, 2004) the term is also used for the solid droplets used in this study.

Determination of partition coefficients. Solutions of the aroma compounds cocktail were prepared in water or lipid and the HS volatile concentrations were measured as a function of solution concentration. The headspace concentration initially increased linearly with solution concentration, but for EH and EO in water, the headspace concentrations reached a plateau value at the aqueous solubility limit and further additions of volatiles lead to the formation of a separate surface phase on the water. The partition coefficients were determined from the slope of the linear portion of the plot (data not shown) and the aroma concentrations used elsewhere in this study were all within the linear region. The gas-oil (K_{go}) and gas-water (K_{gw}) partition coefficients were determined against the lipid ($R^2 = 0.91$) or water ($R^2 = 0.97$) phase concentration while the oil-water partition coefficient (K_{ow}) was calculated from the ratio of gas-water to gas-oil partition coefficients (Table **3.2**).

Table **3.2**: Air-water (K_{aw}), air-oil (K_{ao}) and oil-water (K_{ow}) partition coefficients and surface binding coefficient (K^*_{iw}) of aroma compounds.

Flavor compounds	K_{aw}	K_{ao}	K_{ow}	K^*_{iw} *(m)*
Ethyl Butanoate	7.35×10^{-3}	2.0×10^{-4}	36.75	-
Ethyl Pentanoate	9.02×10^{-3}	7.0×10^{-5}	128.86	2.2×10^{-7}
Ethyl Heptanoate	1.82×10^{-2}	6.0×10^{-6}	3033.33	4.3×10^{-3}
Ethyl Octanoate	2.67×10^{-2}	2.0×10^{-6}	13350	1.6×10^{-5}

It should be mentioned that as bulk eicosane does not show a large supercooling and is solid at the temperature used for the experiments (30°C), n-hexadecane was selected as an analog for gas-liquid lipid partition coefficient determination. The physical properties of the two liquid alkanes are very similar (Weast, 1975) and it is expected that their partitioning behaviors will also be similar. Indeed, in an experiment to compare the effect of two alkanes the HS volatile concentration from both liquid eicosane

and hexadecane emulsion were measured with different lipid content and no significant difference in the results were found (data not shown).

Partitioning behavior of liquid lipid emulsions. Aliquots of the aroma compounds mixture were equilibrated with liquid eicosane emulsions and the headspace concentration measured as a function of emulsion lipid content and emulsion particle size. Similar experiments were also conducted with unhomogenized mixtures of bulk lipid (again hexadecane was used in place of eicosane in the bulk studies to ensure the lipid remained liquid) and water with the same compositions as the emulsions. Gas-emulsion partition coefficient (K_{ge}) values were calculated from the HS concentration data for each emulsion and for the bulk mixture and are plotted as a function of lipid concentration in Figure **3.2**. These data were modeled using Equation 3.3 and the partition coefficients established for the pure bulk phases reported in Table **3.2**. In applying this model it was assumed that the aqueous caseinate-volatile interactions are negligible, and indeed in preliminary work it was observed that repeating the experiment with different concentrations of aqueous caseinate (0.2 and 2% w/w) did not affect the results.

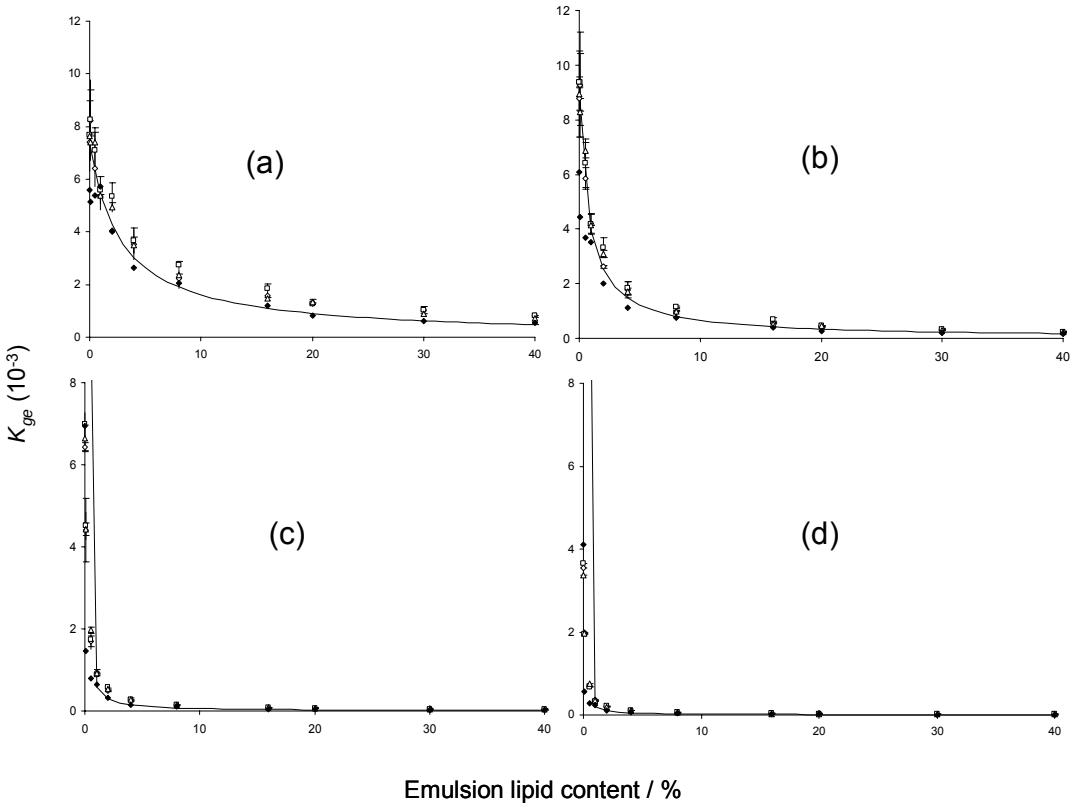

Figure **3.2**: Gas-emulsion partition coefficient (K_{ge}) of aroma compounds as a function of lipid content of emulsions with liquid lipid (a) ethyl butanoate, (b) ethyl pentanoate, (c) ethyl heptanoate and (d) ethyl octanoate. Results for emulsions with different particle sizes (d_{32}) 0.97 μm (◊), 0.44 μm (□) and 0.28 μm (Δ) are shown along with bulk lipid and water mixture (♦). Predicted lines (from Equation 3.3) are shown for each compound alongside the experimental data points. Note the difference in scales for K_{ge} values used in the different plots.

The partition coefficient of all volatiles decreased with lipid content but there was no effect of emulsion particle size. The unhomogenized samples behaved similarly to the homogenized samples (Figure **3.2**). As anticipated, the effect of lipid content was greater for the non-polar volatiles (EH and EO) than for the polar compounds (EB and EP) due to their lower oil-water partition coefficients. The model based on the independent measurements of bulk partitioning behavior (Equation 3.3) agreed reasonably with the experimental results for the emulsions (average r^2 for model

prediction 0.96±0.04). In the next series of experiments these studies were repeated using solid droplets.

Partitioning behavior of solid lipid emulsions. The headspace concentrations of the four volatile compounds were measured as a function of lipid content for emulsions of solid eicosane droplets and the gas-emulsion partition coefficient (K_{ge}) values were calculated from the HS concentration data as before (Figure **3.3**). To allow comparison, average values for liquid lipid droplets measured above are shown alongside these data. (Note that the plots for EH and EO were plotted in a different scale to show the effects of droplet particle size on the K_{ge} values.) The gas-emulsion partition coefficients (K_{ge}) for solid lipid emulsions were higher than those of liquid lipid emulsions for all four aroma compounds. Moreover, the K_{ge} values for EH and EO decreased monotonically with lipid concentration, suggesting an association of aroma molecules with solid lipid droplets.

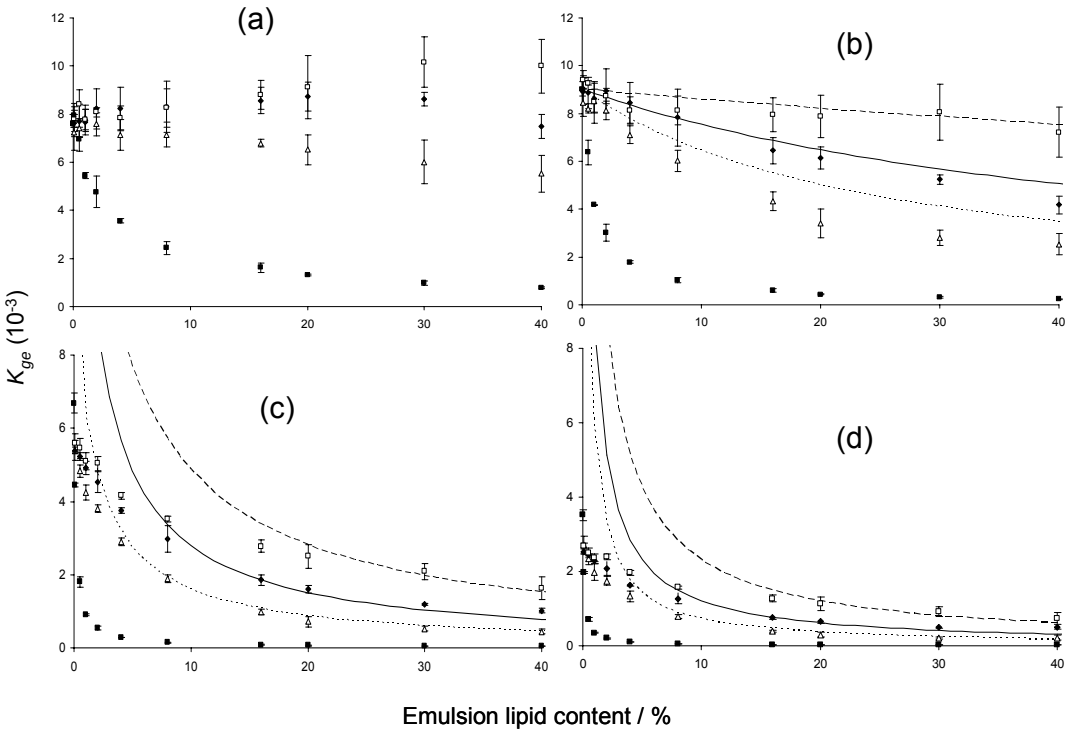

Figure **3.3**: Gas-emulsion partition coefficient (K_{ge}) of aroma compounds as a function of lipid content of emulsions with solid lipid (a) ethyl butanoate, (b) ethyl pentanoate, (c) ethyl heptanoate and (d) ethyl octanoate. Results for emulsions with different particle sizes (d_{32}) 0.97 μm (□), 0.44 μm (♦) and 0.28 μm (Δ) are shown along with the model predicted lines (from Equation 3.4) for three different particle size 0.97 μm (– – –), 0.44 μm (——) and 0.28 μm (----). For comparison the average values from the corresponding liquid lipid emulsion (■) are also shown. Note the difference in scales for K_{ge} values used in the different plots.

Notably the smaller solid particles had a bigger effect on K_{ge} than the larger ones suggesting the interaction may depend on droplet surface area rather than volume. The specific surface area (m^2m^{-3}) of the solid emulsions was calculated from

$$A_s = \frac{6\phi}{d_{32}} \tag{3.4}$$

(where ϕ is the lipid volume fraction and d_{32} is the volume-surface mean diameter) and used to replot the data from Figure **3.3** (as Figure **3.4**). Plotted in terms of

interfacial area, K_{ge} is independent of particle size, supporting the hypothesis that the bound volatiles are adsorbed at the droplet surface. The effect is more significant for the higher molecular weight volatiles (more hydrophobic) EH and EO than EB and EP indicating that polarity of aroma compounds influence their surface adsorption ability. The term volatile binding is used here to describe any physical association of aroma compounds (adsorption as well as absorption) to lipid phase.

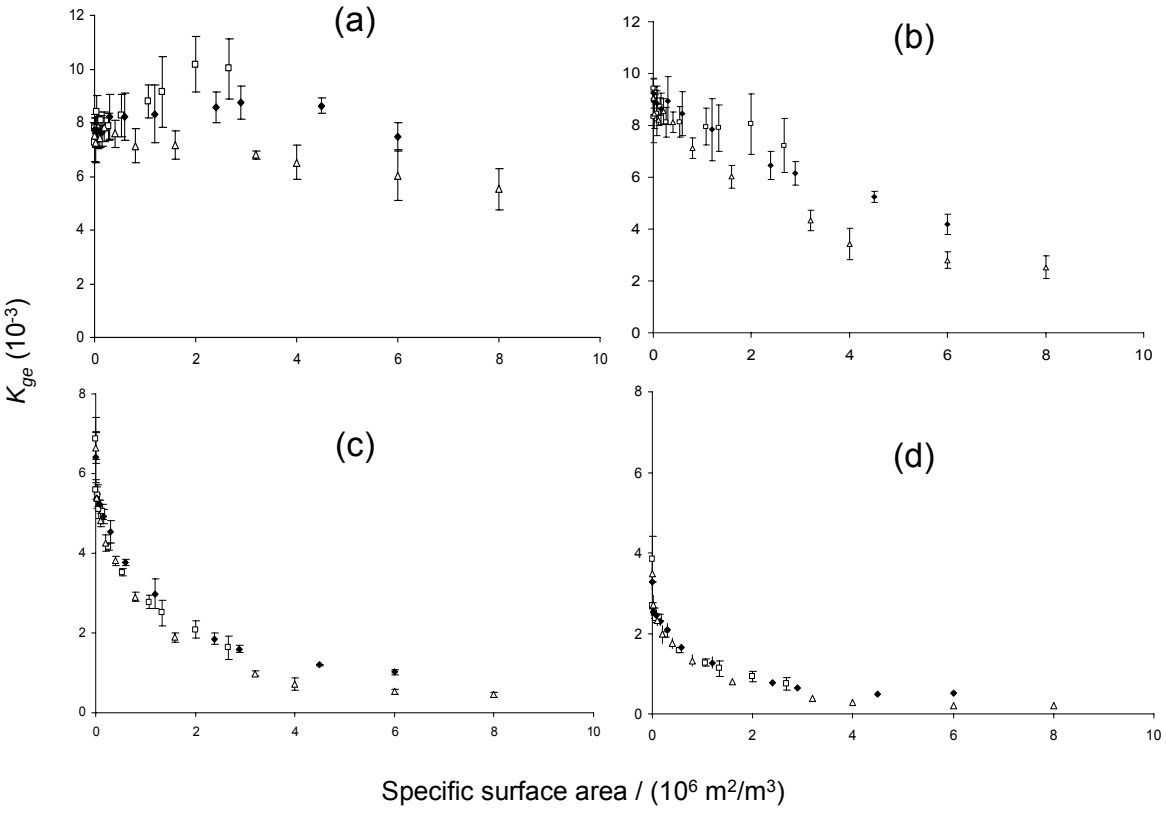

Figure **3.4**: Gas-emulsion partition coefficient (K_{ge}) of aroma compounds as a function of specific surface area of lipid droplets of emulsions with solid lipid (a) ethyl butanoate, (b) ethyl pentanoate, (c) ethyl heptanoate and (d) ethyl octanoate. The particle sizes (d_{32}) of emulsions with solid lipid droplets were 0.97 μm (□), 0.44 μm (♦) and 0.28 μm (Δ).

This type of surface adsorption was proposed by Maier (Maier, 1975) who showed that although the amount of volatiles bound by solid trilaurin was much less than that bound by liquid tributyrin, the initial rate of sorption was much faster for the solid lipid indicating the process occurred at the surface. However, this is in contrast with the findings of McNulty et al. (1973b) and Roberts et al. (2003) who proposed that only liquid oil could bind aroma compounds. One reason for the apparent disparity between the present work and the Roberts et al. (2003) paper may be due to the relatively low-fat emulsions used in their experimental design (1.38% wt/vol) and consequently less interfacial area to adsorb aroma compounds. Also a partially crystalline lipid was used in Roberts et al. (2003) study in comparison with complete solid lipid used in the present work.

In order to model aroma release from emulsion with solid lipid droplets an additional term is required to account for surface binding in Equation 3.3 (McClements, 2004):

$$\frac{1}{K_{ge}} = \frac{\phi_o}{K_{ow}} + \frac{\phi_w}{K_{gw}} + \frac{K^*_{iw}.A_s}{K_{gw}} \tag{3.5}$$

where A_s is the interfacial area per unit volume of emulsion and K^*_{iw} is the apparent surface binding coefficient defined as:

$$K^*_{iw} = \frac{\Gamma_i}{C_w} \tag{3.6}$$

where Γ_i is the surface load, i.e., volume of aroma compound per unit interfacial area ($\mu l/m^2$).

To model the binding effects of solid emulsion droplets it was assumed that the volatiles can only interact with the surface of the crystalline lipid and thus the first term on the right hand side of Equation 3.5 can be neglected.

Surface load (Γ_i) was calculated from the data shown in Figure **3.4** and the air-water partition coefficient in Table **3.2** assuming that volatiles present in the HS are at equilibrium with the emulsion aqueous phase and that the total amount of aroma compounds added are distributed between the HS, the aqueous phase and the surface of solid droplets (Figure **3.5**). However, this calculation was not performed for EB, as this compound showed no measurable surface binding. The surface load increased slowly with equilibrium aqueous phase concentration (C_w) up to a critical value, then rapidly beyond that. It should be noted that the sharp increase in surface load which occurs at a high aqueous phase concentration corresponds to a very dilute emulsion (<1% lipid).

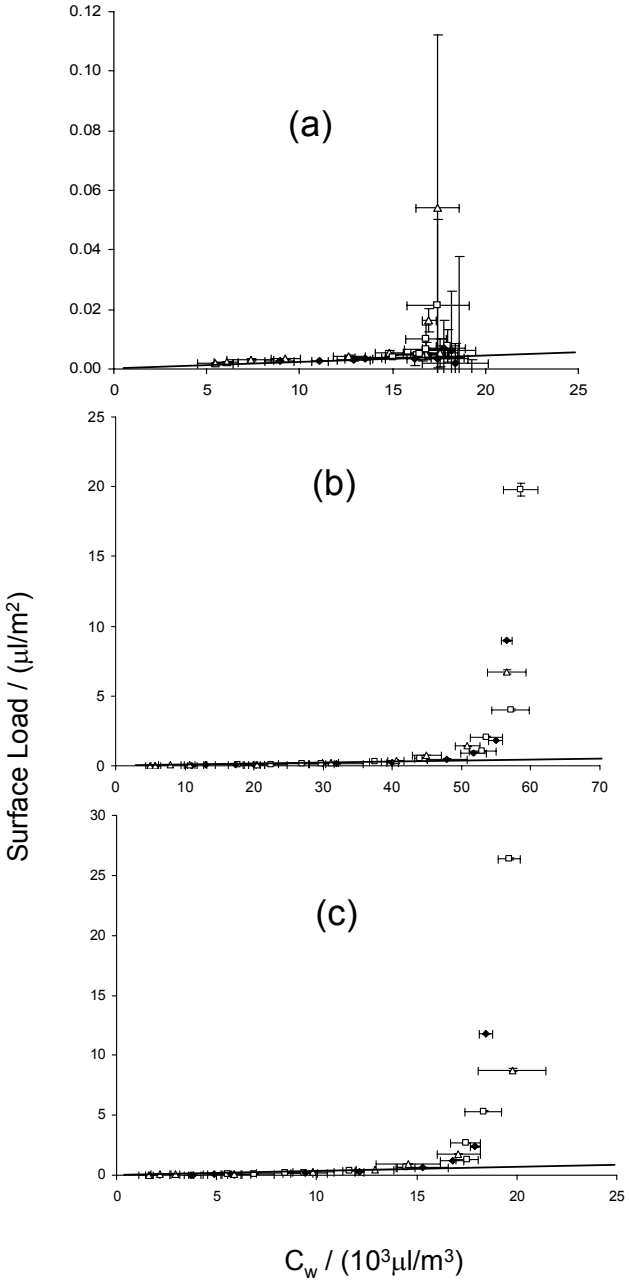

Figure **3.5**: Surface adsorption isotherm of aroma compounds (a) ethyl pentanoate, (b) ethyl heptanoate and (c) ethyl octanoate at 30ºC. Values of surface load (volume of aroma compounds adsorbed per unit area of droplet surface) are plotted as a function of aqueous phase aroma concentration. Results for emulsions with solid lipid particle sizes (d_{32}) 0.97 μm (□), 0.44 μm (♦) and 0.28 μm (Δ) are shown along with the best fit line to the linear portion of the graph. Note the difference in scales used in the different plots.

At low values of C_w, below the critical value, K^*_{iw} was calculated from the slope of the best fit line to the linear portion of the curve (Figure **3.5**) and reported in Table **3.2.** However this value is only representative below the critical value and does not account for the behavior at higher C_w. The K^*_{iw} calculated in this manner was used in Equation 3.5 to calculate the corresponding gas-emulsion partition coefficient (K_{ge}). The model predicted K_{ge} values agreed well with the experimental data (Figure **3.3,** average r^2 for model prediction 0.85±0.13) but overestimated the experimental partition coefficients at lower lipid contents (ϕ <~10%). Lower lipid content emulsions have higher aqueous volatile concentrations and consequently lie beyond the critical value seen in Figure **3.5** where the simple single value of K^*_{iw} cannot be expected to adequately model the data. (It was not possible to model the EB data by this method as adequate measurement of K^*_{iw} was not obtained due to the small amount of adsorption to the solid lipid surface.)

Figure **3.5** represents a surface adsorption isotherm for volatiles onto solid lipid droplets and bears some physical similarity to the moisture sorption isotherm of some sugars (Bronlund and Paterson, 2004; Lammert, Schmidt and Day, 1998; Mathlouthi and Roge, 2003). In dry conditions, sugars adsorb small amounts of moisture roughly proportional to the humidity of the gas surrounding them but at a critical humidity the moisture content of the sugars rapidly increases as they dissolve in the adsorbed water. Extending the physical analogy to the current case it seems adsorption at low values of C_w follows a simple proportionality, but at the critical value the system suddenly changes so the amount of adsorbed volatile increases. My hypothesis is that the initial adsorption is of isolated volatile molecules but at the critical level the adsorbed molecules begin to interact to an extent that they can be treated as a separate thermodynamic phase and begin to dissolve the solid lipid. More volatile added will rapidly dissolve in this new phase increasing the amount bound. This seems to be true for the relatively non-polar compounds (EO and EH) as more polar compound have less surface affinity (EB). However, if this hypothesis is correct, dispersions of solid particles in aqueous phases with high C_w (i.e., low lipid, high added volatiles) should effectively dissolve in the

aroma molecules and have no detectable crystallinity. Similar associations were seen in studies of solid lipid nanoparticles used for drug delivery by Bunjes, Drechsler, Koch and Westesen (2001) who proposed that while a portion the solute firmly associated with solid particle (either incorporated into crystal structure or adsorbed on surface), excess adheres as a liquid phase to the droplet surface. Westesen, Bunjes and Koch (1997) also found formation of liquid triglycerides at higher drug load on solid lipid nanoparticles indicating similar behavior as observed here. In the drug delivery studies, however, the drug components were added to lipid phase before homogenization, whereas in this study the aroma compounds were added after homogenization and droplet crystallization. Nevertheless, as shown below, the lipid- volatile interactions were reversible with respect to droplet crystallization and similar behavior is expected if the volatiles were added to lipid before homogenization.

To test the hypothesis, DSC was used to measure the ratio of the melting enthalpies between emulsions prepared with and without added volatiles (only the emulsion with d_{32} = 0.44 μm was used) and the difference between the two enthalpies was expressed as solid fat content (Figure **3.6**). The surface loads of EH (from Figure **3.5**) are shown along with the solid fat content data. EP and EO also follow similar behavior as EH in Figure **3.6**, however, only the data for EH were shown to maintain clarity. The particles remained crystalline for $\phi > 4\%$ but at lower lipid contents the solid fat content rapidly decreases. This transition coincides with the critical point in the surface binding isotherm and supports the hypothesis that the crystalline droplets can be dissolved if sufficient volatile adsorbs to their surface.

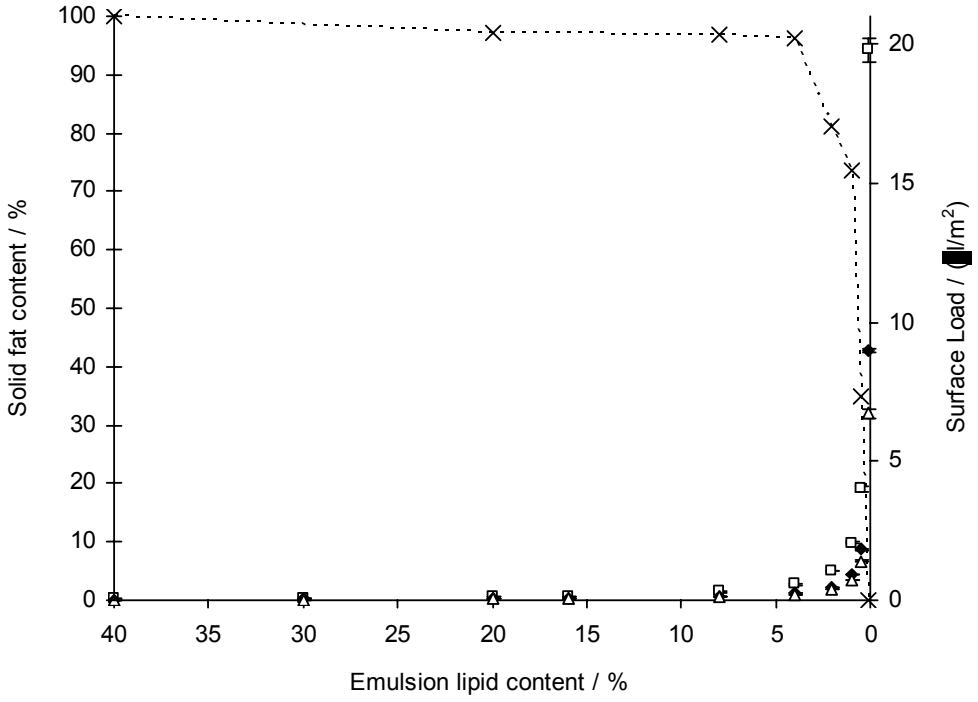

Figure **3.6**: Calculated values of percent solid lipid in emulsions as a function of lipid content (--X--). Percent solid lipid were calculated from the difference between the melting enthalpies of lipid in emulsions (d_{32} = 0.44μm) prepared with and without added volatiles. Surface loads of only ethyl heptanoate were shown as a function of emulsion lipid content along side the solid fat content data to maintain clarity. Particle sizes (d_{32}) of emulsions are 0.97 μm (□), 0.44 μm (♦) and 0.28 μm (Δ)

Reversibility. Finally, the reversibility of the interactions between volatiles and the solid and liquid emulsion droplets, the aqueous phase and the headspace was tested in a time series experiments in which flavored emulsions were temperature cycled to produce alternately solid and liquid particles. The concentration of headspace volatiles above samples of emulsion (ϕ=20% and 40% w/w, d_{32}=0.44μm) were measured at 30ºC over several days. The experiment started with liquid lipid emulsions and at intervals, the emulsions were (i) crystallized (cooling to 10ºC) then reheated to the analysis temperature (30ºC) before continued monitoring (now with solid lipid droplets) and (ii)

melted (heating to 50ºC) once more before returning again to 30°C (with liquid lipid droplet). Three separate vials were used for each analysis and then discarded.

The HS concentrations of all the aroma compounds were plotted as a function of time in Figure **3.7** for both 40% (w/w) and 20% (w/w) lipid emulsions. The HS concentrations of all compounds increased dramatically on droplet crystallization (74 h) as the volatiles were expelled from the solid lipid (although a smaller fraction will adsorb at the solid surface). Thereafter the HS concentration from solid droplet emulsions were measured for several days and no significant change were observed. On re-melting (507 h) the aroma compounds were reabsorbed by liquid lipid and the HS volatile concentrations returned to the same levels as at the beginning of the experiment. Further temperature cycles were also repeatable, indicating the lipid-volatile interactions were reversible. Figure **3.7** also showed that emulsions with more solid lipids (40% w/w) had less aroma compounds in the headspace because they had more solid surface for aroma adsorption. However, for the EB 40% solid lipid droplet emulsion had a higher HS concentration than the corresponding 20% emulsion as this compound does not measurably bind to the solid surface.

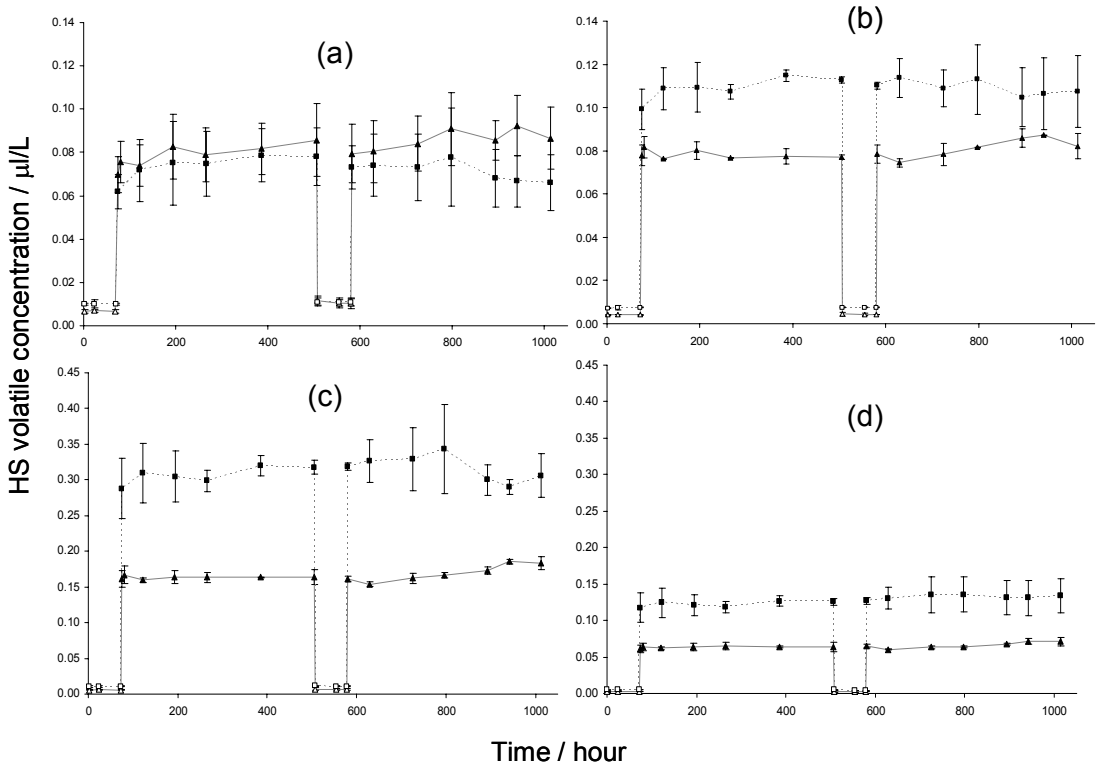

Figure **3.7**: HS concentrations of aroma compounds at 30ºC from 40% emulsion (▲) and 20% emulsion (■) with liquid lipid (open symbol) and solid lipid (closed symbol) as a function of time (a) ethyl butanoate, (b) ethyl pentanoate, (c) ethyl heptanoate, and (d) ethyl octanoate. Note the difference in scales for HS volatile concentration used in the different plots.

The fact that the binding of volatiles was reversible suggests the process is thermodynamically driven and, at least in this case, the compounds are not trapped in the lipid structure. This is in contrast with the results of Roberts et al. (2003) who proposed that absorbed aroma compounds in liquid oil were entrapped by solid fat during crystallization. However, the chemical nature of the lipid used (hydrogenated palm fat) was considerably different than pure n-eicosane used in the present study and this could influence flavor-fat interactions considerably. In the study of controlled drug release using solid lipid nanoparticles it was observed that while lipids forming crystals with perfect lattice lead to drug expulsion, complex lipid mixtures forming less perfect crystals

can accommodate the drugs (Muller, Mader and Gohla, 2000). Similarly, in the present work, n-eicosane crystallized in pure form (Ueno, Hamada and Sato, 2003) and mutually excluded all the foreign materials present.

3.4 Conclusions

From this work it can be concluded that: (i) the interactions of volatile molecules with liquid lipid emulsions can be described in terms of a three-phase partitioning (Equation 3.3), (ii) more non-polar volatiles can interact with the surface of solid lipid droplets, (iii) the binding of volatiles on solid lipid surfaces is proportional to the aqueous concentration up to a critical value then rapidly increases. The critical point corresponds to dissolution of the solid lipid in a phase of adsorbed volatile, (iv) the binding is thermodynamically driven and is reversible.

Acknowledgements

This work was partially funded by a grant from the Center for Food Manufacturing (The Pennsylvania State University).

3.5 References

Bakker, J.; Mela, D. J., Effect of emulsion structure on flavor release and taste perception. In *Flavor-Food Interactions*, McGorrin, R. J.; Leland, J. V., Eds. American Chemical Society: Washington, D.C., **1996**; Vol. 633.

Bronlund, J.; Paterson, T., Moisture sorption isotherms for crystalline, amorphous and predominantly crystalline lactose powders. *International Dairy Journal* **2004,** 14, (3), 247-254.

Bunjes, H.; Drechsler, M.; Koch, M. H. J.; Westesen, K., Incorporation of the model drug ubidecarenone into solid lipid nanoparticles. *Pharmaceutical Research* **2001,** 18, (3), 287-293.

Buttery, R. G.; Guadagni, D. G.; Ling, L. C., Flavor compounds: volatilities in vegetable oil and oil-water mixtures. Estimation of odor thresholds. *Journal of Agricultural and Food Chemistry* **1973,** 21, (2), 198-201.

Carey, M. E.; Asquith, T.; Linforth, R. S. T.; Taylor, A. J., Modeling the partition of volatile aroma compounds froma cloud emulsion. *Journal of Agricultural and Food Chemistry* **2002,** 50, 1985-1990.

Charles, M.; Lambert, S.; Brondeur, P.; Courthaudon, J.; Guichard, E., Influence of formulation and structure of an oil-in-water emulsion on flavor release. In *Flavor Release*, Roberts, D. D.; Taylor, A. J., Eds. American Chemical Society: Washington, D.C., **2000**; pp 342-355.

Coupland, J. N., Crystallization in emulsions. *Current Opinion in Colloid & Interface Science* **2002,** 7, (5-6), 445-450.

Cramp, G. L.; Docking, A. M.; Ghosh, S.; Coupland, J. N., On the stability of oil-in-water emulsions to freezing. *Food Hydrocolloids* **2004,** 18, (6), 899-905.

Dubois, C.; Sergent, M.; Voilley, A., Flavoring of complex media: a model cheese example. In *Flavor-Food Interactions*, McGorrin, R. J.; Leland, J. V., Eds. American Chemical Society: Washington, D.C., **1998**; Vol. 633, pp 213-226.

Friel, E. N.; Taylor, A. J., Effect of salivary components on volatile partitioning from solutions. *Journal of Agricultural and Food Chemistry* **2001,** 49, (8), 3898-3905.

Guichard, E., Interactions between flavor compounds and food ingredients and their influence on flavor perception. *Food Rev. Int.* **2002,** 18, (1), 49-70.

Harrison, M.; Hills, B. P.; Bakker, J.; Clothier, T., Mathematical model of flavor release from liquid emulsion. *Journal of Food Science* **1997,** 62, (4), 653-658.

Laing, D. G.; Jinks, A., Flavour perception mechanisms. *Trends in Food Science & Technology* **1996,** 7, (12), 387-389.

Lammert, A. M.; Schmidt, S. J.; Day, G. A., Water activity and solubility of trehalose. *Food Chemistry* **1998,** 61, (1-2), 139-144.

Landy, P.; Courthaudon, J. L.; Dubois, C.; Voilley, A., Effect of interface in model food emulsions on the volatility of aroma compounds. *J. Agric. Food Chem.* **1996,** 44, (2), 526-530.

Maier, H. G., Binding of volatile aroma substances to nutrients and foodstuffs. In *Proceedings of international symposium on aroma research*, Maarse, H., Groenen, P.J., Ed. Pudoc: Wageningen, **1975**; pp 143-157.

Mathlouthi, M.; Roge, B., Water vapor sorption isotherms and the caking of food powders. *Food Chemistry* **2003,** 82, (1), 61-71.

McClements, D. J., *Food Emulsions - Principles, Practices, and Techniques*. 2nd ed.; CRC Press: New York, **2004**.

McNulty, P. B.; Karel, M., Factors affecting flavor release and uptake in O/W emulsions, 1. Release and uptake models. *Journal of food Technology* **1973a,** 8, 309-318.

McNulty, P. B.; Karel, M., Factors affecting flavor release and uptake in O/W emulsions, 2. Stirred cell studies. *Journal of Food Technology* **1973b,** 8, 319-331.

McNulty, P. B.; Karel, M., Factors affecting flavor release and uptake in O/W emulsions, 3. Scale-up model and emulsion studies. *Journal of Food Technology* **1973c,** 8, 415-427.

Meynier, A.; Garillon, A.; Lethuaut, L.; Genot, C., Partition of five aroma compounds between air and skim milk, anhydrous milk fat or full-fat cream. *Lait* **2003,** 83, 223-235.

Muller, R. H.; Mader, K.; Gohla, S., Solid lipid nanoparticles (SLN) for controlled drug delivery - a review of the state of the art. *European Journal of Pharmaceutics and Biopharmaceutics* **2000,** 50, (1), 161-177.

O'Neill, T. E., Flavor binding by food proteins: an overview. In *Flavor- Food Interactions*, McGorrin, R. J.; Mela, D. J., Eds. American Chemical Society: Washington, D.C., **1996**; pp 58-74.

Overbosch, P.; Afterof, W. G. M.; Haring, P. G. M., Flavor release in the mouth. *Food Reviews International* **1991,** 7, (2), 137-184.

Philippe, E.; Seuvre, A. M.; Colas, B.; Langendorff, V.; Schippa, C.; Voilley, A., Behavior of flavor compounds in model food systems: a thermodynamic study. *J. Agric. Food Chem.* **2003,** 51, (5), 1393-1398.

Pionnier, E.; Nicklaus, S.; Chabanet, C.; Mioche, L.; Taylor, A. J.; Le Quere, J. L.; Salles, C., Flavor perception of a model cheese: relationships with oral and physico-chemical parameters. *Food Quality and Preference* **2004,** 15, (7-8), 843-852.

Rabe, S.; Krings, U.; Berger, R. G., Influence of oil-in-water emulsion characteristics on initial dynamic flavour release. *Journal of the Science of Food and Agriculture* **2003,** 83, (11), 1124-1133.

Roberts, D. D.; Pollien, P., Relative influence of milk components on flavor compounds volatility. In *Flavor Release*, Roberts, D. D.; Taylor, A. J., Eds. American Chemical Society: Washington, D.C., **2000**; pp 321-332.

Roberts, D. D.; Pollien, P.; Watzke, B., Experimental and modeling studies showing the effect of lipid type and level on flavor release from milk-based liquid emulsions. *Journal of Agricultural and Food Chemistry* **2003,** 51, 189-195.

Roberts, D. D.; Taylor, A. J., Flavor release: a rationale for its study. In *Flavor Release, ACS symposium series*, Roberts, D. D.; Taylor, A. J., Eds. American Chemical Society: Washington, D.C., **2000**; Vol. 763, pp 1-3.

Seuvre, A. M.; Espinosa Diaz, M. A.; Voilley, A., Transfer of aroma compounds through lipidic-aqueous interface in a complex system. *J. Agric. Food Chem.* **2002,** 50, 1106-1110.

Taylor, A. J.; Linforth, R. S. T., Flavour release in the mouth. *Trends in Food Science & Technology* **1996,** 7, (12), 444-448.

Ueno, S.; Hamada, Y.; Sato, K., Controlling polymorphic crystallization of n-alkane crystals in emulsion droplets through interfacial heterogeneous nucleation. *Crystal Growth & Design* **2003,** 3, (6), 935-939.

Voilley, A.; Espinosa Diaz, M. A.; Landy, P., Flavor release from emulsions and complex media. In *Flavor Release*, Roberts, D. D.; Taylor, A. J., Eds. American Chemical Society: Washington, D.C., **2000**; pp 142-152.

Weast, R. C., *Handbook of Chemistry and Physics*. 56 ed.; CRC press: Cleveland, Ohio, **1975**.

Wedzicha, B. L., Distribution of low molecular weight food additives in dispersed systems. In *Advances in Food Emulsions*, Dickinson, E.; Stainsby, G., Eds. Elsevier: London, UK, **1988**; pp 329-371.

Westesen, K.; Bunjes, H.; Koch, M. H. J., Physicochemical characterization of lipid nanoparticles and evaluation of their drug loading capacity and sustained release potential. *Journal of Controlled Release* **1997,** 48, (2-3), 223-236.

Chapter 4

Flavor binding by Solid and Liquid Emulsion droplets: Surface Adsorption and Droplet Dissolution Model

Abstract

The binding of a mixture of flavors (ethyl butanoate, ethyl pentanoate, ethyl heptanoate and ethyl octanoate) to model emulsions (n-eicosane stabilized with sodium caseinate) was studied by headspace gas chromatography. Emulsified eicosane shows deep supercooling, so by adjusting the temperature history it was possible to produce solid and liquid droplets with the same composition at the same experimental temperature (30°C). The binding of flavors by the liquid droplets could be modeled well in terms of the bulk oil-gas and water-gas headspace partition coefficients and the volume fraction of the phases. However, the binding of flavor by solid droplets depended on the specific surface area suggesting a surface-binding mechanism. Repeated melting and crystallization of the droplets showed all binding effects were reversible.

An effective surface binding coefficient was defined for each flavor as the ratio of aqueous to interfacial concentration. This value was constant up to a critical value at which point it increased dramatically as the droplets bound much more volatile. The increase coincided with an apparent dissolution of the solid droplets in the adsorbed volatile (as measured by a decrease in the measured melting enthalpy). Using the surface binding coefficient and bulk partition coefficients it is possible to model the volatile binding by solid and liquid emulsion droplets.

4.1 Introduction

The concentration of volatile molecules in the headspace is amongst the most important parameters determining the sensory qualities of a food. The perceived aroma depends both on the total concentration of volatiles in the product but also the extent to which they are bound by the food. For a system at equilibrium, the distribution of a given volatile between the food and the headspace gas is given by its partition coefficient:

$$K_{ge} = \frac{c_g}{c_e} \tag{4.1}$$

where c_g and c_e are the concentrations of the volatile compounds in the headspace and the food respectively. (Formally this should be written in terms of activity, but as the concentrations of volatiles are typically very low, the differences are negligible). In a multiphase food, the volatiles will distribute between all of the available phases according to the relevant partition coefficients and these can be combined into an effective partition coefficient for the food; for example in a food emulsion the effective partition coefficient (K_{ge}) is related to both the volume fraction of oil (ϕ_o) and the gas-oil (K_{go}) and gas-water (K_{gw}) partition coefficients respectively:

$$\frac{1}{K_{ge}} = \frac{\phi_o}{K_{go}} + \frac{(1-\phi_o)}{K_{gw}} \tag{4.2}$$

Equation 4.2 has proved useful in modeling the effects of changing liquid oil concentration on the headspace concentration of volatiles above an emulsion (Bakker and Mela, 1996; Charles, Lambert, Brondeur, Courthaudon and Guichard, 2000; Harrison, Hills, Bakker and Clothier, 1997) however the interaction with solid fats is less clear, with some workers arguing that solid fat does not interact with volatile molecules (McNulty and Karel, 1973; Roberts, Pollien and Watzke, 2003) while others suggest

there may be some binding of the aroma compounds to the crystalline fat (Maier, 1975). The goal of this work is to examine in more detail the interactions between solid fat and aroma molecules in a model food emulsion.

4.2 Materials and Methods

Unless otherwise stated, all ingredients were purchased from the Sigma Chemical Company (St. Louis, MO). Emulsions were prepared by mixing n-eicosane (40% w/w, Fisher Scientific, Springfield, NJ)) with sodium caseinate solution (2 wt%, containing 0.02 wt% thimerosal as an antibacterial agent) using a high-speed blender (Brinkmann Polytron, Brinkmann Instruments Inc., Westbury, NY) then re-circulated through a twin-stage valve homogenizer (Niro Soavi Panda, GEA Niro Soavi, Hudson, WI) for several minutes at different pressures (15-60 MPa) to achieve multiple passes through the valves. The particle size distribution of the emulsions were characterized by static light scattering (Horiba LA 920, Irvine, CA) using a relative refractive index of 1.15. The initial emulsion was diluted with deionized water to produce a series of samples with different oil contents and aliquots (2 mL) were added to 20 mL headspace (HS) vials. Emulsified alkanes show deep and stable supercooling (Cramp, Docking, Ghosh and Coupland, 2004), so a emulsions of either wholly liquid droplets or wholly solid droplets were prepared by either cooling the vials directly to 30°C, or by cooling to 10°C to induce homogeneous nucleation then reheating to 30°C. The solid and liquid droplets were stable at this temperature over several weeks (no change in measured particle size, no apparent creaming, no change in droplet melting or crystallization enthalpy).

A stock aroma mixture was prepared from ethyl butanoate (EB), ethyl pentanoate (EP), ethyl heptanoate (EH) and ethyl octanoate (EO) mixed in a volumetric ratio of 1:2:20:20 and diluted in an equal volume of ethyl alcohol. Aliquots of the stock mixture were added to the vials so that the final concentrations (μL/L) of aroma compounds in the emulsion were EB 10, EP 20, EH 200 and EO 200. The vials were sealed with poly-

(tetrafluoroethylene)/ butyl rubber septa and equilibrated at 30ºC for at least 1 hour prior to analysis. Other measurements showed that the values reached after one hour remained constant for over a week suggesting the samples had reached equilibrium in this time.

After equilibration, a sample of the headspace gas (1 mL) was withdrawn using an autosampler (Combi-Pal, CTC Analytics, Carrboro, NC, USA) and injected into a gas chromatograph (Agilent 6890, Agilent Technologies, Palo Alto, CA, USA) operating in splitless mode and equipped with a DB-5 capillary column (30 m×0.32 mm i.d. with a 1 μm film thickness) and a flame ionization detector. The operating conditions were as follows: inlet temperature 200ºC, detector 250ºC, oven program 30ºC for 1 min, then increase at 35ºC min^{-1} 200ºC and held for 2 min; carrier hydrogen constant flow rate 2.0 mL min^{-1}. Static headspace concentrations were determined from peak areas using a standard calibration curve ($R^2 = 0.99$). All measurements are expressed as the mean and standard deviation of at least two full experimental replications.

4.3 Results and Discussions

4.3.1 Preliminary Modeling

Although a cocktail of four volatiles was measured, the trends seen were similar for all, and only EH will be reported for clarity. K_{ge} decreased with increasing oil volume fraction for model emulsions containing liquid and solid eicosane droplets (Figure **4.1**) but more rapidly for liquid than solid. For the liquid droplets (Figure **4.1**a), K_{ge} depended only upon the volume fraction of oil; indeed an unemulsified mixture of the same ingredients showed the same trend. K_{ge} also decreased with fat volume fraction of solid droplets (Figure **4.1**b) and while this effect is smaller than that seen for liquid droplets, it establishes some positive interaction between solid fat droplets and aroma molecules. The magnitude of the interaction with solids is greater for smaller droplets suggesting it occurs at the surface rather than in the bulk of the crystalline droplet.

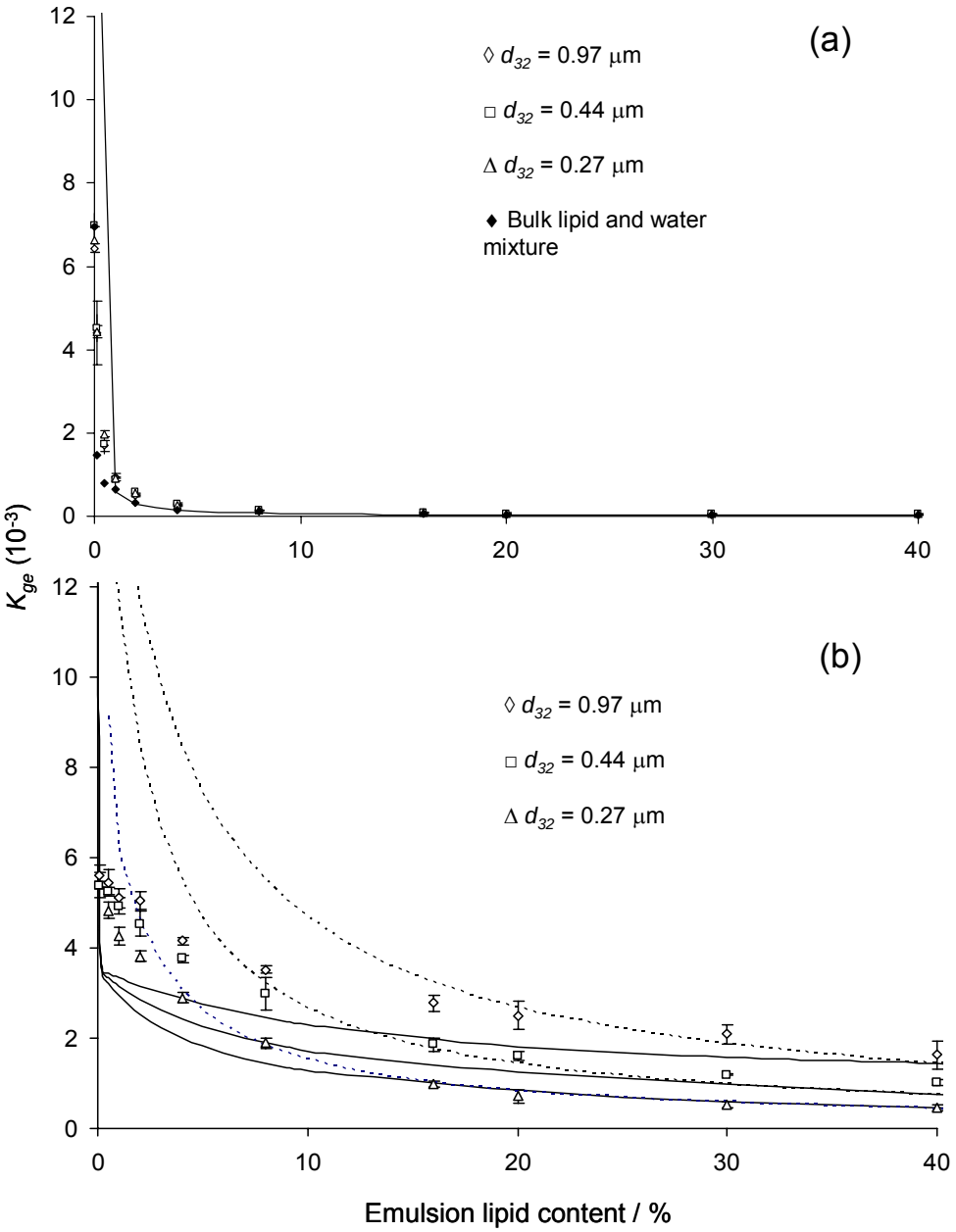

Figure **4.1**: K_{ge} of EH with an eicosane emulsion of (a) liquid and (b) solid droplets with various particle sizes. The lines in (a) are calculated from bulk partition coefficients using a volume partitioning model (Equation 4.2). The broken lines in (b) are calculated based on a surface-binding model fit to ϕ_o>0.1 (K^*_{iw}=4.5 x10^{-6} m). The solid lines in (b) are based on the combined surface binding/droplet dissolution model described in the text.

K_{ge} was modeled as a function of liquid oil volume fraction using independently measured bulk partition coefficients (K_{go}=6 x 10^{-6}, K_{gw}=0.0182) using Equation 4.2. The equation fits the data well over most of the concentration range (Figure **4.1**a) suggesting that the most important interactions are volume partitioning of the aroma molecules and other effects (e.g., Kelvin pressure effects, surface binding of the volatile) are not important enough to be seen in the liquid oil emulsion data.

The particle size effect seen in the solid fat data cannot be adequately represented solely by a volume based model and suggest that interfacial binding may be important. The presence of a binding surface can be incorporated into Equation 4.2 as an additional two-dimensional phase (Chapter 3):

$$\frac{1}{K_{ge}} = \frac{\phi_o}{K_{go}} + \frac{(1-\phi_o)}{K_{gw}} + \frac{K^*_{iw}.A_s}{K_{gw}} \qquad (4.3)$$

where A_s is the interfacial area per unit volume of emulsion (expressed as $6\phi_o/d_{32}$) and K^*_{iw} is the surface binding coefficient defined as the ratio of surface excess concentration, i.e., volume of aroma compound per unit interfacial area, to aqueous concentration. As a first approximation, EH was assumed to interact at the surface of the solid droplets and not with the bulk of the crystal (i.e., ϕ_o=0). Equation 4.3 was used to model the headspace concentration of EH in equilibrium with solid droplets, and although there was a reasonably good fit to the higher oil volume fraction samples (broken lines in Figure **4.1**b correspond to the best fit value of K^*_{iw}= 4.5 x10^{-6} m from a statistical fit to the data with ϕ_o>0.1), the model overestimated the headspace concentration at lower oil volume fractions.

Because the effect of surface binding is much smaller than the effect of partitioning into liquid oil, I cannot discount the possibility of similar binding occurring at the liquid oil-water interface. If Equation 4.3 were applied to the liquid droplet data a similar value of K^*_{iw} (or even a value several orders of magnitude greater) causes no

appreciable change in the model curve. For the remainder of the work it will be assumed that surface binding occurs at all lipid-water interfaces with this binding coefficient regardless of whether the droplets are solid or liquid. However, the importance of surface binding in emulsions is only expected when there is no liquid oil present.

4.3.2 The Nature of the Interaction

In an effort to better understand the nature of the interactions, a coarse eicosane emulsion was prepared with a median droplet size of about 10 μm allowing easy observation under the microscope. Various concentrations of solid droplets were mixed with the aroma cocktail and observed under polarized light using an Olympus BX40 microscope (Melville, NY) equipped with a video camera (Sony 3CCD, PXC-970MD, New York, NY) using X200 magnification lenses. Image manipulation was performed using the PAX-it 4.2 software (Franklin Park, NJ). In the absence of added aroma mixture, the droplets appeared as bright specs under polarized light (Figure **4.2**a, c) but in the presence of the added aroma, many of the solid droplets in the more dilute emulsion had apparently disappeared, suggesting the crystals had dissolved in the added aroma (Figure **4.2**d). Clearly, some critical ratio of aroma to solid fat is necessary to achieve this as the same amount of aroma stock added to more concentrated emulsions caused no observable change (Figure **4.2**b).

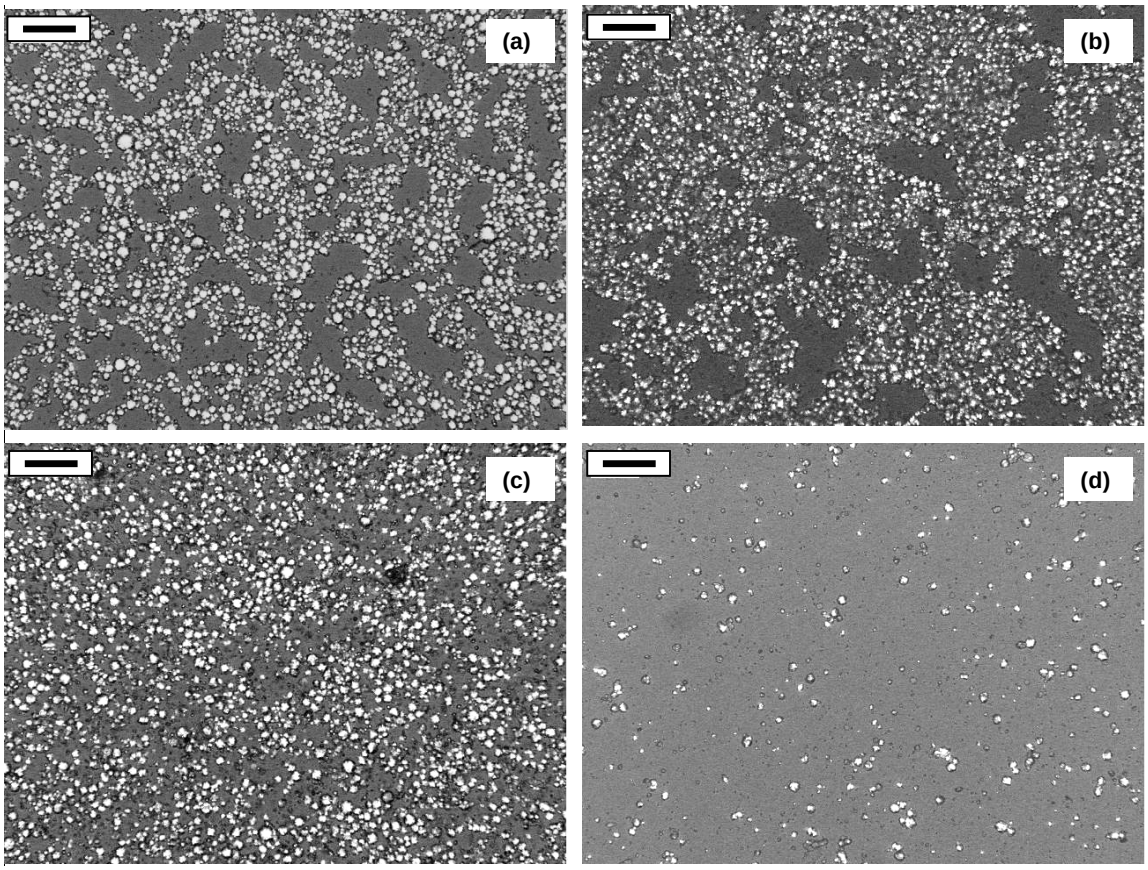

Figure **4.2**: Polarized light micrographs of a coarse solid eicosane emulsion. (a) 20% eicosane, no added aroma, (b) 20% eicosane, with added aroma, (c) 5% eicosane, no added aroma, (d) 5% eicosane, with added aroma (scale bar=40 μm).

It is not possible to make a direct comparison between the large droplets used in the microscopy study and the smaller ones used in the headspace GC work and the smaller droplets could not be adequately observed microscopically. However, similar behavior was measured using differential scanning calorimetry (DSC) to compare the melting enthalpies of fine eicosane droplets prepared with and without added aroma (Chapter 3). Samples (~15 mg) were sealed into aluminum pans and placed in a differential scanning calorimeter (Perkin-Elmer DSC-7, Norwalk, CT) alongside an empty pan as a reference. The melting enthalpies of eicosane in emulsions with different oil content (d_{32} = 0.44 μm) prepared with or without added volatiles were measured by first cooling to 10°C then reheating at 5°C min^{-1} to 50°C. The ratio of the two enthalpies was used as a measure of the effect of the added aroma on the solid fat content of the droplets. At high oil to aroma ratios (i.e., high oil volume fractions) the melting enthalpy of the eicosane was unaffected by the presence of the aroma (hence almost all eicosane remain in the solid state) but at low oil to aroma ratios (i.e., low oil volume fractions) the melting enthalpy of the samples containing aroma was much lower than those prepared without (i.e. much lower solid fat content of eicosane with aroma) (Figure **4.3**). This supports the hypothesis that the eicosane can dissolve in the aroma if sufficient is present and adsorbed to the surface. Any successful model must account for both the effects of the aroma on the phase behavior of the crystal as well as the potential binding of the aroma to the solid and liquid phases present.

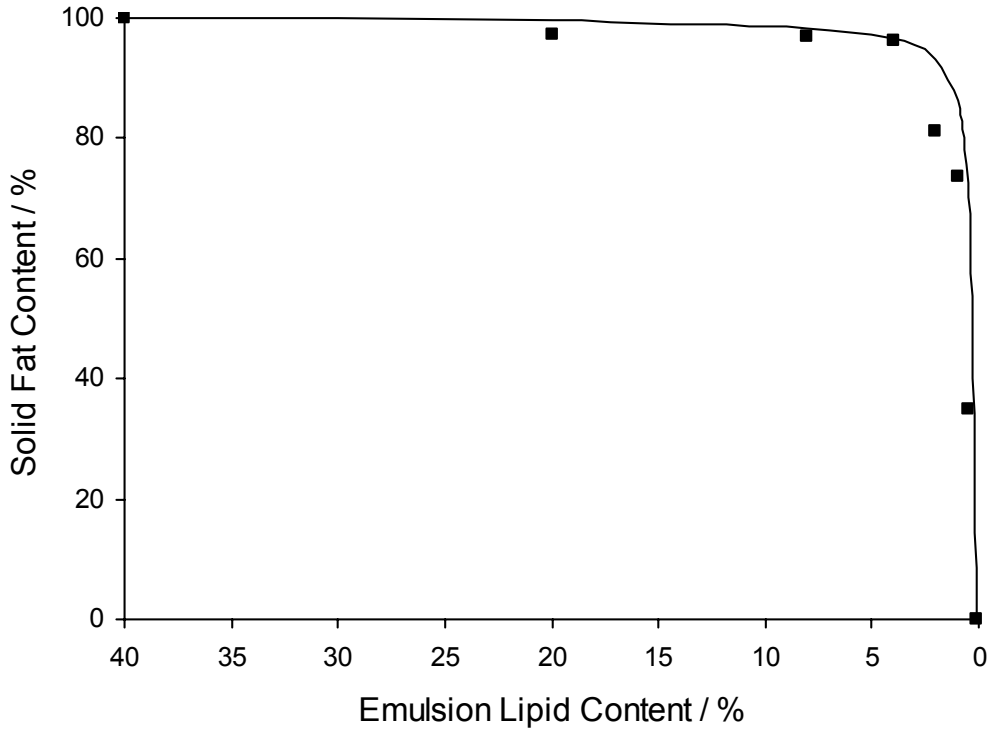

Figure **4.3**: Solid fat content of eicosane emulsions prepared by mixing different concentrations of fully solid droplets with aroma (data from Figure 3.6 has been used). Line showing fit from model described in the text.

4.3.3 Surface Binding and Droplet Dissolution Model

The effects of solid and liquid fat in the droplets on the aroma release properties of the emulsion can be taken into account using a modified form of Equation 4.3:

$$\frac{1}{K_{ge}} = \frac{\phi_o(1-\phi_{sf})}{K_{go}} + \frac{(1-\phi_o)}{K_{gw}} + \frac{K^*_{iw}.A_s}{K_{gw}} \tag{4.4}$$

where ϕ_{sf} is the solid fat content (the proportion of the total lipid in the emulsion that is crystalline). Next, a mass balance for the EH, expressed in terms of concentration (c) and volume (V) of the gas and emulsion phases (subscripts g and e respectively) can be written as:

$$V_{EH} = c_e V_e + c_g V_g \tag{4.5}$$

where V_{EH} is the total volume of EH added to the vial. As the gas and emulsion are at equilibrium (Equation 4.1), K_{ge} can be substituted in:

$$c_e = \frac{V_{EH}}{V_e + K_{ge} V_g} \tag{4.6}$$

The EH in the emulsion is divided amongst the liquid oil (subscript o), aqueous phase (subscript w) and inter-phase (i.e., assuming no direct incorporation into crystalline eicosane or binding at the liquid oil-solid fat surface):

$$c_e V_e = c_w[V_e(1-\phi_o) + K_{ow} V_e \phi_o (1-\phi_{sf}) + K^*_{iw} A_s V_e \phi_o] \tag{4.7}$$

Rearranging and substituting for the oil-water partition coefficient ($K_{ow} = c_o/c_w$):

$$c_o = \frac{K_{ow} c_e V_e}{[V_e(1-\phi_o) + K_{ow} V_e \phi_o (1-\phi_{sf}) + K_{iw}^* A_s V_e \phi_o]} \quad (4.8)$$

and finally by substituting for c_e from Equation 4.6 we have an expression for the concentration of EH in the liquid oil phase:

$$c_o = \frac{K_{ow} V_{EH}}{(V_e + K_{ge} V_g)[(1-\phi_o) + K_{ow} \phi_o (1-\phi_{sf}) + K_{iw}^* A_s \phi_o]} \quad (4.9)$$

K_{ge} can be calculated from Equation 4.4 and all the other parameters are known, so Equation 4.9 can be used to calculate the concentration of EH in the oil phase as a function of solid fat content for emulsions of different volume fraction (Figure **4.4**). As expected, in the completely liquid oil emulsions (zero solid fat fraction), the concentration of EH in the oil phase decreases with oil volume fraction. However, as the droplets crystallize, the EH is progressively confined to a smaller volume of liquid oil and while some of it redistributes to other phases, the oil-phase concentration increases at an increasing rate.

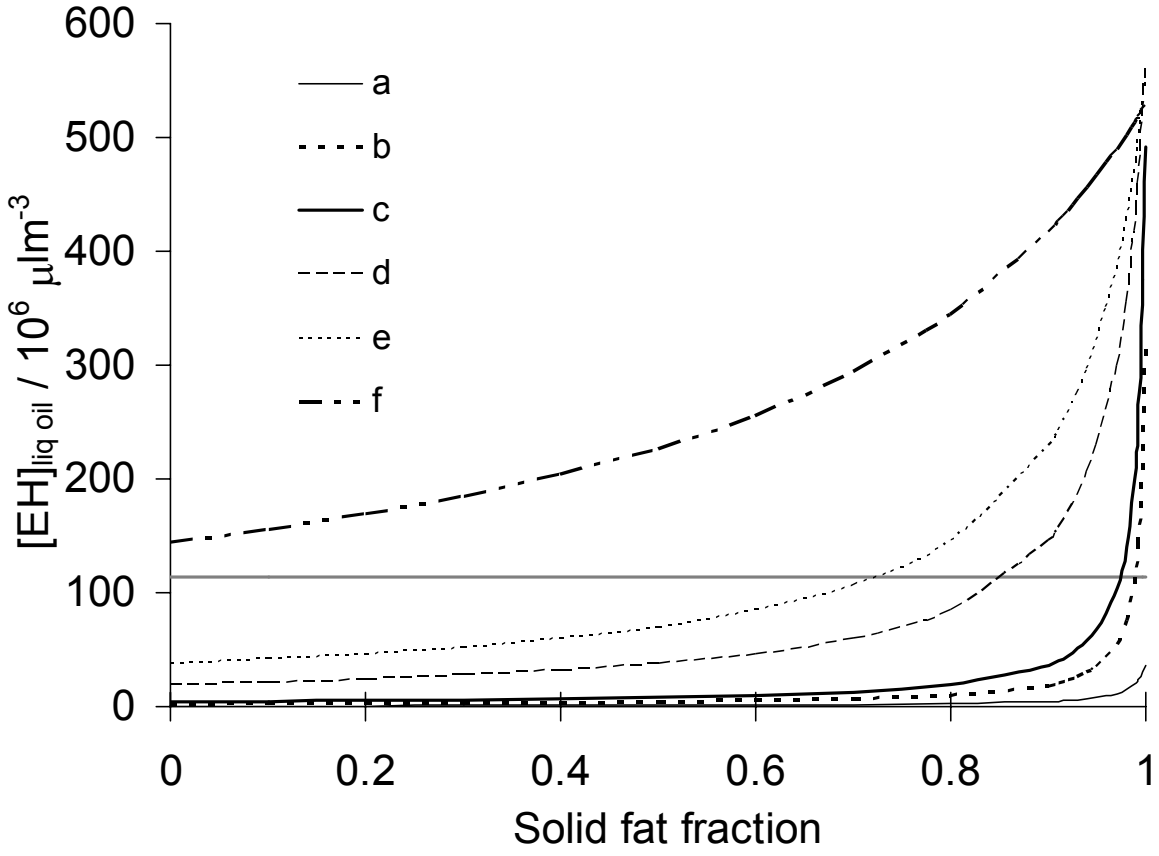

Figure **4.4**: Concentration of EH in the liquid oil phase ($[EH]_{liq\ oil}$) of different concentrations of emulsions crystallized to different extents calculated from bulk partition coefficients and binding of the aroma to the droplet surfaces (K^*_{iw}=4.5 x10^{-6} m). Emulsions with different oil concentration: (a) 40%, (b) 10%, (c) 5%, (d) 1%, (e) 0.5%, (f) 0.1% are shown with the curved lines. The straight line shows the limiting value of solid fat content from the eicosane-aroma phase diagram.

However, in a real system there must be equilibrium between the crystalline eicosane and the liquid eicosane in solution with the aroma molecules at the temperature of the experiments. The phase diagram of the eicosane – aroma mixture was constructed from the DSC melting points of samples containing different proportion of eicosane and aroma compounds. In this case samples were temperature cycled in the DSC from 50 to -20 to 50ºC at 5ºC min^{-1} (Figure **4.5**). At 30°C, where all headspace measurements were made, crystalline eicosane is at equilibrium with a solution of 46.8% aroma mixture (i.e., 1.14 x 10^8 µl/m^3 of EH). This limiting value of c_o has also been plotted in Figure 4.4 and the maximum solid fat content (ϕ_{sf}) for an emulsion of given volume fraction is calculated as the intersection of the line with the corresponding curve. The limiting solid fat content calculated from the phase diagram and from the bulk partition coefficients were plotted in Figure **4.3** and agreed well with the measured solid fat content of the droplets suggesting the dissolution observed should be expected from the phase behavior of the ingredients. Finally the gas emulsion coefficients were calculated using these values of ϕ_{sf} in Equation 4.4 and are plotted alongside the experimental measurements in Figure **4.1**b. While the quality of fit is not perfect (r^2 = 0.94±0.02), the trends are similar to those seen in the experimental data and does not have the large overestimate in K_{ge} at low oil contents predicted by the simple surface binding model.

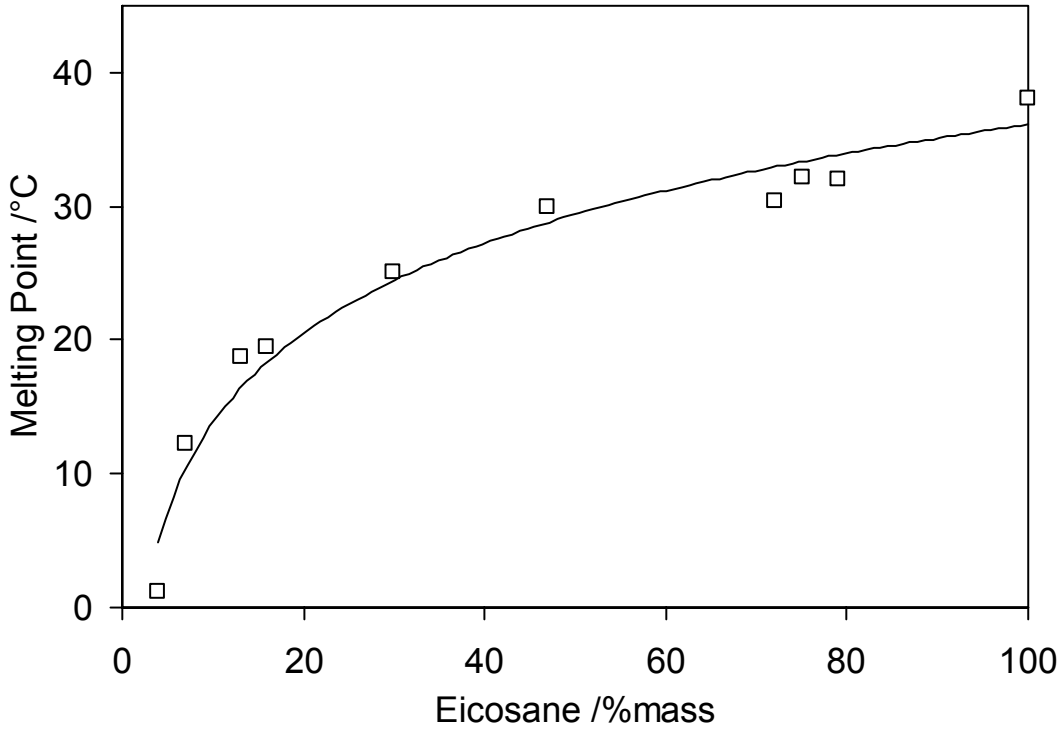

Figure **4.5**: Phase diagram of eicosane – aroma mixture. The melting point of different eicosane – aroma mixtures were plotted against weight fraction of eicosane.

It appears that at a high fat surface-aroma ratio the volatiles simply adsorb at the droplet surfaces and can be modeled by a simple surface-binding coefficient. However if the amount of aroma per unit surface exceeds a certain value, the solid droplets will begin to dissolve in the aroma according to their phase diagram. The additional liquid phase formed produced a much larger reservoir for the aroma and reduces the amount in the headspace. Simple estimations based on the geometry of the molecules involved suggest the critical amount of adsorbed material needed to initiate dissolution is much less than the monolayer. The model proposed is based on independent measurements of the bulk thermodynamic properties of the independent phases (gas- liquid oil and gas- water partition coefficients and aroma-fat phase diagram) and the only adjustable parameter is the surface binding coefficient measured from a best fit at high oil concentration where presumably the amount of liquid oil is negligible. The quality of fit is acceptable but far from perfect. The region where deviations are important is extremely difficult to model because as EH has such a high affinity for liquid oil, even a tiny error in the calculated solid fat content will lead to a huge difference in the result.

4.4 Conclusions

The distribution of volatile molecules between a liquid emulsion and the headspace can be modeled in terms of the volume partition coefficients. There are weaker interactions between solid fat droplets and aroma molecules but these are more complex. A small amount of added aroma can bind at the droplet surface, but larger amounts can dissolve the crystalline droplets according to the phase diagram and partition into the liquid oil. The melting and dissolution of droplets in a food emulsion can have a huge effect in the concentration of headspace volatiles and may be a way to engineer a small molecule delivery system.

4.5 References

Bakker, J.; Mela, D. J., Effect of emulsion structure on flavor release and taste perception. In *Flavor-Food Interactions*, McGorrin, R. J.; Leland, J. V., Eds. American Chemical Society: Washington, D.C., **1996**; Vol. 633.

Charles, M.; Lambert, S.; Brondeur, P.; Courthaudon, J.; Guichard, E., Influence of formulation and structure of an oil-in-water emulsion on flavor release. In *Flavor Release*, Roberts, D. D.; Taylor, A. J., Eds. American Chemical Society: Washington, D.C., **2000**; pp 342-355.

Cramp, G. L.; Docking, A. M.; Ghosh, S.; Coupland, J. N., On the stability of oil-in-water emulsions to freezing. *Food Hydrocolloids* **2004,** 18, (6), 899-905.

Harrison, M.; Hills, B. P.; Bakker, J.; Clothier, T., Mathematical model of flavor release from liquid emulsion. *Journal of Food Science* **1997,** 62, (4), 653-658.

Maier, H. G., Binding of volatile aroma substances to nutrients and foodstuffs. In *Proceedings of international symposium on aroma research*, Maarse, H., Groenen, P.J., Ed. Pudoc: Wageningen, **1975**; pp 143-157.

McNulty, P. B.; Karel, M., Factors affecting flavor release and uptake in O/W emulsions, 2. Stirred cell studies. *Journal of Food Technology* **1973,** 8, 319-331.

Roberts, D. D.; Pollien, P.; Watzke, B., Experimental and modeling studies showing the effect of lipid type and level on flavor release from milk-based liquid emulsions. *Journal of Agricultural and Food Chemistry* **2003,** 51, 189-195.

Chapter 5

Aroma Release from Solid Droplet Emulsions: Effect of Lipid Type

Abstract

Aroma compounds partition between the different phases of a food emulsion and the headspace but only those in the headspace will be perceived. Phase transitions in the lipid droplets profoundly affect the position of the partitioning equilibria and hence headspace aroma concentration. The release of four volatile aroma compounds (ethyl butanoate, pentanoate, heptanoate and octanoate) from eicosane, hydrogenated palm fat or Salatrim® emulsions stabilized with sodium caseinate were investigated as a function of fat crystallization, particle size and droplet concentration. For all compounds, the headspace aroma concentration in equilibrium with solid droplet emulsions was significantly higher than that in equilibrium with liquid droplet emulsions. The partitioning of volatile aroma compounds from emulsion does not depend on the type of liquid oil used but the interactions between solid fat droplets and aroma compounds are significantly influenced by the nature of the crystalline fat. Notably, partitioning into the headspace was much lower for solid triglyceride droplet emulsions than for solid alkane emulsions.

5.1 Introduction

The perception of food aroma begins with the release of stimulating volatile molecules from the food and their transport to appropriate receptors in the nose (Keast, Dalton and Breslin, 2004; Taylor, 1996). Aroma release depends on the distribution of aroma compounds within the different phases of food and with the gas phase above it both before and during consumption. However, the complex nature of real foods makes it difficult to separate the effect of different interaction on overall aroma release and simple model systems are frequently used. As well as being part of real foods, emulsions are extensively used as model systems because they can be prepared and characterized precisely.

In an oil-in-water emulsion, volatile aroma compounds distribute themselves between the oil droplets, aqueous phase and the surface of the droplets according to the equilibrium partition coefficients (i.e. the ratio of concentrations of aroma compounds in two different phases). The overall partition coefficient of aroma compound from an emulsion to the gas phase above it can also be expressed as a function of individual partition coefficients according to the following mass balance equation (Chapter 3, Ghosh, Peterson and Coupland 2006a):

$$\frac{1}{K_{ge}} = \frac{\phi_o}{K_{ow}} + \frac{1-\phi_o}{K_{gw}} + \frac{K^*_{iw}.A_s}{K_{gw}} \qquad (5.1)$$

where, K_{ge}, K_{ow} and K_{gw} are the overall gas-emulsion, oil-water and gas-water partition coefficients, respectively, ϕ_o is the oil volume fraction in emulsion and A_s is the interfacial area per unit volume of emulsion. K^*_{iw} is the surface binding coefficient defined as the ratio of surface excess concentration, i.e., volume of aroma compound per unit interfacial area, to aqueous concentration. Because the effect of surface binding is much smaller than the effect of partitioning into liquid oil, the importance of surface

binding in emulsions can only be seen where there is no liquid oil present or the oil phase is in a solid state (Chapter 4, Ghosh, Peterson and Coupland, 2006b). The importance of K^*_{iw} in partitioning of aroma compounds in emulsions containing solid n-eicosane droplets has been shown in Chapter 3. It was observed that solid eicosane droplets can significantly absorb aroma compounds at the solid droplet surface with more effective binding for more hydrophobic compounds (Chapter 3). However, these findings are in contrast with observations of Roberts and coworkers (2003) and McNulty and Karel (1973) who proposed that only liquid lipid could bind aroma compounds. Another hypothesis proposed by Roberts et al. (2003) was that if the aroma compounds were present during fat crystallization they could be trapped inside the solid fat matrix formed on solidification, but, again this effect was not observed in Chapter 3. Possibly these contradicting results may be due to the fact that Roberts et al. (2003) used complex triglycerides (hydrogenated palm fat) while in the present study pure alkane was used (n-eicosane, Chapter 3).

The goal of the present work was to compare the binding of aroma compounds to solid and liquid emulsion droplets prepared from both alkane and triglycerides. The effect of volatile type (an homologous series of ethyl esters), lipid type (n-eicosane, hydrogenated palm stearin, and Salatrim®) and droplet size on the portioning behavior was considered. Hydrogenated palm stearin (HPS) was used because it has been previously used to study the effect of solid fat on flavor release (Roberts et al., 2003). Salatrim® (Short And Long chain Acyl TRIglyceride Molecules) is a family of structured triglycerides prepared with a combination of short (2, 3 or 4 carbon) and long chain (18 carbon) fatty acids. It was hypothesized that this diversity of chain length might accommodate foreign aroma compounds in its crystal structure. In another experiment, volatile partitioning from two different solid droplets emulsions where aroma compounds were present before or after fat crystallization was performed to test for possible aroma entrapment by solid droplets.

5.2 Materials and Methods

Materials. Partially hydrogenated palm stearin (27 Stearin®) and Salatrim® (Benefat 1H®) were the donations from Loders Croklaan (Channahon, IL) and Danisco (New Century, KS) respectively. Eicosane and hexadecane was purchased from Fisher Scientific (Springfield, NJ). All other chemicals were obtained from the Sigma Chemical Company (St. Louis, MO).

Emulsion preparation. Emulsions were prepared by mixing molten fat (20 wt%) with sodium caseinate solution (2 wt% containing 0.02% thimerosal as an antibacterial agent) using a high-speed blender (Brinkmann Polytron, Brinkmann Instruments Inc., Westbury, NY) for 30 seconds. The coarse emulsions were then re-circulated through a twin-stage valve homogenizer (Niro Soavi Panda, GEA Niro Soavi, Hudson, WI) at different pressures to achieve a range of droplet sizes. To prevent fat crystallization during emulsion preparation, all ingredients were used at elevated temperature and the homogenizer was rinsed several times with hot water before and after homogenization. The particle size distributions of the emulsions were characterized by laser diffraction particle sizing (Horiba LA 920, Irvine, CA) using a relative refractive index of 1.15. The emulsions were stored at a temperature greater than 50ºC to prevent fat crystallization. Samples of emulsions were diluted with deionized water to prepare emulsions with different oil contents.

Thermal Analysis. The crystallization and melting behavior of bulk and emulsified lipids were determined using a differential scanning calorimeter (Perkin-Elmer DSC-7, Norwalk, CT). The instrument was calibrated against indium prior to use. Aliquots (~15 mg) of bulk and emulsified lipids were temperature cycled in the DSC from 70ºC to -40ºC to 70ºC and 70°C to 10°C to 70°C, respectively. The heating and cooling rate was 5ºC min^{-1}.The crystallization and melting points of bulk and emulsified lipids were taken from the onset temperature of peaks on the thermogram using Pyris data

analysis software (version 3.52, Perkin-Elmer Corporation, Norwalk, CT). All analyses were conducted in triplicate.

Addition of aroma compounds to emulsions. A stock aroma solution was prepared by mixing four aroma compounds, ethyl butanoate (EB), ethyl pentanoate (EP), ethyl heptanoate (EH) and ethyl octanoate (EO) in a volumetric ratio of 1:2:20:20 and diluting to a 50% solution in ethanol. The concentrations of the aroma compounds were selected based on their oil-water partition coefficient values so that a quantifiable gas chromatograph peak would be obtained for each compound.

Samples of emulsions were cooled to 10ºC to induce crystallization in the lipid droplets. Stock aroma solution (860 μL/L of emulsion) was added to the solid droplet emulsions and equilibrated for 24 hours at 10ºC. The final concentrations (μL/L) of aroma compounds in emulsion were EB, 10; EP, 20; EH, 200; and EO, 200. Aliquots (2ml) of each aroma added emulsion sample was placed into a 20 mL headspace vial (MicroLiter Analytical Supplies, Inc., Suwanee, GA, USA) and were sealed with poly-(tetrafluoroethylene)/ butyl rubber septa (MicroLiter Analytical Supplies, Inc., Suwanee, GA, USA). The sealed vials were then temperature cycled to produce (i) solid droplets, (ii) liquid droplets and (iii) droplets first melted then recrystallized.

(i) Solid droplet emulsions (i.e., Solid I samples) were prepared by cooling the samples to 10°C to ensure complete crystallization of the lipid, then bringing to the experimental temperature specific for the different type of lipids (i.e., 30ºC for n-eicosane and 10ºC for HPS and Salatrim® emulsions, see Table **5.1**).

(ii) Liquid emulsion droplets (i.e., Liquid samples) were prepared by heating the Solid I samples (according to temperature scheme of Table **5.1**) to melt the droplets then re-cooling to the experimental temperatures specific for each type of lipid (30º, 40º and 50ºC for n-eicosane, Salatrim® and HPS emulsions, respectively).

(iii) Finally, recrystallized droplets (i.e., Solid II samples) were made by cooling the Liquid samples back down to 10°C to induce droplet crystallization and either reheating to 30ºC for n-eicosane emulsion or holding at 10ºC for HPS and Salatrim® emulsions.

After each phase transition was complete (1 hour at the temperature given in Table **5.1**) the samples were maintained at their measurement temperature for a minimum of 24 hours to allow equilibration prior to HS volatile measurement. At each stage, three separate vials were used to measure the HS volatile concentration and then discarded. Due to their differing melting and crystallization properties, the different fats were studied at different temperatures. Later we will show how it is possible to normalize the data to remove the temperature effect and compare different types of lipid.

It should be noted that "solid" and "liquid" in this work refers to the droplets; the overall emulsions were liquid throughout the experiment and phase transitions in the dispersed phase caused no apparent change in their bulk properties.

Headspace analysis by gas chromatograph. Aliquots (1 ml) of the headspace above the emulsion in each vial was sampled using a Combi-Pal autosampler (CTC Analytics, Carrboro, NC) and injected into an Agilent 6890 GC (Agilent Technologies, Palo Alto, CA) equipped with a DB-5 capillary column (30 m×0.32 mm i.d. with a 1 μm film thickness) and a flame ionization detector. The operating conditions were as follows: sample was injected in splitless mode; the inlet temperature was 200ºC, the detector temperature was 250ºC, the oven program was 30ºC for 1 min, then increased at 35ºC min^{-1} from 30 to 200ºC and held for 2 min; and the carrier constant flow rate was 2.0 mL min^{-1} (He). Static HS concentrations were determined from peak areas using a standard calibration curve ($R^2 = 0.99$). All measurements were expressed as the mean and standard deviation of at least three full experimental replicates.

5.3 Results and Discussion

Physical Properties of the Emulsions. By varying the homogenization conditions, it was possible to manufacture emulsions with different droplet size distributions (Table **5.1**). The droplet size distribution for all the emulsions were unimodal with an average standard deviation of the distribution of ~0.23±0.2 μm. The emulsions were physically stable over the course of the experiment (i.e., no changes in measured droplet size, no apparent creaming).

Table **5.1**: Emulsion preparation conditions for different lipid types and the temperature program for equilibrium flavor release experiments.

Emulsion used	Droplet size category	Homogenization conditions		Mean droplet size (d_{32}) (μm)	Temperature cycle program of emulsions for HS GC analysis		
		Pressure (bar)	Number of passes		solid droplets	melting solid droplets	liquid droplets
Eicosane	large	110±10	2	1.04	30ºC	50ºC	30ºC
	medium	220±20	2	0.55			
	small	320±20	10	0.20			
HPS	large	110±10	2	0.91	10ºC	70ºC	50ºC
	medium	220±20	2	0.54			
	small	320±20	10	0.26			
Salatrim	large	110±10	2	1.24	10ºC	50ºC	40ºC
	medium	220±20	2	0.50			
	small	320±20	10	0.24			

The melting and cooling thermograms of the lipids in both their bulk and emulsified forms are shown in Figure **5.1**. On cooling, both bulk and emulsified lipids crystallized with a single major peak with the exception of bulk eicosane, which showed two exothermic peaks (a shallow peak followed by a sharp one) (Figure **5.1** a). We are unclear why a pure alkane would consistently show a split exothermic peak, but its presence does not affect the overall goal of the research and is not pursued further. The eicosane and Salatrim® samples showed a single peak on heating corresponding to the

melting of the crystals (Figure **5.1** a and c) while HPS had a more complex melting thermogram due to several polymorphic phase transitions (Figure **5.1** b). According to Kloek, Walstra and van Vliet (2000) the first endothermic peak of HPS (at around 45ºC) corresponds with the melting of the α polymorph followed by an exothermic peak due to recrystallization to a more stable β' or β polymorph. Finally at around 55ºC, the stable polymorph melts leading to the final exothermic peak (Figure **5.1** b). At sufficiently high temperature (50ºC for n-eicosane and Salatrim® and 70ºC for HPS) the solid lipid droplets melt leading to liquid droplet emulsions.

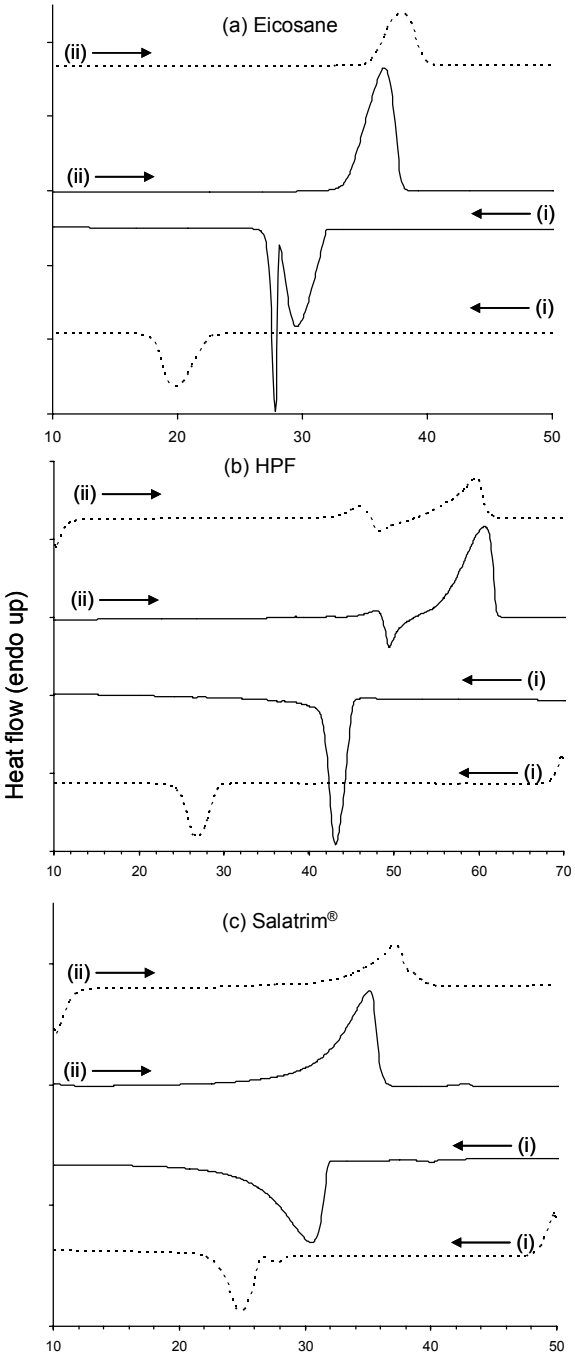

Figure **5.1**: Thermogram of bulk (—) and emulsified (----) fats (a) eicosane, (b) HPF and (c) Salatrim® during (i) cooling and (ii) heating. Emulsions were 20 wt% lipid stabilized with 2 wt% sodium caseinate solution and was temperature cycled at 5°C $min^{-1.}$

The onset of crystallization and melting peaks of bulk and emulsified lipids (from the DSC thermogram) has been plotted in Figure **5.2** for comparison. The emulsified lipids crystallize at a lower temperature than the corresponding bulk oils while the melting points of the bulk and emulsified forms are similar (Figure **5.2**). The deep supercooling required to initiate crystallization in emulsion oil droplets has been observed in a wide range of systems and is sometimes attributed to the majority of the lipid being isolated from potential nucleation catalysts and therefore nucleating homogeneously (Coupland, 2002). Eicosane has a deeper supercooling than the two triglycerides (HPS and Salatrim®) and this might be due to a difference in the number of potential nucleation catalysts for the triglycerides. The supercooled emulsions were very stable and it was possible to maintain liquid emulsion droplets below their thermodynamic freezing point for several weeks without any measurable crystallization.

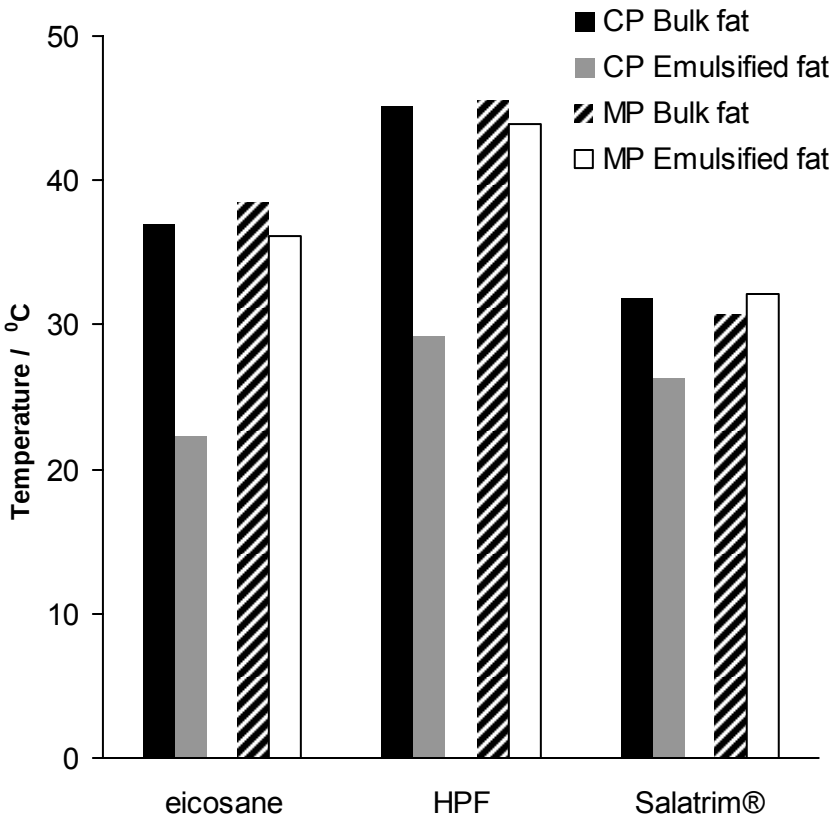

Figure **5.2**: Onset of crystallization point (CP) and melting point (MP) of bulk and emulsified fats from the DSC thermogram.

Equilibrium aroma release from emulsions. The gas-emulsion partition coefficient (K_{ge}) was calculated from the HS volatile concentration data for each emulsion assuming that volatiles present in the HS are at equilibrium with the emulsion and that the total amount of aroma compounds added are distributed between the HS and the emulsion. In earlier work, it has shown that the volatiles selected do not measurably interact with sodium caseinate in the emulsion (Chapter 3). Because different samples were measured at different temperatures it was necessary to account for the effect of temperature on K_{ge} before making a comparison between them. This can be done by

normalizing the measured K_{ge} to the gas-water partition coefficient at the same temperature, i.e.:

$$K_{ge/w} = \frac{K_{ge}}{K_{gw}} \tag{5.2}$$

Therefore $K_{ge/w}$ denotes the release of volatile aroma compound in the HS from an emulsion relative to the release of that compound from water at the same temperature and concentration and by converting K_{ge} to $K_{ge/w}$ we were able to compare all the HS GC measurements done at different temperatures for different lipid emulsions (Figure **5.3-5.5**). This approach has also been used by Roberts et al. (2003) to compare relative headspace volatile concentration from emulsions at different temperatures.

Aroma release from liquid lipid emulsions. The calculated values of $K_{ge/w}$ are plotted as a function of emulsion liquid lipid content and droplet size in Figure **5.3**. The partitioning of volatiles into the HS decreases with emulsion lipid content and but there are no differences between the types of oil used (i.e., n-eicosane, HPS and Salatrim®) or emulsion droplet size. Partitioning in liquid oil droplets depends on the total volume of the droplets and is therefore a function of the affinity between the oil and aroma and the amount of oil present but not the droplet size (Chapter 3). In this case the amount of aroma partitioning into the emulsion increased with volatile molecular weight but was unaffected by lipid type. This is expected as the gas-oil partition coefficients of alkanes and triglycerides at any particular temperature are very similar (Table **5.2**). Indeed all of the liquid droplet data can be well-described by Equation 5.1 using these values for the partition coefficients and neglecting any surface binding terms (i.e. the Buttery model, Chapter 3).

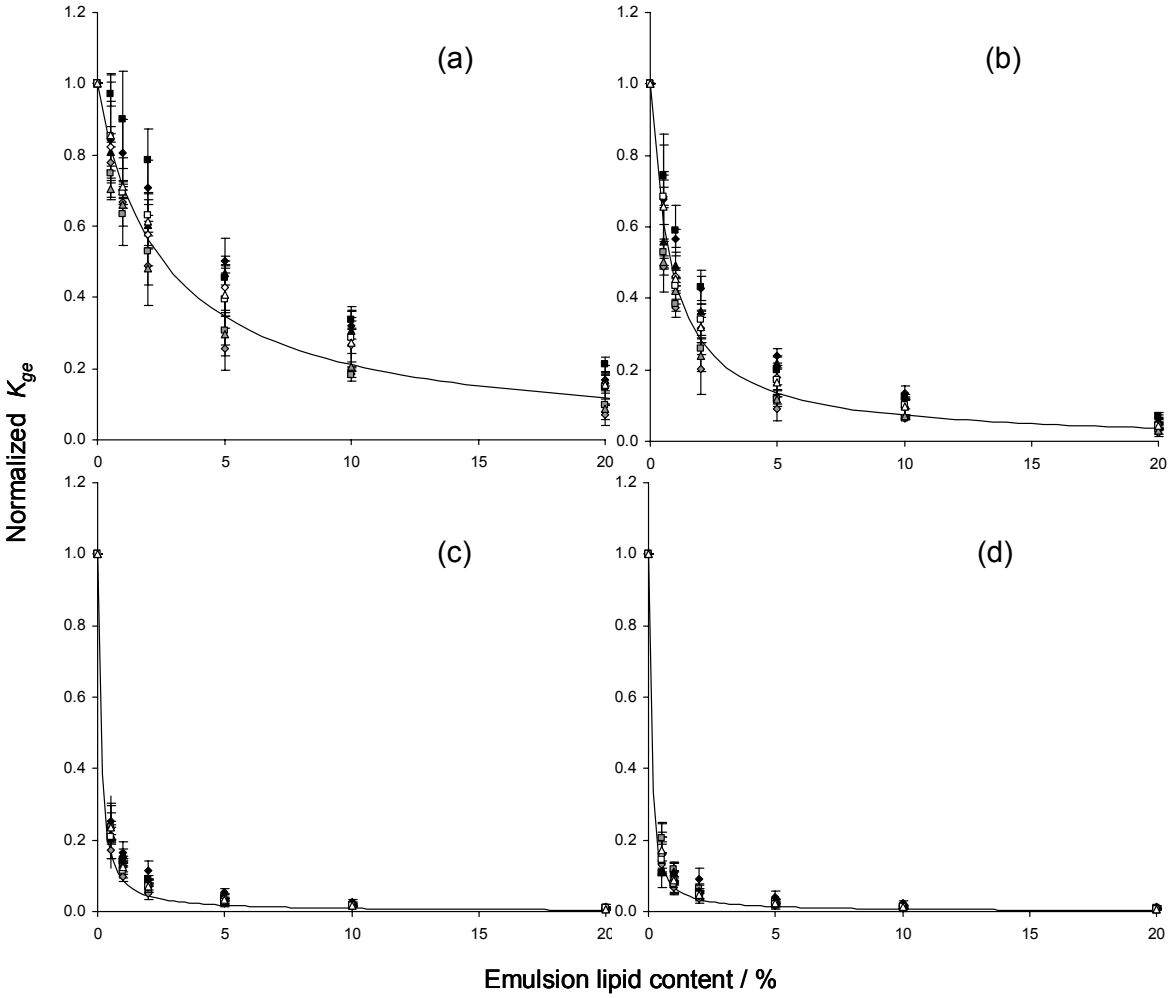

Figure **5.3**: Normalized gas-emulsion partition coefficient ($K_{ge/w}$) of aroma compounds as a function of lipid type and lipid content of emulsions with liquid lipid (a) ethyl butanoate, (b) ethyl pentanoate, (c) ethyl heptanoate and (d) ethyl octanoate. Results for emulsions with different particle sizes (d_{32}) large (◊), medium (□) and small (Δ) are shown for n-eicosane (open symbol), HPS (closed black symbol) and Salatrim® (grey symbol) emulsions. Model prediction using Buttery equation (Equation 3.3) has also been shown by lines.

Table **5.2**: Gas-oil partition coefficients of aroma compounds at 30°C. As bulk eicosane and HPS are solid at the experimental temperatures, hexadecane and corn oil were used as a model alkanes and triglyceride respectively. The partition coefficients were measured according to the method mentioned in Chapter 3

Aroma compounds	Gas-alkane partition coefficient	Gas-triglyceride partition coefficient
Ethyl Butanoate	1.9×10^{-4}	1.4×10^{-4}
Ethyl Pentanoate	6.4×10^{-5}	5.6×10^{-5}
Ethyl Heptanoate	6.5×10^{-6}	8.1×10^{-6}
Ethyl Octanoate	2.2×10^{-6}	3.0×10^{-6}

Aroma release from solid lipid emulsions. The values of $K_{ge/w}$ for solid droplet emulsions were higher than those for the corresponding liquid droplet emulsions suggesting the interaction between aroma and emulsion is weaker. However, for all lipid types, the $K_{ge/w}$ values for EP, EH and EO decreased monotonically with solid lipid concentration, suggesting some sort of association of aroma compounds with the solid fat (Figure **5.4,** Figure **5.5,** and Figure **5.6**). Regardless of aroma type, the $K_{ge/w}$ of solid eicosane emulsion was highest followed by solid HPS and solid Salatrim® emulsions (Figure **5.7**). Interestingly, while $K_{ge/w}$ for EB varied with solid Salatrim® droplet concentration in a similar manner to the other aroma compounds, it was not affected by eicosane or HPS solid droplet concentration.

As noted previously (Chapter 3), the values of $K_{ge/w}$ for solid droplet eicosane emulsion were lower for small droplets than for large droplets (Figure **5.4**) because the aroma adsorbs at the solid droplet surface. Eicosane crystallizes in pure form with tightly arranged aliphatic chains organized in a triclinic crystal structure (Ueno, Hamada and Sato, 2003) and presumably with few defects that might accommodate aroma molecules in the crystal lattice. Thus, it is expected that when n-eicosane crystallizes, it excludes all

aroma compounds from the crystalline matrix. A similar exclusion of foreign materials from crystalline alkane droplets was also postulated by Okuda, McClements and Decker (2005) who found that crystallization of *n*-octadecane (which has a similar crystal structure to n-eicosane according to Ueno et al., 2003) in mixed octadecane-methyl linolenate oil-in-water emulsion droplets leads to separation of methyl linolenate from the solid octadecane. The extent of surface binding increases with aroma molecular chain length and presumably the lack of a droplet concentration effect of EB was because this molecule is relatively hydrophilic and did not tend to associate with the droplet surface.

For the triglyceride emulsions (Figure **5.5**, Figure **5.6**), the values of $K_{ge/w}$ decreased with solid droplet concentration but there was no effect of particle size on aroma volatility suggesting a different mode of interaction was important in these systems dependent on phase volume not interfacial area. This could either be because (i) there is some liquid oil residual in the "solid" droplet which acts as a reservoir for the aroma, or (ii) the aroma compounds co-crystallize with the fat.

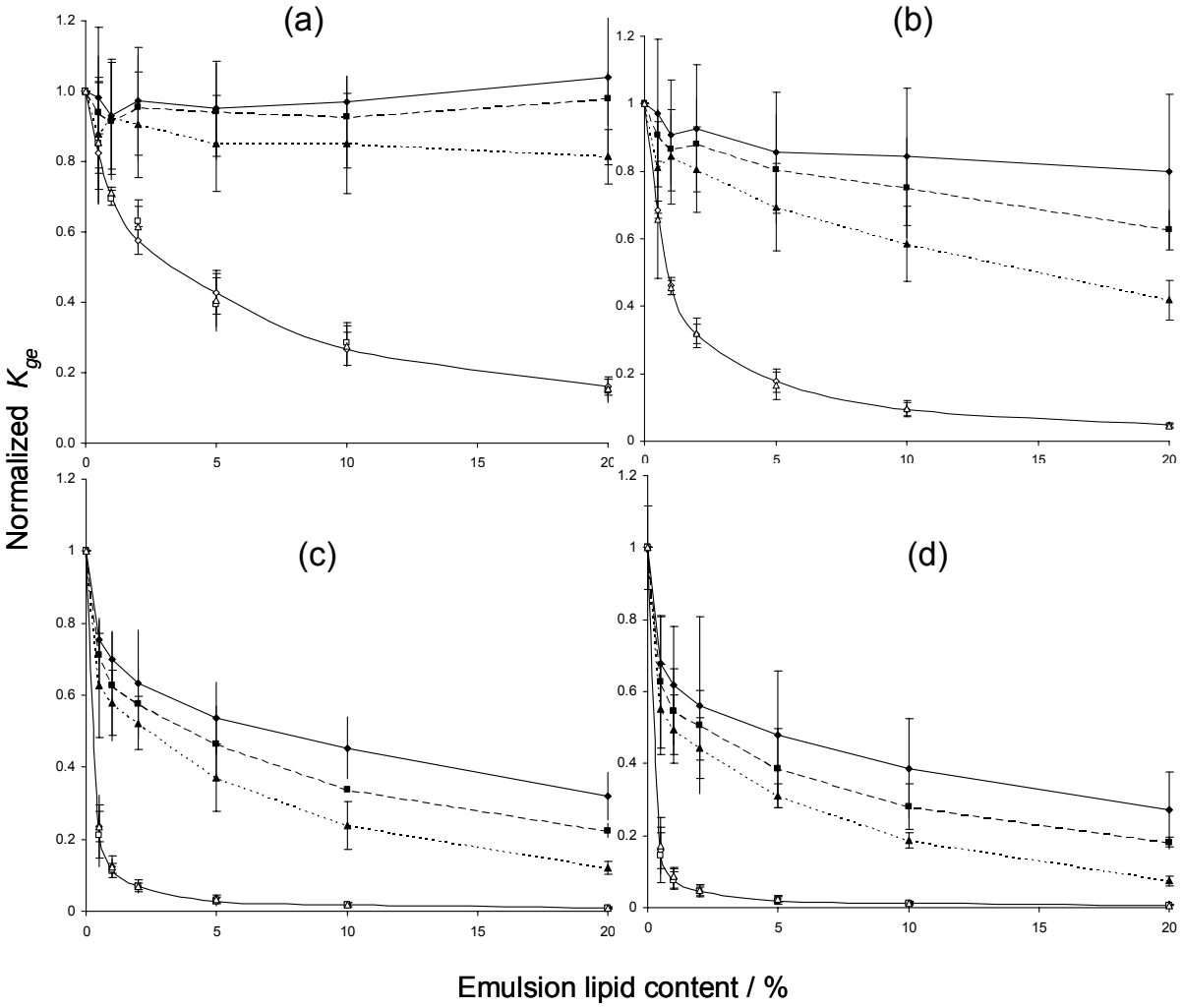

Figure **5.4**: Normalized gas-emulsion partition coefficient ($K_{ge/w}$) of aroma compounds as a function of lipid content of emulsions with liquid lipid (open symbol) and solid lipid (closed symbol) droplets (a) ethyl butanoate, (b) ethyl pentanoate, (c) ethyl heptanoate and (d) ethyl octanoate. Results for **eicosane** emulsions with different particle sizes (d_{32}) highest (◊), medium (□) and lowest (Δ) are shown.

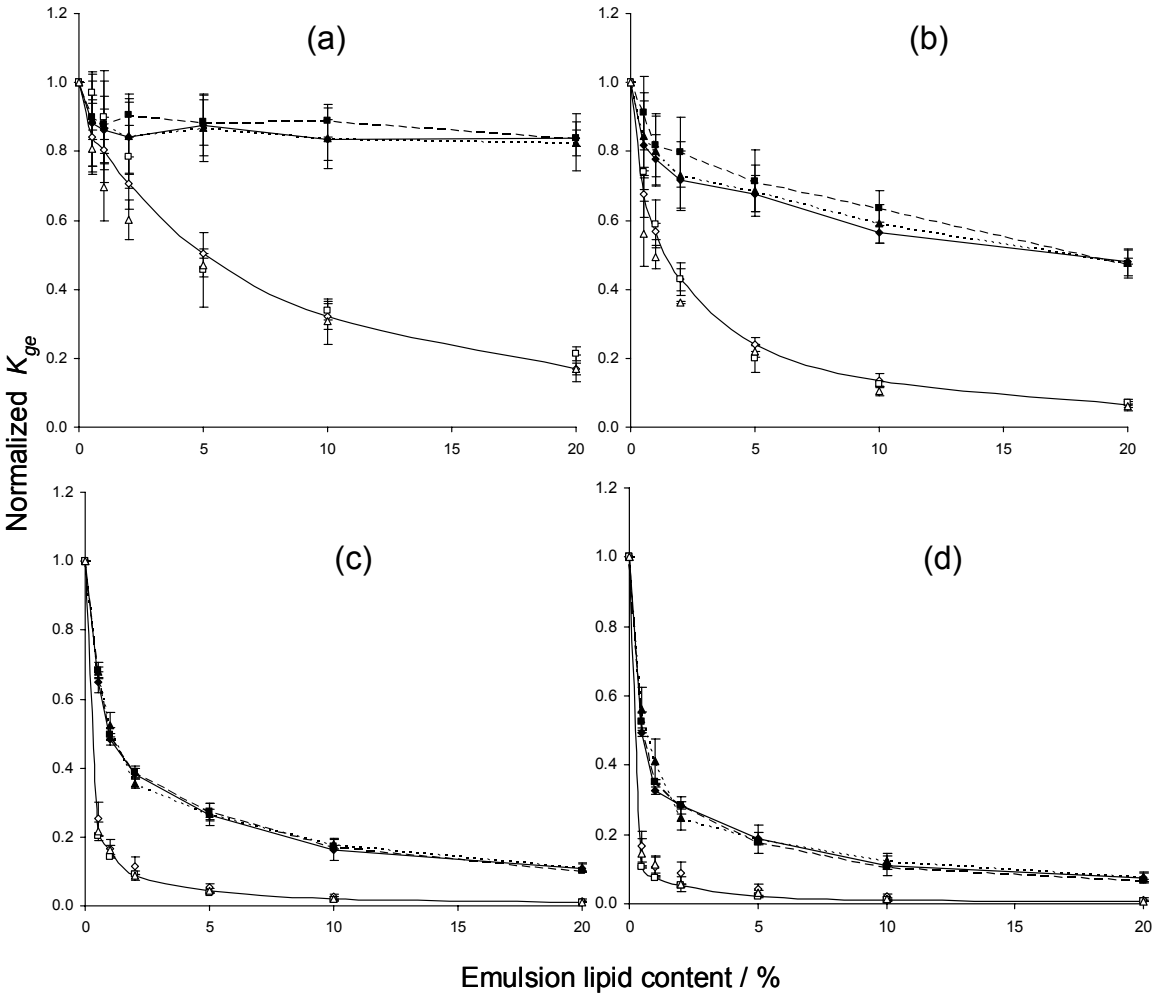

Figure **5.5**: Normalized gas-emulsion partition coefficient ($K_{ge/w}$) of aroma compounds as a function of lipid content of emulsions with liquid lipid (open symbol) and solid lipid (closed symbol) droplets (a) ethyl butanoate, (b) ethyl pentanoate, (c) ethyl heptanoate and (d) ethyl octanoate. Results for **HPS** emulsions with different particle sizes (d_{32}) highest (◊), medium (□) and lowest (Δ) are shown. Solid lipid data points are connected for each particle size while only one line has been used to connect the liquid lipid data points

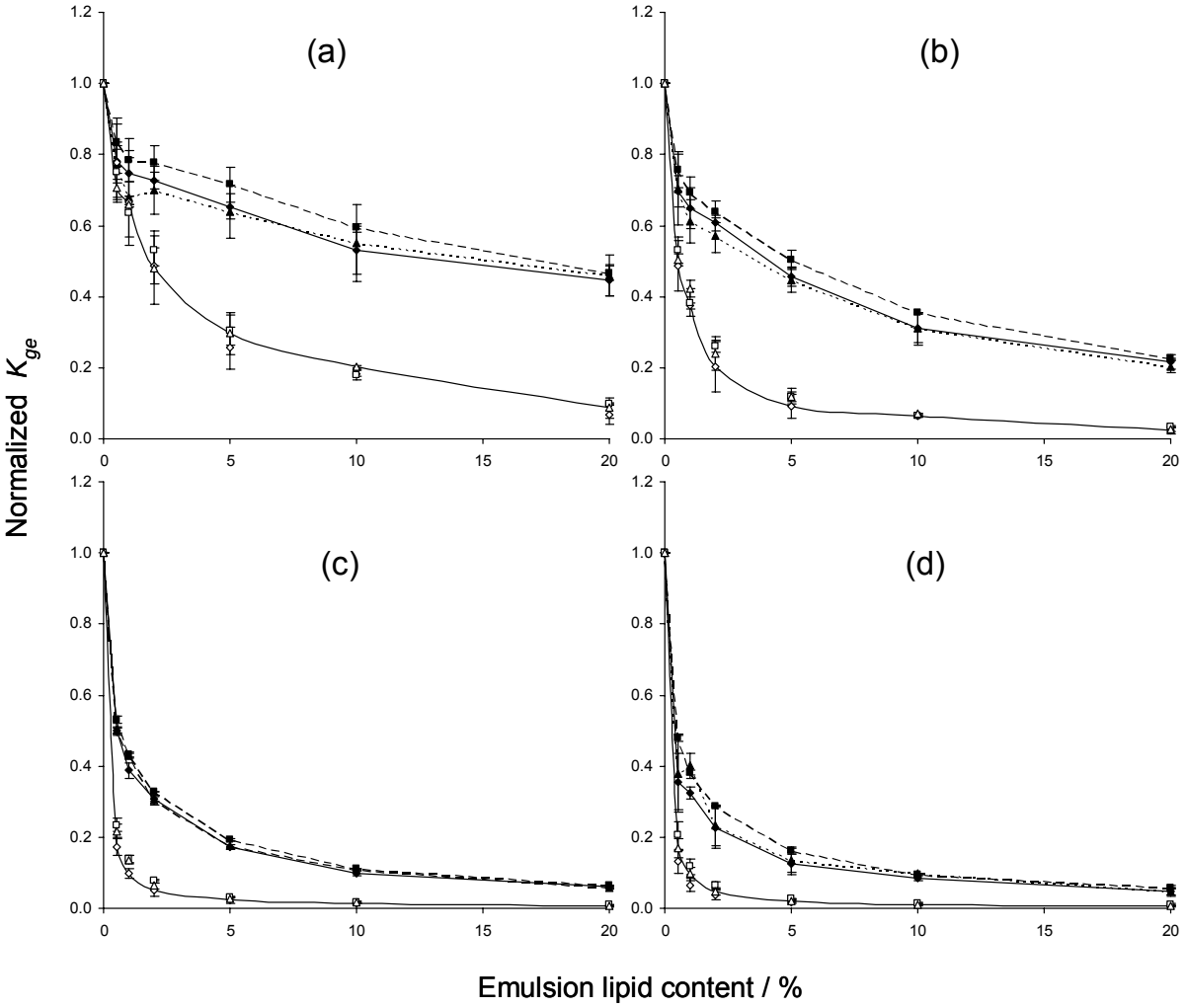

Figure **5.6**: Normalized gas-emulsion partition coefficient ($K_{ge/w}$) of aroma compounds as a function of lipid content of emulsions with liquid lipid (open symbol) and solid lipid (closed symbol) droplets (a) ethyl butanoate, (b) ethyl pentanoate, (c) ethyl heptanoate and (d) ethyl octanoate. Results for **Salatrim**® emulsions with different particle sizes (d_{32}) highest (◊), medium (□) and lowest (Δ) are shown. Solid lipid data points are connected for each particle size while only one line has been used to connect the liquid lipid data points

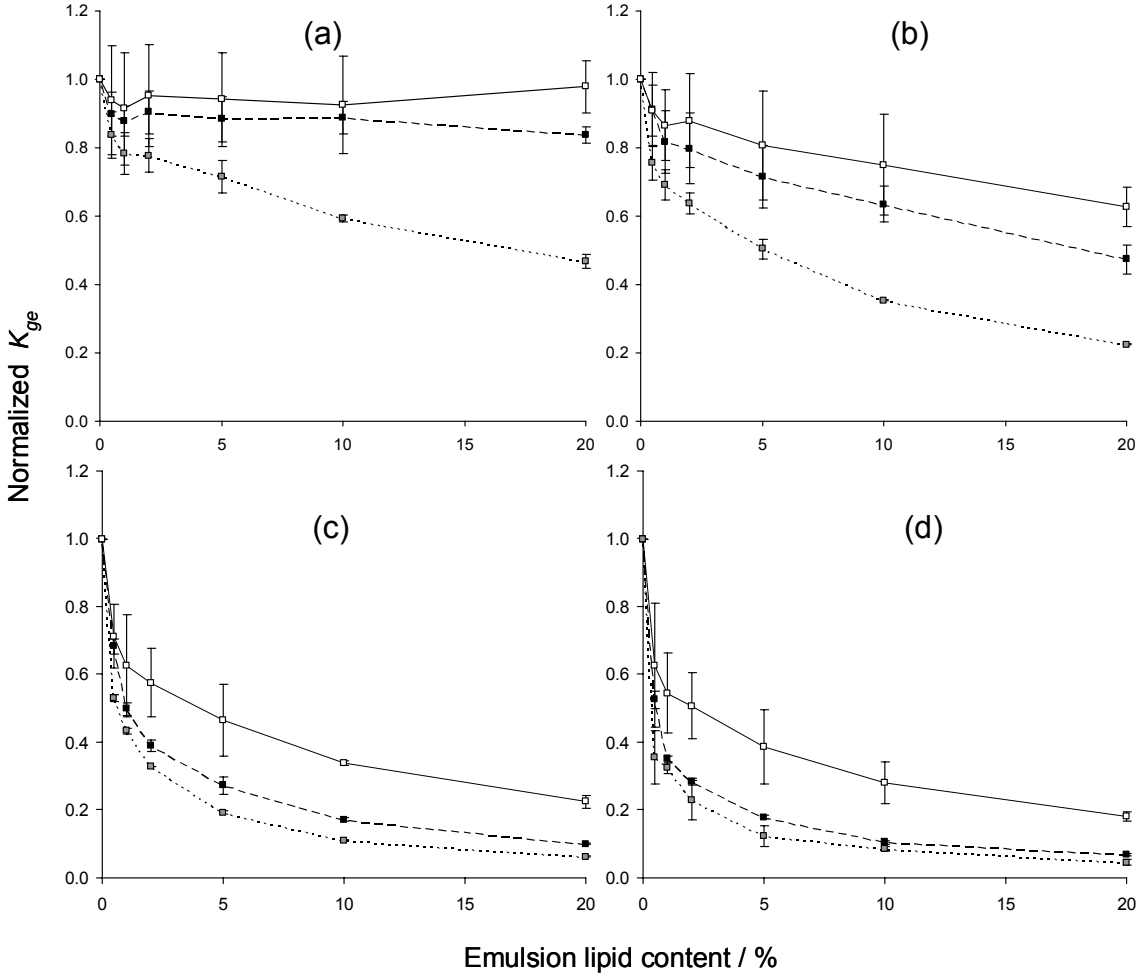

Figure **5.7**: Normalized gas-emulsion partition coefficient ($K_{ge/w}$) of aroma compounds as a function of lipid content of emulsions with solid lipid droplets (a) ethyl butanoate, (b) ethyl pentanoate, (c) ethyl heptanoate and (d) ethyl octanoate. Results for emulsions with different lipid types n-eicosane (□), HPF (■) and Salatrim® (▨) are shown for d_{32} = ~0.5 μm.

(i) Residual Liquid Oil. The first of these proposed mechanisms may be reasonable for the solid Salatrim® droplets because, according to the manufacturers, the solid fat content of this fat is only 91% at 10°C (the measurement temperature). If the residual liquid oil is responsible for the interactions of the aroma molecules with the droplets, then the value of $K_{ge/w}$ for "solid" droplet Salatrim® emulsions should be equal to those of a similar liquid droplet emulsion with a lower fat content. A modified form of the Buttery equation (Equation 4.2) was used to model the data and test this hypothesis (Chapter 4):

$$\frac{1}{K_{ge}} = \frac{\phi_o(1-\phi_{sf})}{K_{go}} + \frac{(1-\phi_o)}{K_{gw}} \tag{5.3}$$

where, ϕ_{sf} is the solid fat content of the lipid (taken as 91% for Salatrim®). Equation 5.3 is similar to Equation 5.1 with the exception that only the liquid fraction of the lipid is assumed to interact with the emulsion and no surface binding effects are considered. The prediction from the model is shown alongside the data for EH in Figure **5.8** (r^2= 0.97). While the trends in the data and the model are similar and the fit is better than the 100% liquid oil line (also shown) the quantitative fit agreement of theory and experiment is only moderate. The best fit of Equation 5.3 shown in Figure **5.8** assuming the solid fat content of the solid Salatrim® was 95%. The actual value of the solid fat content of the droplets under measurement conditions is hard to specify precisely and may differ significantly from the bulk measurements reported by the manufacturer (Dickinson and McClements, 1995). However, these calculations give an indication that even a small amount of liquid oil in an apparently solid fat may be all that is required to bind an appreciable amount of flavor. In the eicosane droplets there was presumably no or very little liquid oil so the only interactions could be at the surface.

A similar approach was taken for the solid HPS emulsions and the best fit between theory and experiment was obtained for a solid fat content of 97% (Figure **5.8**). The theoretical line fits the experimental data well (r^2= 0.98), but how reasonable is the

assumption that there is 3% liquid oil in these samples? HPS has a capillary melting point of 60^{o}C (from the supplier specifications) and we do not expect any liquid to be present in the pure fat at 10^{o}C but perhaps the presence the aroma compounds forms a liquid aroma-fat solution phase at the fat crystal grain boundaries. The presence of liquid oil at the grain boundaries was shown in the images included in Marangoni's recent book (Litwinenko, 2005). In this case, the partitioning of the aroma into the solid fat droplets depends on the phase behavior of the aroma-fat system and the volumes of the phases and not on the droplet size.

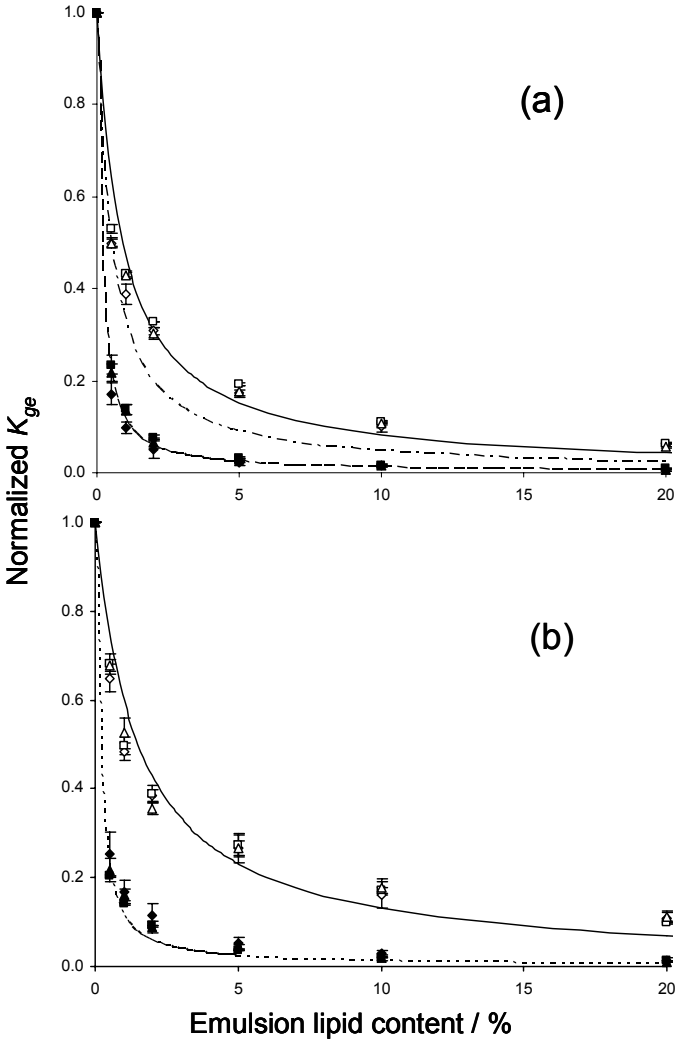

Figure **5.8**: Normalized gas-emulsion partition coefficient ($K_{ge/w}$) of ethyl heptanoate (EH) as a function of lipid content of emulsions with solid lipid droplets. Data for (a) Salatrim® and (b) HPS emulsions with different particle sizes (d_{32}) highest (◊), medium (□) and lowest (Δ) are shown along with the model (Equation 5.3) predicted line for (a) 9% (— - —), 5% (——)and (b) 3% (——) liquid oil content. The gas-oil and gas-water partition coefficients values of EH were taken as 8.1×10^{-6} and 1.82×10^{-2}, respectively. Also shown pure liquid oil emulsion data (closed black symbol) and theoretical prediction (----) from Buttery model (Equation 4.2)

(ii) Co-crystallization. An alternative mechanism for the interaction between solid fat and aroma compounds is the co-crystallization of two chemicals. Although, aroma partitioning from emulsified triglycerides can be explained from their liquid oil content, there are structural differences that might also explain aroma partitioning. Emulsified HPS crystallizes into a mixture of unstable α and more stable β/β' polymorphs (Figure **5.1** b). The aliphatic chains of crystalline triglycerides are disordered in the α form, packed with an intermediate density in the β' form and most densely packed in the β form (Sato, 2001). It has been proposed that because of lower packing density, α crystals would be able to support a greater load of co-crystallized solute (Bunjes and Koch, 2005; Muller, Mader and Gohla, 2000). Therefore, it is expected that solid HPS droplets would be able to accommodate some aroma compounds in its crystalline matrix as well as any potential surface adsorption and hence lower HS aroma concentration compared to the n-eicosane emulsion. A similar argument was used in reference to the incorporation of a drug into solid lipid nanoparticles (Muller, et al., 2000), drug molecules will be excluded from the lipids forming crystals with perfect lattice (e.g. monoacid triclycerides) (Westesen, Bunjes and Koch, 1997) whereas they can be incorporated into the less perfect crystal structure of complex triglycerides (Muller, et al., 2000).

Salatrim® has a highly asymmetrical molecular structure and hence packing into a definite crystalline polymorph is difficult (Narine and Marangoni, 1999a; 1999b). Narine et al. (1999a) proposed that the solid phase of Salatrim® is characterized by random arrangement of platelet-like growth. This type of growth would lead to more surface area in solid Salatrim® droplets compared to HPS droplets and hence space for more aroma adsorption. The situation is somewhat similar to the physical structure of co-crystallized flavor and sugar agglomerate where flavor molecules are included between numerous micro-sized irregular sugar crystals (Chen, Veiga and Rizzuto, 1988; Zeller and Saleeb, 1996).

Reversibility of aroma-solid lipid interaction. Solid I samples were prepared by adding a stock aroma solution to solid droplet emulsions. However, if the aroma molecules were present in liquid oil droplets before fat crystallization, will they be entrapped inside the crystalline solid lipids? To test this hypothesis, Solid II samples were prepared by re-crystallizing aroma added liquid droplet emulsions and $K_{ge/w}$ were measured. The partitioning behavior of Solid I and Solid II samples were similar irrespective of lipid type (Figure **5.9,** Figure **5.10,** and Figure **5.11**). This indicated that at equilibrium the amount of aroma incorporated into the solid phase or adsorbed on the solid lipid surface is constant and defined by the thermodynamic properties of the phases. There is no evidence of any "entrapment" of volatiles within the crystal droplet.

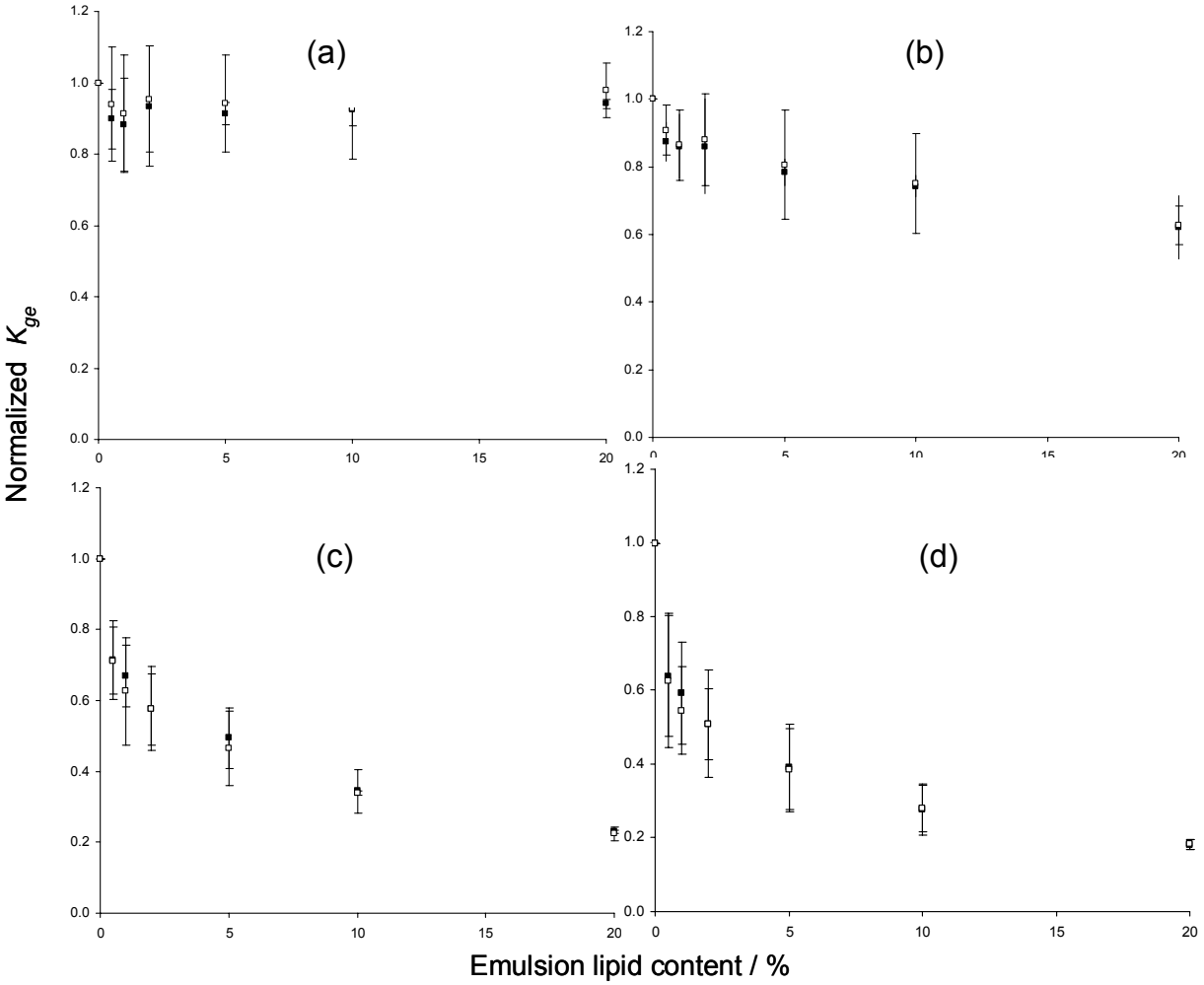

Figure **5.9**: Normalized gas-emulsion partition coefficient ($K_{ge/w}$) of aroma compounds as a function of lipid content of eicosane emulsions (d_{32} ~0.5 μm) with solid lipid droplets comparing Solid I (open symbol) and recrystallized Solid II (closed symbol) samples (a) ethyl butanoate, (b) ethyl pentanoate, (c) ethyl heptanoate and (d) ethyl octanoate.

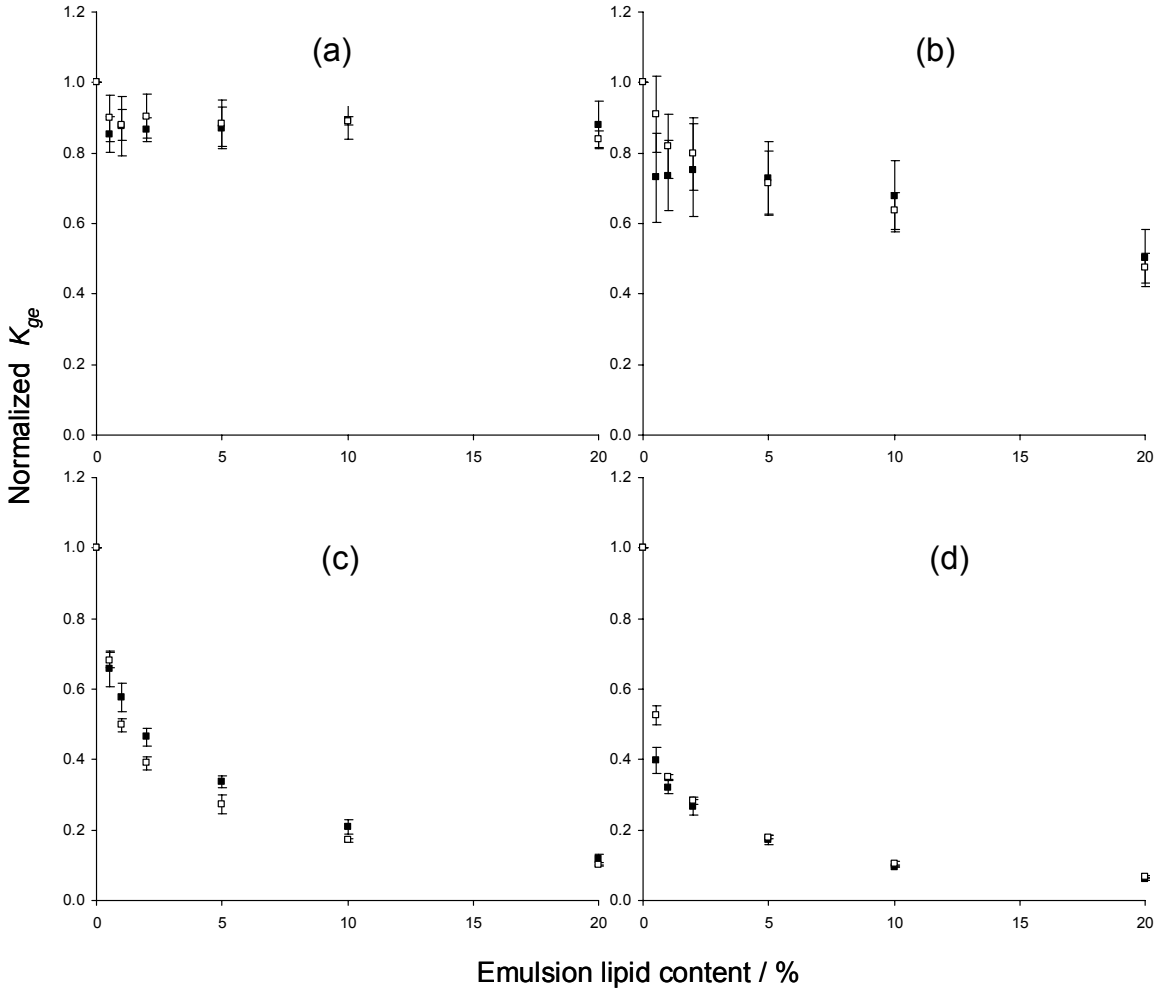

Figure **5.10**: Normalized gas-emulsion partition coefficient ($K_{ge/w}$) of aroma compounds as a function of lipid content of **HPS** emulsions (d_{32} ~0.5 μm) with solid lipid droplets comparing Solid I (open symbol) and recrystallized Solid II (closed symbol) samples (a) ethyl butanoate, (b) ethyl pentanoate, (c) ethyl heptanoate and (d) ethyl octanoate.

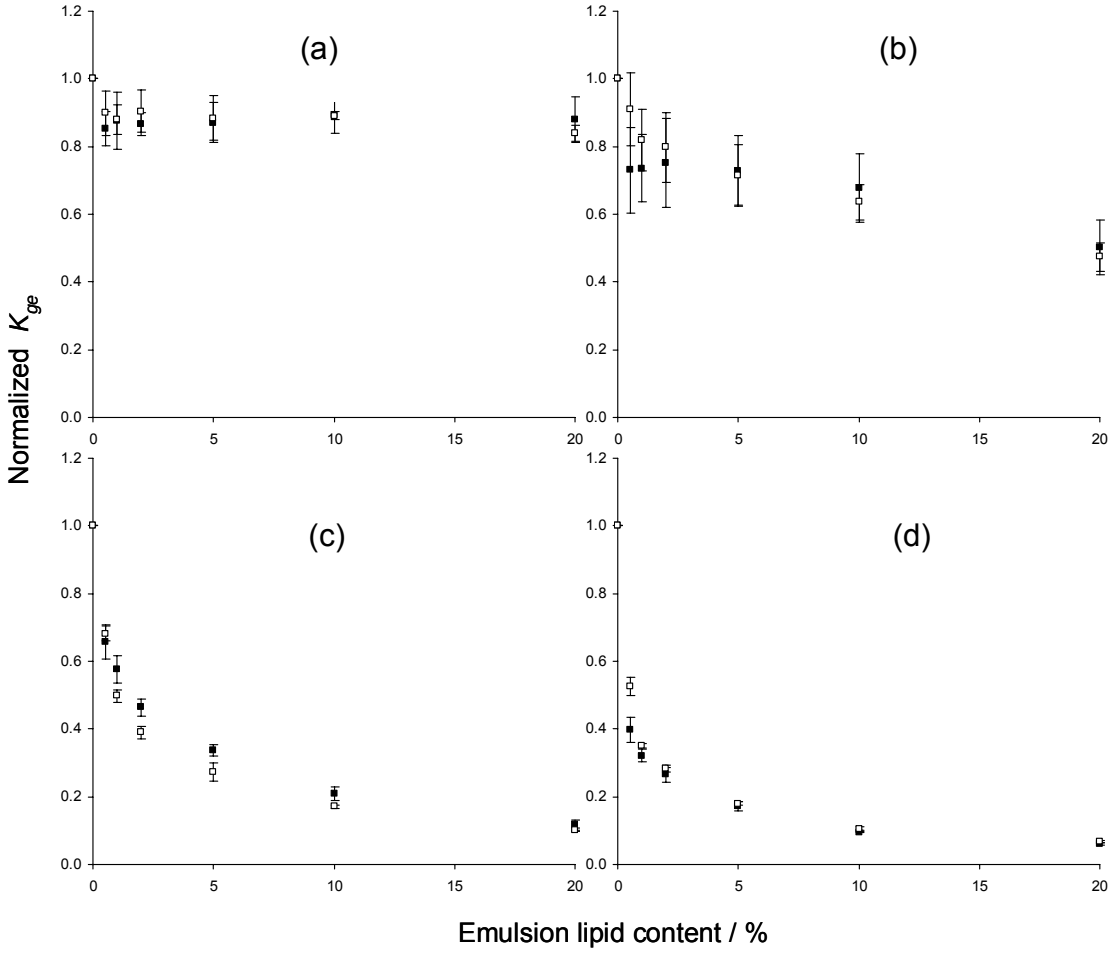

Figure **5.11**: Normalized gas-emulsion partition coefficient ($K_{ge/w}$) of aroma compounds as a function of lipid content of **Salatrim**® emulsions (d_{32} ~0.5 μm) with solid lipid droplets comparing Solid I (open symbol) and recrystallized Solid II (closed symbol) samples (a) ethyl butanoate, (b) ethyl pentanoate, (c) ethyl heptanoate and (d) ethyl octanoate.

5.4 Conclusion

The partitioning of volatile aroma compounds dependent on the composition of the system (oil concentration, aroma type) but not on the type of liquid oil used in the emulsions. Interactions between solid fat droplets and aroma compounds are much weaker than those with liquid oil droplets but are significantly influenced by the nature of the solid fat. n-Alkanes, crystallize in pure form and excludes all aroma compounds from the solid droplets (although some can adsorb to the droplet surfaces). Aroma compounds also interact with complex triglyceride mixtures in food lipids but the mechanism of interaction is different and dependant on the volume not the surface area of the droplets. This could be explained by presence of liquid oil residual at the crystal grain boundaries in the “solid” droplet which can act as a reservoir for the aroma or alternatively, as triglycerides crystallize in a mixture of different polymorphs, their less perfect crystal structure may allow the co-crystallization of aroma compounds..

5.5 References

Bunjes, H.; Koch, M. H. J., Saturated phospholipids promote crystallization but slow down polymorphic transitions in triglyceride nanoparticles. *Journal of Controlled Release* **2005,** 107, 229-243.

Chen, A. C.; Veiga, M. F.; Rizzuto, A. B., Cocrystallization - an Encapsulation Process. *Food Technology* **1988,** 42, (11), 87-90.

Coupland, J. N., Crystallization in emulsions. *Current Opinion in Colloid & Interface Science* **2002,** 7, (5-6), 445-450.

Dickinson, E.; McClements, D. J., *Advances in Food Colloids*. Chapman & Hall: New York, **1995**.

Ghosh, S.; Peterson, D. G.; Coupland, J. N., Effects of droplet crystallization and melting on the aroma release properties of a model oil-in-water emulsion. *Journal of Agricultural and Food Chemistry* **2006a,** 54, (5), 1829-1837.

Ghosh, S.; Peterson, D. G.; Coupland, J. N. In *Flavor binding by solid and liquid emulsion droplets*, Food Colloids Conference, Montreux, Switzerland; Dickinson, E., Ed. Royal Society of Chemistry, UK, **2006b**; in press.

Keast, R. S. J.; Dalton, P. H.; Breslin, P. A. S., Flavor interaction at the sensory level. In *Flavor Perception*, Taylor, A. J.; Roberts, D. D., Eds. Blackwell Publishing: Oxford, UK, **2004**; pp 228-249.

Kloek, W.; Walstra, P.; van Vliet, T., Nucleation kinetics of emulsified triglyceride mixtures. *Journal of American Oil Chemists Society* **2000,** 77, (6), 643-652.

Litwinenko, J. W., Fat crystal network: microstructure DVD Image Archive. In *Fat Crystal Networks*, Marangoni, A. G., Ed. Marcel Dekker: New York, 2005

McNulty, P. B.; Karel, M., Factors affecting flavor release and uptake in O/W emulsions, 2. Stirred cell studies. *Journal of Food Technology* **1973,** 8, 319-331.

Muller, R. H.; Mader, K.; Gohla, S., Solid lipid nanoparticles (SLN) for controlled drug delivery - a review of the state of the art. *European Journal of Pharmaceutics and Biopharmaceutics* **2000,** 50, (1), 161-177.

Narine, S. S.; Marangoni, A. G., Difference between cocoa butter and Salatrim® lies in the microstructure of the fat crystal network. *Journal of American Oil Chemists Society* **1999a,** 76, (1), 7-13.

Narine, S. S.; Marangoni, A. G., Microscopic and rheological studies of fat crystal network. *Journal of Crystal Growth* **1999b,** 198/199, 1315-1319.

Roberts, D. D.; Pollien, P.; Watzke, B., Experimental and modeling studies showing the effect of lipid type and level on flavor release from milk-based liquid emulsions. *Journal of Agricultural and Food Chemistry* **2003,** 51, 189-195.

Sato, K., Crystallization behavior of fats and lipids - a review. *Chemical Engineering Science* **2001,** 56, (7), 2255-2265.

Taylor, A. J., Volatile flavor release from foods during eating. *Critical Reviews in Food Science and Technology* **1996,** 36, (8), 765-784.

Ueno, S.; Hamada, Y.; Sato, K., Controlling polymorphic crystallization of n-alkane crystals in emulsion droplets through interfacial heterogeneous nucleation. *Crystal Growth & Design* **2003,** 3, (6), 935-939.

Westesen, K.; Bunjes, H.; Koch, M. H. J., Physicochemical characterization of lipid nanoparticles and evaluation of their drug loading capacity and sustained release potential. *Journal of Controlled Release* **1997,** 48, (2-3), 223-236.

Zeller, B. L.; Saleeb, F. Z., Production of microporous sugars for adsorption of volatile flavors. *Journal of Food Science* **1996,** 61, (4), 749.

Chapter 6

Temporal Aroma Release Profile of Solid and Liquid Droplet Emulsions

Abstract

The release kinetics of four model aroma compounds was measured from coarse (d_{32}= 1.0 μm) and fine (d_{32}= 0.25 μm) eicosane and hydrogenated palm stearin (HPS) emulsions with either solid or liquid lipid droplets. For both lipids, the release of aroma compounds from emulsions with solid droplets was higher than emulsions with liquid droplets. This difference was greater for higher molecular weight and less polar aroma compounds. The release rate from solid eicosane droplets increased with particle size but no such effect was observed for HPS emulsions and release from solid HPS was slower than solid eicosane. By manipulating the aroma content, the initial aroma release profile of the solid droplet emulsion can be matched to that of a liquid droplet emulsion but at a fraction of the flavor load.

6.1 Introduction

During most of the interactions with food that lead to sensation, the aroma molecules are not at equilibrium and their distribution will change with time. For example, when a package of food is opened and air is drawn over the surface of the food during sniffing, the concentration of volatile molecules reaching the aroma sensitive receptors in the nose changes dynamically. While the thermodynamics of flavor partitioning can give the equilibrium aroma concentration under the new condition, it does not say anything about the timescale needed to get there. As food consumption occurs over a short timescale, knowledge of kinetics of aroma release from food is necessary in order to have a better control of the perceived quality of the food.

Dynamic aroma release from food can be measured by directly sampling the exhaled gas as a human being eats or drinks the sample. However, the oral processing of food as well as release of aroma through the retronasal or orthonasal pathway can be affected by various physiological factors and vary markedly from individual to individual. Thus, more precisely controlled model mouths are used by several researchers to measure the kinetics of volatile release from foods (van Ruth, Roozen and Cozijsen, (1994); Roberts and Acree, (1995); Rabe Krings, Banavara and Berger, (2002). These systems have the advantage of thoroughly controlling the experimental conditions but inevitably, the conditions selected may not be representative of real consumption.

Various types of model mouths have been developed to simulate some of the processes occurring during eating such as mechanical mixing and addition of saliva. In some of the earlier in vitro methods, gas is passed either over (i.e. flushing) or through (i.e. purging) the food product to strip off the volatiles which were trapped for subsequent analysis in a GC (van Ruth, et al., 1994). Recently with the development of new

analytical techniques, continuous measurements of dynamic headspace samples were possible (Marin, Baek and Taylor, 2000; Marin, Baek and Taylor, 1999). The model mouth system used in the present work is similar to those used by Marine, Baek and Taylor (1999 and 2000). The food sample is mixed inside a temperature controlled, stirred glass vessel and inert carrier gas is passed over the sample to strip off the volatiles from the headspace directly to an atmospheric pressure chemical ionization – mass spectrometer (APCI-MS) for real time quantification of aroma release into the headspace.

It has been shown previously that equilibrium partitioning of aroma compounds from an oil-in-water emulsion was significantly influenced by phase transitions in the lipid phase (Chapter 3) and that aroma- solid triglyceride (hydrogenated palm stearin) interactions are stronger than that from aroma- solid eicosane interactions (Chapter 5). However, these measurements were performed under equilibrium conditions, and in order to better understand how dispersed phase crystallization might influence actual aroma release, the kinetic properties must also be studied. In the present study, temporal aroma release profiles from emulsions with solid and liquid droplets were determined using the model mouth system described above. Both eicosane and hydrogenated palm stearin (HPS) were used, and the differences in temporal release profile due to the nature of the fat, effect of droplet crystallinity and droplet size were investigated. Finally, based on the release profile of solid and liquid droplet emulsions, a novel technique for the reduction of aroma load of emulsions was proposed.

6.2 Materials and Methods

Materials. Hydrogenated palm stearin (27 Stearin®) was donated by Loders Croklaan (Channahon, IL). Eicosane was purchased from Fisher Scientific (Springfield, NJ). All other chemicals were obtained from the Sigma Chemical Company (St. Louis, MO).

Emulsion preparation. Emulsions were prepared by mixing molten fat (20 wt%) with sodium caseinate solution (2 wt% with 0.02% thimerosal to prevent microbial growth) using a high-speed blender (Brinkmann Polytron, Brinkmann Instruments Inc., Westbury, NY) for 30 seconds. The coarse emulsions were then re-circulated through a twin-stage valve homogenizer (Niro Soavi Panda, GEA Niro Soavi, Hudson, WI) at different pressures to achieve different droplet size distributions. To prevent fat crystallization during emulsion preparation, all ingredients were used at elevated temperatures and the homogenizer was rinsed several times with hot water. The particle size distributions of the emulsions were characterized by laser diffraction particle sizing (Horiba LA 920, Irvine, CA) using a relative refractive index of 1.15. The emulsions were stored at a temperature greater than 50ºC to prevent fat crystallization prior to use. Samples of emulsions were diluted to 2 wt% with deionized water and were used for the kinetic release study.

Thermal Analysis. The crystallization and melting behavior of bulk and emulsified lipids were determined using a differential scanning calorimeter (Perkin-Elmer DSC-7, Norwalk, CT). The instrument was calibrated against indium prior to use. Aliquots (~15 mg) of bulk and emulsified lipids were temperature cycled in the DSC from 70°C to 10°C to 70°C. The heating and cooling rate was 5ºC min^{-1}.The crystallization and melting points of bulk and emulsified lipids were taken from the onset

temperature of peaks on the thermogram using Pyris data analysis software (version 3.52, Perkin-Elmer Corporation, Norwalk, CT). All analyses were conducted in triplicate.

Preparation and addition of aroma compounds to emulsions. A stock aroma solution was prepared by mixing four aroma compounds, ethyl butanoate (EB), ethyl pentanoate (EO), ethyl heptanoate (EH) and ethyl octanoate (EO) in a volumetric ratio of 1:2:20:20 and diluting to a 50% solution in ethanol. Emulsions were transferred to screw top glass conical flasks and stock aroma solution (5 μL/L) was added to the emulsions, sealed with air tight cap and mixed for 1 hour with continuous stirring. The final aroma concentrations (μL/L) in emulsions was EB, 0.058; EP, 0.116; EH, 1.16; and EO, 1.16. Aliquots (200 ml) of this aroma added emulsions were transferred to separate glass flasks, sealed with air tight caps and were temperature cycled as described below to produce either solid or liquid droplet emulsions.

Liquid droplet emulsions were produced by transferring the samples directly to water baths pre-set to 30°C. Solid droplet emulsions were produced by cooling the samples to 10°C to ensure complete crystallization then reheating to the experimental measurement temperature (30ºC). The temperature cycles allowed us to compare the interaction of aroma compounds with solid and with liquid droplets at the same temperature (see below). Samples were stored for at least 24 hours before measuring the dynamics of aroma release as it has been previously shown that this is sufficient time for equilibration of the aroma compounds among the different phases of the emulsion (Chapter 5).

Real time aroma release analysis by APCI-MS. To measure the dynamics of aroma release from solid and liquid droplet emulsions a glass vessel (volume 330 ml) similar to one shown in Figure **6.1** was used. The glass vessel had an inlet for gas flow and an outlet for gas-aroma mixture which was connected to a Quattro II/Micromass mass spectrometer (Waters, Milford, MA) with an atmospheric pressure chemical ionization (APCI) inlet via an interface set at 65^{o}C. The third opening in the glass vessel

is designed for both sample addition and for adjusting the split flow condition of the nitrogen gas used during the experiment. The jacket around the vessel was attached to a water bath to control the temperature during the experiment and an air tight Teflon cap was used to seal the top of the vessel. A magnetic stir bar was added to stir the liquid contents of the vessel at 300 rpm.

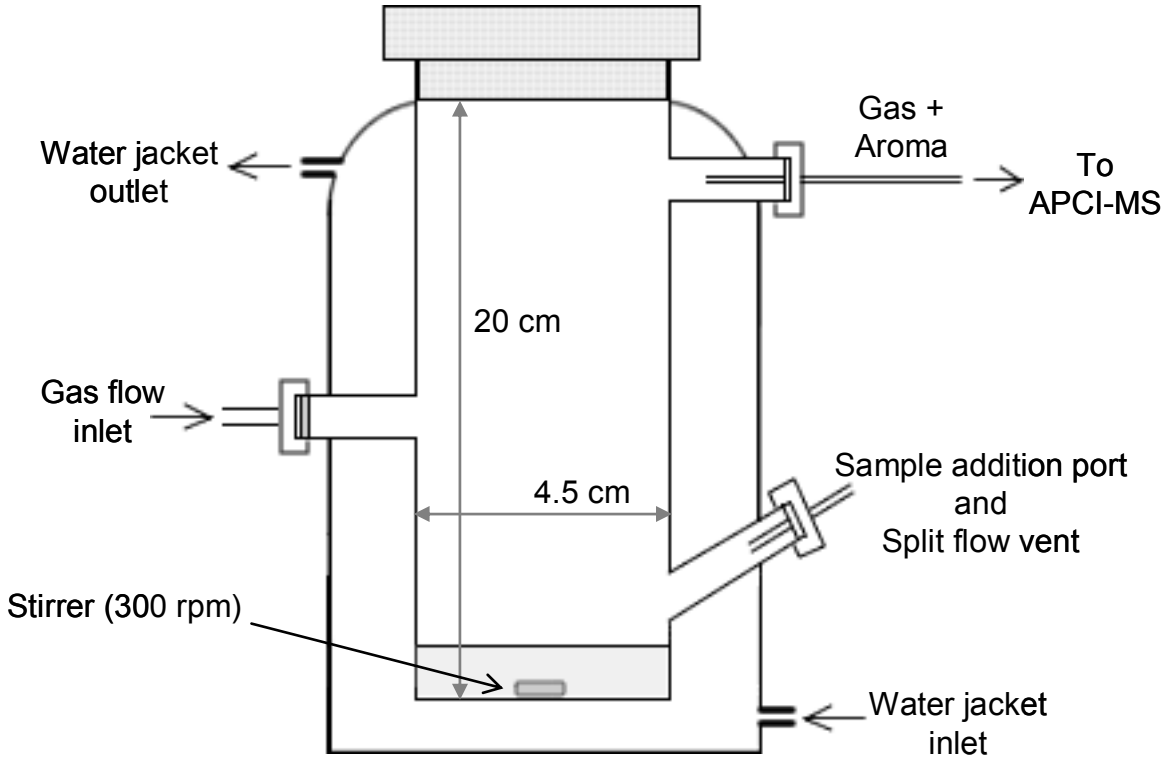

Figure **6.1**: Schematic diagram of the model mouth.

An aliquot (20 ml) of emulsion with added aroma compounds was sealed into the glass vessel and, after 15 seconds, the nitrogen gas flow valve (flow rate 320 ml min^{-1}) was opened and the volatile aroma compounds released into the headspace were carried away to the APCI-MS inlet. The total flow of nitrogen was split in two parts, flow to the MS was 5 ml min^{-1} and the remainder was vented to the atmosphere. The operating conditions of the APCI inlet used were: Select Ionization Mode (SIM); block temperature, 120°C; transfer line, 65°C; corona discharge, 3.5 kV, cone voltage, 12V. Ions monitored were 117 $[M + H]^+$ for EB, 131 $[M + H]^+$ for EP, 159 for EH and 173 $[M + H]^+$ for EO. The amount of each aroma compound in the carrier gas was measured in real time by the MS and the change in intensity was plotted as a function of time by the MassLynx v4.0 Sp2 software (Waters, Milford, MA). The release profile results for EB were very noisy and it was not possible to distinguish the effect of different samples so they are not reported.

The concentration of aroma compounds in the headspace was determined using a standard calibration curve (Schober and Peterson, 2004). Seven different levels of aroma compounds (0.087, 0.174, 0.348, 0.696, 1.044, 1.392, and 1.636 μg) dissolved in pentane were injected into a specialized air tight water-jacketed 1.12 L deactivated glass vessel. The vessel was maintained at 40^{o}C and the gas phase was mixed with a magnetic stirrer at 300 rpm. After 3 minutes of stirring, the liquid had completely evaporated providing a known concentration of volatiles in the air inside the container. These were measured by connecting the vessel to the APCI-MS instrument using the same operating conditions as described above except that no nitrogen gas flow was used and instead a venturi suction flow rate of 5 ml min^{-1} was applied. The volatiles from the deactivated glass vessel were sampled for 40 seconds and the average peak height (ion intensity) for each sample was plotted against the known weight of aroma compound per liter of air to construct calibration curves ($r^2 \geq 0.99$).

6.3 Results and Discussion

Physical Properties of the Emulsions. By varying the homogenization conditions, it was possible to manufacture emulsions with two different droplet size distributions (Table **6.1**). The droplet size distribution for all the emulsions were unimodal with an average standard deviation of the distribution of ~0.18±0.2 μm. The emulsions were physically stable over the course of the experiment (i.e., no changes in measured droplet size, no apparent creaming).

Table **6.1**: Emulsion preparation conditions and particle size for different lipid types and the normalized gas-emulsion partition coefficients (K_{ge}) for 2% lipid emulsions containing solid and liquid lipid droplets. The normalized K_{ge} values are reported in order to compare aroma partitioning at two different temperatures (30°C for eicosane and 40°C for HPF emulsion). It was calculated by dividing the original gas-emulsion partition coefficient values by gas-water partition coefficient values at the respective temperature.

Emulsion used	Homogenization conditions		Mean droplet size (d_{32}) (μm)	Normalized K_{ge} of EH from 2% emulsion	
	Pressure (bar)	Number of passes		Liquid droplet	Solid droplet
Eicosane	110±10	2	1.04	0.07±0.01	0.63±0.1
	320±20	10	0.20	0.07±0.02	0.52±0.07
HPS	110±10	2	0.98	0.10±0.03	0.38±0.01
	320±20	10	0.26	0.09±0.01	0.36±0.01

The melting and cooling thermograms of the emulsified lipids are shown in Figure **6.2**. On cooling, emulsified lipids crystallized with a single major peak at around 22° and 32°C for eicosane and HPS, respectively. The eicosane samples showed a single peak (at 36°C) on heating corresponding to the melting of the crystals while HPS had a

more complex melting thermogram due to several polymorphic phase transitions between 44^{o} to 60^{o}C (Figure **6.2**) (Kloek, Walstra and van Vliet, 2000). The emulsified lipids crystallized at a lower temperature than the corresponding bulk oils while the melting points of the bulk and emulsified forms were similar (data not shown). The deep supercooling required to initiate crystallization in oil droplets has been observed in a wide range of emulsions and is usually attributed to the majority of the lipid being isolated from potential nucleation catalysts and therefore nucleating homogeneously (Coupland, 2002). Eicosane has a deeper supercooling than HPS and this might be due to a difference in the number of potential nucleation catalysts for the triglyceride. The supercooled emulsions were very stable and it was possible to maintain liquid emulsion droplets below their thermodynamic freezing point for several weeks without any measurable crystallization.

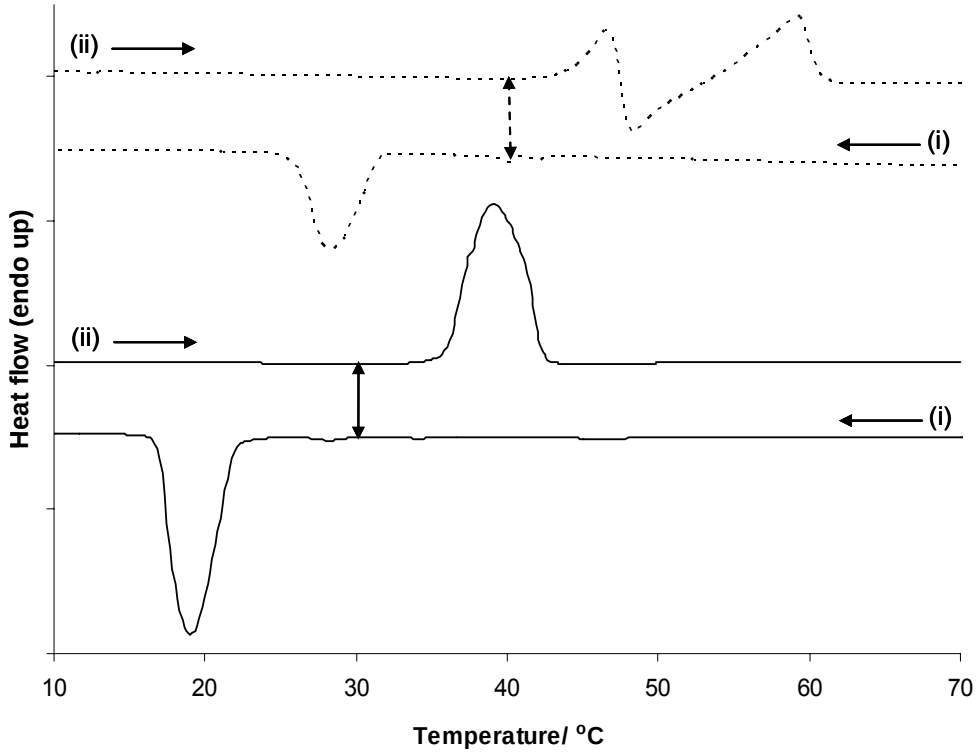

Figure **6.2**: Thermogram of eicosane (—) and HPS (-----) emulsions during (i) cooling and (ii) heating. Arrows on the temperature axis indicates the temperature of the experimental measurements for solid and liquid droplet emulsions. Emulsions were 20 wt% lipid stabilized with 2 wt% sodium caseinate solution and was temperature cycled at $5^{o}C\ min^{-1}$.

The temperature for measuring the release profile of different lipid emulsions are shown by arrows on the thermogram (Figure **6.2**). For example, an eicosane emulsion could be cooled from 70^{o}C to 30^{o}C to have liquid droplets, or it could be cooled further to 10^{o}C and reheated back to 30^{o}C to have emulsions with solid droplets. Similar conditions can also be found for HPS emulsions at 40^{o}C. Thus by varying the temperature history of the emulsion, it was possible to produce emulsions with either complete solid or complete liquid droplets at the same temperature. These conditions were used to compare the results from solid and liquid droplet emulsions at the same temperature. It should be noted that solid and liquid in this context refers to the properties of the droplets. The overall emulsions were fluids with no apparent differences in their physical properties.

Dynamics of aroma release from liquid droplet emulsions. Release profiles of aroma compounds from liquid droplet emulsions are shown in Figure **6.3**. As the flow of nitrogen started, the aroma compounds that had accumulated in the headspace during the 15 s non-gas flow time as the vessel were sealed, were swept away from the glass vessel to the APCI-MS detector. For all samples, the aroma concentration increased sharply to a maximum value in a very short period of time and thereafter decreased slowly with time as the rate at which aroma compounds are swept out of the glass vessel exceeds the rate at which they are released into the gas phase by the emulsion. No droplet size effect on the release profile was observed for liquid droplet emulsions irrespective of types of aroma and lipid used. For both eicosane and HPS emulsions, the maximum amount of aroma released decreased with the molecular weight of the aroma compounds. For example, the maximum aroma concentration in the headspace of eicosane emulsion for EO, EH and EP was about 26.6, 71.3 and 368.9 ng/L per ppm of aroma compounds added, respectively (Figure **6.3)**

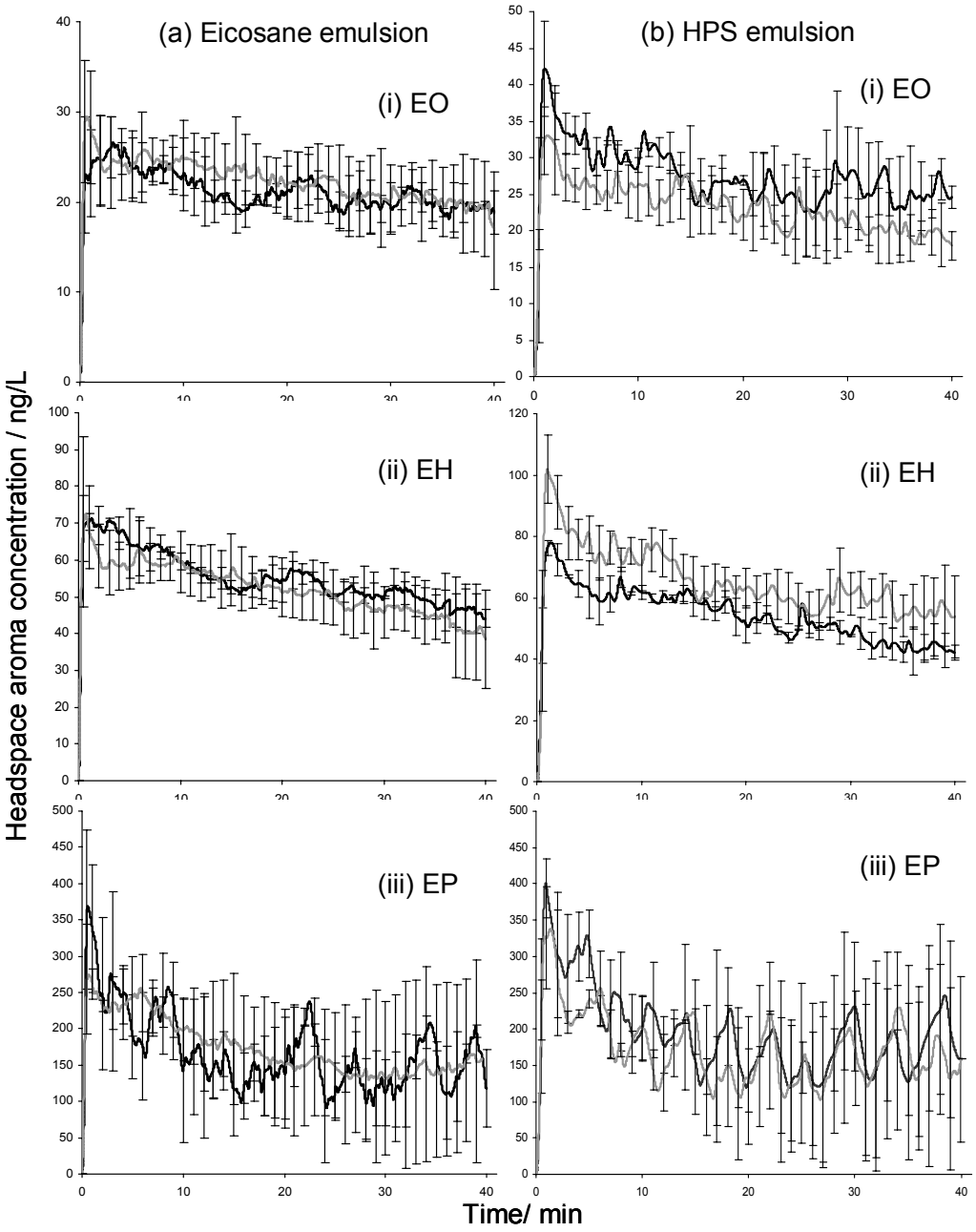

Figure **6.3**: Aroma release profile of liquid droplet emulsions (a) Eicosane and (b) HPS. Results for emulsions with different particle sizes (d_{32}) 0.2 μm (━━) and 1.0 μm (━━) are shown for different aroma compounds: (i) EO, (ii) EH and (iii) EP. The error bars represent one standard deviation (n=3).

Dynamics of aroma release from solid droplet emulsions. Figure **6.4** shows the release profiles of aroma compounds from eicosane and HPS solid droplet emulsions along with liquid droplet data for comparison. For all samples, the gas phase aroma concentration maximum is significantly higher for solid droplet emulsions than that for liquid droplet emulsions. In Chapter 5, I showed that more aroma partitions into liquid oil droplets compared to solid fat droplets and so the headspace concentration above the liquid droplets is lower. This can also be observed from the normalized gas-emulsion partition coefficient (K_{ge}) values of solid and liquid droplet emulsion reported in Table **6.1**. The lower thermodynamic driving force for release explains why the initial peak in the dynamic release curves for liquid droplet emulsions is less than that for solid droplet emulsions. Similarly the faster decay rate from the maximum value for the solid droplet emulsions is because much of the aroma originally present has been swept out by the gas flow and the emulsion is not capable of replenishing the headspace concentration. for example, the total concentration of EO in a solid droplet emulsion decreased by about 20% over the 40 minutes of gas flow while the corresponding loss from the liquid droplet emulsion was only about 2% of the EO originally present in the emulsion.

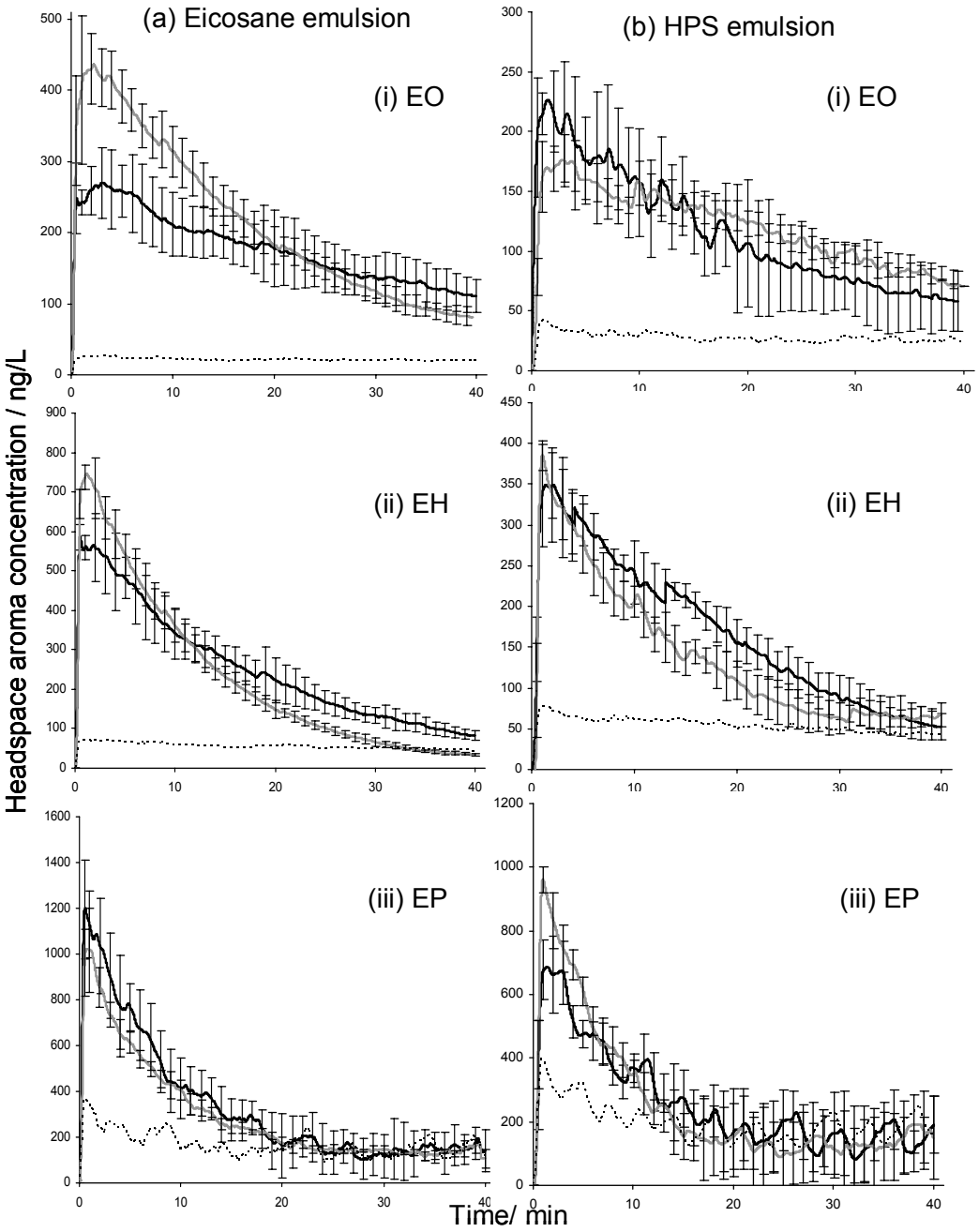

Figure **6.4**: Aroma release profile from solid droplet emulsions (a) Eicosane and (b) HPS. Results for emulsions with different particle sizes (d_{32}) 0.2 μm (▬) and 1.0 μm (▬) are shown for different aroma compounds: (i) EO, (ii) EH and (iii) EP. For comparison a release profile of the corresponding liquid lipid emulsion (- - -) is also shown. The error bars represent one standard deviation (n=3).

The smaller solid eicosane droplets had a lower maximum headspace EH and EO concentration and lower decay rate of the headspace concentration compared to the larger solid eicosane droplets (although this difference was not observed for EP) (Figure **6.4** a). No droplet size effect was observed for the solid HPS emulsions (Figure **6.4** b). Again, this difference in the dynamics of aroma release is similar to the difference in equilibrium aroma concentrations reported in Chapter 5, i.e., the gas-emulsion partition coefficient (K_{ge}) for emulsions containing small and large droplets of solid eicosane are different while those of the corresponding HPS emulsions are similar (Table **6.1**).

If differences in the equilibrium partition coefficient are responsible for differences in the dynamics of release then the release from a solid droplet HPS emulsion should be lower than release from solid droplet eicosane emulsion (Table **6.1**, K_{ge} for solid eicosane emulsions > K_{ge} for solid HPS emulsions). To test this hypothesis, the release kinetics from solid droplet emulsions for the two lipids were compared at a temperature where both are solid (i.e., 30°C, Figure **6.3**). As expected, for all aroma compounds, the initial maximum concentration is lower for solid HPS emulsions than that for solid eicosane emulsions (Figure **6.5)** and the difference in release kinetics are caused by differences in thermodynamic partitioning.

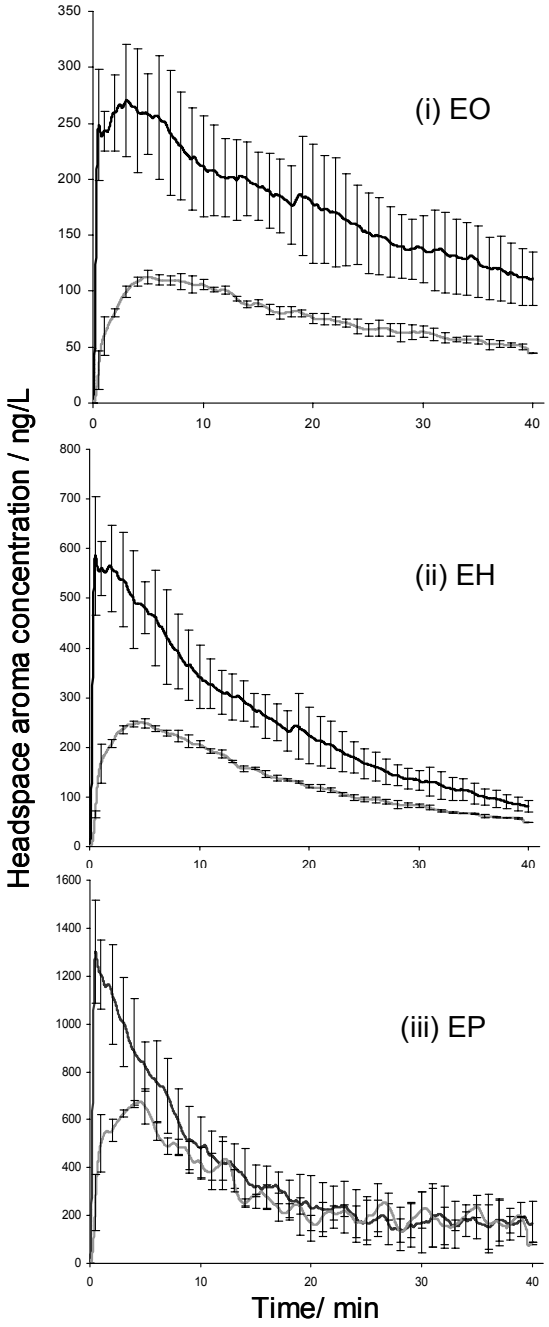

Figure **6.5**: Comparison of aroma release profiles of solid droplet eicosane (—) and HPS (—) emulsions (d_{32}=0.2 μm) at 30°C. (i) EO, (ii) EH and (iii) EP. The error bars represent one standard deviation (n=3).

Reduction of aroma load for solid droplet emulsion. The initial maximum headspace concentration under dynamic conditions is higher than for solid droplet emulsions than liquid droplet emulsions (Figure **6.4) (i.e.,** the initial maximum concentration of volatile released from HPS emulsion was about 7, 6 and 2.6 times higher for solid than liquid HPS emulsion for EO, EH and EP, respectively). Based on this difference, it should be possible to formulate a lower-aroma solid droplet emulsion to match the initial release properties of a high-aroma liquid droplet emulsions. To test this hypothesis, solid droplet emulsions were prepared with a new, modified aroma stock. The composition of the modified aroma stock was calculated by reducing the amount of each aroma in the original aroma stock by an amount equal to the ratio of solid vs. liquid droplet maximum concentrations. For example, the amount of EO in the reduced aroma stock was obtained by dividing the amount in the original aroma stock by 7 (i.e., the ratio of maximum concentration from solid to liquid droplet emulsion having same amount of aroma). The final reduced aroma concentration (μL/L) in the solid droplet emulsion was EB, 0.058; EP, 0.058; EH, 0.25; and EO, 0.22. The release profiles from solid HPS emulsions prepared with the reduced aroma stock is plotted in Figure **6.6** along with the data for liquid HPS emulsions with the original, more concentrated aroma stock (from Figure **6.3** b). Because, food consumption occurs over a short time scale, the data for only the first 5 minutes of the release profile is shown in Figure **6.6**. It can be seen that for all aroma compounds, the initial maximum release and subsequent decrease from solid droplet emulsion with reduced aroma was similar to that from liquid emulsion with the higher aroma content. Thus, liquid droplet food emulsion can be replaced in such a system by a solid droplet emulsion with lower aroma content and could potentially offer considerable savings of these food ingredients (e.g., in this case the percent reduction for each aroma compound was: EP, 50%; EH, 78.3%; and EO, 81.5%). Nevertheless, it should be noted here that, the above experiment was done in a model system and release of aroma from human breath as sell as sensory analysis should be considered before the above system can be applied to real food.

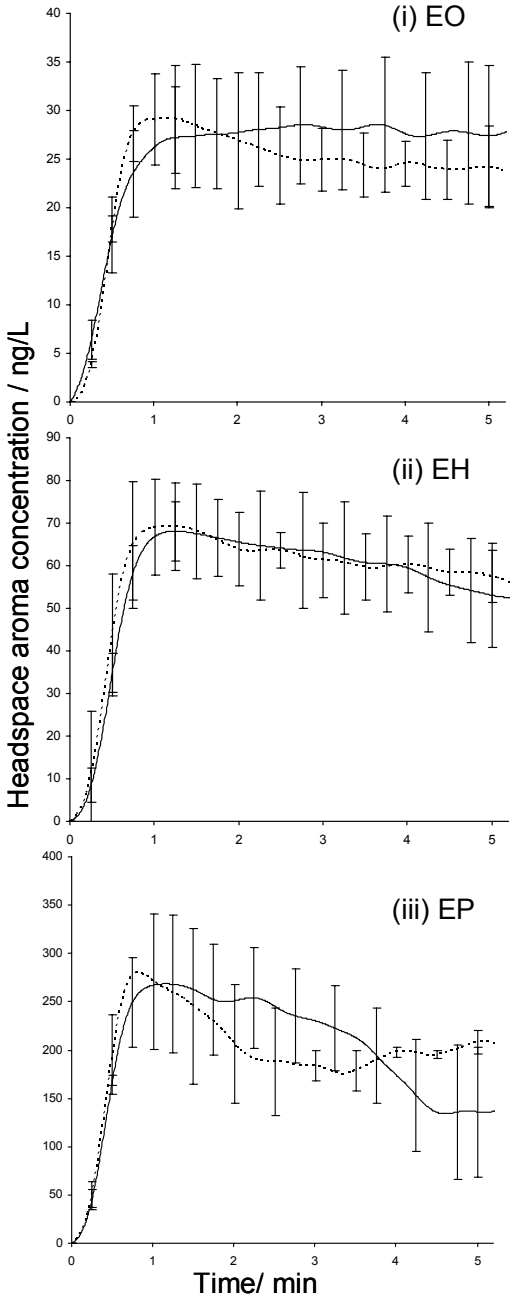

Figure **6.6**: Average aroma release profiles of HPS solid droplet emulsion *(d_{32}*=0.2 μm) prepared with reduced concentration aroma stock (—) compared to the corresponding liquid droplet emulsion with original higher concentration aroma stock (---). (i) EO, (ii) EH and (iii) EP. The error bars represent one standard deviation (n=3).

Change in aroma release profile during melting. During food consumption, some fats in the food will melt at the mouth temperature (~38^{o}C). As I have shown here, the release profiles from solid and liquid droplet emulsions are very different so melting during consumption would be expected to cause a sudden change in aroma levels. This hypothesis was tested as follows: the aroma release profile of an eicosane emulsion was measured initially at 30^{o}C and then, 20 minutes after the gas flow started, the temperature of the sample inside the glass vessel was increased to 40^{o}C to melt the solid eicosane droplets. The resulting release profile data is shown in Figure **6.7**. For both EO and EH, the initial increase in the temperature of the emulsion led to an initial increase in the aroma release (Figure **6.7**) as the volatility of the aroma compounds increased with temperature. This was quickly followed by a sudden decrease in the release rate leading to a final low and almost constant release of aroma with time because as the droplets melt, aroma compounds from the surrounding aqueous phase partition into the newly formed liquid oil phase. It may be possible to use this phenomenon to generate novel sensations from a flavor delivery system that changes phase during consumption.

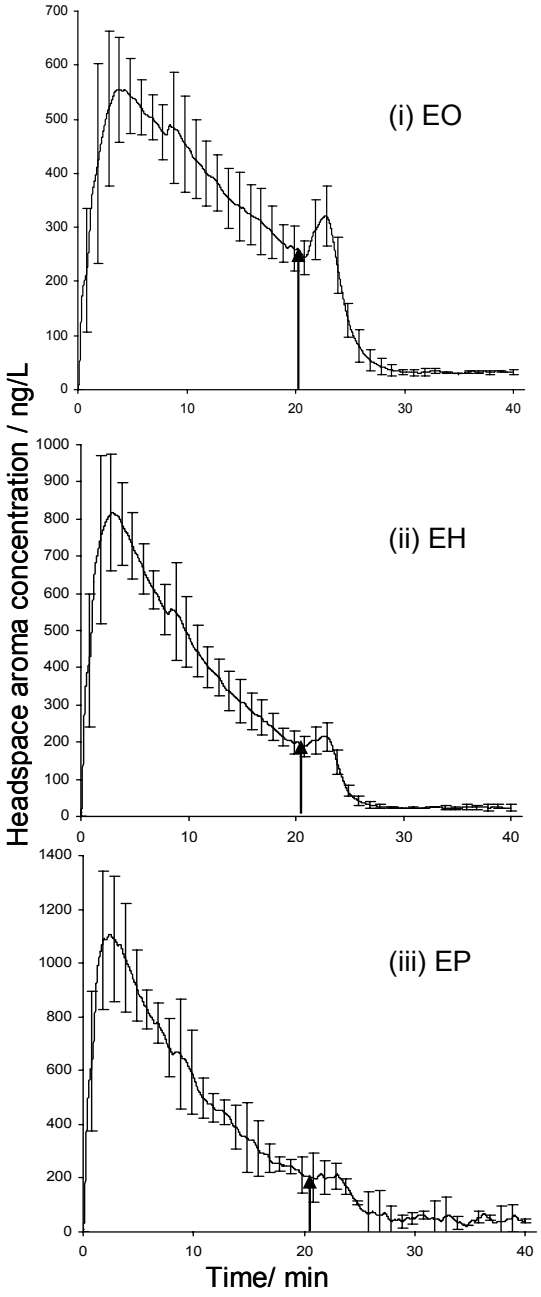

Figure **6.7**: Fat melting during dynamic aroma release from a solid eicosane emulsion (d_{32}=0.2 μm). The experiment started at 30°C and after 20 min (shown by an arrow) the temperature was increased to 40°C. (i) EO, (ii) EH and (iii) EP. The error bars represent one standard deviation (n=3).

6.4 Conclusion

The dynamic aroma release profiles of food emulsions are significantly influenced by the nature of lipid used and its crystallinity. The initial release from solid droplet emulsion is higher than that from liquid droplet emulsion. Triglycerides such as HPS have lower gas-emulsion partition coefficients than simple crystalline alkanes resulting in a lower release rate. Using this effect, the aroma content of a solid droplet emulsion can be reduced and yet still match the release profile of a liquid droplet emulsion. Furthermore, any, melting of solid droplets in the mouth would lead to a sharp decrease in headspace aroma concentration. Importantly, this result has been obtained from an *in vitro* study and further research using human breath analysis and sensory analysis is necessary before this could be confidently applied in real foods.

6.5 References

Coupland, J. N., Crystallization in emulsions. *Current Opinion in Colloid & Interface Science* **2002,** 7, (5-6), 445-450.

Kloek, W.; Walstra, P.; van Vliet, T., Nucleation kinetics of emulsified triglyceride mixtures. *Journal of American Oil Chemists' Society* **2000,** 77, (6), 643-652.

Marin, M.; Baek, I.; Taylor, A. J., Flavor release as a unit operation: a mass transfer approach based on a dynamic headspace dilution method. In *Flavor Release*, Roberts, D. D.; Taylor, A. I., Eds. American Chemical Society: Washington, DC, **2000**; pp 153-165.

Marin, M.; Baek, I.; Taylor, A. J., Volatile release from aqueous solutions under dynamic headspace dilution conditions. *Journal of Agricultural and Food Chemistry* **1999,** 47, (11), 4750-4755.

Rabe, S.; Krings, U.; Banavara, D. S.; Berger, R. G., Computerized apparatus for measuring dynamic flavor release from liquid food matrices. *Journal of Agricultural and Food Chemistry* **2002,** 50, (22), 6440-6447.

Roberts, D. D.; Acree, T. E., Simulation of retronasal aroma using a modified headspace technique: investigation of effects of saliva, temperature, shearing, and oil on flavor release. *J. Agric. Food. Chem.* **1995,** 43, 2179-2186.

Schober, A. L.; Peterson, D. G., Flavor release and perception in hard candy: influence of flavor compound-compound interactions. *Journal of Agricultural and Food Chemistry* **2004,** 52, 2623-2627.

van Ruth, S. M.; Roozen, J. P.; Cozijnsen, J. L., Comparison of dynamic headspace mouth model systems for flavour release form rehydrated bell pepper cuttings. In *Trends in Flavor Research*, Maarse, H.; van der Heij, D. G., Eds. Elsevier: London, **1994**; pp 59-64.

Chapter 7

Conclusions

7.1 Conclusions

The goal of this work was to investigate the effect of fat crystallization on the aroma release properties of oil-in-water emulsions.

Objective 1: Thermodynamics of aroma- solid fat interactions in emulsions

The first objective of the study was to understand the thermodynamics of aroma-solid fat interactions in oil-in-water emulsions. This was accomplished in Chapter 3, 4 and 5. It was found that while the partitioning of volatile molecules with liquid eicosane emulsions can be understood in terms of a three-phase partitioning, the interactions with solid droplets required a surface interaction term. A surface binding coefficient was defined as the ratio of amount of aroma compound adsorbed per unit interfacial area to the aqueous concentration (Chapter 3). Because the effect of surface binding is much smaller than the effect of partitioning into liquid oil, we were not able to discount the possibility of similar binding occurring at the liquid oil-water interface. However, because of the large aroma-affinity of liquid oil, the effect of surface binding would only be significant when there is no liquid oil present. The amount of aroma compounds adsorbed on solid lipid surfaces is proportional to the aqueous concentration up to a critical point then rapidly increases with subsequent increases in aqueous concentration. At the critical point the solid droplets begin to dissolve in the adsorbed aroma according to the volatile-lipid phase diagram (Chapter 4). The additional liquid phase formed produced a much larger reservoir for the aroma and reduces the amount in the headspace. The model developed in Chapter 3 was further modified considering this droplet

dissolution effect where the critical solid fat content was calculated from the aroma-solid phase diagram (Chapter 4). While the quality of fit was not perfect, the trends are similar to those seen in the experimental data and quantitatively better than the original surface-binding model. In particular, the simple surface binding model predicts an increase at lower oil contents not seen in the experimental data or in the new model that allows dissolution.

The partitioning of individual volatile aroma compounds was not affected by the type of liquid oil used in an emulsion, however, interactions between solid fat droplets and aroma compounds are significantly influenced by the nature of fat (Chapter 5). Importantly, the partitioning of volatiles by solid triglycerides was dependant on the volume not surface area of the droplets. This was explained by presence of liquid oil residual at the crystal grain boundaries in the "solid" droplet which can act as a reservoir for the aroma or alternatively, as triglycerides crystallize in a mixture of different polymorphs, their less perfect crystal structure may allow the co-crystallization of aroma compounds. Also, it made no difference to the headspace volatile concentration if the aromas were added before or after lipid crystallization discounting the idea that there can be any kinetic entrapment by crystalline fat.

Objective 2: Kinetics of aroma release from solid and liquid droplet emulsions

The second objective of the study was to understand the kinetics of aroma release from solid and liquid droplets in oil-in-water emulsions. This was accomplished in Chapter 6 by measuring the aroma release under non-equilibrium condition from emulsions placed in a sealed, stirred, thermostatted glass vessel. The rate of release from solid droplet emulsions was found to be higher than that from liquid droplet emulsions. It was proposed that as liquid oil is a large reservoir for aroma compounds compared to solid fat, more aromas would be partitioned into the liquid droplets leading to a lower release rate from liquid droplet emulsions compared to solid droplet emulsion.

Furthermore, release form solid droplet emulsions, involves surface adsorption and desorption of the of aroma compounds, and is therefore droplet size dependent. Smaller droplets with larger surface area slow down the release of aroma compounds compared to larger droplets. On the other hand, as aroma-liquid oil interaction is a volumetric effect and the release rate through liquid droplet emulsions was not influenced by the droplet size.

When kinetics of aroma release from solid eicosane emulsion was compared with a solid triglyceride (HPS) emulsion it was observed that release rate from solid HPS emulsion was significantly lower than that from solid eicosane emulsion (Chapter 6). It was proposed that since solid HPS have lower gas-emulsion partition coefficients than simple crystalline alkanes, the release rate would also be slower.

7.2 Future Work

Partitioning into solid triglycerides. In the present work, the model developed for aroma-solid fat interaction was based on eicosane emulsion and it includes surface binding and droplet dissolution effect. However, it was also found that complex triglycerides like HPS would be able to accommodate aroma compounds into its crystalline structure. In order to understand solid triglyceride crystals- aroma interaction, it would be useful to track the aroma compound in the environment of the crystalline matrix using technique such as nuclear magnetic resonance (NMR) spectroscopy. This technique has been used in pharmaceutical industry to track drug molecules in solid lipid nanoparticles (Westesen, Bunjes and Koch, 1997).

The behavior of flavor delivery systems in vivo. In the present study it has been shown that a solid droplet emulsion with reduced aroma content could be used to replace a liquid droplet emulsion with higher amount of aroma. However, the conclusions were drawn using aroma release from a “model mouth” and before further validation using real

food, breath analysis and sensory studies are necessary. Release profiles of aroma compound into breath can be taken as a measure of perceived aroma during eating and drinking process (Taylor and Linforth, 2000). If the breath release profiles of solid-droplet emulsions with reduced aroma were similar those of liquid-droplet emulsions with more aroma that would confirm the application of solid droplet emulsions as a flavor delivery system. On the other hand time-intensity sensory studies with trained judges would be necessary in order to understand how the solid droplet emulsion with reduced aroma would be perceived in human brain as compared to the original liquid droplet emulsion during the actual eating or drinking process.

7.3 Applications

Solid lipid nanoparticles for pharmaceutical delivery. Solid lipid nanoparticles (SLN) was used as an alternative carrier system of drug molecules compared to traditional colloidal carriers in order to have a better control on sustained release potential of drugs (Muller, Mader and Gohla, 2000). However, researchers in this field never used any drug-SLN binding isotherm or mathematical model to predict release of drug from these emulsions. In order to have a better knowledge of drug release potential thermodynamic models explaining binding properties of drug and SLN would be useful. The fact that the solid alkane excludes any aroma compounds from its crystalline matrix and above a critical point began to dissolve in the adsorbed aroma was also observed during controlled drug release study using pure solid triglyceride (e.g. tristearin and tripalmitin) nanoparticles (Bunjes, Drechsler, Koch and Westesen, 2001; Jores, 2004). The aroma- solid fat interaction model developed in the present work can be modified in order to take into account the release of non-volatile components from sold droplet emulsions. Such a model can be used to predict drug- SLN interaction so that an improved estimation of release potential of a particular drug would be possible.

Flavor delivery emulsions. Emulsions are extensively used as flavor delivery systems in several food products, particularly beverages. These emulsions constitute a very small part of the total beverage by volume but significantly influence its perceived quality. In the present work it was shown that by manipulating the aroma content, the initial aroma release profile of the solid droplet emulsion could be matched to that of a liquid droplet emulsion with higher aroma content (Chapter 6). Using the technique significant cost savings on aroma compounds would be possible. However, the release profile of solid droplet emulsions could be significantly affected by fat melting at mouth temperature during food consumption. It was observed that melting fat in emulsion leads to a sharp decrease in aroma release and hence care should be taken in selection of lipid that could be used as a flavor delivery medium. Also melting fat in the mouth could be used to absorb off flavor compounds during food consumption.

7.4 References

Bunjes, H.; Drechsler, M.; Koch, M. H. J.; Westesen, K., Incorporation of the model drug ubidecarenone into solid lipid nanoparticles. *Pharmaceutical Research* **2001,** 18, (3), 287-293.

Jores, K. Lipid nanodispersions as drug carrier systems - a physicochemical characterization. Ph.D. Thesis, Free University of Berlin, Berlin, Germany, **2004**.

Muller, R. H.; Mader, K.; Gohla, S., Solid lipid nanoparticles (SLN) for controlled drug delivery - a review of the state of the art. *European Journal of Pharmaceutics and Biopharmaceutics* **2000,** 50, (1), 161-177.

Taylor, A. J.; Linforth, R. S. T., Techniques for measuring volatile release in vivo during consumption of foods. In *Flavor Release*, Roberts, D. D.; Taylor, A. J., Eds. American Chemical Society: Washington, DC, **2000**.

Westesen, K.; Bunjes, H.; Koch, M. H. J., Physicochemical characterization of lipid nanoparticles and evaluation of their drug loading capacity and sustained release potential. *Journal of Controlled Release* **1997,** 48, (2-3), 223-236.

Appendix A

Factors affecting the freeze-thaw stability of emulsions

Abstract

Many food emulsions are frozen to provide long-term stability to the product or as a necessary part of the food itself (e.g., ice cream) but very often the thawed emulsion is significantly destabilized and sometimes completely broken down into an oily and an aqueous phase. The phase behavior of the frozen emulsion and hence the potential stresses can be calculated from the composition of the aqueous phase. For example a 20% o/w emulsion prepared with 10% sucrose in the aqueous phase when frozen to -20°C about 85% of the aqueous phase has frozen to ice leaving the unfrozen phase concentrated to about 62% with respect to droplets and 67% with respect to sucrose. The high volume fraction and expanding ice press the droplets together and the high sugar (and other solute) concentration) can affect the interdroplet forces. A combination of these effects can lead to the membrane separating the droplets rupturing and is responsible for the coalescence seen on thawing. The published studies on freeze-thaw stability of emulsions are reviewed within the framework provided by the phase diagram calculations.

A.1 Introduction

Many food emulsions are frozen, either to improve their shelf life (e.g., sauces and some beverages) or as a necessary part of the product (e.g., ice cream, frozen cocktails). When frozen emulsions are thawed, they are sometimes at least partly broken down (e.g., oil on the surface of a defrosted cheese sauce) and in other cases apparently unchanged (e.g., frozen cream). Some examples of the range of changes seen in emulsions after they have been frozen and thawed are illustrated in Figure **A.1**. The freshly prepared emulsions (40% hexadecane) were homogeneous liquids but a variety of degrees and types of destabilization were seen depending on the surfactant system used ranging from creaming to gelation and complete separation of the emulsion into an aqueous and oil layers.

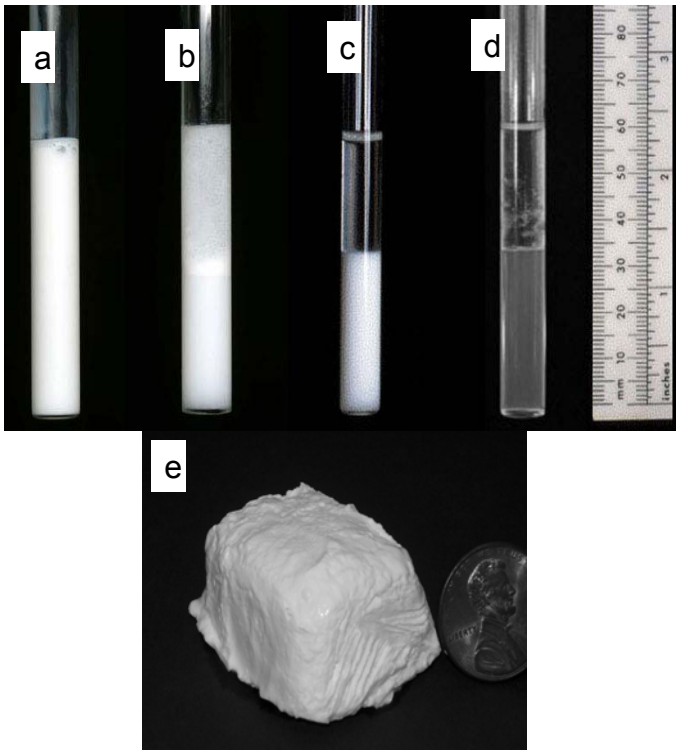

Figure **A.1**: Photographs of (a) an unfrozen n-hexadecane emulsion shown along with freeze-thawed emulsions stabilized with (b) sodium caseinate, (c) Tween 20 and (d) poly (sodium-4-styrene sulfonate). The semi-solid paste seen in (e) was prepared by freezing a cube of the Tween 20 stabilized emulsion then warming to allow the water but not the fat to melt. The emulsions were 40% oil-in-water stabilized with 2% surfactant solution.

An indication of the mechanism of destabilization is given by optical micrographs taken at different stages of the freezing cycle (Figure **A.2**). Upon freezing, the solid crystalline oil droplets are excluded from the space taken up by the ice and are forced into close proximity with one another in the restricted phase volume remaining (Figure **A.2**b; note the ice crystals themselves are not directly visible in this image). When the ice melts (Figure **A.2**c), a network of crystalline solid droplets remains intact (and responsible for the paste-like self supported cryogel shown in bulk scale, Figure **A.1**e) but on further heating the droplets melt and rapidly coalesce (Figure **A.2**d) leading to oiling off. This suggests that the freezing conditions cause the membranes surrounding individual droplets to rupture, allowing some oil-to-oil contact. In freeze-thaw stable

emulsions, there is no permanent interaction caused between the droplets and they dissociate after the ice melts. However, the stresses induced by freezing, and the capacity of different ingredient combinations to resist them is poorly understood.

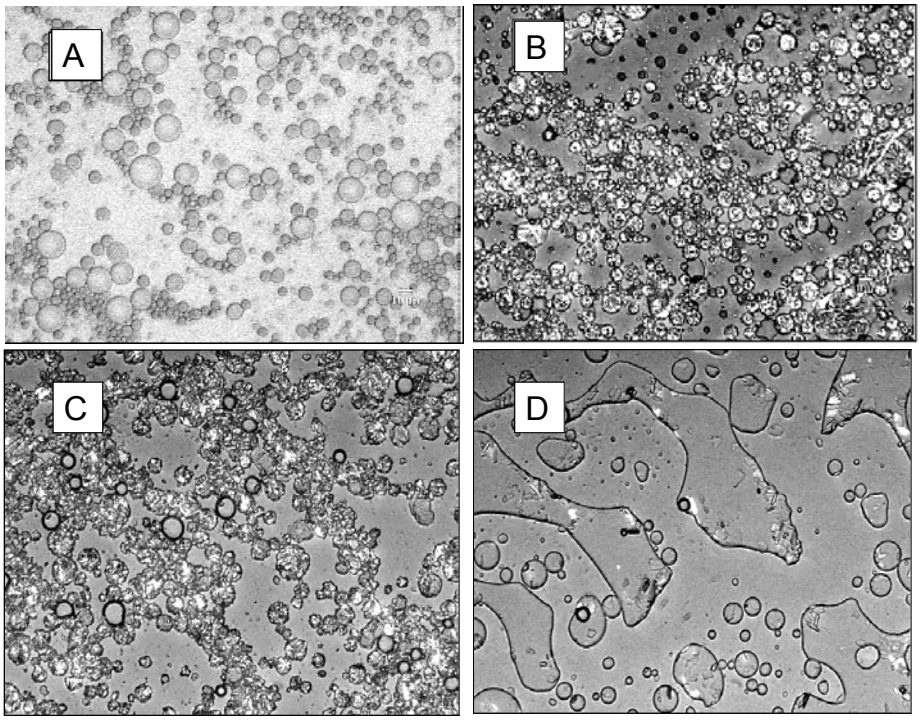

Figure **A.2**: Optical micrograph of a coarse 40 wt.% *n*-hexadecane emulsion (a) before freezing, (b) ice present, (c) ice melted but fat still solid, (d) fat melted. The images represent a time/temperature sequence for a single field of view. Polarized light was used to illustrate the crystalline fat in (b), (c) and (d) but not in (a) where there was no detectable crystallinity. Scale bar is 20 μm.

In this work, a simple phase diagram is used to calculate some of the stresses that may be induced in an emulsion by freezing. After this some of the variables that have been considered in studies of freeze-thaw stability are examined in the light of these stresses and attempt to identify the most critical factors.

A.2 Phase Behavior in Frozen Emulsions

A phase diagram of the aqueous phase can be used to gain some insight into the environment of the emulsion droplets in the frozen state. For some example calculations, a 20% oil in water emulsion with 10% sucrose in the aqueous phase will be used by assuming that the phase behavior of the aqueous phase is solely dependant on the sucrose phase diagram (Figure **A.3**). The aqueous phase does not begin to freeze until -0.7°C, but below that temperature the amount of ice increases at a decreasing rate and the concentration of sucrose in the unfrozen phase increases to about 67% at -20°C. The sucrose is concentrated below its eutectic point with water but does not reach the glass transition concentration (approximately 85% at -20°C). Other solutes will be concentrated along with the sucrose as ice forms in the aqueous phase. The ionic strength of the solution will increase perhaps ten fold during typical freezing conditions (i.e., ¬90% of the water frozen to ice), and the pH will decrease. However, as pH varies with the logarithm of hydrogen ion concentration a reduction of perhaps only one unit is expected.

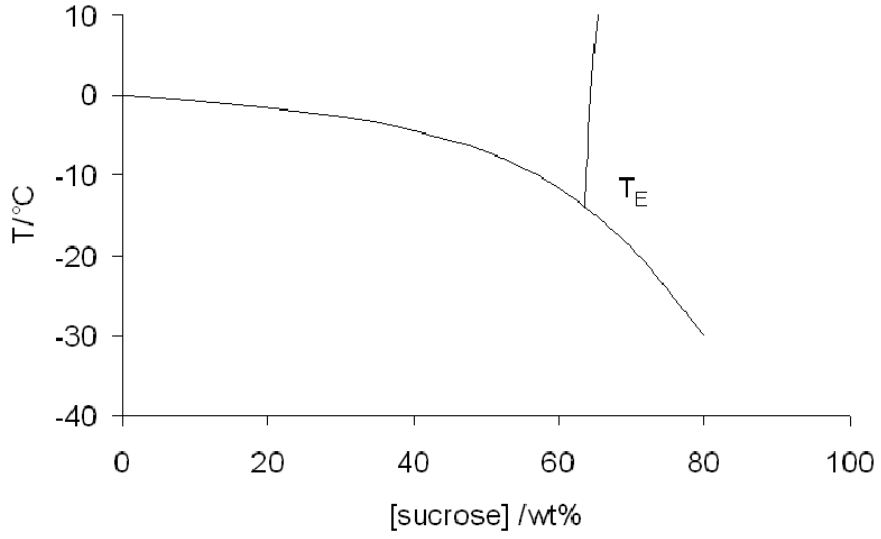

Figure **A.3**: Phase diagram of sucrose (data from Appendix C).T_E is the eutectic point.

Using mass balance equations, the proportion of the water frozen into ice has been calculated (Figure **A.4**). As the temperature is decreased, the amount of ice increases to a maximum of about 85% at -20°C. Ice is less dense than water, so will expand causing increasing internal stresses within the sample. The concentration of oil droplets in the unfrozen phase will also increase as the liquid water is removed. In this example the dispersed phase volume fraction will reach approximately 62% at -20°C (Figure **A.4**); approaching close packing for a typical emulsion. The actual frozen volume fraction will increase with initial (unfrozen) droplet concentration and decrease with sucrose concentration and temperature. Figure **A.5** shows some calculations of the conditions required to produce a close packed emulsion (arbitrarily taken as a mass fraction of 70%); samples below and to the right of the line would have a lower volume fraction and therefore be less stressed and more stable.

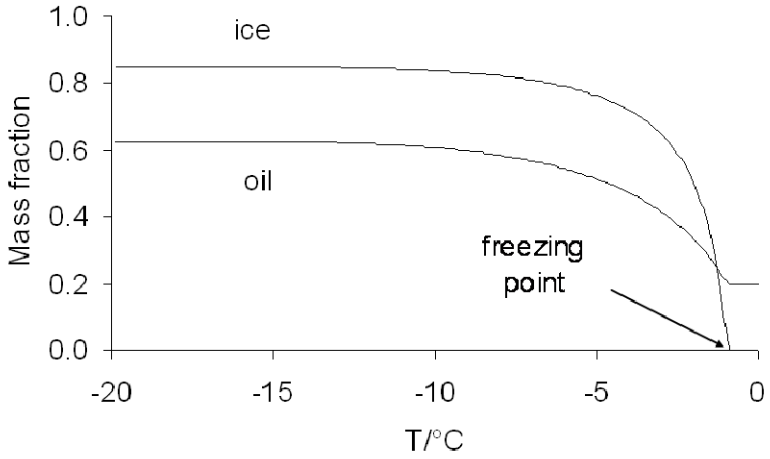

Figure **A.4**: Proportion of the aqueous phase frozen and oil droplet concentration in the unfrozen portion calculated as a function of temperature. The initial emulsion was 20% oil and 10% sucrose and the ice content was assumed to be controlled by the sucrose phase diagram.

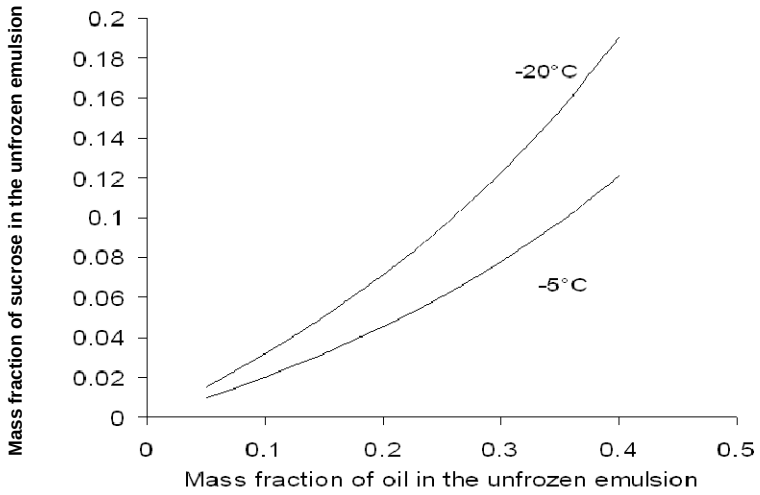

Figure **A.5**: The effect of initial sucrose concentration on the minimum initial oil concentration needed to produce a close-packed (i.e., ϕ_{oil}=0.7) emulsion in the frozen state at two different temperatures. Samples with compositions below and to the right of the line would be expected to be more stable.

For two droplets to coalesce, they must be forced into close proximity so that the film of water separating them will drain out and bring the two surfactant layers into dry contact. Finally, the resultant Newton black film must rupture to allow the droplets' contents to flow together (van Aken, 2003). From the phase diagram, two major groups of effects that may influence this process in the frozen state can be seen. Firstly, the increase in solute concentration changes the chemical environment for the interfacial proteins and surfactants. The concentrated sugars are weakly interacting co-solutes which change the properties of the adsorbed layer (Baier & McClements, 2005). The presence of sugar cosolutes typically stabilizes globular proteins against denaturation, while enhances the rate of aggregation of denatured proteins. High sugar concentrations can also dehydrate the aqueous portions of surfactant and change the bending energy of the interface and hence the free energy for the coalescence transition state (Kabalnov & Wennerstrom, 1996). High salt concentrations screen the electrostatic repulsion between droplets make them easier for the ice to force together. The second major group of effects of freezing is a consequence the fact that the frozen emulsion is highly

concentrated, probably at or beyond close packing, and the droplets are under pressure from the expanding ice. In this respect, the frozen state closely parallels the conditions in the highly concentrated emulsions produced by Van Aken and others (van Aken, 2002; van Aken & van Vliet, 2002; van Aken & Zoet, 2000) when they centrifuged emulsions at high speeds to study coalescence processes.

The various factors affecting the freeze-thaw coalescence of emulsions can be divided into those which affect the ability for the ice to transmit force to the interdroplet lamella (i.e., amount of ice formed, capacity of the lipid droplets to transmit force) and those which strengthen the interdroplet lamella against the applied force (i.e., type and conformation of interfacial material and the colloidal forces acting). In the next sections various factors that have been shown to affect the stability of thawed emulsions (by a combination of chemical and mechanical stresses in the frozen state) will be considered.

A.3 Effect of Lipid Composition

When emulsion droplets are trapped and concentrated between growing ice crystals they will remain stable only as long as the membrane separating the droplets remains intact. One role of the lipid type is to affect the ways the forces produced by the ice is transmitted to the membrane. Cramp, Docking, Ghosh, & Coupland (2004) (Appendix B) prepared polyoxyethylene sorbitan monolaurate (Tween 20) stabilized emulsions from a homologous series of n-alkanes and froze them overnight at -20°C. On thawing, the emulsions whose droplets remained liquid at freezer temperatures (i.e, decane) were stable while the emulsions whose droplets were crystalline (dodecane to octadecane) were partly destabilized. Under the pressure of the ice, the liquid droplets were presumably able to deform to some extent while the crystalline droplets focused the stress at the point of contact between the droplets and forces the surfactant out of the intervening gap.

Solid alkane droplets are typically spherical, with diameters slightly smaller than the corresponding liquid droplets because of the increase in lipid density on crystallization. Other types of fat form more complex microstructures within droplets and under certain conditions crystals can extend several droplet diameters away from the original surface (Spicer & Hartel, 2005). Sharp crystals would be expected to concentrate the stress between droplets even more than solid spheres and therefore be less stable. Thanasukarn, Pongsawatmanit, & McClements (2004b) studied the freeze-thaw stability of hydrogenated palm oil emulsion stabilized by Tween 20, casein and WPI and in all cases, the percentage destabilization was higher than that the corresponding for n-hexadecane emulsion studied by Cramp et al. (2004) (Appendix B). For example, for casein stabilized emulsions (20 wt.% oil-in-water) following freeze thaw, approximately 90% of the hydrogenated palm oil droplets were destabilized (Thanasukarn et al., 2004b) compared to only 27% of the n-hexadecane droplets (Appendix B). Although different methods were used by two research groups, it seems that that triglyceride emulsions are much less stable to freeze-thaw compared to alkane emulsions.

A more chemically specific role for lipids was suggested by Saito, Kawagishi, Tanaka, Tanimoto, Okada, Komatsu, & Handa (1999) who showed a trolein emulsion stabilized with dipalmitoyl phosphatidylcholin and egg phosphatidylcholin surfactants and found that both were freeze-thaw stable, while a tricaprylin emulsion stabilized with egg phosphatidylcholin was not. The authors proposed that the medium chain triglyceride trycaprylin penetrated into the surface layers of egg phosphatidylcholin more than the long chain triolein and decreased the spontaneous curvature of surface membrane. If the membrane cannot curve, it cannot readily form a channel in the bilayer separating closely adjacent droplets which leads to coalescence (Kabalnov et al., 1996).

The amount as well as the type of fat present is important in determining the freeze-thaw stability of an emulsion. Concentrated unfrozen emulsions will have higher dispersed phase volume fractions in the frozen state and therefore greater stresses that may lead to destabilization (Figure **A.5**). Droplet concentration has not been widely

considered as a variable in freeze-thaw studies; however, an observation made by Ghosh, Cramp, & Coupland (2006) (Appendix C) offers some support. In that work, 40% hexadecane emulsions stabilized with sodium caseinate were diluted in water and in protein solutions prior to freeze thaw. In a group of emulsions with similar aqueous composition, the dilute (5%) emulsion was stable while the concentrated emulsions (20-40%) were significantly destabilized.

A.4 Effect of Aqueous Sugars

Increasing the sugar concentration in the aqueous phase of the emulsion reduces the amount of ice formed on freezing (Figure **A.5**) and hence the pressure exerted on the concentrated emulsion. It may also affect the conformation of proteins/surfactants at the interface. Ghosh et al. (2006) tested the effect of six different types of sugars (0-3 wt% sucrose, glucose, fructose, maltose, trehalose and corn syrup solids) on the freeze-thaw stability of 20% n-hexadecane emulsions stabilized with sodium caseinate. Fructose was least effective in stabilizing emulsions on a molar basis while corn syrup solids were most effective, although differences between the sugars were relatively small (Appendix C). For sucrose, these authors found that fat destabilization decreased from ~27% to 2% when amount of sucrose in the emulsions increased from 0 to 2 wt% while in a similar study with hydrogenated palm oil emulsions stabilized with WPI, Thanasukarn, Pongsawatmanit, & McClements (2004a) showed that the addition of 20% sucrose decreased the fat destabilization from >90% to 14% . However, sucrose (up to 40 wt.%) did not improve the freeze-thaw stability of similar emulsions stabilized with Tween 20 (Thanasukarn, Pongsawatmanit, & McClements, 2006a). In some cases, even the small amount of sugar inherent in commercial protein preparations can be important. For example, a 40 wt% hexadecane emulsion stabilized with caseinate was 33% destabilized following freeze-thaw, but if the protein was first dialyzed to remove the residual lactose it was 50% destabilized (unpublished results).

It seems the effectiveness of sugar as a freeze-thaw stabilizer varies dramatically from system to system. While the effect of the sugars on the mechanical forces exerted by the ice would be expected to be similar for similar aqueous phases, the capacity of the membrane to resist that force would vary from system to system and would also be affected by the chemical stresses exerted by the concentrated solute. For example, Saito et al. (1999) again used the surface curvature model to explain the protective effect of maltose on a frozen tricaprylin emulsion stabilized with egg phosphatidylcholin. They suggested that the sugar was incorporated into the hydrophilic portions of the surfactant, preventing the spontaneous curvature needed to form a pore in the membrane separating two droplets in the frozen state that would lead to droplet coalescence

A.5 Effect of Aqueous Salts

Like sugars, added salts can change the amount of ice formed in a frozen emulsion. However, the concentrated salt solutions in the unfrozen phase can have a much greater effect than sugars on the interdroplet interactions. High salt concentrations would be expected to screen the electrostatic repulsion between droplets make them easier for the ice to force together to form a Newton black film. Thanasukarn et al. (2004b) showed that an emulsion which was only 14% destabilized in the absence of salt was about 48% destabilized in the presence of 150 mmol kg^{-1} added NaCl. If the effect of salt was merely due to its effect on the phase diagram, it would be expected to have a stabilizing effect on the emulsion while the opposite result seen points to the role of salt on the electrostatic interactions between the droplets. It is important to remember that the aqueous concentration of salts in the frozen emulsion is several times that originally added to the unfrozen emulsion.

On the other hand, other workers have seen salts as protecting against freeze thaw. Komatsu, Okada, & Handa (1997) showed 0.5 M NaCl or LiCl provided freeze-thaw protection to a soybean oil (200 mg/ml) emulsion containing 2.2% glycerin and

stabilized with egg phosphatides (12 mg/ml). Similar suppressive effects were found for other salts (RbCl, CsCl and KCl), but, they were not as effective as NaCl and LiCl and the effectiveness decreased in the following order: LiCl = NaCl > RbCl ~ CsCl ~ KCl (Komatsu et al., 1997). They also showed that the added salt reduced the magnitude of the ζ–potential on the emulsions from -21 mV to about 0 mV with increase in salt (NaCl, LiCl) concentration from 0.2 to 0.5 M. One would expect that the loss in electrostatic repulsion would make the emulsions more vulnerable to freeze-thaw destabilization but these authors argued that in this case the salt together with glycerin suppressed ice formation and had a net stabilizing effect. The salts were not stabilizing in the absence of glycerin.

A.6 Effect of Surfactant Composition

When droplets come under pressure from an expanding ice phase, the main resistance to coalescence is the interfacial layer and so, as might be expected, changing the composition of the interface has important effects on the freeze-thaw stability of emulsions (Figure **A.1**). It is important to note however, that it is still unclear how the freezing of either the droplets or the continuous phase affects adsorption at the interface. At least for alkane droplets, which are usually not prone to partial coalescence, crystallization of the lipid does not lead to any emulsion destabilization suggesting that some surfactant remains adsorbed to the crystal-liquid interface. This is supported by some unpublished measurements from our laboratory in which it has been shown that crystallization and melting of n-octadecane droplets does not affect the ζ–potential of surfaces stabilized with SDS, sodium caseinate or poly (sodium-4-styrene sulfonate). Even if one can eliminate droplet crystallization as a major factor affecting the interfacial composition the same cannot be said for aqueous freezing. Freezing the aqueous phase markedly changes the environment of the surface protein and may lead to a change in the amount adsorbed or its conformation.

Cramp et al. (2004) showed that amount of destabilization of a 40% hexadecane emulsion following one freeze-thaw cycle decreased in the sequence Tween 20 (63%) > SDS (49%) > WPI (32%) ~ sodium caseinate (29%). Thus, the protein emulsifiers were better at protecting the emulsions than small molecule surfactants but still were not completely effective. It was proposed that a thick interfacial layer could be responsible for increased stability of protein stabilized emulsions. However, Thanasukarn et al. (2004b) showed hydrogenated palm oil emissions prepared with Tween 20 and caseinate were unstable to freeze-thaw while WPI provided better protection. One reason for the different trends seen by the two groups may be the different types of oils used.

The general trend that thicker layers provide better protection is supported by a series of papers from McClements and co-workers on the freeze-thaw stability of droplets stabilized by multilayer of surfactants and/or polymers (Aoki, Decker, & McClements, 2005; Ogawa, Decker, & McClements, 2003; Thanasukarn, Pongsawatmanit, & McClements, 2006b). For example, Thanasukarn et al. (2006b) used a 5 wt.% hydrogenated palm oil emulsion stabilized with 10 mmol/kg SDS, 0.3 wt.% chitosan, 100 mM acetic acid buffer and 0 to 2.2 wt% pectin to study the effect of freeze-thaw stability. The primary emulsion droplets were made with SDS at the surface; this was then coated with a layer of chitosan in secondary emulsion and a layer of pectin to form the tertiary emulsion. After a freeze-thaw cycle (-40º, 24 h to 37ºC 24 h) the primary emulsion was highly coalesced, the secondary emulsion was flocculated and the tertiary emulsion above a certain level of pectin (≥ 2 wt.%) was stable. This study is also notable in showing extensive freeze-thaw induced flocculation, and some of the micrographs show large clumps of unidentified polymer insolubilized by the process.

Recently it was shown that an emulsion (n-hexadecane-in-water) stabilized with sodium caseinate was stable to freeze-thaw if the amount of aqueous protein content is above a critical level (Appendix C). One mechanism for this effect is that the unadsorbed protein can act as particles which provide some kinetic stability of the system as they must diffuse out of the lamella before the interdroplet film can thin and rupture (Giasson,

Israelachvili, & Yoshizawa, 1997). Alternatively, the aqueous protein might provide a reservoir of additional protein that can limit the hypothetical desorption of protein as the solvent conditions change on freezing.

A.7 Conclusion

The process of freezing and thawing is highly destabilizing to many food emulsions. Unusually, even protein stabilized emulsions can show a large degree of coalescence and in some cases complete phase separation into an oil and water phase. The frozen state imposes two important groups of potentially destabilizing effects to a food emulsion. First, the aqueous phase is concentrated with respect to all aqueous solutes. High concentrations of solute may dehydrate the interfacial proteins/surfactants changing their conformation, surface activity and spontaneous curvature. High concentrations of salts can screen out any dielectric repulsion between droplets and make them easier to force into close proximity. Second, the dispersed phase volume fraction increases as the amount of liquid water is reduced and the droplets will come under strain from the expanding ice phase. The published literature does not provide a complete picture of the relative importance of these mechanisms and it is suggested that a profitable line of investigation would be to compare the stability of a thawed emulsion with the stability of a similar emulsion (a) prepared with very high amounts of added sugar/salt, i.e., to impose the chemical stress of freezing, and (b) concentrated by intense centrifugation, i.e., to apply the mechanical stress of freezing.

Acknowledgements

I am grateful to Dr. Darrell Velegol of Department of Chemical Engineering, Pennsylvania State University for helpful discussion.

A.8 References

Aoki, T., Decker, E. A., & McClements, D. J., Influence of environmental stresses on stability of O/W emulsions containing droplets stabilized by multilayered membranes produced by a layer-by-layer electrostatic deposition technique. *Food Hydrocolloids* **2005** 19, (2), 209-220

Cramp, G. L., Docking, A. M., Ghosh, S., & Coupland, J. N., On the stability of oil-in-water emulsions to freezing. *Food Hydrocolloids* **2004,** 18, (6), 899-905

Ghosh, S., Cramp, G. L., & Coupland, J. N., Effect of aqueous composition on the freeze-thaw stability of emulsions. *Colloids and Surfaces a-Physicochemical and Engineering Aspects* **2006**, 272, (1-2), 82-88

Giasson, S., Israelachvili, J., & Yoshizawa, H., Thin film morphology and tribology study of mayonnaise. *Journal of Food Science* **1997**, 62, (4), 640-&

Kabalnov, A., & Wennerstrom, H., Macroemulsion stability: The oriented wedge theory revisited. *Langmuir* **1996**, 12, (2), 276-292

Komatsu, H., Okada, S., & Handa, T., Suppressive effects of salts on droplet coalescence in a commercially available fat emulsion during freezing for storage. *Journal of Pharmaceutical Science* **1997**, 86, (4), 497

Ogawa, S., Decker, E. A., & McClements, D. J., Influence of environmental conditions on the stability of oil in water emulsions containing droplets stabilized by lecithin-chitosan membranes. *Journal of Agricultural and Food Chemistry* **2003**, 51, (18), 5522-5527

Saito, H., Kawagishi, A., Tanaka, M., Tanimoto, T., Okada, S., Komatsu, H., & Handa, T., Coalescence of Lipid Emulsions in Floating and Freeze-Thawing Processes: Examination of the Coalescence Transition State Theory. *Journal of Colloid and Interface Science* **1999**, 219, (1), 129-134

Spicer, P. T., & Hartel, R. W., Crystal comets: Dewetting during emulsion droplet crystallization. *Australian Journal of Chemistry* **2005**, 58, (9), 655-659

Thanasukarn, P., Pongsawatmanit, R., & McClements, D. J., Impact of fat and water crystallization on the stability of hydrogenated palm oil-in-water emulsions stabilized by whey protein isolate. *Colloids and Surfaces a-Physicochemical and Engineering Aspects* **2004a**, 246, (1-3), 49-59

Thanasukarn, P., Pongsawatmanit, R., & McClements, D. J., Influence of emulsifier type on freeze-thaw stability of hydrogenated palm oil-in-water emulsions. *Food Hydrocolloids* **2004b**, 18, (6), 1033-1043

Thanasukarn, P., Pongsawatmanit, R., & McClements, D. J., Impact of fat and water crystallization on the stability of hydrogenated palm oil-in-water emulsions stabilized by a nonionic surfactant. *Journal of Agricultural and Food Chemistry* **2006a**, 54, (10), 3591-3597

Thanasukarn, P., Pongsawatmanit, R., & McClements, D. J., Utilization of layer-by-layer interfacial deposition technique to improve freeze-thaw stability of oil-in-water emulsions. *Food Research International* **2006b**, 39, (6), 721-729

van Aken, G. A., Flow-induced coalescence in protein-stabilized highly concentrated emulsions. *Langmuir* **2002**, 18, (7), 2549-2556

van Aken, G. A., Coalescence Mechanisms in Protein-Stabilized Emulsions. In *Food Emulsion*, Fourth ed.; Friberg, S. E., Larsson, K., Sjoblom, J., Ed. Marcel Dekker, Inc.: New York, **2003**; pp 299-325.

van Aken, G. A., & van Vliet, T., Flow-induced coalescence in protein-stabilized highly concentrated emulsions: Role of shear-resisting connections between the droplets. *Langmuir* **2002**, 18, (20), 7364-7370

van Aken, G. A., & Zoet, F. D., Coalescence in highly concentrated coarse emulsions. *Langmuir* **2000**, 16, (18), 7131-713.

Appendix B

On the Stability of Oil-in-Water Emulsions to Freezing

Abstract

Oil in water emulsions (40 wt%) were prepared from a homologous series of n-alkanes (C10-C18). The samples were temperature cycled in a differential scanning calorimeter (two cycles of 40°C to -50°C to 40°C at 5°C min^{-1}) and in bulk (to -20°C). The emulsions destabilized and phase-separated after freeze-thaw if the droplets were solid at the same time as the continuous phase and were more unstable if a small molecule (SDS or polyoxyethylene sorbitan monolaurate) rather than a protein (whey protein isolate or sodium caseinate) emulsifier was used. The unstable emulsions formed a self-supporting cryo-gel that persisted between the melting of the water and the melting of the hydrocarbon phase. Microscopy provides further evidence of a hydrocarbon continuous network formed during freezing by a mechanism related to partial coalescence which collapses during lipid melting to allow phase separation.

B.1 Introduction

Emulsions are defined as a fine dispersion of one liquid in a second largely immiscible liquid. However in foods this definition is often relaxed to allow phase transitions in one or both phases and the presence of multiple colloidal species (Dickinson 1992). Phase transitions in emulsions are important as they affect the functional properties and stability of the products they contain (Walstra 1996).

When a liquid is cooled below its equilibrium melting point, the process of crystallization is thermodynamically favorable because the free energy of the solid becomes less than the liquid state (Hartel 2001). However a liquid may persist below its melting point for a considerable period of time because of the free energy barrier that must be overcome before nucleation can occur. In bulk liquids, impurities in the melt or at the surface of the vessel can act as sites for nucleation and crystallization can proceed relatively rapidly by a heterogeneous mechanism. However, when the liquid is finely divided into emulsion droplets so that the number of oil droplets is much larger than the number of impurities, the vast majority of the oil is effectively pure and crystallization nuclei must arise spontaneously, i.e., homogeneous nucleation (Skoda and Van den Tempel 1963). The situation is further complicated in emulsions as first, the surfactant may affect nucleation (i.e., surface heterogeneous nucleation, McClements, Dungan, German, Simoneau and Kinsella 1993) and secondly, collision between solid droplets and undercooled liquid droplets can induce crystallization in the liquid (i.e., interdroplet heterogeneous nucleation, McClements and Dungan 1997).

Most real food oils, notably milk fat, are semicrystalline over a wide temperature range. Collision between semisolid droplets in an emulsion can promote destabilization via partial coalescence, in which a fat crystal from one droplet penetrates the lamella

separating two colliding droplets (Walstra 1996). As the crystal is wetted better by the oil than water, the residual liquid oil flows out to reinforce the linkage point between them. With time, the droplets fuse more closely to reduce the total surface area of the oil exposed to aqueous phase, but the irregular doublet shape of the partially coalesced droplets is maintained by the mechanical strength of the fat crystal network. Upon heating, the fat crystal network melts, allowing full coalescence.

Recently a differential scanning calorimetry method was used to measure emulsion breakdown due to partial coalescence during temperature cycling as a function of oil type, dispersed phase volume fraction, and cooling rate (Vanapalli, Palanuwech and Coupland 2002). Small molecule surfactant stabilized triacylglycerol emulsions broke down under these conditions, while alkane emulsions were completely stable. Furthermore, triacylglycerol emulsions stabilized with protein-based surfactant were more stable to partial coalescence (Palanuwech and Coupland 2003). Previous studies have involved exclusively dispersed phase transitions, but here continuous phase freezing is also considered. Alkanes are selected as the model oil for most of this work as they have been previously shown to be resistant to partial coalescence in an unfrozen emulsion and so it is possible to ascribe destabilization to the process of freezing itself. By studying a homologous series of alkanes, freezing and melting characteristics relative to those of the continuous phase is controlled.

B.2 Methods and Materials

Materials. Whey protein isolate (WPI, ~90 % protein) was donated by Avonmore West, Inc. (Twin Falls, ID) and sodium caseinate was purchased from Fisher Scientific (Springfield, NJ). All other reagents were obtained from the Sigma Chemical Company (St. Louis, MO). Alkanes are sometimes identified by their carbon number; thus tetradecane is C14.

Emulsion preparation. Emulsions were prepared by mixing oil (40 wt%) with a 2 wt% surfactant solution (*i.e.*, 1.2% surfactant in the finished emulsion) in a high-speed blender (Brinkmann Polytron, Brinkmann Instruments Inc., Westbury, NY) for 30 seconds. The crude emulsions were then re-circulated through a twin-stage valve homogenizer (Niro Soavi Panda, GEA Niro Soavi, Hudson, WI) for several minutes at a pressure of 90 ± 10 bar to achieve multiple passes through the valves. Emulsions were prepared and homogenized at room temperature (23±2°C), with the exception of the octadecane emulsion, which was heated to ~35°C prior to homogenization to ensure the oil was liquid (melting point 27.3ºC). The emulsions were characterized by laser diffraction particle sizing (Horiba LA 920, Irvine, CA) using a relative refractive index of 1.5. The Sauter mean droplet size (d_{32}) of all the emulsions produced under the given conditions was 0.52 ± 0.16 μm, independent of surfactant type and with a standard deviation of the distributions of approximately 0.15 μm. The emulsions were stable at room temperature for several days (no change in particle size).

Freeze-thaw protocol. The samples of emulsion were transferred into thin-walled glass tubes (internal diameter 10.25±1.8 mm). They were then held for 17 ± 2 hours at either room temperature (23 ± 1ºC) or -20 ± 1ºC before being heated to 41 ± 1ºC.

Unstable emulsions were defined as those samples with visible surface oil after the freeze-thaw cycle.

Microscopy. Microscopy was used to identify different end products of emulsion breakdown, as well as to characterize the effect of the freeze-thaw process on emulsions. To demonstrate the freeze-thaw effects, coarse emulsions were made by adding 20 wt% hexadecane to a 2 wt% Tween 20 solution and mixing in a high-speed blender for 15 seconds. The mean droplet size (d_{32}) of these coarse emulsions was approximately 2 μm, with many larger particles. This larger particle size and lower oil concentration was needed to more clearly visualize the freeze-thaw process. The sample was placed on a microscope slide and frozen on a block of dry ice (-78.5°C) then transferred to a temperature-controlled stage (CTS-4ICA, Physitemp Instruments Inc., Clifton, NJ) at -12±2ºC. The sample slide was then heated on the thermal stage to 20ºC in increments of 5ºC using a temperature controller (TS-4, Physitemp Instruments Inc., Clifton, NJ). Micrographs (x400 magnification) were taken at intervals in the freeze-thaw process using an Olympus BX40 microscope (Melville, NY) equipped with a video camera (Sony 3CCD, PXC-970MD, New York, NY). Image manipulation was performed using the PAX-it 4.2 software (Franklin Park, NJ). When necessary, a polarizer was used to identify crystalline features.

Thermal Analysis. The crystallization and melting behavior of emulsions and pure fats were determined using a differential scanning calorimeter (Perkin-Elmer DSC-7, Norwalk, CT). The instrument was calibrated against indium. About 15-20 mg samples were sealed in aluminum pans and placed inside the DSC alongside an empty reference pan. It was then cooled from 40°C to -50°C, held for 1 minute, and then heated to 40°C at 5.0°C min^{-1}. The temperature cycle was repeated to identify any changes in the emulsion induced by the freeze-thaw. The freezing and melting points of the continuous and dispersed phases were taken from the onset temperatures of peaks on the thermogram. All analyses were conducted in triplicate.

B.3 Results and Discussion

A thermogram showing the thermal events occurring during the cooling and heating of a hexadecane emulsion stabilized with Tween 20 is provided in Figure **B.1.** On first cooling, there is a crystallization peak due to the oil at -1.2°C and the aqueous phase at -21.5°C. On reheating, the aqueous phase melts at -1.1°C and the oil at 14.9°C. The large degree of supercooling (16.1°C) for the emulsified oil is probably due to homogeneous nucleation in the finely divided emulsion droplet. The supercooling in the water is common in small, static samples. One interesting distinction is that while liquid water is typically only transiently stable at these deep supercoolings, supercooled oil droplets can remain liquid for many hours (McClements et al. 1997). On second and subsequent cooling cycles the water froze at a similar temperature but the oil crystallized at a much higher temperature, (12.4°C) close to the freezing point of bulk hexadecane measured under similar conditions (12.7°C). Subsequent heating cycles were similar to the first shown.

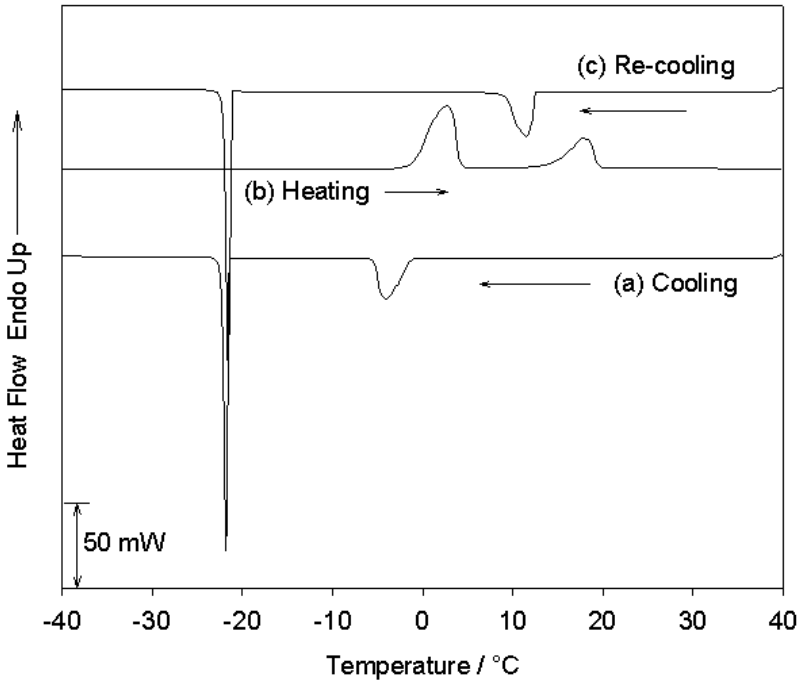

Figure **B.1**: Thermogram of a Tween 20 stabilized n-hexadecane emulsion (a) cooling, (b) heating, (c) re-cooling. Emulsions were 40 wt% oil stabilized with 2 wt% Tween 20 and were cooled and heated at 5°C min^{-1}.

Previously, this type of change in the freezing profile of an emulsified oil sample has been interpreted in terms of emulsion destabilization (Vanapalli et al. 2002). The initially fine emulsion crystallizes at a low temperature by a homogeneous mechanism, then partially coalesces on melting, and fully coalesces on reheating to form much larger droplets that, on second cooling, crystallize by a predominantly heterogeneous mechanism at a higher temperature. However, while this type of partial coalescence was readily induced in hydrogenated palm oil emulsions, n-alkane emulsions were completely stable to temperature cycling (between -10°C and 40°C, i.e., without continuous phase freezing) (Vanapalli et al. 2002). It was hypothesized that the pure alkane crystallized very rapidly and was not present for a useful amount of time as a mixture of solid and liquid fat necessary for partial coalescence. However in the previous studies the continuous phase remained liquid. The results reported here suggest that n-hexadecane emulsions *will* coalesce but only if the continuous phase freezes.

To understand more about the process of destabilization, bulk and microscopic observations of the samples were undertaken. On melting the water in a previously frozen emulsion, a semi-solid paste was formed (Figure **B.2**a), which on further heating (beyond the melting point of the fat ~10°C) melted and phase separated (Figure **B.2**b). An optical micrograph of a similar frozen emulsion is shown in Figure **B.3**b and c. The ice crystals are present in the open areas of the slide and the oil droplets are forced into the space surrounding them where they form a network. The oil droplets appear crystalline under polarized light and the larger droplets studied here often contain multiple crystals (Figure **B.3**b). On melting the water (Figure **B.3**c) some particles gain some diffusional mobility but the network formed on freezing is largely intact. It is this network that is responsible for the paste like quality seen at bulk scale (Figure **B.2**a). The droplets are still crystalline, but on further heating the crystals melt abruptly and the droplets rapidly coalesce (Figure **B.3**d).

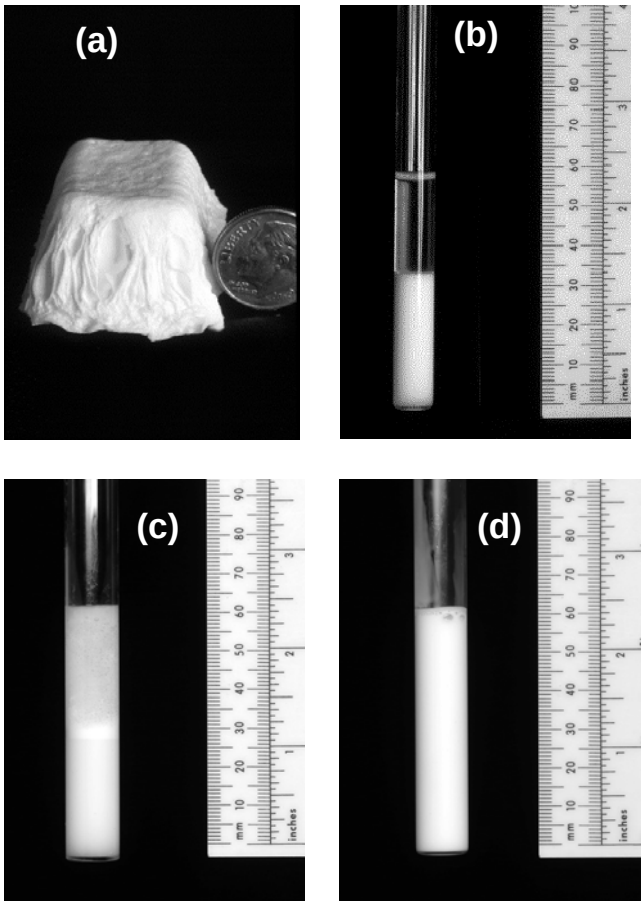

Figure **B.2**: Photographs of thawed n-hexadecane emulsion. (a) The gelled structure present before (b, c) the fat melts and the emulsion phase separated. Thawed emulsions prepared with (b) Tween 20 and (c) sodium caseinate are shown alongside a (d) similar, unfrozen emulsion for comparison. The semi-solid paste seen in (a) was prepared by freezing a cube of emulsion then removing the frozen block from the container and warming to allow the water but not the fat to melt.

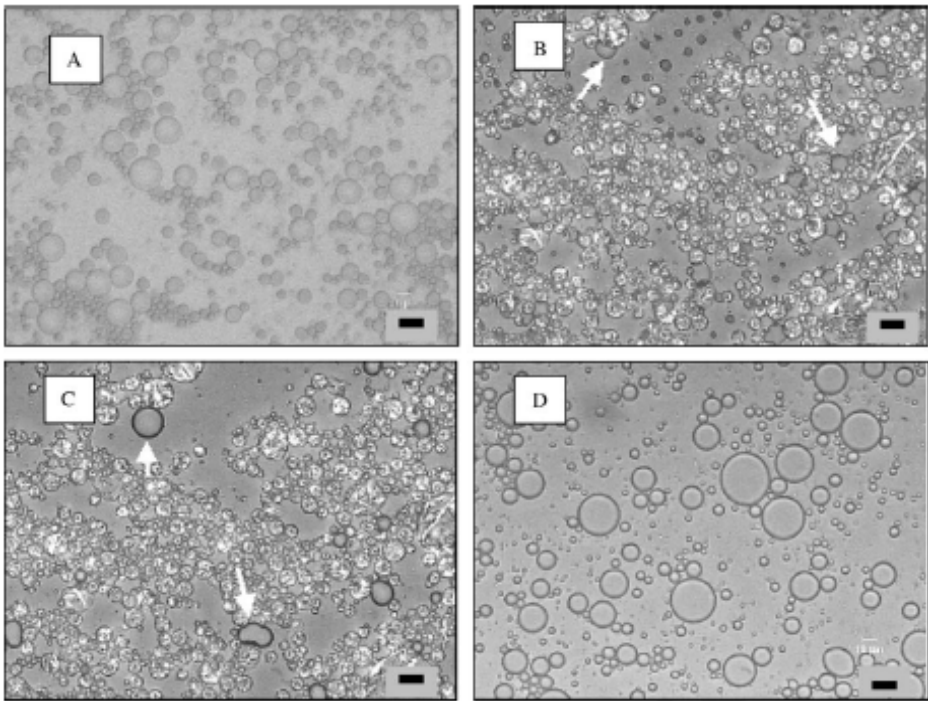

Figure **B.3**: Micrographs taken of an n-hexadecane emulsion (a) before freezing, (b) ice present, (c) ice melted but fat still solid, (d) fat melted. The images represent a time/temperature sequence for a single field of view. Note in (b) and (c) several air bubbles have formed (marked by arrows) that have been reabsorbed before (d) was taken. These bubbles appeared to form from and be reabsorbed into crystallizing and melting oil droplets respectively. Polarized light was used to illustrate the crystalline fat in (b) and (c) but not in (a) and (d) where there was no detectable crystallinity. Scale bar is 20 μm.

Similar experiments were conducted with emulsions of a homologous series of n-alkanes. The freezing and melting points of oils decreased with chain length while the freezing point of water was largely unchanged (Figure **B.4**). Emulsion stability was defined as those emulsions without visible surface oil after freezing to -20°C in bulk and then thawing. By this definition, the longer-chain alkanes (C14, C16, and C18) destabilized after a freeze-thaw cycle, while the shorter ones (C10) remained stable. The C12 sample destabilized even though the freezing point by DSC (-23±0.2°C) was lower than the freezer temperature, presumably because the highly supercooled oil crystallized during storage overnight in the freezer at -20°C. The distinction between these samples appears to be that while the aqueous phase froze in all cases, the shorter chain alkanes

remained in a liquid state and did not coalesce at –20°C. Support for this observation was provided in a subsequent experiment, where decane emulsions were cooled to -80°C (i.e., below the freezing point of the oil droplets), in which case they too destabilized.

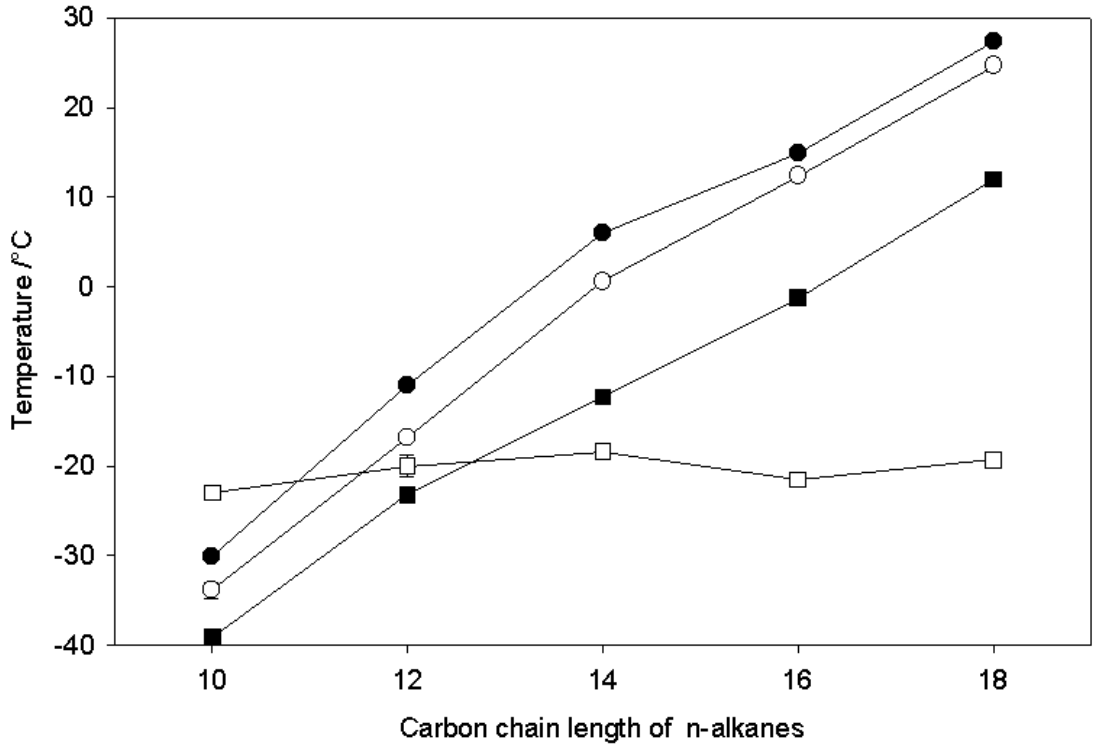

Figure **B.4**: Melting and freezing points of bulk and emulsified n-alkanes and the freezing point of water. Emulsions were 40 wt% oil stabilized with 2 wt% Tween 20 and were cooled and heated at 5°C min^{-1}. Freezing point of emulsified oil (■), freezing point of bulk oil (○), melting point of emulsified and bulk oil (●), melting point of aqueous phase (□).

Frequently, a "bubbly" layer was seen between the bulk oil and bulk aqueous phases of the thawed and phase separated emulsion, and the lower (aqueous) layer was turbid, suggesting emulsion breakdown was not complete. The bubbly layer seen at bulk scale was also observed microscopically and shown to be a complex mixture of partially phase-inverted emulsion (Figure **B.5**). While the extent of breakdown was not

quantified, qualitatively the C10 and C12 samples (destabilized by freezing to -80°C) were more turbid and had a more extensive bubbly layer than the C14, C16, and C18 samples. No explanation for these differences in phase separation is offered.

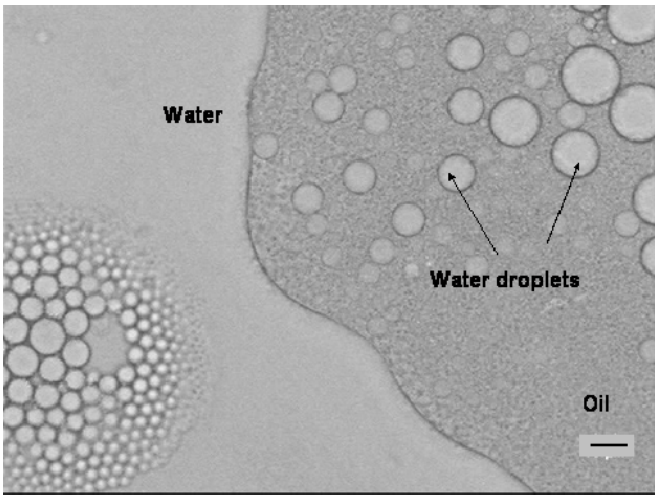

Figure **B.5**: Micrographs of the bubbly phase in a thawed and phase-separated emulsion (hexadecane emulsion stabilized with Tween 20). Scale bar is 20 μm.

Experiments were conducted to attempt to alter the structure of the ice and fat crystals formed. Changing the cooling and heating rate (0.5, 5.0 and 15.0°C min^{-1}, Table **B.1**) delayed the temperatures of the phase transitions, but did not alter the instability of the emulsions (here defined as a change in the DSC thermogram between first and second cooling of a Tween 20 stabilized emulsion). Furthermore, adding sucrose (up to 12 wt%) to the Tween 20-stabilized emulsions caused no changes in freeze-thaw stability. However, changing the surfactant type led to wide discrepancies in the freeze thaw stability of emulsions (Table **B.2**). The small molecule surfactants (SDS and Tween 20) were unstable while protein emulsifiers (WPI and caseinate) were apparently stable to freeze-thaw in DSC experiments (even after 5 cycles of cooling and heating).

Table **B.1**: Melting and freezing points of emulsified n-hexadecane and the emulsion aqueous phase at various cooling/heating rates.

Cooling and heating rate / °C min^{-1}	Oil freezing point/°C		Oil melting point/°C	Aqueous freezing point /°C
	(first cooling)	(second cooling)		
0.5	-0.54±0.5	12.9±0.4	14.0±0.4	-20.2±1.3
5.0	-1.2±0.1	12.4±0.0	14.9±0.3	-21.5±0.3
15.0	-3.0±0.1	11.2±0.3	17.1±0.2	-23.4±0.8

Table **B.2**: Freezing point of emulsified n-hexadecane stabilized with various surfactants.

Surfactant	Freezing point/ °C		Melting point / °C
	(first cooling)	(second cooling)	
Tween 20	-1.2±0.1	12.4±0.0	14.9±0.3
SDS	1.0±0.3	12.8±0.4	16.4±0.1
Na Caseinate	-0.5±0.4	-0.4±0.3	16.3±0.2
WPI	-0.5±0.4	-0.4±0.3	15.8±0.5

Surprisingly, despite their apparent stability in the DSC studies, in bulk experiments, some freeze-thaw instability in protein-stabilized emulsions was observed (Figure **B.2** b). While the small molecule-stabilized samples separated into two layers, the protein-stabilized samples separated into three layers: an upper free oily layer with aqueous "bubbles", an intermediate water-continuous creamy layer and a lower turbid layer. The density of the lower layer was 988.36 kg m^{-3} and that of the cream layer was

889.04 kg m^{-3} corresponding to an oil mass fraction of approximately 2.75% and 40.95% in the two phases respectively. The amount of free oil was much less in the protein-stabilized emulsions than in the small molecule surfactant stabilized emulsions. To better quantify the degree of emulsion destabilization the amount of free oil after freeze-thaw was measured by solvent extraction (Palanuwech, Potineni, Roberts and Coupland 2003). Briefly, hexane and emulsion (volume ratio 3:1) were mixed then allowed to stand for 30 minutes before decanting the solvent layer. The extraction was repeated five times then the combined solvent extracts were evaporated to dryness and the mass of extracted fat measured. Extractions were conducted both before and after a freeze-thaw treatment on n-hexadecane emulsions stabilized with either Tween 20, SDS, WPI or sodium caseinate.

Almost no oil could be extracted from the freshly prepared (unfrozen) emulsions suggesting the emulsion droplets were capable of protecting the emulsified lipid (Figure **B.6**). However, after freeze-thaw step, significantly more oil could be extracted from all samples, reaffirming the emulsions were partially destabilized. The amount of extractable fat decreased in the sequence Tween 20>SDS>WPI~Sodium caseinate (Figure **B.6**). Thus the protein emulsifiers were better at protecting the emulsion from freeze-thaw than the small molecule emulsifiers but still were not completely effective. A slight thickening of the thawing protein-stabilized samples was observed between the melting of the ice and the melting of the hydrocarbon rather than the self-supporting cryo-gel seen in the surfactant-stabilized systems. Previously it was observed that protein emulsifiers were better than small molecule surfactants at protecting triacylglycerol emulsions from partial coalescence (without a continuous phase transition) and argued this was due to the presence of a thicker interfacial layer (Palanuwech et al. 2003).

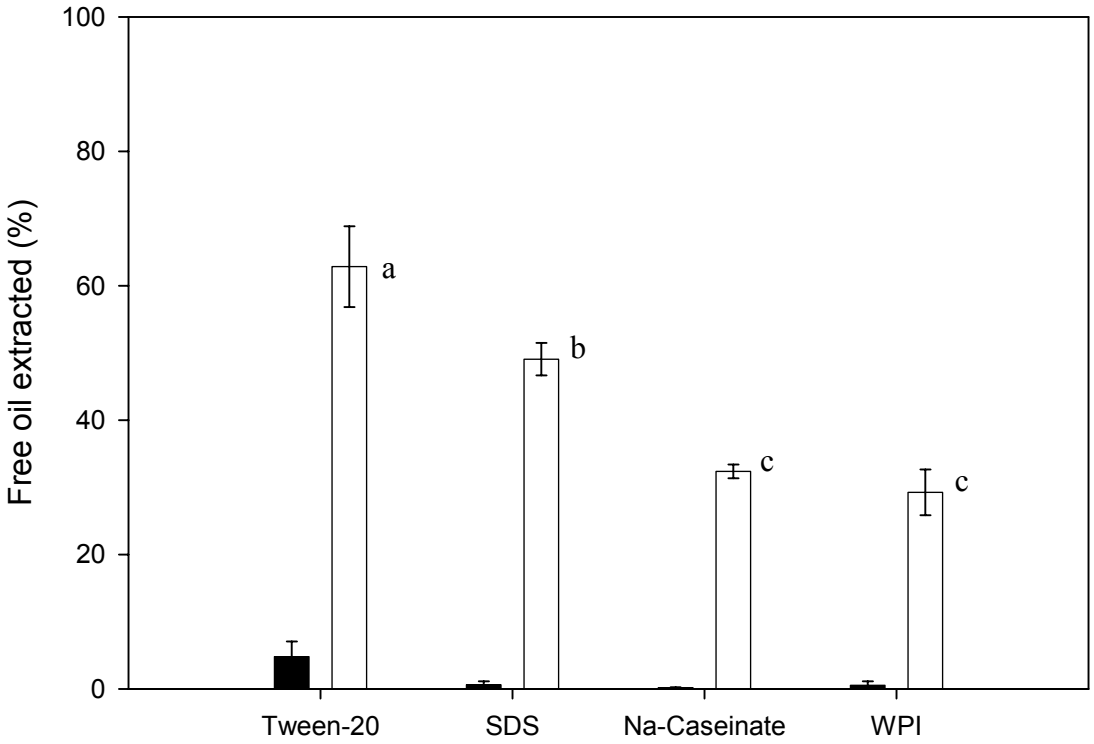

Figure **B.6**: Percentage of the total oil present that could be solvent-extracted from emulsions stabilized with different surfactants both before (■), and after (□) freeze thaw. Error bars represent the standard deviation of six replicate experiments. Thawed samples marked with similar letters were not significantly different (P> 0.05)

It is interesting that despite this destabilization seen in the protein stabilized samples both in solvent extraction measurements and in bulk observations, there was typically no characteristic changes in DSC profile even after multiple temperature cycles. In other experiments the DSC was programmed to mimic the cooling, holding, and heating conditions used in the bulk experiment but again no changes in the thermogram were seen. It is not immediately clear why the DSC method should prove unreliable in this case. One possibility is the very small sample size means that once nucleation occurs the sample freezes faster than the bulk emulsion and this somehow affects the stability of the dispersed droplets. Interestingly, of the 25 different samples of sodium caseinate

stabilized n-hexadecane emulsions prepared in this study only two of them consistently gave thermograms characteristic of freeze-thaw instability while the others were consistently completely stable. The solvent extraction measurements gave a more typical scatter of experimental data around the mean.

It is apparent that freezing the continuous phase will force the droplets into the confined spaces between droplets. If the oil is liquid during this process there is no permanent network formed and the emulsion will readily redisperse on melting. On the other hand, if the droplets are solid and particularly if they are surrounded with small-molecule surfactant, they will remain connected even after melting the ice and then coalesce as the fat melts. The situation is somewhat similar to experiments conducted on the stability of thin films in concentrated emulsions (Bibette 1992). In this work, Bibette was able to calculate the critical pressure for film rupture of lamellae separating emulsion droplets in a concentrated emulsion from the osmotic pressure applied to draw water out of the system. In the present study, the water is withdrawn by freezing and the pressure is further applied by the expansion of the water on freezing. Together these effects force droplets into close proximity. The liquid droplets are probably able to deform somewhat to accommodate the pressure, but the solid droplets cannot. The surfactant may be squeezed out of the gap separating the two droplets, creating some oil-to-oil contact that would lead to full coalescence on melting. The destabilization mechanism here is similar to partial coalescence, in that oil-to-oil contact is achieved without full coalescence but in this case the presence of liquid oil to reinforce the linkage is not necessary. Protein emulsifiers are more resistant to the pressure caused by freezing, probably because of their stronger steric effects (Palanuwech et al. 2003) or because their higher molecular weight makes them slower to diffuse from the lamellae region.

B.4 Conclusion

Although alkane emulsions are stable to dispersed phase transitions, they will destabilize following a continuous phase transition unless the oil remains liquid while the aqueous phase is solid. The degree of destabilization is greater for protein-stabilized than for small molecule-stabilized emulsions. The destabilization follows a two-stage process, first a network of crystalline fat droplets forms during freezing and second the network collapses and the droplets coalesce during droplet melting. The network formed on freezing is similar to partial coalescence seen in unfrozen media and may also be relevant in ice cream quality (Goff 1997). The breakdown seen in some thawed emulsions would clearly be a quality defect in real frozen food products (e.g., sauces).

Acknowledgement

This work was partially funded by a grant from the Mark and Nancy Speizer Undergraduate Research Fund in Food Science. I am grateful to co-authors Grace Cramp and Andrea Docking for allowing me to use this paper as a part of my thesis and to Leslie Grant for technical assistance.

B.5 References

Bibette, J., Stability of thin-films in concentrated emulsions. *Langmuir* **1992,** 8, (12), 3178-3182.

Dickinson, E., *An introduction to food colloids*. Oxford University Press.: New York, 1992.

Goff, H. D., Colloidal aspects of ice cream - a review. *International Dairy Journal* **1997**, 7, (6-7), 363-373.

Hartel, R. W., *Crystallization in foods*. Aspen Publishers Inc.: Gaithersburg, MD, 2001.

McClements, D. J. and S. R. Dungan, Effect of colloidal interactions on the rate of interdroplet heterogeneous nucleation in oil-in-water emulsions. *Journal of Colloid Interface Science* **1997**, 186: 17-28.

McClements, D. J.; Dungan, S. R.; German, J. B.; Simoneau, C. and Kinsella, J. E., Droplet size and emulsifier type affect crystallization and melting of hydrocarbon-in-water emulsions. *Journal of Food Science* **1993**, 58, (5), 1148-1151.

Palanuwech, J. and Coupland, J.N., Effect of surfactant type on the stability of oil-in-water emulsions to dispersed phase crystallization. *Colloids and Surfaces A-Physicochemical and Engineering Aspects* **2003**, 223, 251-262

Palanuwech, J.; Potineni R.; Roberts, R.F. and Coupland, J. N., A method to determine free fat in emulsions. *Food Hydrocolloids* **2003**, 17, 55-62

Skoda, W. and van den Tempel, M.. Crystallization of emulsified triglycerides. *Journal of Colloid Science* **1963**, 18, 568-584.

Vanapalli, S. A.; Palanuwech, J. and Coupland, J.N., Stability of emulsions to dispersed phase crystallization: Effect of oil type, dispersed phase volume fraction, and cooling rate. *Colloids and Surfaces A-Physicochemical and Engineering Aspects* **2002**, 204, (1-3), 227-237.

Walstra, P., Dispersed systems: Basic considerations. In *Food chemistry,* Fennema, O. R., Ed. Marcel Dekker, Inc.: New York, **1996**; pp 95-156.

Walstra, P., Emulsion Stability. In *Encyclopedia of emulsion technology*, Becher, P., Ed. Marcel Dekker: New York, **1996b**; Vol. 4, pp 1-62.

Appendix C

Effect of Aqueous Composition on the Freeze-Thaw Stability of Emulsions

Abstract

The freeze-thaw induced coalescence of sodium caseinate stabilized n-hexadecane emulsions was investigated as a function of added protein (0-2 wt%), fat (0-40 wt%) and aqueous sugar (0-2 wt% sucrose, maltose, glucose, corn syrup solids) contents. For all variables there was a critical dependence on aqueous phase composition. Emulsions were stable to small decreases in aqueous protein or sugar content to a critical point below which the extent of destabilization increased linearly. It is hypothesized that the stability of frozen emulsions depends on the mechanical capacity of the lamellae separating them to resist the pressure of the growing ice phase. Sugar serves to reduce the amount of ice (as measured by differential scanning calorimetry) and hence the pressure, while aqueous protein reinforces the lamellae.

C.1 Introduction

Emulsions are thermodynamically unstable because of their large interfacial area and droplet coalescence and phase separation is an inevitable consequence. For two droplets to coalescence, they must first approach to close proximity, then the film of water separating them must drain, and finally the resultant Newton black film must rupture and allow the two droplets' contents to flow together (van Aken, 2003). In many cases the repulsive forces between droplets (i.e., disjoining pressure, (Derjaguin, 1987; Dickinson, 1992) is sufficient to limit droplet approach and film drainage while in other cases the mechanical strength of the film can resist rupture.

Coarse emulsions (e.g., a vinaigrette dressing made by shaking together oil and vinegar) are prone to coalescence as the lower internal pressure allows significant deformation of large droplets to form a polyhedral structure separated by large planar films vulnerable to rupture. On the other hand, fine emulsions act as hard spheres and to overcome the disjoining pressure and force droplets into close proximity separated by a Newton black film external pressure must be applied via centrifugation (van Aken and Zoet, 2000) or osmotic dehydration (Bibette, 1992). These highly concentrated emulsions (ϕ>close packing, i.e., liquid foams) will coalesce if the thin films separating the droplets rupture.

Film rupture can occur due to incomplete coverage of the droplet surface by the stabilizer leading to exposed patches of dispersed phase at the interface (van Aken, 2004). Nucleation and growth of such patches on the surface cause film rupture followed by coalescence of the adjoining droplets (Kashchiev and Exerowa, 1980). Films formed between saturated interfaces can also rupture following the spontaneous formation of a channel between adjacent oil droplets. The tendency of such a channel to form depends

on the bending energy and surface curvature of the interfacial membrane (i.e., coalescence transition state theory, (Kabalnov and Wennerstrom, 1996)). The geometrical concerns leading to bending energies are rarely expressed for surface proteins, however it is clear that the relatively thick hydrophilic layer present at protein coated surfaces would tend to resist spontaneous channel formation and may account for the relative stability of protein-stabilized emulsions to coalescence (van Aken, 2004). A film which is quiescently stable (i.e., limited spontaneous pore formation) may still rupture in response to mechanical forces, leading to droplet coalescence. Van Aken and coworkers (van Aken, 2002; van Aken and van Vliet, 2002; van Aken and Zoet, 2000) showed that this mechanism of coalescence occurs in highly concentrated emulsions prepared by centrifugal concentration of an initially dilute emulsion. They also showed that coalescence at rest occurred only in emulsions whose surfaces were not saturated with surfactant (van Aken and Zoet, 2000), whereas emulsions with saturated surfaces only coalesced after yielding to an applied stress (van Aken, 2002; van Aken and van Vliet, 2002).

The highly concentrated emulsions used in coalescence studies rarely occur in commercial emulsions (with the possible exception of mayonnaise and some cosmetics). However when an oil-in-water emulsion is frozen, the oil droplets are forced together to very high volume fractions and the interactions between droplets in the unfrozen portion may be similar to those between droplets in a liquid foam. Unsurprisingly emulsions frequently show considerable oiling-off following a freeze-thaw cycle (Cramp, Docking, Ghosh and Coupland, 2004; Thanasukarn, Pongsawatmanit and McClements, 2004b).

Sugars are important cryoprotectants in freeze-tolerant plants and animals (Troshin, 1963) and simple sugars such as sucrose and sorbitol and high molecular weight maltodextrins have been known to stabilize food proteins against denaturation by freezing (Carvajal, MacDonald and Lanier, 1999; McClements, 2002). Based on the cryoprotective effects of sugars in biological systems and simple proteins, it is expected that they would have a similar role in frozen food emulsions. Indeed, Saito et. al. (Saito,

Kawagishi, Tanaka, Tanimoto, Okada, Komatsu and Handa, 1999) reported the ability of maltose to protect a frozen emulsion against coalescence. They suggested that either sugar may work as a spacing matrix between the droplets, thus preventing fusion, or alternatively interactions between the maltose and the phospholipid surface monolayer may give rise to higher bending energy of the interfacial membrane, thus increasing the free energy of the coalescence transition state. In another recent study Thanasukarn et. al. (Thanasukarn, Pongsawatmanit and McClements, 2004a) also showed that incorporation of sucrose into emulsion aqueous phase can improve the stability of whey protein isolate stabilized hydrogenated palm oil emulsion to freezing.

Emulsion freeze-thaw stability is important in developing frozen sauces and desserts and knowing the factors influencing freeze-thaw stability of emulsion will help us to control the product formulations for improved storage stability. In the present work the effects of oil volume fraction and added protein and sugar on the extent of freeze-induced coalescence in model emulsions is considered.

C.2 Materials and Methods

Materials. Hexadecane and hexane was purchased from Fisher Scientific (Springfield, NJ). Trehalose and corn syrup solids (dextrose equivalent 36, as provided by the manufacturer) were donated by Cargill, Inc. (Wayzata, MN) and sucrose was purchased from Florida Crystals Food Corp (Palm Beach, FL). All other reagents were obtained from the Sigma Chemical Company (St. Louis, MO). The protein content of sodium caseinate used in this work was found to be 91.6 ± 0.6 % (see below for analytical methodology).

Sample preparation. The model system selected for this study is a fine dispersion of n-hexadecane droplets stabilized with sodium caseinate. Similar emulsions have been widely used as model systems in our laboratory and others (Awad, 2002;

Cramp, et al., 2004; Dickinson, Kruizenga, Povey and van der Molen, 1993) as they are relatively simple and stable over several weeks. Previously it was shown that caseinate-stabilized alkane emulsions are stable to dispersed phase crystallization (Palanuwech, 2003) but can be partially destabilized by continuous phase freezing (Cramp, et al., 2004). In the present work the composition of the aqueous phase was modified and its effects on emulsion freeze-thaw stability were examined.

Emulsions were prepared by mixing n-hexadecane (40 wt%) with sodium caseinate solutions (2 wt%) in a high-speed blender (Brinkmann Polytron, Brinkmann Instruments Inc., Westbury, NY) for 30 seconds. The crude emulsions were then re-circulated through a twin-stage valve homogenizer (Niro Soavi Panda, GEA Niro Soavi, Hudson, WI) for several minutes at a pressure of 230 ± 10 bar to achieve multiple passes through the valves. The emulsions were characterized by laser diffraction particle sizing (Horiba LA 920, Irvine, CA) using a relative refractive index of 1.15. The de Brouckere mean droplet size (d_{43}) of all the emulsions was 0.44 ± 0.06 μm, and the standard deviation of the distributions was approximately 0.12 μm. The emulsions were stable at room temperature for several days (no change in particle size, no extractable fat).

The freeze-thaw stability of the emulsions was measured by transferring aliquots into thin-walled glass tubes (internal diameter 11 mm) and holding for 17 ± 2 hours at -20 ± 1ºC or at room temperature (23 ± 1ºC) as a control. Samples were then re-heated to 40 ± 1ºC to melt the solid fat before determining the free (extractable) fat.

Determination of Free Fat. The degree of emulsion destabilization was measured by the amount of free oil after freeze-thaw by solvent extraction method. Samples of emulsion (5 g) were transferred to Mojonnier flasks (FMC Corporation, Chicago, IL) and extracted with hexane (hexane to emulsion volume ratio 3:1). The organic extracts were evaporated to dryness (at 110°C) in a Soxtec Extraction Unit (Foss Tecator, Eden Prairie, MN) and the extractable fat weighed. The extraction was repeated five times to ensure complete extraction of destabilized fat. Preliminary experiments

showed that no fat could be extracted from a freshly prepared emulsion by this method while a free fat spike could be quantitatively recovered and five extractions were sufficient to recover all the extractable fat. Therefore it is concluded that solvent extraction is a suitable method to measure the extent of emulsion freeze thaw destabilization. In this work emulsion destabilization is defined as the proportion of the total fat in a sample that can be extracted by this method after a single freeze-thaw cycle. All measurements are expressed as the mean and standard deviation of at least three full experimental replicates.

Determination of Aqueous Protein. Samples of emulsions were centrifuged at 1.5×10^4 g for 20 minutes in a high speed centrifuge (IEC B-20A, Needham Heights, MA) at 20ºC. The clear aqueous layer at the bottom of the centrifuge tubes were withdrawn with a syringe and filtered through 0.45 μm filter. The nitrogen content of the aqueous solutions was determined by combustion using a nitrogen analyzer (Leco, St. Joseph, MI). A Kjeldahl factor of 6.38 was used to calculate crude protein content from the nitrogen measurement. The protein content of sodium caseinate was also measured by this method.

C.3 Results and Discussions

Stock emulsions (40 wt% oil) were diluted in varying concentrations of caseinate solutions to prepare a series of samples with similar oil contents (5 wt%) but varying protein concentrations. The aqueous protein concentration and freeze-thaw destabilization were measured by the standard methods and the results are reported in Figure **C.1**. The aqueous protein concentration increased with the protein concentration in the diluent solution: ([aqueous protein] = 0.86 [diluent protein] + 0.07, r^2>0.99) indicating that because the stock emulsion was prepared with an excess of protein, very little of the protein added subsequently adsorbed to the interface. The freeze-thaw stability of the emulsion increased dramatically with small initial increase in aqueous

protein concentration (i.e., while an emulsion with 0.09% aqueous protein was 47.7% destabilized by freeze thaw, the same emulsion with 0.2% aqueous protein was almost completely freeze-thaw stable). Clearly protein plays an important role in protecting emulsions from freeze-thaw induced coalescence but because the amount of aqueous and adsorbed protein were closely correlated it was not possible to see which fraction was most important.

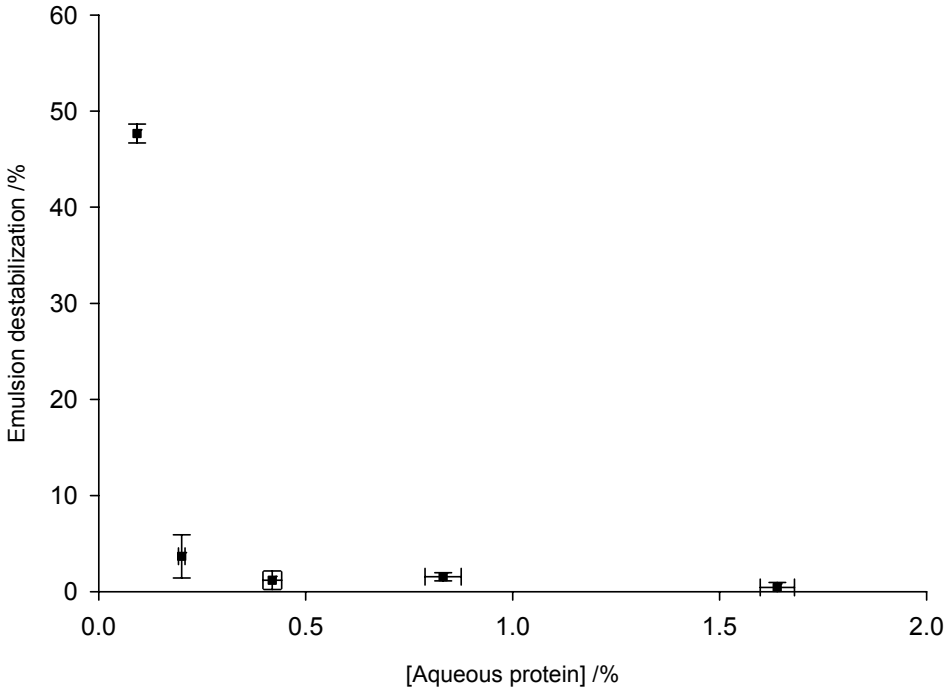

Figure **C.1**: Effect of aqueous protein concentration on the freeze-thaw destabilization of 5 wt% hexadecane emulsions. Samples were prepared by dilution a 40 wt% emulsion in different concentrations of sodium caseinate solution. Emulsion destabilization is defined relative to the total amount of fat in the system. The values are the mean of three experimental replications and the errors bars are one standard deviation.

In a second similar series of experiments the effect of oil fraction on the freeze-thaw stability of emulsions was investigated. Samples were prepared by diluting a stock emulsion (40 wt% oil) to different extents. Because the effect of dilution is likely to be convoluted with small changes in protein concentration, two series of experiments were

conducted – one in which the emulsions were diluted in 2 wt% caseinate solution and one where they were diluted deionized water. The emulsion freeze-thaw stability and aqueous protein concentration of the protein-diluted and water-diluted samples are reported in Figure **C.2**. Note that while the absolute amount of fat extracted increased with the amount of oil in the emulsion, the differences discussed refer to the proportion of the oil present that is extractable after freeze-thaw.

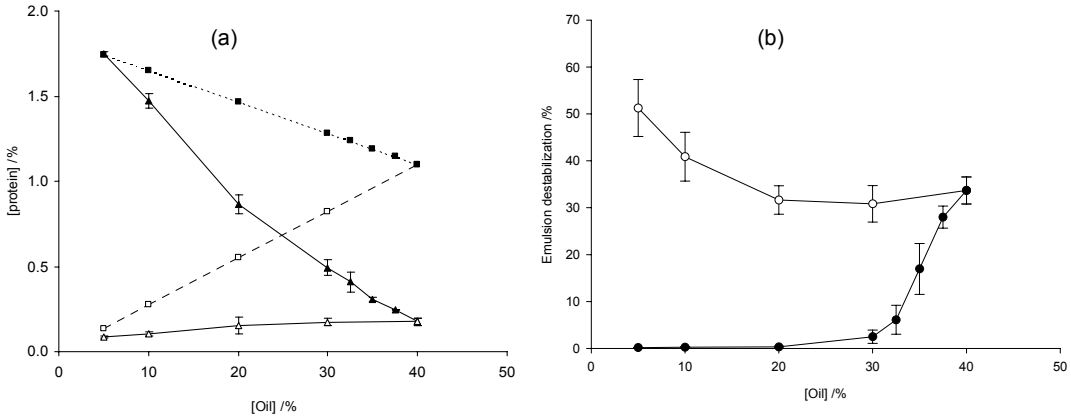

Figure **C.2**: Effect of dilution on the aqueous protein concentration (a) and freeze-thaw stability (b) of sodium caseinate stabilized hexadecane-in-water emulsions. Samples were prepared by diluting a 40 wt% stock emulsion in either water (open symbols) or 2% sodium caseinate (filled symbols) solution. Experimental values of aqueous protein (Δ, ▲) are plotted along with total protein content (□, ■) of the emulsions. Emulsion destabilization is defined relative to the total amount of fat in the system. The values are the mean of three experimental replications and the errors bars are one standard deviation.

For the samples diluted in sodium caseinate solution both the aqueous and total protein concentration increased with the degree of dilution (Figure **C.2**a). In the most dilute samples the protein added in the diluent solution is so large it is almost equal to the overall protein content of the emulsion. In the samples diluted in deionized water both the aqueous and total protein was low and decreased with the extent of dilution (Figure **C.2**a). The samples diluted in protein solution became much more stable as the oil concentration was decreased from 40% oil (33.7% destabilization, 0.18% aqueous

protein) to 30% oil (2.5% destabilization, 0.49% aqueous protein) while for all the samples diluted in deionized water, freeze-thaw destabilization of all of the sample was relatively high and decreased with oil mass fraction (i.e., 33.7% of the oil extractable from the 40 wt% emulsion to 51.2% of the oil extractable from the 5 wt% emulsion) (Figure **C.2**b).

The rate of coalescence is conventionally defined as a product of droplet collision rate and collision efficiency (Vanapalli, 2003). Assuming a constant collision efficiency, reaction rate is then a second order reaction with respect to droplet number, so it can be said that for a given reaction time the amount of coalescence should increase with the square of droplet concentration (i.e., volume fraction). In this work emulsion destabilization is presented relative to the total amount of fat present and therefore this parameter is expected to increase monotonically with oil volume fraction. Clearly this relation is not seen (Figure **C.2**b), suggesting the droplet collision model is inappropriate in this case. A better picture of the destabilization event may then be to imagine the droplets confined in the spaces between ice crystals. The close-packed droplets are under pressure from the expanding ice phase and in these circumstances the balance of forces acting on the film separating the droplets will govern the stability of the emulsion. Evidence of such clusters of solid droplets was observed by microscopy of a similar system in previous work (Cramp, et al., 2004) and by neutron scattering in a study of the freeze and pressure destabilization of a water-in-oil microemulsion by Steytler et al. (Steytler, Robinson, Eastoe, Ibel, Dore and Macdonald, 1993).

[Interestingly the water-in-oil microemulsion was stable to freezing in the work by the Steytler group (Steytler, et al., 1993) and no phase separation observed upon melting of the continuous alkane phase. However, the dispersed phase (water) was always in liquid state in the study of Steytler et al. (Steytler, et al., 1993), whereas in the present experiments the droplets (emulsified hexadecane, freezing point -1ºC) were solid at the emulsion freezing temperature (-20ºC). In previous studies (Appendix B) it was observed that if the oil droplets are liquid during the freezing process, no permanent

network will be formed and the emulsion will readily redisperse on melting. On the other hand, if the droplets are solid and particularly if they are surrounded with small-molecule surfactant, they will remain connected even after melting the ice and then coalesce as the fat melts.]

The ability of the interdroplet film to resist the pressure from the ice phase and allow the emulsion to remain stable on thawing increased with the amount of added protein, and led to an increase in emulsion stability (Figure **C.1**). Because in the dilution experiments almost all the protein added remained in the aqueous phase, data from Figure **C.2**a and Figure **C.2**b was replotted to show the extent of emulsion destabilization as a function of aqueous protein concentration (Figure **C.3**). Here it can be seen that emulsion destabilization was independent of aqueous protein concentration for aqueous protein>0.5 wt% but increased dramatically for lower concentrations. No such simple relation was seen if the data in Figure **C.2** was replotted in terms of total protein (data not shown) suggesting that a certain minimum amount of non-adsorbed aqueous protein in the lamella separating the droplets is necessary to resist the pressure from the expanding ice but protein added beyond this caused no further increase in emulsion stability (Figure **C.3**).

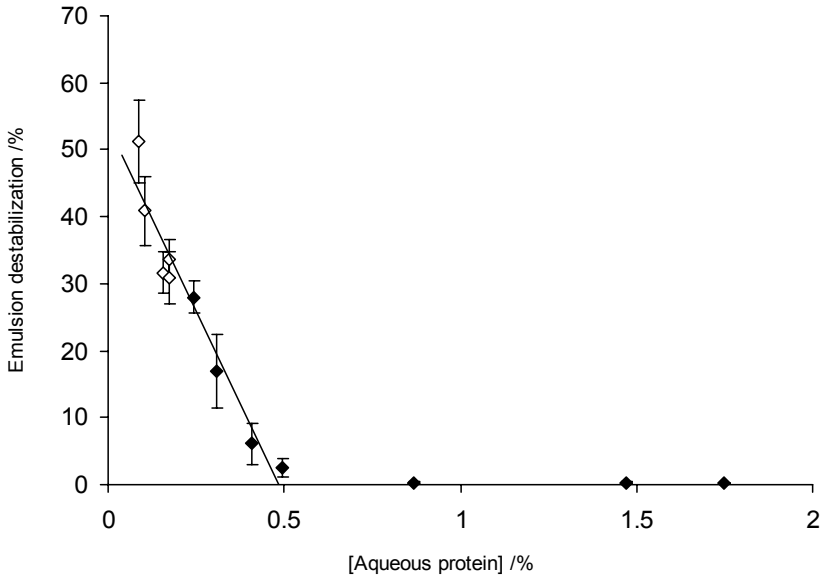

Figure **C.3**: Effect of aqueous protein concentration on the freeze-thaw stability of sodium caseinate stabilized hexadecane-in-water emulsions. Data are replotted from Figure C.2a (aqueous protein concentration) and 2b (relative emulsion destabilization). Water-diluted emulsions are shown with open symbols and 2% caseinate-diluted emulsions are shown with filled symbols.

There are various mechanisms the unadsorbed protein could contribute to the "strength" of the lamellae in the frozen emulsion. First, the increased amount of polymer in that phase may increase its viscosity or even form a transient gel that is able to mechanically resist deformation. Another possibility is the unadsorbed proteins act as particles and provide some kinetic stability of the system as they must diffuse out of the gap before a Newton black film can form (Giasson, Israelachvili and Yoshizawa, 1997). Isrealachvili (Israelachvili, 1997) showed that adsorbed polymer can produce a short range stabilizing repulsive force between the colloidal particles leading to 'steric stabilization' of a colloid. Based on this steric repulsive force it is expected that externally added protein between two protein-covered surfaces would also produce similar stabilization against coalescence.

Another factor could influence emulsion stability in frozen state is the removal of dissolved gas during freezing of aqueous phase. Pashley described apparent decrease in hydrophobic effect after the dissolved gasses were removed from a sample by repeated freeze-thaw cycling under a vacuum (Pashley, 2003). While the samples studied here were also frozen it is unlikely that similar levels of degassing would be achieved as the present work was conducted at atmospheric pressure. However, it was possible that the decrease in dissolved gas in the frozen state would reduce the hydrophobic effect to some extent. Pashley (2003) showed that that this would lead to spontaneous dispersion of oil in the degassed medium. In the present work lipid droplets were crystalline, so unlikely to spontaneously disperse, but it was possible that the emulsifier sodium caseinate could desorb from the surface (as there is less hydrophobic effect to hold it there) and be unable to quickly readsorbed on thawing to prevent coalescence. More protein present in the system could allow faster readsorbtion on thawing.

This analysis shows the critical value of aqueous phase composition on the freeze-thaw stability of emulsions but does not eliminate the possibility of an affect due to oil content. In Figure **C.1** the 5 wt% emulsion with 0.2 wt% aqueous protein was almost completely stable, while in Figure **C.3** there is a group of emulsions with similar aqueous protein contents (0.15-0.18 wt%) but widely varying oil contents (20, 30, 40 wt% oil) all of which were significantly destabilized. The only difference between these samples is the lower oil content in the former, and while this effect was not investigated systematically, it makes sense that a lower fat emulsion would have more ice at freezing temperature and therefore greater pressure on the droplets and proportionally more destabilization.

If the capacity of an emulsion to withstand freezing to depend on the mechanical properties of the interdroplet film and therefore the amount of aqueous solids present, then any factor that decreased the forces applied would be similarly expected to increase the freeze-thaw stability of the emulsions. Solutes are known to decrease the amount of

ice present at a given temperature and have previously been shown to stabilize emulsions to freezing (Thanasukarn, et al., 2004a). So in the next series of experiments the effects of various types of added sugar on the amount of ice formed and on the freeze-thaw stability of emulsions were investigated.

Samples of emulsion were diluted in stock (60 wt%) sugar solution and deionized water to prepare samples with 20% oil and 0.5, 1, 2 and 3% of the different sugars. (Note sugar concentration is expressed here relative to the total mass of the emulsion. As these sugars are exclusively water soluble their aqueous concentrations would be 0.625, 1.25, 2.5 and 3.75% respectively.) To better see the differences, emulsion destabilization in these studies is expressed relative to the degree of destabilization of similar emulsions prepared without added sugar.

When small amounts of simple sugars were added, the relative freeze-thaw instability of the emulsions dramatically decreased (Figure **C.4**). On molar basis fructose was the least effective in stabilizing emulsions and corn syrup solids is most effective although differences among the sugars were relatively minor.

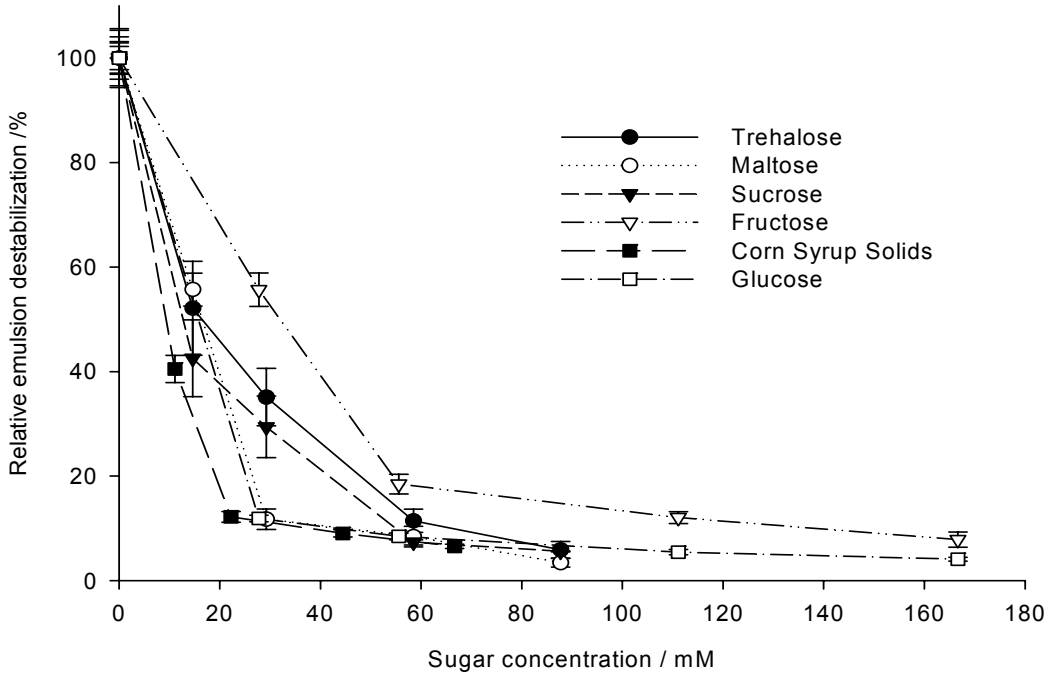

Figure **C.4**: Effect of added sugars on the freeze-thaw stability of sodium caseinate stabilized hexadecane-in-water emulsions. Emulsion destabilization is expressed as percent free oil extracted relative to that of an unmodified (no sugar added) emulsion after one freeze-thaw cycle. Molecular weight of corn syrup solids was calculated from its dextrose equivalent.

[The sudden transition was initially explained (incorrectly) by the fact that the sugars plasticize the caseinate in the unfrozen phase and allows it to remain in a flexible rubbery state better able to resist the pressure of the ice without cracking. Indeed, it has been showed that the presence of fructose (2:1, sodium caseinate: fructose) reduces the Tg of sodium caseinate (Kalichevsky, 1993). However this hypothesis was rejected as the glass transition temperatures (Tg, measured by differential scanning calorimetry) of all of the model aqueous phases were lower than the freezing temperature (-20°C) (data not reported) regardless of the sugar amount/type and regardless of the stability of the emulsion.]

To better understand the properties of the aqueous phase under these conditions, phase diagrams were measured using the method of Ponsawatmanit and Miyawaki (1993) for three different sugars (corn syrup solids, sucrose and fructose). Briefly sugars were dissolved in sodium caseinate solution similar in protein content to the emulsion aqueous phase (i.e., 0.15%) and aliquots (~15 mg) were cooled in the DSC (Perkin-Elmer DSC-7, Norwalk, CT) to -70^{o}C to ensure complete freezing, and then slowly reheated (0.5°C/min) to 40ºC. A model aqueous phase was used instead of the whole emulsion to obtain clear data without the thermal transitions due to the lipid phase.

The onset of melting temperature of the frozen solutions was plotted as a function of sugar concentration The state diagram (Figure **C.5**) is similar to that developed by other workers (Hartel, 2001; Ponsawatmanit, 1993) in the absence of sodium caseinate with freezing point decreasing with increased sugar content and the relative effects of the sugars being fructose>sucrose>corn syrup solids.

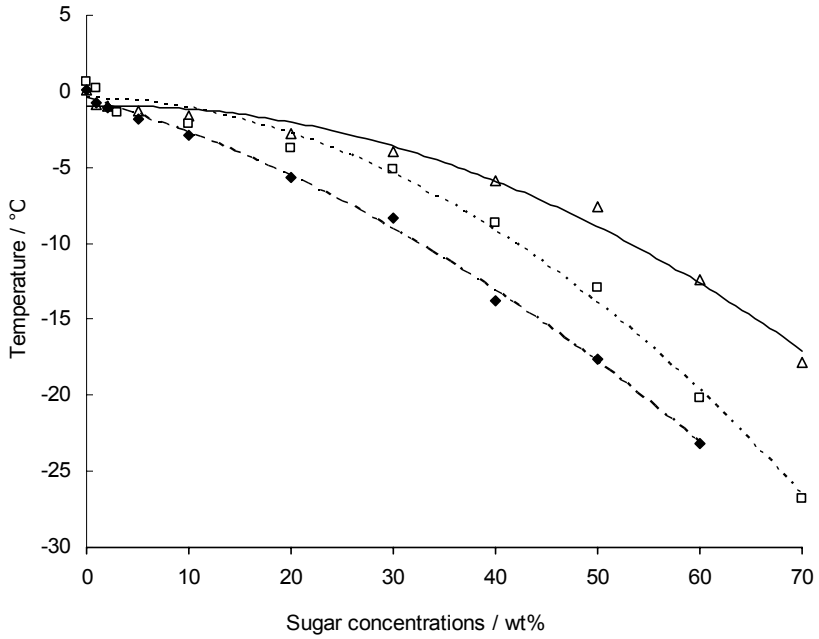

Figure **C.5**: Freezing point depression curves for corn syrup solids (Δ), sucrose (□) and fructose (♦), dissolved in 0.15% sodium caseinate solution.

From Figure **C.5**, at the freezing temperature used for the emulsions in the present work (-20°C) the equilibrium sucrose concentration was 60.3%. Therefore at -20°C, a 20% oil-in-water emulsion with 3% total added sucrose (i.e., 3.7% aqueous sucrose), would consist of solid oil droplets, ice crystals, and a certain amount of unfrozen 60.3% sucrose solution. To maintain mass balance there must be 6.1% unfrozen aqueous phase and the remainder (93.9%) ice. Similar calculations were made for the other sugar types and concentrations (data from Figure **C.5**) to determine the dependence of emulsion freeze thaw stability on the amount of unfrozen phase present at freezer temperature (Figure **C.6**). Emulsions with no added sugar have minimal unfrozen water present and those emulsions were maximally destabilized. From this point emulsion destabilization steeply decreases with increase in unfrozen water content and reached a plateau for more than approximately 3% unfrozen water content. Probably this amount of water is sufficient to maintain a hydration layer around the droplets sufficient to prevent the ice

from crushing them and rupturing the membrane between them. It should be noted that the addition of sugar may also have some influence on the properties of the proteins (Belyakova, Antipova, Semenova, Dickinson, Merino and Tsapkina, 2003). However, sugars were added after the emulsions were formed, hence adsorption at the interface would likely be less affected. In addition the levels of sugar used in this work were relatively low.

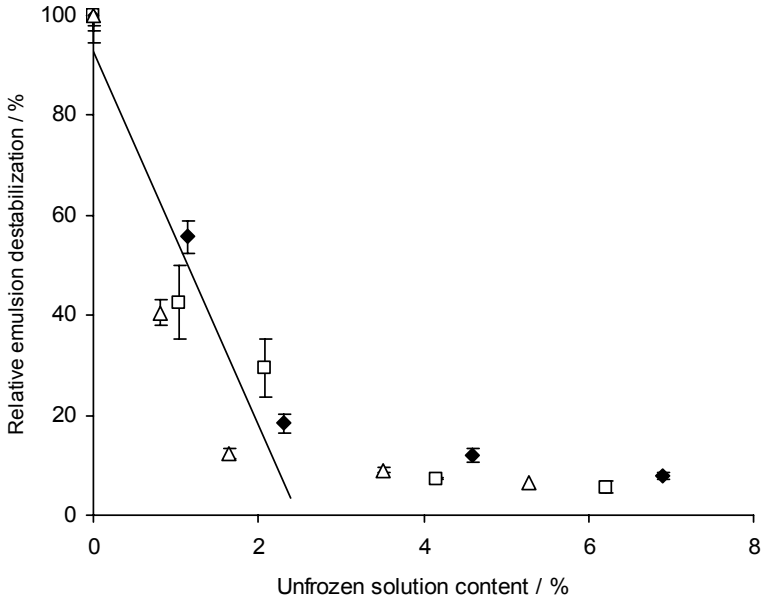

Figure **C.6**: Emulsion destabilization after freeze-thaw cycle as a function of unfrozen solution content at freezing temperature (-20°C). Unfrozen aqueous phase was varied by the addition of different amount of sugar in the emulsions. Emulsion destabilization is expressed as percent free oil extracted relative to that of an unmodified (no sugar added) emulsion after one freeze-thaw cycle. (□) sucrose, (♦) fructose and (Δ) corn syrup solids. A linear regression is shown for sugar concentrations <3%.

C.4 Conclusion

In summary, two different stabilizing mechanisms of sugars and proteins on emulsion freezing could be observed. Presence of sugars reduces the amount of ice which in turn reduces the compressive force on the droplets. A similar freezing point depression effect of proteins is not expected because of its very high molecular weight. Instead, addition of aqueous protein increases the resistance of the thin film separating the droplets to the applied force of expanding ice.

However, in both cases, emulsion destabilization showed similar trends (Figure **C.1**, Figure **C.3,** and Figure **C.6**) – resistance to coalescence above a critical composition and a linear increase in destabilization below that. Similar critical limits for destabilization of highly concentrated emulsion were also observed by Van Aken (van Aken, 2002) who showed that flow-induced coalescence in concentrated emulsions occurred only below a critical water content. The author argued that the critical value was related to a critical pressure above which the frictional force between the droplets cannot relax by slip between the adjacent droplet surfaces causing stretching and rupture of the thin film (van Aken, 2002). There is a class of changes described as catastrophes, where small changes to input variables make very little difference until a critical point at which a small additional change will lead to a large change in behavior. The theory has been applied to explain the sudden phase inversion seen in emulsions caused by a small change in dispersed phase volume fraction (Dickinson, 1981). It was suggested that catastrophic inversions were caused by the rapid coalescence of the dispersed phase at the closest packing arrangement of the drops throughout the whole O/W (or W/O) system to form the new continuous phase (Zerfa, Sajjadi and Brooks, 2001). In the present study a discontinuity in the degree of emulsion destabilization in response to small changes in aqueous phase composition was observed which suggests similar catastrophic behavior.

Formulating freeze-thaw stable emulsions is therefore a matter of maintaining a significant amount of unfrozen water or reinforcing the unfrozen phase added polymers.

Small changes in formulation can either have no effect on the stability or a very large effect depending on the position of the critical values.

Acknowledgement

I am thankful to co-other of this paper Grace Cramp for giving permission to use this paper in my thesis. I am also grateful to Leslie Grant for technical assistance.

C.5 References

Awad, T. S., Sato, K., Fat crystallization in O/W emulsions controlled by hydrophobic emulsifier additives. In *Physical properties of lipids*, Marangoni, A. G., Narine, S.S., Ed. Marcel Dekker Inc.: New York, **2002**; pp 37-62.

Belyakova, L. E.; Antipova, A. S.; Semenova, M. G.; Dickinson, E.; Merino, L. M.; Tsapkina, E. N., Effect of sucrose on molecular and interaction parameters of sodium casemate in aqueous solution: relationship to protein gelation. *Colloids and Surfaces B-Biointerfaces* **2003,** 31, (1-4), 31-46.

Bibette, J., Stability of thin films in concentrated emulsions. *Langmuir* **1992,** 8, 3178-3182.

Carvajal, P. A.; MacDonald, G. A.; Lanier, T. C., Cryostabilization Mechanism of Fish Muscle Proteins by Maltodextrins. *Cryobiology* **1999,** 38, (1), 16-26.

Cramp, G. L.; Docking, A. M.; Ghosh, S.; Coupland, J. N., On the stability of oil-in-water emulsions to freezing. *Food Hydrocolloids* **2004,** 18, (6), 899-905.

Derjaguin, B. V., Modern state of the investigation of long-range surface forces. *Langmuir* **1987,** 3, (5), 601-606.

Dickinson, E., Interpretation of emulsion phase inversion as a cusp catastrophe. *Journal of Colloid and Interface Science* **1981,** 84, (1), 284-287.

Dickinson, E., *An introduction to food colloids*. Oxford University Press.: New York, 1992.

Dickinson, E.; Kruizenga, F.-J.; Povey, M. J. W.; van der Molen, M., Crystallization in oil-in-water emulsions containing liquid and solid droplets. *Colloids and Surfaces A: Physicochemical and Engineering Aspects* **1993,** 81, 273-279.

Giasson, S.; Israelachvili, J.; Yoshizawa, H., Thin film morphology and tribology study of mayonnaise. *Journal of Food Science* **1997,** 62, (4), 640-&.

Hartel, R. W., *Crystallization in foods*. Aspen Publishers Inc.: Gaithersburg, MD, 2001.

Israelachvili, J., *Intermolecular and surface forces*. 2nd ed.; Academic Press: San Diego, CA, **1997**.

Kabalnov, A.; Wennerstrom, H., Macroemulsion stability: The oriented wedge theory revisited. *Langmuir* **1996,** 12, (2), 276-292.

Kalichevsky, M. T., Blanshard, J.M.V., Tokarczuk, P.F., Effect of water content and sugars on the glass transition of casein and sodium caseinate. *International Journal of food science and technology* **1993,** 28, 139-151.

Kashchiev, D.; Exerowa, D., Nucleation mechanism of rupture of Newtonian black films. I. Theory. *Journal of Colloid and Interface Science* **1980,** 77, (2), 501-511.

McClements, D. J., Modulation of Globular Protein Functionality by Weakly Interacting Cosolvents. *Critical Reviews in Food Science and Nutrition* **2002,** 42, (5), 417-471.

Palanuwech, J., and Coupland, J.N., Effect of surfactant type on the stability of oil-in-water emulsions to dispersed phase crystallization. *Colloids and Surfaces A-Physicochemical and Engineering Aspects* **2003,** 223, 251-262.

Pashley, R. M., Effect of Degassing on the Formation and Stability of Surfactant-Free Emulsions and Fine Teflon Dispersions. *J. Phys. Chem. B* **2003,** 107, (7), 1714-1720.

Ponsawatmanit, R., Miyawaki, O., Measurement of Temperature-dependent ice fraction in frozen foods. *Bioscience Biotechnology and Biochemistry* **1993,** 57, (10), 1650-1654.

Saito, H.; Kawagishi, A.; Tanaka, M.; Tanimoto, T.; Okada, S.; Komatsu, H.; Handa, T., Coalescence of Lipid Emulsions in Floating and Freeze-Thawing Processes: Examination of the Coalescence Transition State Theory. *Journal of Colloid and Interface Science* **1999,** 219, (1), 129-134.

Steytler, D. C.; Robinson, B. H.; Eastoe, J.; Ibel, K.; Dore, J. C.; Macdonald, I., Effects of Solidification of the Oil Phase on the Structure of Colloidal Dispersions in Cyclohexane. *Langmuir* **1993,** 9, (4), 903-911.

Thanasukarn, P.; Pongsawatmanit, R.; McClements, D. J., Impact of fat and water crystallization on the stability of hydrogenated palm oil-in-water emulsions

stabilized by whey protein isolate. *Colloids and Surfaces A: Physicochemical and Engineering Aspects* **2004a,** 246, (1-3), 49-59.

Thanasukarn, P.; Pongsawatmanit, R.; McClements, D. J., Influence of emulsifier type on freeze-thaw stability of hydrogenated palm oil-in-water emulsions. *Food Hydrocolloids* **2004b,** 18, (6), 1033-1043.

Troshin, A. S. In *The cell and environmental temperature : the role of cellular reactions in adaption of multicellular organisms to environmental temperature*, International Symposium on Cytoecology, Leningrad, 1967, 1963; Pergamon Press: Leningrad, **1963**.

van Aken, G. A., Flow-induced coalescence in protein-stabilized highly concentrated emulsions. *Langmuir* **2002,** 18, (7), 2549-2556.

van Aken, G. A., Coalescence Mechanisms in Protein-Stabilized Emulsions. In *Food Emulsion*, Fourth ed.; Friberg, S. E., Larsson, K., Sjoblom, J., Ed. Marcel Dekker, Inc.: New York, **2003**; pp 299-325.

van Aken, G. A.; van Vliet, T., Flow-induced coalescence in protein-stabilized highly concentrated emulsions: Role of shear-resisting connections between the droplets. *Langmuir* **2002,** 18, (20), 7364-7370.

van Aken, G. A.; Zoet, F. D., Coalescence in highly concentrated coarse emulsions. *Langmuir* **2000,** 16, (18), 7131-7138.

Vanapalli, S. A., Coupland, J.N., Orthokinetic stability of food emulsions. In *Food Emulsions*, Fourth ed.; Friberg, S. E., Larsson, K., Sjoblom, J., Ed. Marcel Dekker, Inc.: New York, **2003**; pp 327-351.

Zerfa, M.; Sajjadi, S.; Brooks, B. W., Phase behavior of polymer emulsions during the phase inversion process in the presence of non-ionic surfactants. *Colloids and Surfaces a-Physicochemical and Engineering Aspects* **2001,** 178, (1-3), 41-48.

VITA

Supratim Ghosh

EDUCATION

- **Doctor of Philosophy in Food Science**, The Pennsylvania State University, University Park, Pennsylvania (January 2003- May 2007)
- **Bachelor of Technology in Chemical Technology** (specialization in Oil Technology), University of Calcutta, India (1996-1999)
- **Bachelor of Science in Chemistry**, University of Calcutta, India (1993-1996)

WORK EXPERIENCE

- Graduate Research Assistant, Department of Food Science, The Pennsylvania State University, University Park, Pennsylvania (January 2003 – May 2007)
- Executive Product Development, Quaker Chemical India Ltd. Kolkata, India (April 2000 – December 2002)
- Oil Technologist, K.N. Oil Industries Ltd. Chhattisgarh, India (June 1999 – March 2000)
- Intern, ITC Agro Tech Ltd. Andhra Pradesh, India

SELECTED PUBLICATIONS AND PRESENTATIONS

- Flavour binding by solid and liquid emulsion droplets; Supratim Ghosh, Devin G. Peterson and John N. Coupland, *Food Colloids: Self Assembly and Material Scienc*e, eds E Dickinson and M Leser, Royal Society of Chemistry, UK, chapter 29
- Effects of droplet crystallization and melting on the aroma release properties of a model oil-in-water emulsion; Supratim Ghosh, Devin G. Peterson and John N. Coupland, *Journal of Agricultural and Food Chemistry*, (54), 2006, 1829-1837
- Characterization of the Aroma - Lipid Interaction in Food Emulsions, Supratim Ghosh, Devin G. Peterson and John N. Coupland. Presented at AOCS annual meeting, May 2006, St. Louis, Missouri
- Effect of lipid phase transition on aroma release properties of model oil-in-water emulsions, Supratim Ghosh, Devin G. Peterson and John N. Coupland. Presented at AOCS annual meeting, May 2005, Salt Lake City, Utah
- Effect of aqueous composition on the freeze-thaw stability of emulsions, Supratim Ghosh and John N. Coupland, Presentation at IFT Annual Meeting, July, 2005, New Orleans, Louisiana.

AWARDS AND SCHOLARSHIPS

- Honored Student Award, American Oil Chemists Society (2005)
- The Robert D. and Jeanne L. McCarthy Graduate Scholarship in Food Science, Penn State University (2006-2007)
- National Scholarship, Govt. of India (1996-1997)